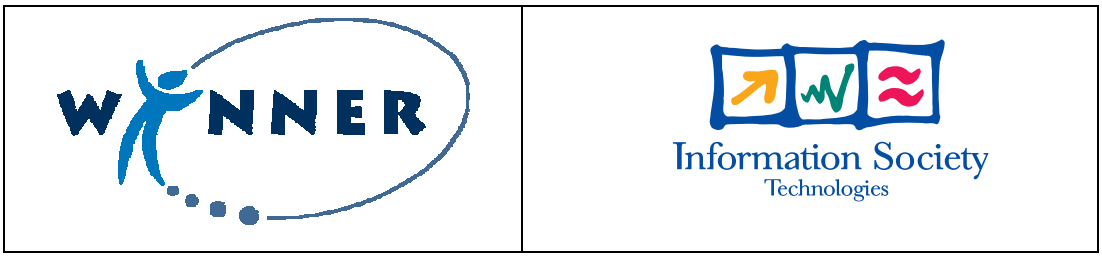

IST-2003-507581 WINNER

D2.10 v1.0

Final report on identified RI key technologies, system concept, and their assessment

Contractual Date of Delivery to the CEC:	*Month 24*
Actual Date of Delivery to the CEC:	23/12/2005
Author(s):	*Johan Axnäs, Karsten Brüninghaus, Martin Döttling, Kari Kalliojärvi, Vaia Sdralia, Kai-Erik Sunell, Mikael Sternad, Ernesto Zimmermann (editors; see author list for full set of authors)*
Participant(s):	*AAU, ACL, CTH, CTH/UU, CTTC, CU, DLR, DoCoMo, EAB, FTR&D, IBM, KTH, LUK, MOT, NTUA, NOK, NOKCH, RWTH, PRL, PUT, SEUK, SM, SM/BenQ, SM/RMR, SM/TUB, SM/TUD, SM/TUHH, SM/UU, TID, TUD, TUI, UniS, UOULU*
Workpackage:	WP2 – Radio Interface
Estimated person months:	*210*
Security:	**PU**
Nature:	**R**
Version:	1.0
Total number of pages:	18080

Abstract: A radio-interface concept for a ubiquitous WINNER radio system is presented and assessed, both in terms of performance and in terms of implementation complexity. The developed radio-interface concept is a packet-oriented, user-centric, always-best concept targeting 100 Mbps sector-throughput for wide-area coverage and 1 Gbps for local-area coverage. It defines a scalable and flexible radio interface based on adaptive and compatible system modes that are tailored to particular situations such as the radio environment, the usage scenario, the economic model, etc. In contrast to the deliverable D7.6, which focuses on the functional architecture of the overall WINNER system concept, and D3.5, which describes protocols and deployment concepts, the present deliverable focuses on the actual design of the radio interface, primarily its lower layers, in order to enable optimisation and evaluation of performance. Results of extensive simulations on link, multi-link, and system levels are presented, supporting important system design choices, exemplifying favourable configurations of the radio interface in different scenarios, and providing an initial system performance estimation. Analyses of system complexity and implementation issues are found not to reveal any major showstoppers that would prevent a cost-efficient implementation at the time of deployment of the WINNER system.

Keyword list: radio interface, physical layer, channel coding, duo-binary turbo codes, LDPCC, pilot grid, self-organised synchronisation, CP-OFDM, adaptive transmission, relays, medium access control, spatial processing, multi-antenna systems, radio resource management, implementation complexity, simulations, multiple access, generalised multi-carrier, serial modulation, time-frequency chunks

Executive Summary

The objective of WP2 and this final deliverable is to identify key technologies for a future broadband radio interface, to develop basic concepts based on these technologies that will lead to a ubiquitous radio system concept, and perform assessments thereof. This is an inherently iterative process, determined not only by pure technical considerations, but also by regulatory and other decisions and restrictions. The snapshot provided in the present deliverable will be further refined and adapted to various external conditions during WINNER Phase II. The present deliverable differs from the overall concept description given in deliverable D7.6 in that it primarily focuses on lower layers, goes more into technical depth, and contains extensive results of simulations and other evaluations in addition to the concept description.

The developed WINNER radio interface concept is a packet-oriented, user-centric, always-best concept. It defines a scalable, flexible, and efficient radio interface. A tool for obtaining such flexibility is to define a small number of compatible system modes that provide a unified interface to higher layers and implement tailored solutions. Within the modes, parameterisations can be used to provide added flexibility and maximum efficiency depending on the particular radio environment, usage scenario, economic model, etc. The always-best solution is further supported by the flexible protocol architecture of the WINNER radio interface and incorporates mechanisms for both long-term and short-term adaptation. Both relaying and advanced spatial processing are integrated parts of the system architecture.

The WINNER radio interface targets fulfilment of the ITU-R M.1645 recommendation according to the views and amendments specified in the WINNER deliverable D7.1. In order to enable detailed system design and appropriate optimisations, the general and user-oriented requirements of D7.1 have been mapped onto more technically oriented design targets on the radio interface for different application scenarios under consideration by WINNER.

The physical layer of the WINNER radio interface uses generalised multi-carrier (GMC) as the transmission format, as this technique enables flexible switching between different forms of multi-carrier and (frequency-domain generated) serial modulation. Specifically, GMC configured as standard cyclic-prefix (CP) OFDM is the preferred option for downlink as well as uplink transmission when terminal power consumption is not a limiting factor (e.g. in short-range scenarios). For all other cases, GMC configured as serial modulation is the preferred option (mainly in the uplink for wide area coverage). The resource allocation in the physical layer is based on a slotted time-frequency chunk pattern that can be adjusted to different propagation scenarios. The chunk and frame durations are short, to ensure a low transmission delay over the radio interface (less than 1 ms). In the case of spatial reuse of resources, each chunk contains several chunk layers. Adaptive modulation supports higher-order modulation up to 64-QAM, and even 256-QAM in short range connections, and uses Gray labelling. Forward error correction coding is based on (quasi-cyclic) block low-density parity-check codes for large code-blocks. Duo-binary turbo codes are additionally considered for medium and smaller block sizes. Convolutional codes are currently foreseen only for very short block lengths (less than 200 information bits).

Generic and baseline transceiver structures have been developed, including a flexible spatial processing architecture, which enables *multi-user spatial domain link adaptation* based on the following basic components: (linear) dispersion codes, directive transmission (beamforming), per stream rate control, and multi-user precoding. This architecture exploits the spatial processing gains (i.e. spatial diversity, SDMA, spatial multiplexing, and interference control) in flexible combinations as required by different scenarios. Apart from the generic architecture, a baseline implementation using adaptive modulation, linear dispersion codes, and linear precoding is also provided.

The WINNER radio interface uses a scattered pilot grid that supports efficient channel estimation, also on chunk basis, with very low overhead. Spatial processing on the one hand limits the potential reuse of pilots for different purposes and on the other hand introduces additional requirements. A classification of pilot types including the effects of spatial processing is provided. The cyclic prefix is used to achieve coarse synchronisation (i.e., on OFDM-symbol level). Training symbols at the beginning of the super-frame enable inter-cell synchronisation, also when no global timing reference (e.g. GPS, Galileo) is available. Efficient means have been developed for compressing the channel quality information feedback required for adaptive transmission and the channel state information required for some multi-antenna schemes. These methods reduce the required feedback overhead to reasonable levels.

The WINNER concept is designed for large bandwidth flexibility and is duplex neutral; there is a time-division duplex (TDD) solution available for use in unpaired spectrum, and a frequency-division duplex (FDD) solution for paired spectrum.

The medium access control (MAC) system layer of the proposed WINNER radio interface allocates the time-frequency-spatial resources to packet flows. Its key element is a resource scheduler, which is assumed to be physically located close to or within each base station and relay node. Functionality for handling and formulating constraints on the allocation to be performed by the resource scheduler is also parts of the MAC system layer. Packets arrive at the MAC in different transport channels intended for control broadcast, contention-based traffic, scheduled point-to-point and scheduled point-to-multipoint traffic. The MAC performs resource allocation on two time scales:

(1) Resource partitioning on a time scale of the super-frame (5–10 ms): The overall allocation of time-frequency-spatial resources to different transport channels is adjusted on this time scale, based on the aggregated demand within each transport channel. Unused guard chunks used for interference avoidance and spectrum sharing are also reserved.

(2) Resource scheduling for the scheduled flows on the time scale of the slot (0.34 ms): The scheduled flows are allocated to time-frequency-spatial resources available for this purpose in the super-frame. There are two options (algorithm variants) for performing resource scheduling: *adaptive allocation* and *non-frequency-adaptive allocation*: With adaptive allocation, individual time-frequency chunks can be allocated to different flows. Fast link adaptation is performed within each chunk, based on predictions of the channel quality. This method offers maximal performance and a high potential for multi-user diversity gains, but it cannot be used at high interference levels and high vehicular velocities. A general framework for adaptive resource scheduling is outlined that enables the allocation to be performed with reasonable complexity. With non-frequency-adaptive allocation, bits from each flow are allocated onto sets of chunks that are dispersed in frequency. Coding and interleaving is used here to combat frequency selective fading. Link adaptation may be performed with respect to shadow fading, but not with respect to frequency-selective fading.. This method is required for control signalling and is the primary method in the case of point-to-multipoint transmission. It offers a robust option for scheduled flows and also serves as a fallback solution for adaptive scheduling. The resource scheduling (adaptive as well as non-frequency adaptive) is fast, offering around 1 ms minimum delay over the radio interface.

The user plane of the MAC system layer can be outlined as follows for the downlink: The arriving packets are separated into retransmission units that are coded. The coded blocks, denoted FEC blocks, are buffered with per-flow queuing. The scheduler allocates resources to flows and then drains the queues with bit-level granularity, to fill the allocated chunks. Contention-based uplink transmission and peer-to-peer communication use a separate set of subcarriers. Cell-wide broadcast messages utilise a set of broadcast OFDM symbols that are located in the preamble of each super-frame.

The choice of multiple access method is intimately connected to the problems of resource partitioning and resource scheduling. For adaptively allocated flows, TDMA/OFDMA is used. In the baseline design, individual chunks are exclusively allocated to flows. For non-frequency-adaptively allocated flows, mapping a flow on a set of chunks would provide insufficient diversity for small packets. The preferred options for solving this problem are presented. The problem of integrating SDMA with the studied time-frequency based multiple access schemes is also discussed.

Radio resource management (RRM) has the overall goal of utilising the given radio resources in an efficient manner. The RRM functions are divided into mode-specific RRM functions that are targeted and optimised for a specific system mode and deployment scenario, mode-generic RRM functions that are shared between the different WINNER system modes or used for their coordination, and cooperative RRM functions which are used for the cooperation of the WINNER system with legacy RANs such as UMTS (including 3GPP long-term evolution) and WLAN. An initial set of algorithms for the RRM functions studied within the WINNER framework is described, including spectrum mapping and allocation, service level controller, mode and RAN selection, handover, admission control, load sharing/congestion control and routing. The location of these RRM algorithms within the RAN architecture is an essential issue. It is envisioned that for the WINNER system with its multiple system modes, a hybrid (hierarchical) approach could be suitable where different decision levels of the same RRM functionality that work at different time scales are located in different nodes. Finally, a first approach to the RRC signalling and a survey of required measurements reports is presented.

Extensive performance assessments of the current WINNER concept and variants thereof have been performed through simulations. Results are presented for link, multi-link and system levels. The insight obtained by such simulations supports important system design choices, allows identification of favourable configurations of the radio interface, and allowed initial system performance estimation. Comparisons with other systems and technologies are made where appropriate. Implementation impact and performance-complexity trade-offs have been analysed in depth in earlier WINNER deliverables and an overview is contained in this deliverable, including electromagnetic field (EMF) exposure aspects.

Authors

Partner	Name	Phone / Fax / E-mail
AAU	Albena Mihovska	Phone: +45 96358639 Fax: +45 98151583 E-mail: albena@kom.auc.dk
ACL	Thorsten Wild	Phone: +49 711 821 35762 Fax: +49 711 821 32185 E-mail: thorsten.wild@alcatel.de
CTH	Tommy Svensson	Phone: +46 31 772 1823 Fax: +46 31 772 1782 E-mail: tommy.svensson@s2.chalmers.se
CTH/UU	Mikael Sternad	Phone: +46 704 250 354 Fax: +46 18 555096 E-mail: mikael.sternad@signal.uu.se
CTTC	Monica Navarro	Phone: +34 93 645 2915 Fax: +34 93 645 2901 E-mail: monica.navarro@cttc.es
	Stephan Pfletschinger	E-mail: stephan.pfletschinger@cttc.es
CU	David Falconer	Phone: +1 613 520 5722 Fax: +1 613 520 5727 E-mail: ddf@sce.carleton.ca
	Chan Tong Lam	E-mail: lamc@sangam.sce.carleton.ca
	Florence Danilo-Lemoine	Phone: +1 613 520 2600 ext. 5691 Fax: +1 613 520 5727 E-mail: fdanilo@sce.carleton.ca

DLR	Armin Dammann	Phone:	+49 8153 28 2871
		Fax:	+49 8153 28 1871
		E-mail:	armin.dammann@dlr.de
	Simon Plass	Phone:	+49 8153 28 2874
		Fax:	+49 8153 28 1871
		E-mail:	simon.plass@dlr.de

DoCoMo	Gunther Auer	Phone:	+49 89 5682 4219
		Fax:	+49 89 5682 4301
		E-mail:	auer@docomolab-euro.com
	Jérôme Bonnet	Phone:	+49 89 5682 4229
		Fax:	+49 89 5682 4301
		E-mail:	bonnet@docomolab-euro.com

EAB	David Astély	Phone:	+46 8 585 301 49
		Fax:	+46 8 585 314 80
		E-mail:	david.astely@ericsson.com
	Johan Axnäs	Phone:	+46 8 404 38 59
		Fax:	+46 8 585 314 80
		E-mail:	johan.axnas@ericsson.com
	Niklas Johansson	Phone:	+46 8 508 77860
		Fax:	+46 8 7575720
		E-mail:	niklas.j.Johansson@ericsson.com
	Göran Klang	Phone:	+46 8 404 4794
		Fax:	+46 8 585 314 80
		E-mail :	goran.n.klang@ericsson.com
	Magnus Olsson	Phone:	+46 8 585 307 74
		Fax:	+46 8 585 314 80
		E-mail:	magnus.a.olsson@ericsson.com
	Per Skillermark	Phone:	+46 8 58531922
		Fax:	+46 8 7575720
		E-mail:	per.skillermark@ericsson.com
	Kai-Erik Sunell	Phone:	+46 8 757 35 61
		Fax:	+46 8 585 314 80
		E-mail:	kai-erik.sunell@ericsson.com

FTR&D	Marie-Hélène Hamon	Phone:	+33 2 99 12 48 73
		Fax:	+33 2 99 12 40 98
		E-mail:	mhelene.hamon@francetelecom.com
	Rodolphe Legouable	E-mail:	rodolphe.legouable@francetelecom.com
	Mylène Pischella	Phone:	+33 1 452 98 963
		Fax:	+33 1 452 94 194
		E-mail:	mylene.pischella@francetelecom.com
	Thomas Sälzer	E-mail:	thomas.salzer@francetelecom.com

IBM	Pedro Coronel	Phone:	+41 1 724 8532
		Fax:	+41 1 724 8955
		E-mail:	pco@zurich.ibm.com
	Wolfgang Schott	Phone:	+41 1 724 8476
		Fax:	+41 1 724 8955
		E-mail:	sct@zurich.ibm.com

KTH	Mats Bengtsson	Phone:	+46 8 790 8463
		Fax:	+46 8 790 7260
		E-mail:	mats.bengtsson@s3.kth.se

LUK	Angeliki Alexiou	Phone:	+44 1793 776620
		Fax:	+44 1793 776725
		E-mail:	alexiou@lucent.com
	Abdelkader Medles	Phone:	+44 1793 776783
		Fax:	+44 1793 776725
		E-mail:	medles@lucent.com

MOT	Markus Muck	Phone:	+33 1 6935 2573
		Fax:	+33 1 6935 7701
		E-mail:	Markus.Muck@motorola.com

NTUA	Elias Tragos	Phone:	+302107721511
		Fax:	+302107722534
		E-mail:	etragos@telecom.ntua.gr

NOK	Carl Eklund	Phone:	+358 50 4836566
		Fax:	+358 7180 36067
		E-mail:	carl.eklund@nokia.com
	Kari Kalliojärvi	Phone:	+358 50 4836232
		Fax:	+358 7180 35935
		E-mail:	kari.kalliojarvi@nokia.com
	Antti Sorri	Phone:	+358 50 4821294
		Fax:	+358 7180 36857
		E-mail:	antti.sorri@nokia.com
	Samuli Visuri	Phone:	+358 50 4868219
		Fax:	+358 7180 36857
		E-mail:	samuli.visuri@nokia.com

NOKCH	Yong Teng	Phone:	+86 10 65392828 2753
		Fax:	+86 10 84210576
		E-mail:	yong.teng@nokia.com

RWTH	Ole Klein	Phone:	+49 241 80 28575
		Fax:	+49 241 80 22242
		E-mail:	ole.klein@comnets.rwth-aachen.de
	Ralf Pabst	Phone:	+49 241 80 25828
		Fax:	+49 241 80 22242
		E-mail:	pab@comnets.rwth-aachen.de

PRL	Keith Roberts	Phone:	+44 1293 815754
		Fax:	+44 1293 815024
		E-mail:	keith.roberts@philips.com

PUT	Zbigniew Dlugaszewski	Phone:	+48 61 665 3916
		Fax:	+48 61 665 2572
		E-mail:	zdlugasz@et.put.poznan.pl
	Adam Piatyszek	Phone:	+48 61 665 3936
		Fax:	+48 61 665 2572
		E-mail:	adam.piatyszek@et.put.poznan.pl
	Michal Wodczak	Phone:	+48 61 665 3913
		Fax:	+48 61 665 2572
		E-mail:	mwodczak@et.put.poznan.pl

SEUK	Thierry Lestable	Phone:	+44 1784 428600 Ext.720
		Fax:	+44 1784 428624
		E-mail:	thierry.lestable@samsung.com
	Vaia Sdralia	Phone:	+44 1784 428600
		Fax:	+44 1784 428629
		E-mail:	vaia.sdralia@samsung.com

SM	Elena Costa	Phone:	+49 89 636 44812
		Fax:	+49 89 636 45591
		E-mail:	elena.costa@siemens.com
	Martin Döttling	Phone:	+49 89 636 73331
		Fax:	+49 89 636 1373331
		E-mail:	martin.doettling@siemens.com
	Jörn von Häfen	Phone:	+49 89 636 46228
		Fax:	+49 89 722 13034834
		E-mail:	joern.von_haefen@siemens.com
	Eiman Mohyeldin	Phone:	+49 89 636 45340
		Fax:	+49 89 636 45591
		E-mail:	eiman.mohyeldin@siemens.com

SM/BenQ Mobile	Karsten Brüninghaus	Phone:	+49 2842 95 1742
		Fax:	+49 2842 95 3387
		E-mail:	karsten.brueninghaus@benq.com

SM/RMR	Bill 'Xinqun' Liu	Phone:	+44 1794 833547
		Fax:	+44 1794 833586
		E-mail:	xinqun.liu@roke.co.uk
	David Thomas	Phone:	+44 1794 833431
		Fax:	+44 1794 833433
		E-mail:	david.Thomas@roke.co.uk

SM/TUB	Eduard A. Jorswieck	Phone:	+49 30 31002860
		Fax:	+49 30 31002863
		E-mail:	jorsey@cs.tu-berlin.de
	Volker Jungnickel	Phone:	+49 30 31002768
		Fax:	+49 30 31002647
		E-mail:	volker.jungnickel@mk.tu-berlin.de
	Malte Schellmann	Phone:	+49 30 31002770
		Fax:	+49 30 31002647
		E-mail:	malte.schellmann@tu-berlin.de
	Aydin Sezgin	Phone:	+49 30 31002868
		Fax:	+49 30 31002863
		E-mail:	aydin.sezgin@mk.tu-berlin.de

SM/TUD	Tobias Frank	Phone:	+49 6151 16 3769
		Fax:	+49 6151 16 53 94
		E-mail:	tobias.frank@nt.tu-darmstadt.de

SM/TUHH	Ting Chen	Phone:	+49 40 42878 2165
		Fax:	+49 40 42878 2281
		E-mail:	t.chen@tu-harburg.de
	Rainer Grünheid	Phone:	+49 40 42878 2166
		Fax:	+49 40 42878 2281
		E-mail:	gruenheid@tu-harburg.de

SM/UU	Stephan Stiglmayr	Phone:	+49 731 50-31531
		Fax:	+49 731 50-31509
		E-mail:	stephan.stiglmayr@e-technik.uni-ulm.de

TID	Emilio Mino	Phone:	+34 91 3374428
		Fax:	+34 91 3374212
		E-mail:	emino@tid.es

TUD	Ernesto Zimmermann	Phone:	+49 351 463 34958
		Fax:	+49 351 463 37255
		E-mail:	zimmere@ifn.et.tu-dresden.de

TUI	Martin Fuchs	Phone:	+49 3677 69 1156
		Fax:	+49 3677 691195
		E-mail:	martin.fuchs@tu-ilmenau.de
	Veljko Stankovic	Phone:	+49 3677 69 1156
		Fax:	+49 3677 691195
		E-mail:	veljko.stankovic@tu-ilmenau.de
	Martin Haardt	Phone:	+49 3677 69 2613
		Fax:	+49 3677 691195
		E-mail:	martin.haardt@tu-ilmenau.de

UniS	Mohammad Abaii	Phone:	+44 1483 683609
		Fax:	+44 1483 686011
		E-mail:	M.Abaii@surrey.ac.uk
	Yajian Liu	Phone:	+44 1483 686015
		Fax:	+44 1483 686011

UOULU	Kari Hooli	Phone:	+358 8 553 2883
		Fax:	+358 8 553 2845
		E-mail:	kari.hooli@ee.oulu.fi
	Juha Karjalainen	Phone:	+358 8 553 7637
		E-mail:	Juha.Karjalainen@ee.oulu.fi
	Zexian Li	Phone:	+358 8 553 2877
		E-mail:	zexian.li@ee.oulu.fi

Table of Contents

Terminology, Acronyms, and Abbreviations

In this chapter abbreviations are explained and fundamental terms are listed, which are not commonly used and/or have specific meaning throughout the document. A short explanation or a reference to the corresponding section that defines this term is given where appropriate.

Term	Description
AC	Admission Control
ACS	Access Control Server
AMA	Alpha-Min Algorithm
BCH	Broadcast (Transport) Channel
BICM	Bit Interleaved Coded Modulation
BLDPCC	Block Low-Density Parity-Check Code
BPA	Belief Propagation Algorithm
BPSK	Binary Phase Shift Keying
BS	Base Station. A stationary network element serving relay nodes or user terminals. Base stations are interconnected with network elements belonging to the RAN.
BSsr	Short-range BS
BSwa	Wide-area BS
CAI	Co-Antenna Interference
CAP	Contention Access Period, in peer-to-peer MAC
CC	Convolutional Code
CCI	Co-Channel Interference
CDC	Common Data (Transport) Channel, for point-to-multipoint communication
CDMA	Code Division Multiple Access
Cell	A cell is defined by the geographical coverage area of a broadcast channel originating from a base station. A BS may control several cells. A cell uses a single PLM on a particular carrier frequency. See also REC.
Chunk	Basic time-frequency resource unit for OFDM links, consisting of a rectangular time-frequency area that comprises n_{symb} of subsequent OFDM symbols and n_{sub} of adjacent subcarriers.
Chunk layer	A time-frequency chunk within one spatial channel (layer).
CoopRRM	Cooperative Radio Resource Management
CP	Cyclic Prefix
CQI	Channel Quality Information, measurement required for (spatial) link adaptation containing condensed information about the channel, e.g., signal-to-interference and noise ratio.
CRC	Cyclic Redundancy Check
CRRM	Common Radio Resource Management
CSI	Channel State Information, measurement required for spatial link adaptation containing detailed information about the channel, e.g., complex-valued channel gain matrix, correlation matrix
CSMA/CD	Carrier-Sense Multiple Access / Collision Detect
CTP	Control Period of DAC physical channel in P2P MAC

Term	Description
DAC	Contention-Based Direct Access (Transport) Channel
DBTC	Duo-Binary Turbo Code
DCT	Discrete Cosine Transform
DFE	Decision Feedback Equalisation
DS-CDMA	Direct Sequence Code Division Multiple Access
DVB	Digital Video Broadcasting
DVB-S	Digital Video Broadcasting – Satellite
DVB-T	Digital Video Broadcasting – Terrestrial
FDD	Frequency Division Duplexing
FDMA	Frequency Division Multiple Access
FDOSS	Frequency Domain Orthogonal Signature Sequences
FD-DFE	Frequency-Domain Decision-Feedback Equalisation
FEC	Forward Error Correction (Coding)
FEC block	FEC coded transmission block with whole or part of RTU as payload
FER	Frame Error Rate
FFT	Fast Fourier Transform
Flow	Packet stream from one source to one or several destinations
FMT	Filtered Multi-Tone
Frame	Timeslot consisting of one uplink and one downlink transmission slot
GAP	Guaranteed Access Period, slotted part of DAC physical channel in P2P MAC
GI	Guard Interval
GMC	Generalised Multi-Carrier
GPS	Global Positioning System
HARQ	Hybrid Automatic Repeat Request
HHO	Horizontal Handover, handover to other cell within the same system
HIS	Hybrid Information System
HPA	High Power Amplifier
HSDPA	High-Speed Downlink Packet Access
IBO	Input Backoff (to transmit HPA, due to PAPR)
ICE	Iterative Channel Estimation
ICI	Inter-Carrier interference
IDCT	Inverse Discrete Cosine Transform
IDD	Iterative Detection and Decoding
IF	Intermediate Frequency
IFDMA	Interleaved Frequency Division Multiple Access
IFFT	Inverse Fast Fourier Transform
IOTA	Isotropic Orthogonal Transform Algorithm
IP	Internet Protocol

Term	Description
IR	Incremental Redundancy
ITU	International Telecommunication Union
ISI	Inter-Symbol Interference
LA	Link Adaptation
LDC	Linear Dispersion Code
LDPCC	Low-Density Parity-Check Code
Link	A link is a radio connection between two network elements of the WINNER access system. It subdivides into *relay links* between base station and relay nodes or between relays and the *user link* between the user terminal and the radio access point.
LLR	Log-Likelihood Ratio
LT	Long-Term
LTE	Long-Term Evolution of 3GPP
MAC	Media Access Control. Name used both to denote a system layer (MAC_{SL}) and a protocol layer (MAC_{PL}) that is implemented in the MAC system layer user plane.
MAI	Multiple Access Interference
MC-CDMA	Multi-Carrier Code Division Multiple Access
MCN	Multi-hop Cellular Network, cellular network that includes relay nodes
MIMO	Multiple Input Multiple Output
MMSE	Minimum Mean Square Error
MSA	Min-Sum Algorithm
MU	Multi-User
OBF	Opportunistic Beamforming
OFDM	Orthogonal Frequency Division Multiplexing
OFDMA	Orthogonal Frequency Division Multiple Access
P2P	Peer-to-Peer transmission
PACE	Pilot-Aided Channel Estimation
PAPR	Peak-to-Average Power Ratio
PARC	Per Antenna Rate Control
PCCC	Parallel Concatenated Convolutional Code (Turbo Code)
PDP	Power Delay Profile
PDU	Protocol Data Unit
PHY	Physical Layer. Name used both to denote a system layer (PHY_{SL}) and a protocol layer (PHY_{PL}).
PHY mode	Basic physical layer transmission strategy, currently two modes are defined: TDD and FDD. Also denoted PLM, Physical Layer Mode.
Physical channel	A set of chunk layers onto which the resource scheduler in the MAC system layer maps data associated with one sub-flow
PLM	Physical Layer Mode, see PHY mode.
PLMN	Public Land Mobile Network
PMP	Peer-to-Multi-Peer transmission

Term	Description
PRP	Pseudo-Random-Postfix
PSAP	Provided Service Access Point
PSRC	Per Stream Rate Control
QoS	Quality of Service
QAM	Quadrature Amplitude Modulation
QC-BLDPCC	Quasi-Cyclic Block Low-Density Parity-Check Code
RAC	Contention-Based Random Access (Transport) Channel
RAN	Radio Access Network
RANG	Radio Access Network Gateway
RAP	Radio Access Point, common term that encompasses both base stations and relay nodes.
RAT	Radio Access Technology
RC	Rate-Compatible
REC	Relay-enhanced cell. The geographical area covered by one broadcast channel from a single base station plus the broadcast channels from its connected relay nodes.
RF	Radio Frequency
RI	Radio Interface
RLC	Radio Link Control: Name used both to denotes a system layer (RLC_{SL}) and a protocol layer RLC_{PL}) that is implemented in the RLC system layer user plane.
RN	Relay Node. A network element serving other RN or UT in a given geographical area via its radio access capabilities. It is wirelessly connected to a base station, another relay node and/or a user terminal and forwards data packets between these network elements.
RNC	Radio Network Controller
RRC	Radio Resource Control. Protocol that provides the signalling for control and feedback messages.
RRM	Radio Resource Management. Control functions implemented in the RLC system layer control plane.
RSB	Resource Scheduling Buffer
RTU	Retransmission Unit, packets upon which HARQ is performed
RUP	Reuse Partitioning
SAP	Service Access Point
SC	Single Carrier
SDMA	Spatial Division Multiple Access
SDU	Service Data Unit
SDFE	Soft Decision Feedback Equalisation
Sector	Azimuth angle partition of a base station coverage area. In the system-level simulations of this document, each sector constitutes a separate cell.
SF	Super-Frame
SF preamble	Initial part of super-frame, transmitted cell-wide in spectrum available everywhere
SF-MMSE	Space-Frequency MMSE

Term	Description
SFTuCM	Space-Frequency Turbo Coded Modulation
SINR	Signal-to-Interference-and-Noise ratio
SISO	Single-Input Single-Output
Site	A location with co-located antenna element that belong to one base station.
SLC	Service Level Control
Slot	short form of Timeslot, see below
SMMSE	Successive Minimum Mean Square Error precoding
SNR	Signal-to-Noise Ratio
SO-RRM	Self-Organised Radio Resource Management
SPIC	Soft Parallel Interference Canceller
ST-WNRA	Space-Time Weighted Nonbinary Repeat Accumulate (Code)
Sub-flow	Data stream after segmentation consisting of FEC blocks
SUD	Single User Detection
Super-frame	Timeslot spanning whole band with place for flows from all transport channels, contains also synchronisation symbols and n_f frames.
System Mode	Specific combinations of algorithm assignations or ranges of algorithm assignations may be referred to as "modes". The two main considered *physical layer modes* (PLM) are based on, and denoted, FDD and TDD. A *System mode* is a PL mode combined with a MAC mode.
Targeted Flow	CDC packet stream to a subset of the multicast receivers within the cell.
TC	Turbo Code
TCP	Transmission Control Protocol
TDC	Targeted Data (Transport) Channel for point-to-point communication.
TDD	Time Division Duplexing
TDMA	Time Division Multiple Access
TEQ	Turbo Equalisation
(Time)slot	Time unit of one contiguous uplink or downlink transmission in FDD or TDD
Transport channel	Interface between the RLC and the MAC layer user planes
UMTS	Universal Mobile Telecommunication System
UT	User Terminal. A physical network element used by the end user to access a service or set of services.
UTRAN	UMTS Terrestrial Radio Access Network
VAA	Virtual Antenna Array
VHO	Vertical Handover, handover between different systems
WLAN	Wireless Local Area Network
ZF	Zero Forcing

Mathematical Symbols and Notation

Symbol	Description
$\mathbf{a}_{c,l}(t,f)$	virtual antenna chunk for chunk *c,* layer *l,* symbol *t;* and subcarrier *f*
B_i	information bits to be transmitted
f	subcarrier
$\mathbf{F}_{c,l}$	precoding matrix for chunk *c* and layer *l*
K	number of users
M_r	number of receive antennas
M_t	number of transmit antennas
N_{data}	number of data symbols per chunk
n_f	number of frames per super-frame
n_{sub}	number of subcarriers per chunk
n_{symb}	OFDM symbols per chunk
Q_c	number of spatial layers in chunk *c*
R_{min}	minimum coding rate
S_c	number of modulated layers in chunk *c*
t	time (OFDM symbol)
T_{chunk}	chunk duration
TO_i	time-out
T_{slot}	MAC slot duration
$\mathbf{x}_{c,l}(t,f)$	antenna chunk for chunk *c,* layer *l,* symbol *t;* and subcarrier *f*

1. Introduction and Radio Interface Structure

The definition of a new radio interface (RI) concept is an inherently iterative process determined not only by pure technical considerations but also by regulatory and other decisions or restrictions. The technical and regulatory processes are mutually dependent. From a design perspective this is clearly a problem since the regulatory framework is needed to provide an optimised solution. On the other hand the regulatory process requires technical arguments and indications to define the system and spectrum framework.

This is the prevailing situation under which the new WINNER system and in particular the new WINNER radio interface is developed. It therefore provides solutions for different system frameworks and a wide range of possible spectrum allocations. This document describes the general WP2 RI concept and current mainstream assumptions based on a consolidation process of previous WINNER deliverables and results. Key technology concepts are assessed against the requirements and assessment criteria derived from WP7 work. System design choices are guided by technical, strategic, and economic aspects. Technical assessment criteria include system performance, implementation aspects, terminal and system complexity, scalability and flexibility. Also of major concern is the interworking with legacy radio technologies and efficient implementation of multi-standard equipment, in particular OFDM-based systems, e.g. like the one discussed in 3GPP long-term evolution (LTE).

The overall requirements, design targets, and key components for the WINNER RI are given in Chapter 1. Chapter 1 also provides some background to the system framework as far as required for the remainder of this document in the form of a top-down survey. The contribution of this deliverable is discussed in the framework of the overall system concept work, including service specification, service architecture, protocols, and system design. Thereafter Chapters 2–4 provide a detailed bottom-up discussion of the system design. The physical layer design, including transceiver diagrams, coding, modulation, spatial processing, synchronisation, and channel estimation, is explained in Chapter 2. Chapter 3 shows the functional design and architecture for the cellular medium access control (MAC) system layer and the MAC for peer-to-peer direct communications. Chapter 4 does the same for radio resource management (RRM) and radio resource control (RRC). Chapter 5 gives an overview on key assessments performed to support design choices, to exemplify favourable configurations of the RI, and to obtain initial performance estimation. For brevity, these chapters focus on major results and key components; further rationale and detail is provided in dedicated appendices for each topic.

1.1 Requirements and design targets

The WINNER system should fulfil the ITU-R Recommendation M.1645 about systems beyond IMT-2000 (i.e. beyond 3G). In particular, 100 Mbps peak aggregate useful data rate for mobile access and 1 Gbps for local area are assumed for these systems. Peak data rates do not, however, give any indication on the quality of service experienced by one user, and a set of amendments and extended system requirements are presented in [WIND71]. A number of them are directly relevant to the radio interface:

- R3.6: Peak spectral efficiency in connected sites of 10 bit/s/Hz/site in wide-area deployments for high load.
- R3.7: Peak spectral efficiency in isolated (non-contiguous) sites of 25 bit/s/Hz/site.
- R3.2: A sustainable average “high end” data rate per link of 50 Mbit/s above Layer 2.
- R3.3: A consistent and ubiquitous data rate per link of 5 Mbit/s above Layer 2.
- R3.12: User speeds ranging from 0–500 km/h should be supported.
- R3.4: A maximum delay over the radio interface of 1 ms at Layer 2.
- R6.7: Maximum bandwidth per radio link: 100 MHz.

Although providing useful indications, these system requirements do not provide sufficient information to completely specify required capabilities and performance of the radio interface. The reason is that several fundamental pieces of information, e.g. the traffic intensity for which the system is to be designed, the admission and congestion strategies, the maximum allowed output power from different types of network nodes in different environments, spectrum availability, etc, are not yet established – but crucial to calculate absolute numbers of many key parameters. This uncertainty is unavoidable since most of the missing parameters are determined by pending political, legal, and strategic decisions of different regulating bodies and in the end by the network operator.

Nevertheless, in order to develop an adequate system concept, technical design targets and guidelines for the radio interface are needed at an early stage. Therefore, a number of scenarios believed to be relevant for the WINNER system have been identified, and for each scenario a set of more technically oriented targets, with details about bit rates and other parameters, have been specified. The scenarios and targets are summarised in Appendix A. In Chapter 5 and its associated appendices (Appendix E, Appendix F, and Appendix G) comparisons of simulation results with these design targets are made. In addition, direct comparisons with the requirements are made to the extent possible. In the latter case, several additional assumptions about missing parameters are needed, and there are many simplified conditions and uncertainties that must be borne in mind when interpreting such results, as further discussed in Chapter 5.

1.2 Key components of the radio interface

In order to meet the requirements discussed above, the WINNER radio interface has been designed as a packet-oriented, user-centric, always-best concept. It defines a scalable and flexible radio interface based on adaptive and compatible system modes tailored to particular situations such as the radio environment, the usage scenario, the economic model, etc. The always-best solution is enabled by several innovative key components, such as

- a flexible multi-mode protocol architecture enabling efficient interworking between different system modes,
- relay-enhanced cells as an integrated part of the concept,
- design and support for operation in shared spectrum and inter-system coordination,
- consequent MAC design for packet-oriented transmission including two-layered resource scheduling and short radio interface delays,
- resource allocation targeting interference avoidance by coordinated scheduling across base stations and relay nodes or using joint (spatial) precoding over distributed antennas,
- physical layer design using generalised multi-carrier (GMC) in different configurations to ensure low complexity, high spectral efficiency, and high granularity of resource elements,
- a spatial multi-user link adaptation concept allowing scalability in link adaptation and multi-user optimisation and being able to adapt to a wide range of deployments, operational scenarios, propagation channel, service requirements, and terminal capabilities,
- novel multi-user precoding techniques developed within WINNER,
- support of self-organised synchronisation of terminals and base station,
- optimisation techniques for overhead and control signalling.

A detailed discussion of these key elements is provided in the conceptual part of this document. The remainder of Chapter 1 is dedicated to introducing the overall WINNER system concept in order to provide the necessary framework and nomenclature.

1.3 Top-down overview of the WINNER system concept

1.3.1 Services, protocols and design

A challenging task in the concept development work is to ensure that the different key components can be embedded into one single radio interface concept that is technically sound for a ubiquitous radio system and its multiple deployment scenarios. A fundamental principle is to study important problems from different perspectives in a systematic manner, taking advantage of the large variety of technical competence that is available in the different working groups. Consequently, the radio interface concept development work is carried out from service-oriented, protocol, and design perspective. The main differences between these three perspectives are that they all represent different levels of abstractions and technical details as illustrated in Figure 1.1. The studies of technical details and the development of abstractions are performed in parallel and complement each other.

The service-oriented view is based on a top-down system engineering approach. A *system* consists of layers and each *system layer* provides services towards the layer above. *Services* and their *users* are first identified starting from the highest layer. Identified services are broken into service components and the

external behaviour of these components (as seen by the users) are modelled with high-level abstractions or provided service access point (PSAP) state-machines[1]. The main goal of this type of representation is to describe services without touching any technical details. The resulting hierarchical structure of these behavioural descriptions is referred to as a *service specification* [WIND76]. The service specification describes the system at the highest level of abstraction.

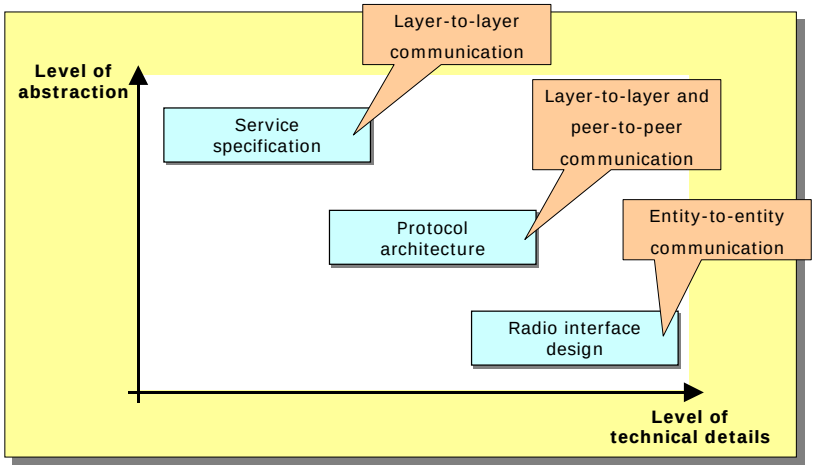

Figure 1.1: The three views on radio interface concept studies.

The service specification is further mapped to a *service architecture* that explains the provided services thus providing the starting point for the protocol view. The service architecture describes the details of provided services by defining service access point (SAP) interfaces between layers. One single PSAP state-machine may be mapped onto one or several SAPs, e.g. (highly-abstract) packet transfer services (as described by the service specification) may be explained with multiple SAPs that are aimed for different purposes such as point-to-point and point-to-multipoint communication. The definition of these interfaces is followed by a description of *protocol architecture* that is a set of radio protocols and *protocol layers* that implements the service architecture.

Protocols are in turn defined as set of rules and formats that govern the communication between protocol peer-entities[2], i.e. communicating parties at the same level, over the air. Even though the placement of control functions and the formal description of protocols is currently under discussions there is a general consensus concerning the overall protocol structure and protocol layers. Currently, the overall structure consists of *radio resource control* (RRC), *radio link control* (RLC), *medium access control* (MAC), and Physical (PHY) protocol layers. The RRC protocol is used by the radio resource management functions. RLC protocol provides reliable packet transfer over the radio interface. The MAC protocol arbitrates access to the shared medium and associates each destination with a unique address. The PHY protocol is responsible for transferring information over a physical link. As the vision is to connect the radio interface to an Ambient Network [AN05], upper layers handle the rest of the functionalities.

The radio protocol architecture is shown in Figure 1.2 where SAPs are illustrated with circles and protocol instances are illustrated with rectangles. For further information about protocols and service-oriented descriptions see [WIND76, WIND35, WIND32, WIND31].

It should be emphasised, that the radio protocol architecture is a very general description about the communication of two nodes over the air. In order to ensure that the radio interface architecture can support all envisioned key technologies and reach the desired performance, *design* and *implementation* related studies are important. Of particular interest is to gain knowledge about the technical feasibility of envisioned key technologies for lower layers. The design view describes the radio interface with the highest level of technical details and it addresses problems that are related to radio interface functions and

[1] In WP7 UML 2.0 is used to describe these state-machines.

[2] This should not be confused with the notion of peer-to-peer communication that later on (throughout this deliverable) refers to direct communication between physical nodes.

detailed algorithmic solutions. Since the main focus of this deliverable is on those lower layer protocols and functions, and the evaluation of their performance, the design perspective is consistently used throughout this document.

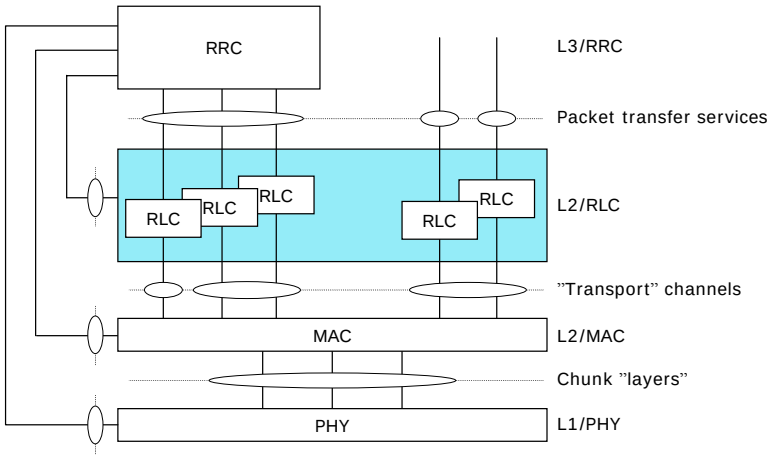

Figure 1.2: WINNER radio protocol layers and interfaces.

1.3.2 System layers, modes, and parameterisation

There are four system layers in the WINNER system concept according to the description in [WIND76]. These layers are further divided into *user plane* and *control plane*. The services that need to operate on individual data units (IP packets or lower layer PDUs) have been placed in the user plane. The control plane services operate on longer time scales and control the operation of the user plane services by way of control signalling.

1.3.2.1 The system layers

The functional role of each system layer is as follows:

IP convergence (IPC) layer

The user plane of the IPC layer receives IP packets from the user of the WINNER RAN, maps them into flows and performs header compression and decompression. The control plane is responsible for RAN association functions as well as macro-mobility (IP level mobility).

Radio link control (RLC) layer

The user plane of the RLC layer provides reliable packet transfer over the radio interface. It also performs confidentiality protection and packet prioritisation in order to meet the quality-of-service (QoS) goals. The control plane takes care of flow establishment and release, location services, load, spectrum, and micro-mobility control. These *radio resource management (RRM)* functions of the control plane will be described in Chapter 4 and Appendix D.

Medium access control (MAC) layer

The MAC user plane provides the service "radio packet transfer", i.e. transmission and reception of packets over the radio interface. An important part of this service is the scheduling of packets. The control plane provides the "MAC radio resource control" service, i.e. acceptance and execution of control messages from higher layers that specify required transmission parameters and boundary conditions. Furthermore it implements "MAC control feedback", i.e. messaging that supports the flow control, the QoS control and the spectrum assignment and other functions at the RLC system layer. There is a tight inter-layer interaction between MAC and physical layers and this is crucial for the performance of the WINNER system. Some functions, such as encoding and decoding, that are traditionally placed in the physical layer are in the WINNER system concept placed in the MAC system layer. The MAC system layer is outlined in Chapter 3 and Appendix C.

Physical (PHY) layer

The PHY system layer handles the physical transmission of flows and of measurements and control signalling directly related to the radio interface. The PHY system layer is not separated into user plane and control plane since it is assumed that all control functionality for the PHY layer resided within the control plane of the MAC system layer. The design of the PHY system layer is one of the major topics of this document. It is described in Chapter 2 and Appendix B.

1.3.2.2 Physical layer modes and flexible parameterisations

The WINNER architecture should be unified yet flexible enough to handle deployments from wide area coverage to high capacity hot spots. A basic goal is that the WINNER radio interface should present a unified set of services to higher layers, yet include some specific parts that provide the required flexibility. To provide flexibility and convergence in a structured way, the definition of *modes* is helpful.

A *physical layer mode (PLM)* can be defined where there is a significant impact (discontinuity in adaptation) of PHY functionality on the radio interface concept. Two PLMs have been defined:

- **Frequency division duplex (FDD)** transmission, performed over paired bands and supporting half-duplex FDD terminals.
- **Time division duplex (TDD)** transmission over unpaired band.

Although any PLM can be configured for any kind of deployment, in this document the FDD mode is evaluated primarily in *wide-area cellular deployment scenarios*, using frequency bands of different width. The TDD PLM has so far primarily been evaluated in short-range cellular deployment.

A *system mode* represents a specific combination of physical layer modes and MAC modes (Section 8.3 of [WIND76]). All higher layer functions are designed to be mode-independent (generic) and form the unified interface of the WINNER system.

There are three MAC modes within the concept:

- **FDD cellular MAC**
- **TDD cellular MAC**
- **MAC for peer-to-peer transmission**, at present designed using the TDD physical layer mode

The combinations of PHY and MAC modes thus define three WINNER system modes.

Parameterisations within modes provide further flexibility and adaptability. Both PLMs use generalised multi-carrier (GMC) transmission, which includes CP-OFDM and serial modulation as special cases (Section 2.2.2). Multiple access is realised in frequency, time, space, and in particular cases also in the code domain. Further details are provided in Section 3.1.6.

The basic time-frequency unit for resource partitioning is denoted a *chunk*. It consists of a rectangular time-frequency area (see Figure 1.3 a) that contains payload symbols and pilot symbols. It may also contain control symbols that are placed within the chunks to minimise feedback delay (in-chunk control signalling). The number of offered payload bits per chunk depends on the utilised modulation-coding formats, and on the chunk sizes. In transmission using multiple antennas, the time-frequency resource defined by the chunk may be reused by spatial multiplexing. A *chunk layer* represents the spatial dimension (Figure 1.3 b).

The chunks and chunk layers are pre-assigned to different types of data flows, on a super-frame time scale (Section 3.1.4 and Appendix C.1.1). They are then used in a flexible way to optimise the transmission performance. For example:

- The antenna resources can be used differently for different flows to/from user terminals.
- Different users may use different variants of GMC, as depicted in Figure 1.4. For example, in uplinks power-constrained users may use single-carrier waveforms within their assigned transmission resources, while other terminals use CP-OFDM. A prerequisite for attaining both efficiency and flexibility is efficient synchronisation of all transmissions within a cell (Appendix B.4).

The coming chapters will describe the concepts used to combine the desired flexibility with the equally desired high efficiency; two goals that are often contradictory and challenging to combine.

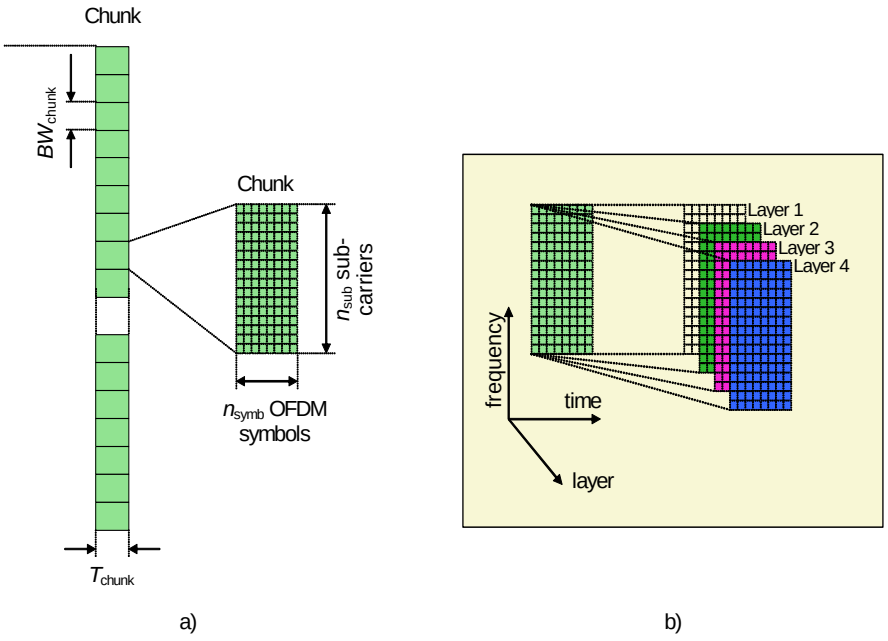

Figure 1.3: a) Multi-carrier downlink physical channel structure and chunks. b) Chunk layers obtained by spatial reuse.

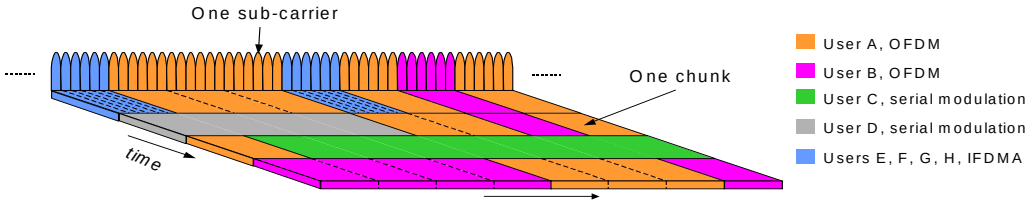

Figure 1.4: Use of different variants of GMC modulation by different uplink users.

1.4 Scope of this document

The radio interface is embedded in the overall WINNER system concept, which defines system layers, services, functional architecture, and protocols as outlined above. While [WIND76] focuses on the functional architecture of the WINNER system concept and [WIND35] describes protocols and deployment concepts, the present report has another focus: The *design* of the lower layers of the radio interface to enable high *performance*, and a preliminary evaluation of the resulting performance.

2. Physical Layer

The design of the physical layer implements several innovative features of the WINNER concept:

- A slotted time-frequency chunk pattern that can be adjusted to different propagation scenarios. The chunk and frame durations are short, which is a basic requirement for a low transmission delay over the radio interface.
- A transmission chain based on generalised multi-carrier (GMC), which enables flexible switching between multi-carrier modulation and (frequency-domain generated) serial modulation.
- A flexible spatial processing is integrated into the transmission and reception chains.
- A scattered pilot grid that supports efficient channel estimation also on chunk basis, at very low overhead. The cyclic prefix is used to achieve coarse intra-cell synchronisation. Additionally, training symbols at the beginning of the super-frame enable inter-cell synchronisation, also in cases where no global timing reference (e.g. GPS) is available.
- Efficient means have been developed for compressing the channel quality information feedback required for adaptive transmission and the channel state information required for some multi-antenna schemes. These methods reduce the required feedback overhead to reasonable levels.

The purpose of this chapter is to present a concise summary of the current selection of technologies for different parts of the WINNER physical layer. To provide the rationale behind this selection, a detailed assessment is given in Appendix B (concept details) and Appendix F (simulation results), including a summary of the results from previous deliverables [WIND21, WIND22, WIND23, WIND24, WIND27].

2.1 Forward error correction

Among the large number of possible options for forward error correction identified in [WIND21], three techniques have been identified as main candidates for the WINNER system [WIND23]: convolutional codes (CC), parallel concatenated convolutional codes (PCCC, Turbo Codes) and low-density parity-check codes (LDPCC). More specifically, Duo-Binary Turbo-Codes (DBTC) and Block-LDPC Codes (BLDPCC) are able to provide excellent performance at medium to large block sizes (200 information bits and beyond) while taking implementation simplicity (e.g. parallelisation, memory requirements) into account already in the code design phase. BLDPCC outperform DBTC at large block lengths and/or high code rates (for a detailed assessment, please refer to Appendix B.2). The use of convolutional codes is currently considered for block lengths below 200 information bits. However, DBTC show very good performance also in this regime, so that CC might eventually not be needed to implement channel coding in the WINNER radio interface.

Table B.1 in Appendix B summarises the relative merits of the three candidate technologies with respect to the most relevant assessment criteria. Details on the assessment can be found in [WIND23] and Appendix B.2. Note that while the discussion on FEC schemes forms part of the PHY chapters, coding in the WINNER system will be mainly implemented in the MAC system layer (MAC-2 sub-layer), as detailed in the Chapter 3. Only convolutional coding as a part of the (spatial) link adaptation within individual chunks will form part of the PHY system layer.

In situations where the channel coding gain (using reasonable code rates, e.g. 1/3 and above) is not sufficient to support reliable transmission, additional spreading can be used to provide reasonable SINR values. This avoids further decoding complexity as would be the case for low-rate channel codes. It is, however, understood that this comes at the expense of lower achievable data rates.

2.2 Modulation and space-time-frequency processing

2.2.1 General resource allocation strategy

The overriding principle for allocating the total available resources is to strive primarily for orthogonal use of time-frequency resources: Non-orthogonality, for example in the form of CDMA, SDMA or contention-based signalling, is allowed only within carefully prescribed subsets of the total resources, designed to limit interference with other parts of the resource pool. Furthermore, some resources have to be reserved as guard bands/guard spaces to preserve the orthogonality. Extension of the orthogonality from single cells/sectors to clusters of neighbouring sectors, can be done for example by

- interference avoidance scheduling between cells, or
- joint (spatial) precoding (and detection) over sectors [SWW+04, LWZ04].

For the spatial dimension, non-orthogonality is unavoidable; spatial reuse of time-frequency resources will always create some interference. The general time-frequency space transmission chain outlined in Appendix B.1 provides means to tailor and control such interference, as outlined in Appendix C.1.7.

2.2.2 Modulation technique

Block signal processing in the frequency domain at both transmitter and receiver, using efficient fast (inverse) Fourier transform (IFFT/FFT) operations, is a natural choice for future high bit rate wireless radio interfaces, as signal processing complexity per data symbol rises only logarithmically with the channel delay spread [FK05]. Furthermore, frequency domain processing enables transmitters to easily and adaptively shape their spectrum occupancy in response to user data rate requirements, user terminal capabilities and the availability of unoccupied spectrum. It also enables flexible choice of bit rates, modulation formats and multiple access schemes, according to the current channel state and user need.

The *generalised multi-carrier* (GMC) technique [WIND21, WIND23] will be used for modulation in WINNER, as it is essential for providing the flexibility needed to fulfil the "always best" principle also on the physical layer. It enables to accommodate a plurality of *multi-carrier* modulation/multiple access schemes, such as different flavours of OFDM (CP-OFDM, IOTA-OFDM, PRP-OFDM), FMT, and MC-CDMA, as well as the following *serial modulation* schemes: single carrier, single carrier DS-CDMA, and IFDMA. This is done by selection of an appropriate mapping strategy (data symbols to subcarriers), guard interval design, and (frequency domain) filtering. The GMC approach is also extremely useful in generating *multi-band* signals, for spectrum flexibility [WIND22].

A small set of the above stated modulation technique options will be sufficient to efficiently adapt the WINNER system to the most relevant deployment scenarios outlined in Appendix A.1. This restriction will also keep the complexity of the WINNER radio interface in terms of implementation options at a reasonable level. To enable the choice of appropriate techniques, their relative merits have been thoroughly studied [WIND21, WIND22, WIND23]. The results of this assessment work are summarised in Table B.3, and the following options have been selected for use in the WINNER system:

- GMC configured as standard CP-OFDM
    - for downlink transmission in the TDD and FDD modes,
    - for uplink transmission when terminal power consumption is not a limiting factor
- GMC configured as serial modulation (DFT precoded CP-OFDM)
    - for uplink transmission in the power limited wide-area case

The above specifications define only the *modulation* technique – the choice of appropriate *multiple access schemes* for the different modes is discussed in Chapter 3. For adaptive transmission, chunk-based OFDMA will be used; for non-frequency adaptive transmission, MC-CDMA in conjunction with FDMA/TDMA is the preferred option while for the serially modulated uplink, FDMA/TDMA is envisioned (e.g. DFT-precoded block OFDMA or IFDMA).

The specific parameterisation of these transmission techniques is governed by the physical channel conditions, as outlined in [WIND23]. Based on this methodology, appropriate parameters have been selected and are summarised in Table 2.1. Non-differential M-QAM modulation (with BPSK as a special case) is proposed for the use in the WINNER system, since channel state information can be made available to the receiver at relatively low pilot overhead in all scenarios, as detailed in Section 2.3. For the wide-area scenario, modulation formats up to 64-QAM are proposed, while for short-range transmission

even 256-QAM appears to be feasible. Gray mapping is proposed, as it is a natural choice for the bit labelling, facilitating the calculation of soft output at the detector with low complexity. The use of other labellings (in combination with a weaker outer code) is also under investigation in the context of iterative equalisation and/or channel estimation.

2.2.3 Modulation parameters

The configuration presented below was used for investigations during the last part of WINNER Phase I. Note that the real WINNER system will be required to support several different configurations (parameter sets), in order to effectively adapt to differing channel conditions and fulfil the "always-best" objective. The parameters listed below are examples for such parameter settings, which can be used to study the relative merits of different techniques. They are, however, not claimed to be optimal, and refined sets of parameters might be used for Phase II. A framework for deriving appropriate parameter sets can be found in [WIND23]. The range of reasonable values is much wider for the TDD mode than for the FDD mode, where parameter ranges are more severely constrained by assumed channel delay spreads and vehicular velocities [WIND23] in the wide-area scenario. All uplink transmissions are embedded in the super-frame and are assumed to be fine-synchronised. The assumed centre frequencies are worst-case values. The use of FFT sizes up to 2048 has been assumed to be reasonable from an implementation point of view.

Table 2.1: Basic transmission parameters used for simulation of GMC based systems

Parameter	FDD mode (2×20 MHz)	TDD mode	Units/notes
Centre frequency	5.0 DL/ 4.2 UL	5.0	GHz
Duplexing method	FDD (paired)	TDD	
FFT BW	20.0	100.0	MHz
Number of subcarriers in GMC	512	2048	Equals length of FFT
Subcarrier spacing	39062	48828	Hz
Symbol length (Excluding cyclic prefix)	25.60	20.48	μs
Cyclic prefix length	3.20	1.28	μs
Total symbol length	28.80	21.76[3]	μs
Number of subcarriers in use	416	1664	[-208:208] and [-832:832] Subcarrier 0 not used
Signal BW	16.25	81.25	MHz
Chunk size in symbols	8×12 = 96	16×5 = 80	Subcarriers × Symbols

2.2.4 Transceiver structure

Figure 2.1 and Figure 2.2 give a general overview of the envisaged structure for the transmitter and receiver in the WINNER system, respectively. The structure is the same for all cases of generalised multi-carrier transmission, only requiring appropriate configuration for some components. The user data is first segmented into flows, which then are individually encoded, segmented and mapped to chunks, where modulation and space-time-frequency processing takes place (cf. Appendix B.1 for details). Afterwards, the modulated chunks are assembled to raw (OFDM) symbols, subjected to an IFFT, the CP is added and the digital baseband data is finally forwarded to the RF processing.

[3] A small symbol roll-off time should be added to the OFDM symbol length, to reduce the out-of-band power. It is here assumed to be included in the guard intervals.

For OFDM transmission, the "GMC" preprocessing block in Figure 2.1 would only contain (optional) frequency domain filtering. For serial modulation, however, it is necessary to subject the modulated symbols to a FFT *prior to* any *frequency domain* (spatial) processing, i.e., modulation has to be done *prior to* the formation of chunks (spatial processing for single carrier transmission may also be done in the time domain). This operation will be done in the GMC processing block of Figure 2.1: a block of M modulated symbols that eventually will be turned into one or more chunks will be passed through an M-point FFT. The M symbols are now in the frequency domain, and are mapped into the specified chunk layers. The remaining processing is equivalent to that for other GMC signals, e.g. OFDM. It should be emphasised that this approach somewhat reduces the flexibility of the system in the case of serial modulation, as all chunks within one serially modulated block will have to undergo the same kind of spatial processing. However, as serial modulation is envisaged for uplink transmission from user terminals only, it will anyway require only a quite basic configuration of the generic spatial processing chain described in detail in Appendix B.1, so this limitation is not very severe.

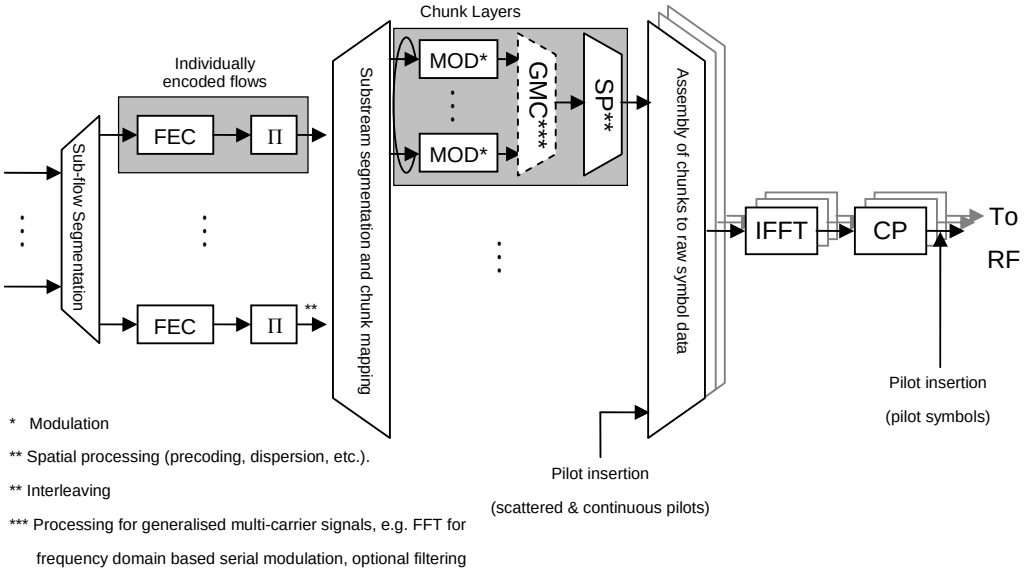

Figure 2.1: Overview of transmitter structure.

The corresponding receiver structure is depicted in Figure 2.2. Optional feedback between soft-input soft-output decoder and space-time equaliser and channel estimator enable iterative detection/Turbo equalisation (TEQ) and iterative channel estimation (ICE) techniques detailed in [WIND21, WIND23] (cf. also the results presented in Appendix F.3). Serial modulation based transmission (frequency domain based single carrier, as well as IFDMA) requires an IFFT in addition to the FFT, in order to support frequency domain equalisation.

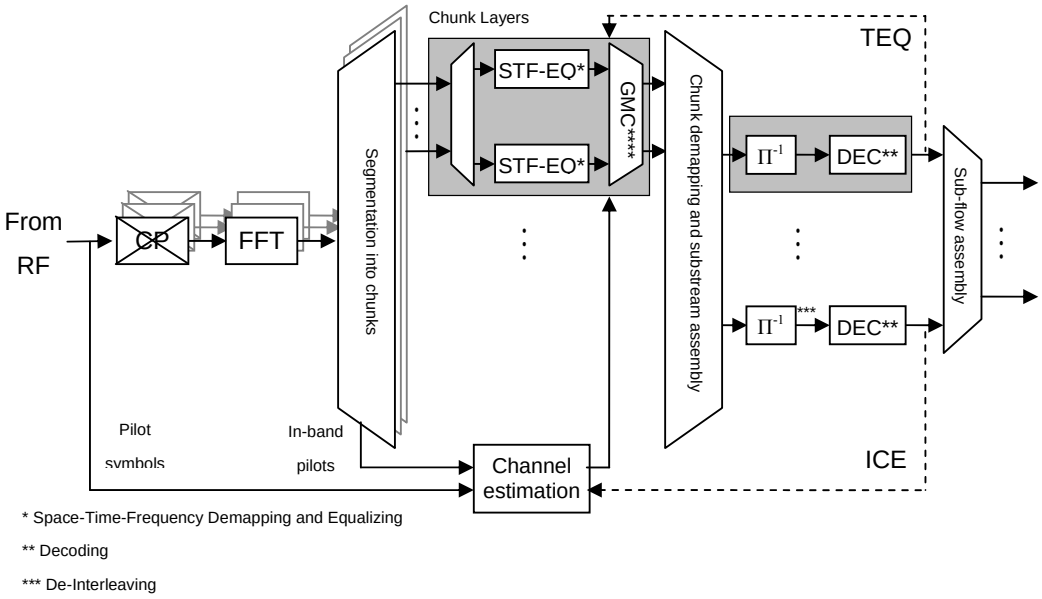

Figure 2.2: Overview of receiver structure.

2.2.5 Space-time-frequency processing

Spatial processing provides performance gain via spatial diversity, spatial multiplexing, SDMA, and enhanced interference management. Spatial diversity adds reliability by transmitting multiple copies of the same data over (potentially) uncorrelated channels. Therefore, diversity efficiently copes with the detrimental effects of fading on the system performance. On the other hand, independent fading in a multi-antenna system can also be seen as a beneficial effect that can lead to a substantial increase of the achievable data rate by performing spatial multiplexing, i.e. transmitting independent data over the uncorrelated spatial channels to one user terminal. A significant contribution to high spectral efficiency is interference avoidance by spatial processing, e.g. based on multi-user precoding at the transmitter in the downlink. The use of beamforming (adaptive or non-adaptive) makes it possible to schedule multiple users on the same time-frequency resource (chunk) within a cell or across multiple cells, and separate them by the SDMA properties of the multi-antenna channel. When channel knowledge is available at the transmitter, it is also possible to distribute complexity between transmitter and receiver in a very flexible manner. Precoding techniques, for example, allow keeping receiver complexity low. Note that, although first investigations are based on traditional cell layouts with sector antennas, precoding with distributed antennas (using a central processing unit and separated radio heads) is seen as a particular deployment form of the proposed WINNER multi-antenna concept that can be of additional benefit for the overall goal of an interference-avoidance radio interface concept.

The WINNER multi-antenna concept is a generic architecture that aims at performing *multi-user spatial domain link adaptation*, based on the following basic components: (linear) dispersion codes, directive transmission (beamforming), per stream rate control, and multi-user precoding [WIND27, DAO05]. This architecture allows fostering the spatial processing gains introduced above in flexible combinations as required by different scenarios, i.e. different combinations of physical layer mode, link direction, transport channel type, deployment, propagation conditions, cell load, traffic type, BS antenna configuration, and terminal capabilities. A generic spatial processing chain that implements the WINNER multi-antenna concept is detailed in Appendix B.1.

2.3 Pilot grid design for channel estimation and synchronisation

2.3.1 Synchronisation

For synchronisation, we have to distinguish between coarse synchronisation (acquisition) where all other relevant system parameters are still unknown, and fine synchronisation (tracking) where a previous coarse estimate is further improved and adapted to variations of, e.g., the local oscillator. Furthermore, there are three quantities, which have to be synchronised in an OFDM system:

- OFDM symbol and frame timing
- Carrier frequency
- Sampling rate

The choice of an appropriate synchronisation strategy for the radio interface is based on several criteria:

- Robustness, expressed in the lock in probability, i.e. the probability of successful acquisition
- Residual synchronisation offsets in the steady state
- Time required to achieve synchronisation
- Required overhead

With respect to synchronisation, the scenarios in which the WINNER radio interface is to operate can be distinguished as follows:

- **Hot spot**: mainly indoor environment, with no significant interference from adjacent BSs.
- **Wireless network with global reference time**: All BSs operate synchronised governed by a global reference clock, which may be provided by the Global Positioning System (GPS) or the European Satellite Navigation System (Galileo).
- **Synchronised wireless network without timing reference**: If no global timing reference is available, synchronisation of the network can be achieved in a self-organised way. Since coordinated operation of a wireless network essentially requires BSs to be synchronised, it is generally believed that the attainable system capacity of a synchronised wireless network exceeds a non-synchronised network.
- **Uncoordinated wireless network**: BSs operate non-synchronised. In this case, the UT needs to be able to distinguish between several signals in order to identify the closest BS.

For synchronisation purposes, different types of pilots are foreseen for the WINNER system concept:

- Two sets of **training symbols** (uplink and downlink), consisting of three OFDM symbols are included in the super-frame preamble for self organised inter- and intra-cell synchronisation. The structure of the training symbols, and the related synchronisation algorithms are described in Appendix B.4.1.
- **Continual pilot subcarriers (or tones)**. They may serve various purposes, such as phase noise compensation, tracking of carrier and sampling frequency offset (see [WIND23], Section 6.2.5.2). In combination with cyclic prefix based synchronisation, differential modulation of the pilot tones allows establishing frame synchronisation, as well as to detect frequency offsets of a multiple of the subcarrier spacing [SFF+99].

Within the WINNER framework a synchronisation concept that can synchronise a wireless network in a self-organised way has been identified in [WIND21]. The algorithm relies on dedicated set of training symbols inserted in the super frame preamble. In Appendix B.4.1 its basic principles are summarised and some enhancements are presented. Simulation results reported in [WIND23] show that both frequency and time synchronisation of all BSs within the cellular network can be achieved after 20 super-frames, with remaining frequency offset of about 1% of the subcarrier spacing and time offset of about 10% of the guard interval, respectively. Since the duration of one super-frame is 8x12 and 8x30 OFDM symbols for the WINNER FDD and TDD modes, respectively, the time to synchronise for this algorithm totals to about 110 ms for 20 super-frames, which may be too long for some applications.

For hot spots or for networks with access to a global timing reference, synchronisation utilizing the cyclic prefix in combination with continual pilot tones is considered to be an appropriate choice [WIND21, WIND23]. This approach is in particular attractive for OFDM systems with a large number of subcarriers, in terms of pilot overhead and performance [BBB+99]. It is demonstrated in Appendix F.4.1 that reliable

acquisition can be achieved within 12 OFDM symbols at SNR > -4 dB. Furthermore, a scattered pilot grid, predominantly used for channel estimation (see Appendix B.4.2), can be used to achieve acquisition in a non-synchronised wireless network. However, numerical results in Appendix F.4.1 suggest, that the carrier frequency offset must not exceed half of the subcarrier spacing for this algorithm to work.

A timing advance strategy which compensates for the propagation delays between signals transmitted from UTs to their assigned BS during uplink is proposed in Appendix B.4.1. The proposed ranging process enables the UTs to estimate the propagation delays of their signals by utilising individual synchronisation tones. This information is subsequently used for a time advanced transmission during uplink, providing a time aligned arrival of different users' signals at the BS. If the synchronisation tones are retransmitted by the UTs after the ranging process is finished, they may further be used for a fine estimation of the carrier frequency offset at the BS.

2.3.2 Channel estimation

For channel estimation purposes, the following types of pilots are foreseen:

- A **scattered pilot grid** is used for OFDM channel estimation and channel prediction. For the pilot grids presented in B.4.2, the pilot overhead is 2.5% and 4% per spatial stream for the WINNER TDD and FDD mode, respectively. In Appendix F.4.1 it is shown that a scattered pilot grid could also be utilised for acquisition in a non-synchronised wireless network.
- In OFDM uplinks that use adaptive transmission, channels from many users have to be estimated and predicted in each chunk. Methods based on simultaneous pilot transmission from all candidate terminals (**overlapping pilots**) can then be used to limit the pilot overhead fraction in the uplink [WIND24].
- For uplink (frequency domain generated) serial modulation, pilot patterns may be generated in the frequency domain in either of two ways. The first way is to use a scattered pilot grid, equivalent to OFDM. Alternatively, pilot patterns for serial modulation in the uplink may be generated in the time domain, in the form of short training blocks time-multiplexed with data blocks. Both techniques are described in Appendices B.4.2 and F.3.1, respectively.

For multi-antenna transmission, a combination of dedicated pilots per flow, common pilots per cell/sector, common pilots per antenna and common pilots per beam are required, as described in Appendix B.4.2. Interference estimates, per chunk layer or averaged over chunk layers, may be obtained as by-products of the pilot-based channel estimation: The residual, i.e. the signal component that cannot be explained through the known pilots and the channel model, is used as interference estimate.

Channel estimation by interpolation in time and frequency based on a scattered pilot grid is considered to be an efficient solution for an OFDM-based radio interface [WIND21, WIND23]. In Appendix B.4.2 a generic framework for the pilot design of GMC signals is described. To this end, a scattered pilot grid is applicable to any GMC signal. Alternatively, short time domain training symbols can be implemented for single carrier signals on the uplink.

During the start of communication, interpolation techniques with limited information about the channel conditions must be used. An unbiased channel estimation scheme, which does not require any information about the channel statistics is proposed and evaluated in Appendix F.3.4. A robust interpolation filter which only assumes knowledge about the CP duration and the maximum velocity expected in a certain environment is another possible choice, cf. results in [WIND23] and Appendix F.3.2. During operation, statistical knowledge about the power delay profile and the Doppler spectrum is accumulated. Channel interpolation utilizing this knowledge can improve performance significantly (see Appendix F.3.3).

Especially in case of dedicated pilots, purely pilot aided techniques may have severe limitations. Conventional channel estimation by interpolation may then require a pilot boost and/or a significant degree of over-sampling. Advanced solutions, such as iterative channel estimation, aim to make a pilot boost redundant, at the expense of increased complexity, cf. results in [WIND23] and Appendix F.3.2. If an iterative receiver structure is already in place, iterative channel estimation offers a good compromise between performance and complexity.

Adaptive transmission requires channel prediction for use in the resource allocation. Channel prediction can be based on common pilot symbols that are also used for other purposes. It should utilise the channel correlation in time and frequency. In Appendix B.5.2, the results obtained by using Kalman state-space algorithms in the frequency domain for prediction are outlined. Similar results are obtained with time-domain extrapolation of channel taps. With these methods, adaptive transmission becomes possible in the WINNER system at vehicular velocities. The channel prediction accuracy estimates (covariances) are furthermore important inputs in the design of the link adaptation and resource scheduling schemes.

3. Medium Access Control (MAC) Layer

The WINNER medium access control (MAC) system layer is designed as **three MACs** (modes):

- **FDD cellular MAC**, including multiple-access, multi-hop and multi-antenna aspects
- **TDD cellular MAC**, including multiple-access, multi-hop and multi-antenna aspects
- **MAC for peer-to-peer transmission**, at present based on the TDD physical layer mode

The first two have a largely identical design and are described briefly in the section below, with additional details in Appendix C.1. See also [WIND76]. The peer-to-peer MAC is outlined in Section 3.2 with further details in Appendix C.2.

3.1 Medium access control for FDD and TDD cellular transmission

3.1.1 Goals and design principles

The cellular MAC design supports and enables several innovative features of the WINNER system:

- The super-frame is designed with pilots that support self-organised synchronisation of all involved base stations, relay nodes and user-terminals. Having a synchronised network enables an improved spectral efficiency in two ways: it makes large guard-bands unnecessary and simplifies interference-avoidance scheduling between cells and relay nodes.
- MACs for FDD and TDD cellular transmission support fast transmission and very low re-transmission delays over the RI. These properties are key to attaining high spectral efficiency via adaptive schemes [WIND24], reliable communication through efficient re-transmission and high data rates for TCP/IP traffic.
- Adaptive transmission is integrated into the design, on all time scales. Up to moderate vehicular velocities, link adaptation and scheduling can be performed with fine granularity in the frequency domain (OFDMA/TDMA). This provides multi-user scheduling gains for mobile as well as stationary terminals. For higher velocities, the transmission only adapts to the path loss and shadow fading. On a super-frame time scale, the resource partitioning can adapt to the traffic demand over different transport channels.
- Multi-antenna transmission can be adjusted in a very flexible way per flow, to obtain an appropriate balance between different objectives: Obtaining multiplexing gains to boost throughput, achieving robustness via diversity transmission, and obtaining SDMA gains by transmitting flows to different user terminals over different spatial channels.
- Operation in spectrum shared with other operators who all use the same physical-layer WINNER mode [WIND63] will be an integral part of the design. Operation in dedicated bands is seen as a special case of this situation. Such single-system shared spectrum use has the potential of *both* improving the flexibility and simultaneously increasing the throughput/spectral efficiency.
- The super-frame and the resource partitioning are designed to work efficiently in conjunction with inter-cell interference-avoidance schemes. They are also designed for relay-enhanced cells, so that base stations and a set of relay nodes can share the total spectral resources efficiently.

In the design of the adaptive transmission system, the different reaction times and control time scales of various control functions have been an important guiding principle. The slower control functions have been placed as RRM functions in the control plane of the RLC system layer (see Appendix D.1). The faster control functions are located in the MAC control plane while the fastest ones, which directly control data flows, are located in the MAC user plane. To minimise transmission time delays due to communication between nodes, a complete MAC layer is assumed to be implemented at each *base station* (BS) and at each *relay node* (RN). Thus, all antenna resources belonging to a BS or a RN can be controlled tightly by the MAC system layer. Cooperative multi-antenna transmission and distributed antenna systems are supported, when all antennas are regarded as encompassing *one BS/RN*.

3.1.2 Control of relay-enhanced cells

The MAC system layer is designed to work in *relay-enhanced cells* (REC), in which a set of nodes (RNs or BS) are linked to each other over the air. (Nodes here refer to logical nodes, cf. [WIND35].) The BS, but not the RNs, has a fixed connection to the RAN. The RNs may be used for improving the coverage

within the cell or for extending the range of the cell. Each RN is connected to one but not more BSs. Some or all UTs may communicate directly with the BS. If RNs are present, some UTs may transmit to/receive from these RNs. The MAC implemented in each RN controls those transmissions. Thus, the RNs essentially control separate sub-cells. The MAC system layer controls flows over a single hop. Flow QoS control over links spanning multiple hops is the responsibility of the RLC layer.

While both heterogeneous and homogenous relaying is under consideration, the cellular MAC design has focused on the more challenging case of homogenous relaying, where RNs and BS use the same PLM and share spectral resources. The total time-frequency resources are partitioned into parts used by the BS, shared parts, and parts used by RNs. This partitioning is computed by RRM functions at a central location in cooperation with the MAC that is implemented at the BS. It is then signalled to all RNs and UTs.

3.1.3 The MAC services and tasks

The MAC system layer for FDD and the TDD cellular transmission has a MAC protocol implemented in its user plane. It also contains resource allocation and planning functions in its control plane. It should provide the following services to the RLC system layer:

- ***Radio packet transfer***, i.e. transmission and reception over the radio interface of packets belonging to any of the transport channels defined below.
- ***MAC radio-resource control***, i.e. acceptance and execution of control messages
- ***MAC control feedback***, i.e. messaging from MAC to RLC that supports the flow control, the QoS control, and the spectrum assignment and other functions at the RLC system layer.

The WINNER *transport channels* are defined as being the interfaces between the RLC protocol layer (in the RLC system layer user plane) and the MAC protocol layer (in the MAC system layer user plane). They define the basic types of radio-packet transfer that are provided.

- Broadcast channel (**BCH**) for broadcasting system information from RLC and higher layers to all terminals inside the coverage area of the cell,
- Contention-based random access channel (**RAC**) for initial access to a BS or RN, and also for BS-to-BS control signalling in the TDD mode,
- Contention-based direct access channel (**DAC**) for contention-based uplink data transfer,
- Common data channel (**CDC**) for scheduled point-to-multipoint communication,
- Targeted data channel (**TDC**) for scheduled point-to-point communication,
- Targeted control channel (**TCC**) for control-plane generated control messages.

MAC flow control and resource allocation is performed two time scales: That of the slot (half frame) and that of the super-frame (Section 3.1.4 below)[4]:

- Time-frequency *resource partitioning* and *spatial scheme control* is planned on a time scale of the super-frame (5–10 ms): The allocation to different transport channels is adjusted on this time scale, based on the aggregated demand within each transport channel. Unused chunks enable flexible spectrum use between WINNER operators/users and adaptive interference avoidance between neighbouring cells and parts of cells.
- *Resource scheduling* (RS) is performed on the time scale of the slot (0.34 ms): The scheduled flows are allocated to time-frequency-spatial resources in one of two ways: *Adaptive* RS utilises the frequency-selective fading. This requires processing of CSI/CQI feedback from the PHY layer. *Non-frequency adaptive* RS uses a diversity-based transmission within the frame.

Adaptive resource scheduling and support for adaptive transmission is a major feature of the design, discussed further in Appendix C.1.6. Detailed transmission schemes for adaptive transmission in both FDD and TDD modes have been presented in Section 3.1 of [WIND24]. Key enabling features are here the use of chunks of appropriate granularity, the use of in-frame control signalling to obtain tight feedback loops, the use of channel prediction to enable adaptive transmission at vehicular velocities (Appendix B.5.2) and appropriate schemes for compressing feedback information (Appendix B.5.3).

[4] We say that a function in a certain system layer works on a given time scale if the reaction time on a control message need not be smaller than the time indicated by the time scale. Thus, the required adaptation speed of a given function that is distributed among different physical nodes is given by this time scale.

3.1.4 The chunk, slot, frame and super-frame structure

As outlined in Section 1.3.2.2, the basic time-frequency unit for resource allocation is the chunk. During the later part of WINNER Phase I, the transmission parameter examples outlined in Table 2.1 have been used for simulation purposes. In the FDD physical layer modes, chunks then comprise 8 subcarriers by 12 OFDM symbols or 312.5 kHz × 345.6 μs. In the TDD physical layer mode, the chunk dimension is 16 subcarriers by 5 OFDM symbols, or 781.25 kHz × 108.0 μs. Using the parameter sets of Table 2.1, an FDD downlink/uplink with 20 MHz FFT bandwidth, is divided into 52 chunks on the 16.25 MHz signal bandwidth. A 40 MHz FFT bandwidth accommodates 104 chunks. The TDD PLM with 100 MHz FFT bandwidth has 104 chunks on 81.25 MHz signal bandwidth. Please see Appendix C.3 for a discussion on chunk dimensioning. [5]

The chunks are organised into *frames*. In the TDD mode, each frame consists of a downlink transmission interval followed by an uplink transmission interval, denoted *slots*, or *time-slots*. In FDD, the frame is also split into two slots. Half-duplex terminals may be separated into two groups, where one group has downlink transmission in the first slot and transmits in uplinks in the other, while the other group uses the opposite scheme (Appendix C.1.2). FDD base stations use full duplex.

The frame duration has been set equal in the two PLMs, to facilitate inter-mode cooperation. With a frame duration of 691.2 μs, an FDD frame consists of two chunk durations, with one chunk per slot. A TDD frame consists of in total 6 chunks and two duplex guard intervals, organised into a downlink slot and an uplink slot. With downlink-uplink asymmetry 1:1, the TDD slot thus consists of three downlink chunks followed by three uplink chunks. See the figure below. The asymmetry ration could be varied from 5:1 to 1:5, but to provide sufficient time for signalling and scheduling calculations during the uplink slot in adaptive transmission, it should not be set larger than 2:1.

The *super-frame* (SF) is a time-frequency unit that contains pre-specified resources for all transport channels; Figure 3.2 illustrates its preliminary design, comprising of a *preamble* followed by n_f frames. Here n_f = 8, resulting in super-frames of approximate duration 5.6 ms. (It could be extended to e.g. 16 frames, if required). The available number of chunks in the frequency direction could vary with the geographical location. It is assumed that for the FDD DL and UL as well as for TDD, there exist frequency bands that are available everywhere. The preamble is transmitted in those commonly available bands. The remainder of the super-frame may use other spectral areas that are available at some locations, or to some operators, but not to others. All of these spectral areas are spanned by one FFT at the receiver and are at present assumed to span at most 100 MHz.

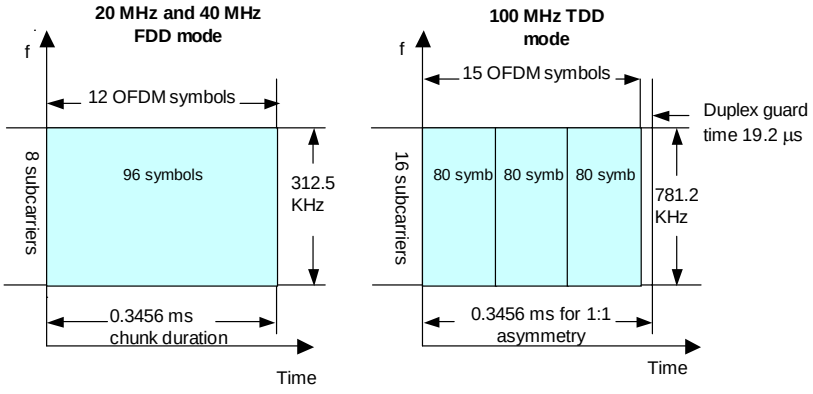

Figure 3.1: Summary of assumed chunk sizes in the two physical layer modes. The figures show a slot (half of the frame) in each case, assuming 1:1 TDD asymmetry.

[5] Note that the dimensions used here differ from the ones assumed in earlier deliverables such as [WIND24], in two ways. 1) The FDD chunk width in frequency has been doubled, since the earlier narrower size contained few symbols and thus incurred a higher pilot and control overhead. 2) In the TDD mode, the chunks have been made shorter. The TDD frame now contains six instead of two chunks. This enables terminals to concentrate their transmission and reception in time, and go into short power saving micro-sleep intervals in-between.

The subsequent main part of the super-frame is shared by the contention-based direct access channel (DAC), the scheduled data channels CDC and TDC, and their related control signalling. It also contains time-frequency-spatial resources that are not to be used, due to interference avoidance constraints. The resource partitioning (allocation) is performed in terms of chunks. It is performed on a super-frame basis but it may be changed between super-frames. The DAC resource is used both for the DAC channel and for the peer-to-peer transmission described in Section 3.2 below. It is organised as a constant set of frequencies over the whole super-frame, to enable the use of carrier-sense multiple access contention based transmission. The resource partitioning is described in more detail in Appendix C.1.1.

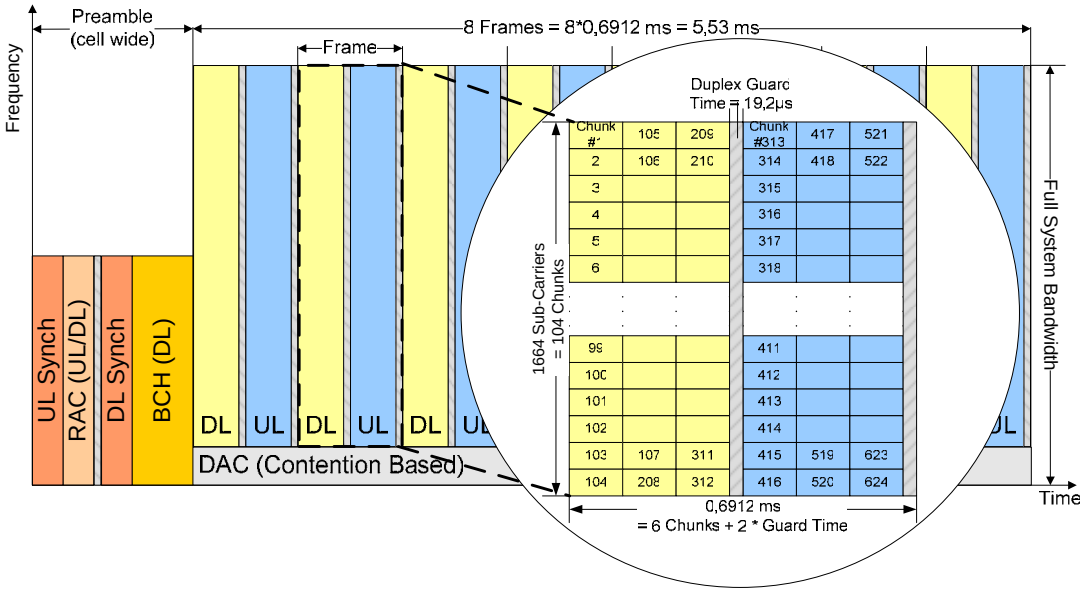

Figure 3.2: WINNER MAC super-frame example consisting of 8 TDD frames with asymmetry 1:1, a preamble and the DAC for contention based peer-to-peer communication. The frame for TDD cellular transmission with its chunk-based substructure has been enlarged.

The super-frame is synchronous in all BS and RN. In the FDD mode, one super-frame is of course required in each of the paired bands. The preamble has the following structure:

- At the beginning of each super-frame there are **two synchronisation slots**, Self-organising synchronisation of terminals and network nodes, as described in [WIND23] and Appendix B.4.1 can be used on a super-frame basis by this design. In the **second slot**, each base station/relay node transmits on four OFDM symbols. The first, the *T-pilot*, is used for coarse synchronisation. In the remaining three symbols, each BS transmits on two adjacent subcarriers, with the others set to zero. On reception, they are used for updating the UT synchronisations. The **first slot** of three OFDM symbols the next super-frame is the *uplink* synchronisation slot. Here, all terminals transmit on the two adjacent subcarriers that were received strongest, i.e. those that were used by the BS/RN closest to them. This part of the iteration is used for self-organizing synchronisation of the base stations and relay nodes, which receive uplink synchronisation symbols from terminals at other BS, that in turn synchronise to those BS. In the FDD mode, the UL synch. slot is in the UL super-frame and the DL synch. slot is in the DL super-frame.
- In-between these synchronisation slots, a short timeslot over the whole band is reserved for the contention-based random access channel (RAC), plus a guard time. This channel enables initial access to a BS or RN. Placing the RAC and its guard time in-between the synchronisation slots gives the RAP sufficient time to process the uplink synch signal and adjust its synchronisation before transmitting the downlink synchronisation signal. The RAC time-slot is in TDD system modes also used for BS-to-BS and RN-to-BS over-the-air control signalling.
- Subsequently, a set of OFDM symbols carries the **downlink preamble control transmission**. It contains the broadcast control channel (BCH) messages from the RLC layer. It also contains a control message that specifies the overall resource allocation used within this super-frame.

3.1.5 Overview of main functions

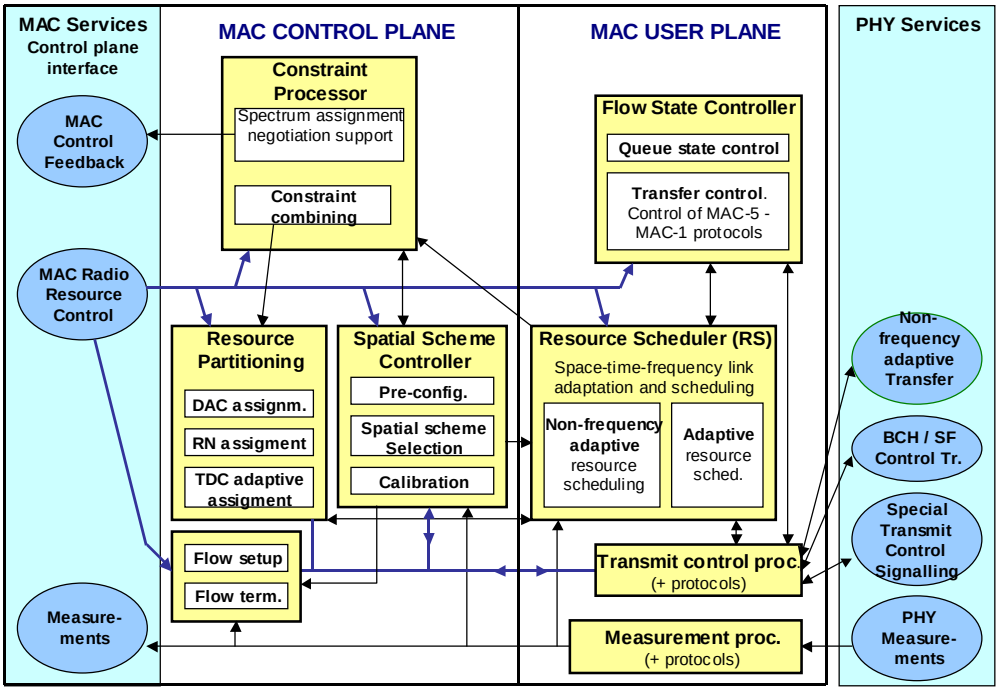

Figure 3.3: FDD and TDD cellular MAC control functions: Services and main function blocks.

The MAC layer is subdivided into a control plane and a user plane. The PHY layer is not subdivided in that way, as all essential control functions for the physical layer reside in the MAC. The main MAC control function blocks are illustrated in Figure 3.3. Control functions that directly control packet transmission on a *slot* time scale reside in the user plane. Slower functions reside in the control plane.

- ***Resource partitioning***. Partitions the super-frame into sets used for adaptive, non-frequency adaptive and DAC transmission, as well as into chunks reserved for use by RNs, BS-to-RN relay links and as guards for interference avoidance with respect to other cells and operators.
- ***Spatial scheme control***. The appropriate spatial transmit scheme is determined for each flow, and it is held fixed within a super-frame. It is influenced by many parameters, including PLM, deployment, transport channel type, cell load, traffic type, BS antenna configuration, terminal capabilities, propagation channel, and interference conditions. Further support functions related to spatial processing, like calibration, are invoked if required.
- ***Flow setup and termination*** performs flow context establishment and release over one hop, supervised by the RRM flow establishment and release functionalities in the RLC system layer.
- ***Constraint processor***. Combines constraints on the use of chunks and chunk layers. These arise from interference between user terminals, interference avoidance scheduling with neighbouring cells and spectrum sharing between operators. The output is in the form of chunk masks that define restricted use of a super-frame's chunks. The constraint processor also processes measurements that support the RRM spectrum assignment/negotiation at the RLC system layer.
- ***Flow state controller.*** Controls the segmentation and FEC coding/decoding of packets and monitors the states of RS queues. It also controls the active/semi-active/passive state of flows.
- ***Resource scheduler (RS).*** Includes adaptive and non-frequency adaptive scheduling algorithms and control of spatial link adaptation. Power control in both uplinks and downlinks is performed under the control of the resource scheduler and is integrated into the optimisation of the transmission parameters. The MAC RS cooperates with the RLS layer flow scheduler, Sect. 4.1.

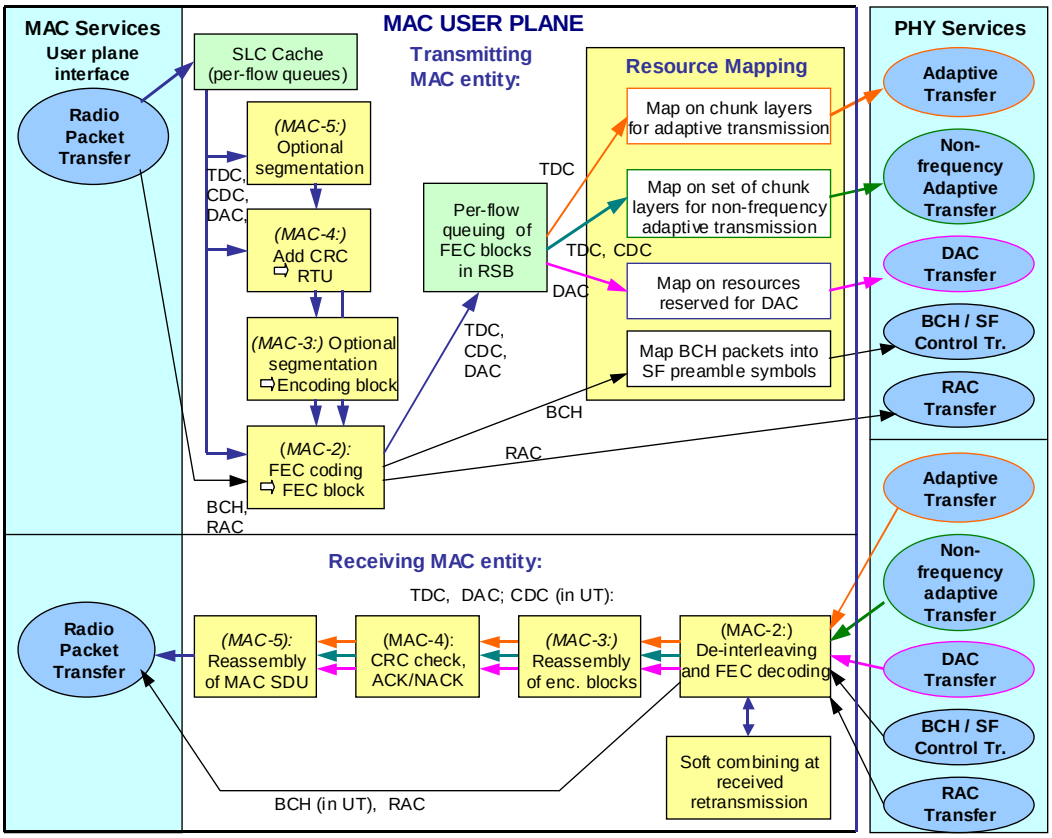

Figure 3.4: FDD and TDD cellular MAC: User-plane services and packet processing.

The data flows in the user plane, shown in Figure 3.4, are processed by three groups of functions:

- ***Transmission: Segmentation, encoding and buffering.*** The flow state controller supervises this sequence. Protocol sub-layers MAC-1–MAC-5 control the transmission and are parameterised to describe the different retransmission options (HARQ). A MAC SDU is drained from the SLC Cache. TDC or DAC packets may be retransmitted. Retransmission can be an option also for CDC point-to-multipoint flows. The TDC, CDC or DAC packet is optionally segmented. A CRC sequence is added, resulting in a Retransmission unit (RTU). The RTU may optionally be segmented into *encoding blocks* that are encoded separately. Coding and interleaving results in *FEC blocks*, which are buffered in the RS buffer on the transmitter side, in one or several queues per flow. There they remain, until acknowledged or dropped. BCH and RAC-packets are transmitted in the super-frame preamble, without retransmission.
- ***Resource mapping***. At transmission, bits from TDC flows are mapped either on chunks reserved for adaptive transmission, or on the sets of chunks intended for non-frequency adaptive transmission. CDC (multicast) flows should use non-frequency adaptive transmission. DAC packets are mapped on the contention-based physical channel. For TDC and CDC, puncturing of the buffered FEC block may be performed and only a part of a FEC block may be transmitted in a scheduling round that comprises a time-slot.
- ***Reception: Decoding and reassembly***. The flow state controller supervises the reception. De-interleaving and FEC decoding is first performed for received FEC blocks belonging to TDC, CDC or DAC packets, followed by the (optional) re-assembly of the RTU. Then, the retransmission unit is optionally checked for transmission errors and a retransmission may be requested. The MAC SDU is finally re-assembled. BCH and RAC packets are received separately in the super-frame preamble and then decoded.

3.1.6 Resource mapping and multiple access

In [WIND26], different *multiple access* (MA) techniques were assessed, for multi-carrier as well as for single-carrier transmission. Subsequently, a set of schemes has been selected as baseline choices for use within the WINNER system. Several of the initially considered schemes turned out to useful. The key distinguishing feature for selecting MA scheme turned out to be not the deployment scenario, but instead the use of *adaptive or non-frequency adaptive transmission*, which place different demands on the utilised resources. The multiple access schemes will therefore differ for different flows.

Flows scheduled for adaptive and non-frequency adaptive transmissions are mapped onto the separate sets of chunks earmarked for these two purposes by the SF resource partitioning (Figure 3.5). The mappings use different MA schemes:

- **Adaptive transmission** (DL/UL) uses **chunk-based TDMA/OFDMA**: Flows are mapped onto individual chunk layers with individual link adaptation per chunk layer. The mapping is exclusive within the cells, i.e. each chunk layer carries data from only one flow.

Chunks are designed to work well for adaptive transmission. See Appendix C.3 for a background on the reasoning used for dimensioning the chunk sizes. In a non-frequency adaptive transmission that is based on channel averaging, there would be a problem in attaining sufficient frequency diversity when transmitting small packets when the packets are mapped directly onto chunks. A small RTU or control packet may fill only one chunk. Two schemes that increase the diversity significantly are selected:

- In **non-frequency adaptive downlinks**, **MC-CDMA** is used within the assigned set of chunks. In the *downlink*, spreading may thus be used to code-multiplex the flows onto sets of chunks assigned for non-frequency adaptive transmission. When code multiplexing is used, spreading is performed only within chunks, to minimise non-orthogonality of the received signals. Orthogonal signalling (TDMA per OFDM symbol or FDMA/IFDMA per subcarrier, without code-multiplexing) are special cases of the scheme. They may be used when appropriate.
- In **non-frequency adaptive uplinks, TDMA/OFDMA is used on an OFDM symbol basis.** For non-frequency adaptive transmission in the *uplink*, code multiplexing is not used, to avoid the need for multi-user detection. Instead TDMA is used on an OFDM symbol basis. Several uplink flows with small FEC blocks may share one OFDM symbol (OFDMA) to improve the rate matching (Figure 3.5, middle part). Either OFDM or frequency-domain generated serial modulation can be used in the uplinks.

Compared to chunk-based OFDMA/TDMA, these schemes provide increased frequency diversity and resources of shorter duration. The shorter time duration (mapping on individual OFDM symbols/GMC slots) provides increased opportunities for terminals to go into power-saving micro-sleep intervals.

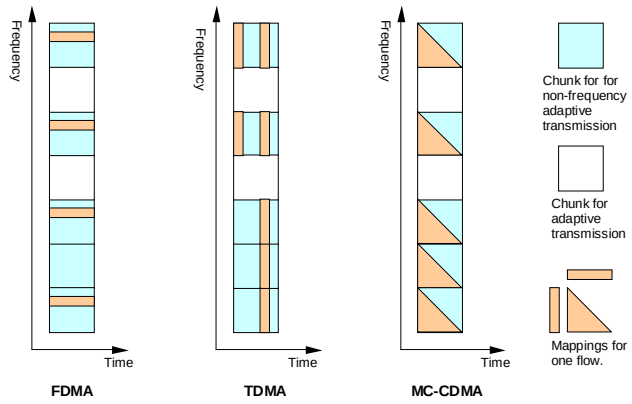

Figure 3.5: Illustration of the mapping of one flow on the chunks earmarked for non-frequency adaptive transmission when using FDMA, TDMA or MC-CDMA within the set of chunks.

The selected multiple access schemes have been evaluated and compared to several alternatives in Appendix G. A summary of relevant results is given below and an additional discussion can be found in Section 5.3.3.

For the case of *adaptive transmission* a gain was, not surprisingly, found when concentrating the transmitted packets to individual chunks, instead of spreading them out over the slot. Spreading them out over all frequencies by e.g. MC-CDMA or TDMA would *average away* the channel variability. Lowering the cannel variability reduces potential multi-user scheduling gain. In Appendix G.4.1 (single-carrier) TDMA that allocates the whole 20 MHz band to only one user is found to result in a reduced multi-user scheduling gain. See also Section 3.1.5.3 in [WIND24] where OFMD-based TDMA was compared to TDMA/OFDMA.

The chunk sizes have been designed to be appropriate for the transmission scenarios used, with reasonably flat channels within chunks. Therefore, as shown in Appendix G.4.3, very little can be gained by *sharing chunk layers between flows* if the throughput is to be maximised. As shown in Appendix G.1.4 and Section 3.3 of [WIND24], chunk sharing can be of advantage in a special case: There are many flows that have the very strict delay requirements and a guaranteed throughput in each slot (0.34 ms). While such delay constraints are extreme for user data, they are applicable for retransmissions and for time-critical control information. Appropriate transmission schemes for these will be studied in WINNER II.

For *non-frequency adaptive transmission*, G.4.2 illustrates the improved performance obtained by paritioning the transmission over a set of resources whose channels have high diversity. As noted above, different methods can be used: MC-CDMA, symbol-based TDMA or subcarrier-based OFDMA. The performance differences between them were investigated and were found to be rather small. Of these schemes, MC-CDMA provides the highest diversity. In Appendix G.1.1, it is concluded that MC-CDMA outperformed OFDMA in terms of cell throughput for all considered loads and scheduling algorithms. In Appendix G.1.2, MC-CDMA provides some advantage while in Appendix G.1.3, OFDMA is found to provide slightly superior performance. Explanations for these differences are discussed in Section 5.3.3.

None of the so far performed investigations added the effect of spatial diversity schemes. It can be expected that the additional use of spatial diversity will lessen the requirement for frequency diversity. This would simplify the resource partitioning problem (Appendix C.1.1), that includes selecting appropriate sets of chunks for adaptive and non-frequency adaptive transmission.

3.2 Medium access control for peer-to-peer transmission

The WINNER system supports peer-to-peer (P2P) and peer-to-multi-peer (PMP) transmission between user terminals under the control of a master device as illustrated in Figure 3.6. The role of the master will be taken by the base station while the terminals act as slaves. All user terminals participating in the peer-to-peer communication are synchronised in time to the master's clock, and use the contention-based direct access channel (DAC) to exchange user data with their peers and control information with the master. In the absence of a BS, a user terminal can also take on the master responsibility if it is equipped with some additional network management functions

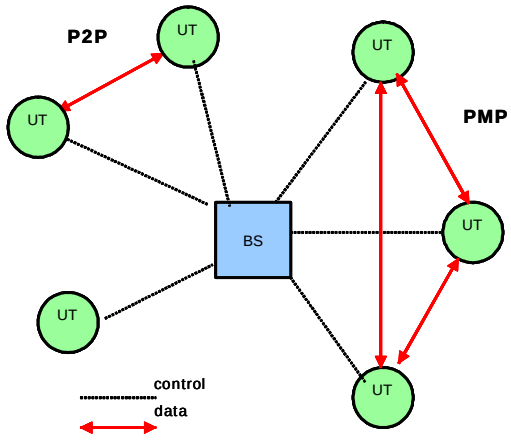

Figure 3.6: Network topologies for peer-to-peer communication.

3.2.1 MAC architecture for P2P transmission

In the WINNER system, peer-to-peer transmission between user terminals is at present designed to be provided by the TDD physical layer mode. Other alternatives will be considered at later stages. In Section

3.1 and Appendix C.1, a MAC is specified for controlling this physical layer in cellular deployment scenarios. Although it supports the exchange of user data between UTs via a base station, it does not allow the direct data transfer between terminals. To enable P2P communication, some new services and functions have to be added to the control- and user-plane of the basic TDD cellular MAC (see Figure 3.7).

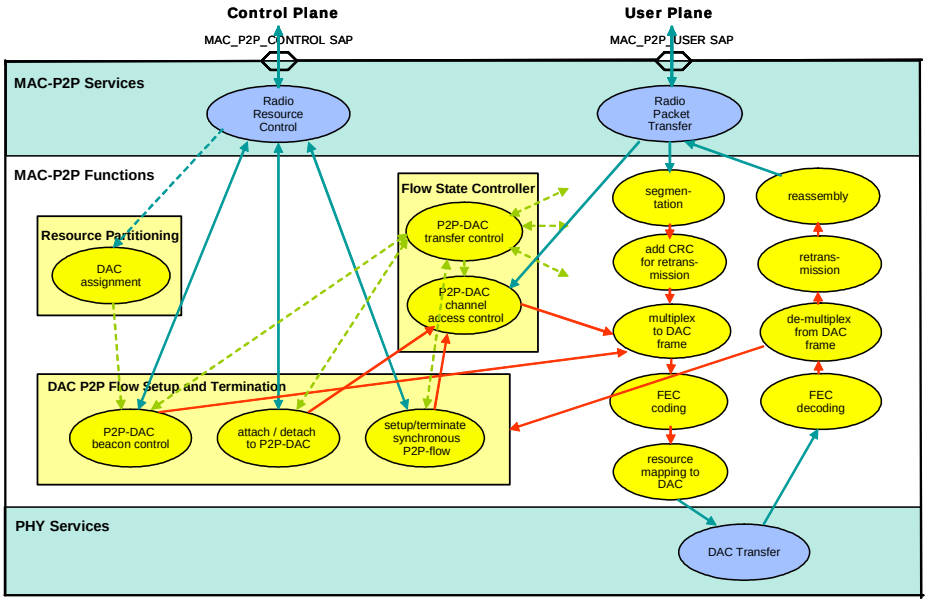

Figure 3.7: MAC services and functions for peer-to-peer transmission

The MAC layer services for P2P transmission are integral part of the *radio_resource_control* and *radio_packet_transfer* service. The P2P-specific services are provided to higher layers at the MAC_P2P_CONTROL and MAC_P2P_USER service access point (SAP).

The MAC layer services are implemented by adding P2P-specific protocol functions to the main function blocks of the TDD cellular MAC. In the control plane of the MAC, the *resource partitioning* unit has to comprise the DAC assignment function for controlling the allocation and release of radio resources. The *flow setup and termination* unit is extended with functions required to setup and terminate P2P data flows over the DAC. These include functions for transmitting and receiving DAC-specific broadcast control information, attaching and detaching UTs to the service provided by the P2P-DAC, and setting-up and terminating synchronous P2P-flows between UTs. In the *flow state controller*, functions are provided for controlling the transmission and reception of radio packets over the DAC. The control of packet segmentation, FEC coding, and retransmission is executed by these functions. The flow state controller also contains functions required to give UTs random access to the P2P-DAC for transmitting control messages to the BS and exchanging P2P data in a contention-based manner between peer terminals. In the user plane of the MAC, additional functions are provided to multiplex control information and user data onto the DAC, and to extract control information and user data from a received decoded radio packet. Note that other MAC functions not directly related to the P2P-DAC service, are not shown in Figure 3.7.

3.2.2 Frame structure of DAC for P2P transmission

The direct access channel is embedded into the super-frame structure of the TDD physical layer mode as shown in Figure 3.2. Successive DAC frames are thus always separated by a preamble that is used to keep time synchronisation between the master and all user terminals involved in P2P transmission.

As shown in Figure 3.8, a DAC frame is further subdivided in three parts, namely the control period, the contention-access period, and the guaranteed-access period. The length of the control period is given by the duration of a TDD DL/UL frame of a scheduled target/common data channel (TDC/CDC). The length of each access period takes on a multiple value of the basic time slot size of 0.3452 ms and may dynamically change from super-frame to super-frame.

- The **control period (CTP)** is composed of two time slots for exchanging MAC control information between the BS and UTs. The first slot is formatted such that, firstly, beacon frames

can be broadcasted from the BS to the UTs to announce the format of the current DAC frame and to communicate management information to the terminals and, secondly, send DL MAC commands from the BS to a dedicated user terminal. In the second time slot, user terminals can send UL commands to the BS and exchange MAC protocol messages with peers. Random channel access for the involved terminals is provided by using a time-slotted ALOHA protocol.

- The **contention-access period (CAP**) may be used to asynchronously transmit protocol messages and/or small amount of user data peer-to-peer between user terminals. Since several UTs can simultaneously access the CAP, the possible contention for medium access is resolved by using a carrier sense multiple access protocol with collision avoidance (CSMA-CA).
- The **guaranteed-access period (GAP)** consists of time slots of fixed length and is used for asynchronous and synchronous P2P transmission between user terminals. Channel access in the GAP of the DAC frame is based on a TDMA method, in which one or several time slots can be allocated to two or more UTs for peer-to-peer communication. For synchronous transmission, time slots are allocated to the UTs on a regular basis in successive DAC frames without limit in time, while for asynchronous transmission, a sequence of consecutive time slots is allocated to start at any arbitrary time instant the transfer of a fixed amount of data. The time slot allocations in the current DAC frame and their usage are broadcasted in the beacon field of the control period.

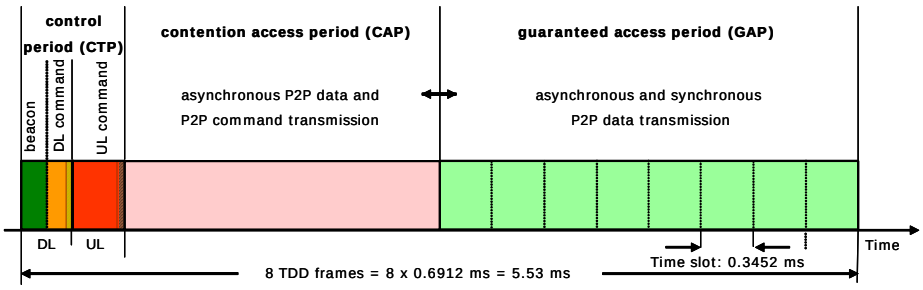

Figure 3.8: DAC frame structure for peer-to-peer transmission.

4. Radio Resource Management (RRM) and Radio Resource Control (RRC)

4.1 RRM functions

Although the term radio resource management (RRM) is often used as a general term for numerous algorithms and protocols used to govern the radio resources, it is in the context of WINNER reserved to denote the control functions implemented in the RLC system layer control plane. Other functions related to management of radio resources, such as scheduling, link adaptation, and power control, were described within the MAC chapter (Chapter 4). The overall goal is to utilise the given radio resources in an efficient manner. The WINNER RRM framework handles flows rather than UTs. A flow is a packet stream from one source to one or several destinations, classified by QoS requirements, source and destination(s). One of the WINNER RRM advantages is that it handles the handover process per flow rather than per UT. Therefore, a UT might send/receive traffic over different cells and routes that match best the requirements of the specific flow. Additionally, it includes functionalities for coordinated spectrum sharing with other radio access networks using the same radio access technology as well as for spectrum sharing with other radio access technologies. Finally, unlike in existing systems, admission control is not responsible for only admitting a new or handover flow to a new cell but also for selecting the best cell among a group of candidate cells that are nominated by the micro mobility functionality. A summary of the RRM functionalities studied herein can be found below while more details are given in Appendix D.

Spectrum control

Spectrum control coordinates flexible spectrum use between multiple WINNER RANs and spectrum sharing with radio access systems using some other radio access technology (RAT). To have more tractable problems, spectrum control is divided into two components, namely, *spectrum sharing* coordinating spectrum sharing with systems using other RAT, and *spectrum assignment,* providing flexible spectrum use between WINNER RANs. Spectrum sharing controls the access to the spectrum in frequency bands, which are shared with other RATs, which are probably legacy systems. Spectrum assignment is divided further into *long-term spectrum assignment* providing slowly varying spectrum assignments for large geographical areas and *Short-term Spectrum Assignment* providing short-term, local variations to the large-scale solution. The detailed implementation of these functionalities remains an open issue, and further development will be carried out in Phase II.

Service level control (SLC)

The SLC performs the management between flows of the same user and/or between different users and is specific for a population of users (e.g. the population within one cell or sector). The SLC provides means to allocate network resources to the traffic associated with the different applications and end-user services (i.e. not radio interface services). The service differentiation is exercised through three different (and parallel) service components, namely *flow Conditioning*, *flow queuing* and *flow scheduling*. The SLC also comprises a *flow monitoring* service component to provide feedback on e.g. load predictions. The *flow scheduling* controls the resource scheduler and the interaction between these two schedulers is assumed to work as follows. The *flow scheduling* should ensure that a sufficient amount of packets are residing in the SLC cache to enable high multi-user gains (i.e. based on predictions about the current rate the *flow scheduling* aims at keeping the overall SLC cache content at some predetermined level, e.g. corresponding to what (on average) may be transmitted within 5 ms). At the same time, the resource scheduler must guarantee that it will (to the furthest extent possible) transmit the packets in the SLC cache within a small amount of time, e.g., in less than 10 ms. Otherwise, the resource scheduler could create head-of-line blocking and too much delay. Effectively, this means that the ultimate decision about if and when (within a few ms timeframe) a packet is transmitted lies with the *flow scheduling* since the resource scheduler sooner or later has to schedule the packets assigned to it. This also means that service classes are transparent to the resource scheduler. Nevertheless, the interface between SLC and RS is still under investigation, e.g. the resource scheduler may also be made aware of the service classes (or at least some priorities of the different flows) to support work-conserving packet pre-emption (i.e. that a higher priority packet can pre-empt the transmission of a lower priority packet destined for the same node) as well as to give preferential treatment of e.g. network control signalling packets.

Mode/RAN selection

Algorithms for the selection of one or several modes/RANs to serve a particular flow/user. The mode selection can be made on different time scales. These include per call or session (slow selection), per packet (fast selection), or triggered by non-traffic related events like changes in radio conditions (mode re-selection). More frequent mode selection leads to larger potential capacity and quality gains (through exploitation of "mode-selection diversity"), but can increase signalling load. In some cases mode selection will require user interaction or be dictated by an application (also referred to as slow selection or even re-selection). The mode selection can either be controlled by a node in the fixed part of the network, a base station, a relay node or by the user terminal. If one operator runs the network, this operator likely prefers network controlled mode selection. If the network is run by different operators, terminal based mode selection is more likely.

Handover

Algorithms for handover between two cells of the same/different mode (intra-system) as well as different radio access systems (inter-system) are studied. In order to allow for a seamless handover within the WINNER RAN, BSs and RNs of the same or different mode can announce their presence to the UTs by broadcasting control messages using orthogonal resources. This scheme is especially helpful for the handover between WINNER FDD and TDD as it allows the UTs to be aware of the presence of BSs and RNs that operate at a different mode without disrupting their normal operation to "sniff" other parts of the spectrum. The case of an inter-system handover between WINNER and legacy RANs is expected to take place either due to loss of coverage of the current system or in case of overlapping coverage due to user/operator preferences or traffic congestion. One solution could be to extend the inter-system handover based on the common RRM (CRRM) framework defined in the 3GPP. Another approach could be location-based handover where user terminals (UTs) make use of foreign measurements and location information. An inter-system handover is performed with the assistance of the cooperative RRM (CoopRRM) entity.

Admission control (AC)

The AC ensures that the admittance of a new flow into a resource constrained network does not violate the service commitments made by the network to already admitted flows. The decision is based on information such as load prediction, statistics of current flows, resource restrictions and physical layer measurements. It is assumed that flow statistics will include:

- throughput per flow, in previous super-frame
- time-frequency-spatial resource use per flow
- spare capacity within cell in previous super-frame
- path loss estimate, and
- interference estimates

In case of limited resources in the candidate cells, a number of different actions may be taken:

- reduce requests for connection/flow in question and/or for lower priority flows
- resource re-partitioning
- lower load in (interference from) neighbouring cells
- handover flows (cell/mode/RAN)
- drop flows.

In the case of multiple RANs and multiple technologies, the admission control must take into account the individual characteristics of each technology in order to make the final decision about admitting or rejecting a user in the network.

Load control

The load control algorithm is triggered in order to ensure that the system is in stable state. It calculates the predicted load per cell based on information such as load prediction, statistics of current flows and resource restrictions. In particular:

- The preventive load control takes care so that the network does not get overloaded and remains stable and attempts to improve the system performance by distributing users/sessions/resources among cells/sectors.
- The reactive load control attempts to bring the load back to stable regions as fast as possible
- The load sharing aims to distribute the load (the offered traffic) and/or resources between "resource owners" (BSs and RNs) such that the resources are efficiently utilised

Potential actions for a "congested cell" are taken. Examples are:

- interaction with the *service level controller* and restriction of incoming traffic
- denial of new flow requests
- change of TDD asymmetry factor
- reduction of requests (e.g. bit rates) for flows (within limits as specified in the flow QoS specification)
- attainment of more resources by resource re-partitioning or lower load in (i.e. lower interference from) neighbouring cells
- handover of flows to another cell/mode/RAN
- dropping of flow(s)

Routing

Algorithms for the selection of the appropriate route/path per flow. It is expected that several paths to a BS will exist due to the deployment of relays. From the architecture perspective, two basic routing strategies are envisioned in multi-hop systems: centralised or distributed. Under the centralised strategy, route determination is performed in a central controller, which normally possesses powerful processing capability and has knowledge on global network status, so that sophisticated routing algorithms could be adopted to optimise the system performance. With the distributed strategy, individual network nodes from the source to the destination jointly perform route determination. This strategy could function when no central controller is reachable, but its performance is normally limited by network nodes' processing capability and knowledge on network status.

4.2 WINNER RRM architecture

As previously described, the WINNER radio interface will encompass a number of modes, each of them targeted and optimised for a specific deployment scenario (and possibly also user scenario). Nevertheless, many of the RRM functions may be shared between the different WINNER modes (e.g. admission control). Hence, the RRM functions could be classified within the three following categories:

1) ***Mode -specific RRM functions***: These are targeted and optimised for a specific mode and deployment scenario in terms of using different parameters specific to the current mode used. In the MAC system layer, they include scheduling, power control, and link adaptation. In the RLC control plane, they include intra-mode handover and routing.

2) ***Generic RRM functions***: These are shared between the different WINNER modes or used for their coordination and include spectrum assignment, service level control, mode selection, buffer management, traffic policing, admission control, congestion control and inter-mode handover.

3) ***Cooperative RRM functions***, which are used for the cooperation of the WINNER system with legacy RANs such as UMTS and WLAN and reside in the Cooperative RRM (CoopRRM) entity. These include spectrum sharing, inter-system handover, admission control, congestion control and RAN selection.

It is very likely that an overlap between the generic and mode-specific RRM functions will exist, where the generic part will administrate the mode-specific part. For efficient management of the resources, the location of the RRM functions within the network architecture is an essential issue as it can affect the performance of the network due to extensive signalling and delays. In a centralised RRM architecture, a central entity monitors and makes decisions regarding the allocation of the resources and it is usually located in a node at the RAN while user terminals have minimal role. For example, in UMTS most of the RRM functionalities are located in the Radio Network Controller (RNC). In addition, terminals and Node B also contribute to parts of RRM, in terms of power and load control. In a distributed RRM architecture the decision entities for each resource management function are located in different nodes including the

user terminal. Furthermore, in a hybrid approach different decision levels of the same RRM functionality that work at different time scales are located in different nodes.

It is envisaged that for the WINNER system with the multiple operating modes, the hybrid approach will be suitable. In particular, extensive delays in the decision making and signalling overload can be avoided by bringing some of the control plane functions closer to the BSs physical nodes. Clearly this adds more complexity to the BSs physical nodes and therefore increases their cost. However, assuming different types of BSs for the wide-area and short-range scenarios, we could restrict the extra functionality to the wide-area BSs (BSwa). In particular, the WINNER vision is that the cells of the different modes will coexist and overlap either completely or partially. This feature could be used in favour of the RRM architecture as the mode generic control plane functions that concern the coordination of the different modes/BSs could be moved to the BSwa, making the BSwa responsible for the control and allocation of resources per wide-area cell including all short-range BSs (BSsr) that fall within its coverage. A requirement for such an approach would be the definition of a communication link between the BSwa and BSsr. This link could be either wired or wireless (e.g. part of the FDD mode interface). More discussion on the RRM architecture can be found in Appendix D.

4.3 Radio resource control

The RRC provides the signalling for these RRM functions, control measurements and reports. Examples of RRC functionalities are:

- Broadcast of information related to the network
- Control of broadcast
- Establishment, maintenance and release of an RRC connection between the UT and WINNER RAN
- Assignment, establishment, reconfiguration and release of PHY resources
- Feature discovery (antenna configuration, relays etc)
- Control of requested QoS
- Measurement reporting and control of the reporting
- Power control (slow)
- Paging
- Initial cell selection and cell re-selection
- RRC message integrity protection
- Timing advance
- Control of synchronisation
- Scanning of PHY resources
- Control of master/slave mode (P2P)

The RRM measurements may be performed regularly, upon request or triggered by some event. To achieve the best possible performance, the time period of the measurements should be chosen such that it may track the variations of the measured quantity. However, since some quantities (like a fading radio channel) undergo not only short-term but also long-term variations, lower measurement frequencies may still be useful. Moreover, the measurement frequency may be adaptive, adjusting the time period according to the variation of the measured quantity. Similarly as for the measurements, the reporting of the measurements can be performed periodically, upon request or be event triggered. The measurement reporting strategy that will be studied further in Phase II, should not be selected independent of the measurement strategy. We may distinguish between the case in which the measurement data itself is reported to the network and the case in which the measurement data is processed in the UT and only a RRM command is reported back to the network. Further details are given in Appendix D.

4.3.1 RRC states

In order for WINNER to be harmonised with the 3GPP LTE work, the same RRC states are proposed.

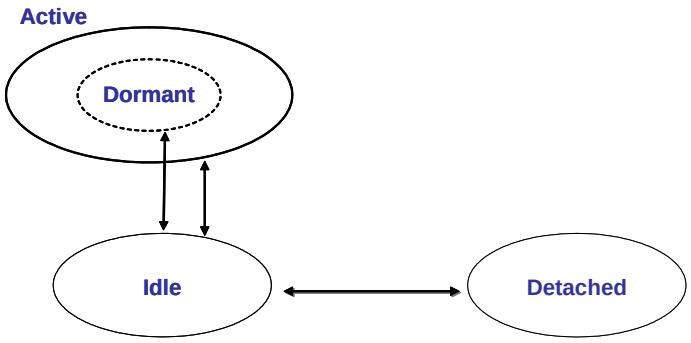

Figure 4.1: RRC states.

These are:

- UT Detached:
  - The location of the UT is not known by the network (e.g. UT is switched off or operating on another RAT system)
- UT Idle:
  - UT performs periodic search for higher priority RAN
  - UT performs cell selection and reselection
  - UT monitors broadcast and paging channels
  - Inherently power saving state
  - UT is handled by radio access network gateway (RANG)
- UT Active (identical to the UTRAN CELL_DCH state [3GPP-TS25.331])
  - UT is transmitting/receiving data on traffic channels
  - UT monitors the directed/common control channels continuously
  - There is a power saving sub-state within the Active state. This is the dormant sub-state where the UT is ready to transmit or receive data on traffic channels and monitors the control channels discontinuously
  - UT is handled by BS

5. Assessment Overview

5.1 General

Assessment of the performance of the developed system concept is an important aspect of the WINNER project. In the case of WINNER, the assessment work has been carried out to some extent by theoretical analysis, but mostly by computer simulations. In WP2 different kinds of simulations are required:

- link level simulations, where the performance of the transmission and reception schemes under study are simulated with the selected fading channel models;
- multi-link simulations, where multiple radio interface links are simulated simultaneously, and thus effects of interference between users can be studied in detail;
- system level simulations, where a coarser view of the physical layer is taken and higher level system functionalities are studied.

At the link level, simulation activities have been focusing on the following topics:

- channel coding schemes
- novel modulation techniques
- channel estimation
- synchronisation
- link adaptive transmission schemes

On the system and multi-link level, the number of simulation alternatives is significantly higher. Emphasis has been put on

- multiple access technologies (TDMA, FDMA, CDMA, SDMA and combinations thereof)
- resource scheduling (frequency/time adaptive or non-adaptive)
- spatial processing
- multi-user detection

In addition, implementation impact in terms of computational complexity and RF requirements are vital to consider. The outline of the rest of this chapter is as follows: In Section 5.2, the main challenges in performing the assessment work are discussed, in Section 5.3, performance results, implementation impact, and performance-complexity trade-offs are discussed, and in Section 5.4, comparisons with requirements and design targets from Section 1.1 and Appendix A are made.

5.2 Challenges

In the assessment work within WINNER WP2 there are two major challenges, discussed in the following along with the strategies used to cope with them:

1. There are a **huge number of details and possible combinations** of different functionalities. In order to carry out a comprehensive assessment of the system concept, all realistically possible combinations would have to be assessed and the associated performance checked. However, for a complex system as WINNER, a fully comprehensive assessment is simply not possible to carry out with any reasonable amount of resources. It is thus important to carefully select the areas on which the assessment work is focused. The broad experience in designing communication systems that the WINNER personnel possesses helps significantly in this focusing, and different partners have taken on to study different key aspects. Also, earlier results in previous WINNER deliverables are reused whenever possible to obtain as broad and accurate assessment as possible of the system capabilities.
2. As different partners provide results, it means that special emphasis needs to be put on the **calibration and cross-verification of the simulation environments**, in order to ensure that system components are modelled in a similar manner in different simulators. At link level, the calibration is a straightforward operation and easy to carry out. In the system level simulators the calibration is a much more challenging task due to significantly higher complexity, larger number of parameters, and larger number of issues (e.g. radio propagation related, traffic

models, functionalities of the system etc.) that need to be modelled. Moreover, the setup of one gigantic system simulator covering all aspects of a system in one study is simply not feasible. Hence, smaller system simulators dedicated to a specific topic studied by a partner can often provide more technical insight. This fact is clearly reflected in the evaluation results in the appendices. Link level results (Appendix F) from different partners are typically jointly presented in the same graphs whenever appropriate, whereas multilink and system level results (Appendix G) from different partners are normally presented in different sections, each with its own topic. A detailed set of common simulation assumptions have been specified (Appendix E) to make the different studies as comparable as possible, but nevertheless, comparisons of absolute system-level performance between different partners cannot normally be directly made, as the results may be sensitive to several details in the modelling approach.

5.3 Summary of results – performance and complexity

This section summarises major findings regarding performance and implementation issues, the details of which can be found in the appendices of the present deliverable (primarily Appendix F and Appendix G) and in earlier WINNER deliverables. It should be noted that many additional results, not directly discussed here, can be found in the deliverables [WIND23], [WIND24], and [WIND26].

5.3.1 Analogue RF

In analogue RF implementation no major showstoppers have been identified. With the assumed SNR requirement of 30 dB, the RF sections of handheld terminals can be constructed using high-end components of today, and the required components are expected to be available for the mass market when WINNER systems are to be deployed. Zero-IF RF architecture seems to be the most promising solution. Power consumption of analogue parts is generally expected to be within acceptable limits, but with some restrictions for the use of higher order modulation schemes in combination with the large signal bandwidths and multiple antenna techniques. However, it is clear that power consumption in user terminals can become a limiting factor, since the development of battery and heat dissipation technologies is not expected to be as rapid as the development of other analogue parts or the digital processing technologies.

The requirements for the asynchronous TDD network (where interference between UL and DL on adjacent carriers may be substantial) with TDMA were found technically unfeasible, taking into account the significant performance degradation and loss of area coverage. To overcome this problem either synchronised networks or channel specific RF filtering should be used. The latter is costly, spectrally inefficient and unattractive to handheld terminals due to large size. Therefore, synchronised networks for TDD operation are strongly preferred.

European and international electromagnetic field (EMF) exposure requirements and standards [HP98][OJEC99][CENELEC01] will be possible to fulfil for user terminals with the uplink output power levels used in the evaluations in this deliverable (200 mW for handheld device and 400 mW for laptop), and with designs and intended use similar to those of existing 2G/3G terminals. With downlink power levels and antenna installations similar to those used for 2G/3G, the EMF exposure requirements and standards [HP98][OJE99][CENELEC02] for radio base stations will also be fulfilled.

5.3.2 Digital baseband

In the following subsections, the different components of a transmitter/receiver chain are first discussed individually. An assessment of the overall link throughput is then provided, followed by a subsection focusing further on multi-antenna aspects.

5.3.2.1 Forward error correction

Decoding of the error control code is typically a dominant factor in the digital baseband processing complexity, especially for single antenna systems. On the other hand, advanced forward error correction schemes based on iterative decoding provide substantial improvements in link layer performance.

In this report, the performance and complexity of two main candidate techniques, DBTC and BLDPCC, have been compared in detail (cf. Appendices B.2 and F.2). The main finding is that DBTC provides best performance when the block length of the code is small, while BLDPCC provides better performance at large block lengths. The threshold block length where the advantage changes from one code to the other depends on the code rate. DBTC show good performance already at block sizes around 100 information bits, so CC might not be required for error control coding in the WINNER radio interface. This is subject of further study. The performance differences are in many cases rather small (<0.5 dB) and other factors

than performance may also affect the selection of coding technique. BLDPCC show slightly lower (maximum) decoding complexity than DBTC – and provides the inherent capability to reduce power consumption when channel conditions are good.

Overall, the assessment showed that even for these advanced coding schemes, decoders are expected to be implementable for data rates of 300 Mbps and beyond (see Appendix B.2.1), in particular given the predicted increase in semiconductor computational power and the advances in parallelisation of decoding techniques. The peak data rates of 1 Gbps can be somewhat challenging not only due to the power consumption but also due to increased clock rates at which the limits of the digital processing hardware (with respect to scaling and clocking limits, current leakage, heat dissipation etc.) become more and more visible. For these reasons solutions like lower complexity codes and even analogue decoding should be kept in mind. Encoding of the error control code is of negligible complexity for all considered coding schemes.

DBTC and BLDPCC represent the state of the art, and such techniques are also under discussion in multiple standardisation activities [3GPP-WG1#42][80211n04][80211n-05][80216e-05], and have in some cases already been standardised [DVB00]. Since basically all advanced coding schemes now come very close to the performance limits predicted by coding theory, the coding schemes in these systems can be expected to have similar performance (and complexity) as those selected for the WINNER radio interface.

5.3.2.2 Modulation

A variety of modulation/demodulation techniques have been investigated and good performance has been found to be achievable with low or moderate complexity already in previous deliverables [WIND21, WIND22, WIND23]. However, the selection of an appropriate modulation technique depends on a large number of aspects beyond complexity and basic performance, as for example flexibility, achievable spectral efficiency, robustness to RF imperfections, requirements on the RF (HPA backoff), and last but not least also on their suitability for implementation of different multiple access schemes and spatial processing methods. Aspects directly related to physical layer performance and RF aspects of modulation schemes have been assessed in [WIND21, WIND22, WIND23], and are therefore treated in less detail here. Based on the assessment of modulation techniques summarised in Appendix B.3.1, GMC transmission configured as CP-OFDM (for DL transmission, and for UL transmission in short-range scenarios) and serial modulation (mostly for the UL in wide-area scenarios) are the preferred options for the WINNER radio interface. See also Appendix G.7.1 for a comparison of single carrier and CP-OFDM on theUL. The employed multiple access schemes are presented in Chapter 3 and evaluated in Appendix G.

CP-OFDM is a well-established technique that is in use in a large number of systems, such as DVB-S, DVB-T and IEEE 802.11 (WiFi). It is currently also under discussion for the use in 3GPP LTE and IEEE 802.16e. Serial modulation/single carrier is under discussion in 3GPP LTE due to its advantages for uplink transmission from (power constrained) user terminals.

5.3.2.3 Synchronisation and channel estimation

The choice of an appropriate synchronisation strategy for the WINNER radio interface is based on several criteria, such as robustness, residual synchronisation offsets, acquisition delay, and required overhead. Two different types of pilots are foreseen for the WINNER system concept: time and frequency multiplexed pilots, in the form of OFDM training symbols and continuous pilot subcarriers, respectively. In combination with cyclic prefix based synchronisation, differential modulation of continuous pilot subcarriers allows to establish frame synchronisation, as well as to detect arbitrary frequency offsets (see Appendix F.4.1 for details). Additionally, a set of *training symbols* are included in the super-frame preamble for self organised inter- and intra-cell synchronisation (cf. Appendix B.4.1). A timing advance strategy is proposed, enabling a time aligned arrival of different users' signals at the BS.

Channel estimation by interpolation in time and frequency based on a *scattered pilot grid* is considered to be an efficient solution for the WINNER radio interface. In Appendix B.4.2 a generic framework for the pilot design of GMC signals is described. The pilot overhead is only 2.5% and 4% per spatial stream for the WINNER TDD and FDD mode, respectively. For multi-antenna transmission, dedicated pilots per flow, common pilots per cell/sector, common pilots per antenna and common pilots per beam are required, depending on the spatial scheme selected. Especially in case of dedicated pilots, purely pilot aided techniques may have severe limitations, requiring a pilot boost and/or a significant degree of over-sampling. Advanced solutions, such as iterative channel estimation, aim to make a pilot boost redundant, at the expense of increased complexity.

Adaptive transmission with respect to resource and physical layer processing requires channel prediction, which can be based on common pilot symbols that are also used for other purposes. Adaptive transmission becomes possible in the WINNER system at vehicular velocities. The channel prediction accuracy estimates (covariances) are furthermore important inputs in the design of the link adaptation and resource scheduling schemes. See Section 3.1 of [WIND24] for their use and impact.

5.3.2.4 Physical layer throughput

The overall link level performance is assessed in Appendix F.1 with throughput simulations for different scenarios and different physical layer parameters. The focus is on the throughput achievable with a standard CP-OFDM system using different modulation/coding schemes; under the assumption of ideal channel estimation and synchronisation. The results are presented for the SISO case both for FDD and TDD, as well as for the 2x2 MIMO case for FDD and the 4x4 MIMO case for TDD. The obtained throughput figures indicate that at an S(I)NR between 20 to 25 dB, a spectral efficiency for the single link of 3 bit/s/Hz is achievable in the SISO case, when considering the WINNER A1/C2 NLOS tapped delay line channel models for the TDD and FDD mode, respectively. For the MIMO case, a link spectral efficiency of 4.5 and 9 bit/s/Hz in the 2x2 and 4x4 MIMO case, respectively can be achieved at a target S(I)NR of 25 dB (using the same channel models).

At a bandwidth of 100 MHz, the target of 1 Gbps at short ranges in isolated cells appears hence to be achievable. For the wide area case, achievable spectral efficiencies (and data rates) depend very much on the interference situation – cf. the multi-link and system level results in the following section.

5.3.2.5 Multi-antenna processing

The spatial processing aspects of the WINNER radio interface concept are described in Appendix B.1. There the mapping of the data bits to the available space-time-frequency resources is described in detail. Impacts of multiple transmit and/or receive antennas to the physical layer (e.g. to synchronisation, channel estimation) can be seen throughout the Appendix B. Use of two antennas in the terminal is envisaged to be the baseline case as it provides substantial gains compared to single antenna at only moderate extra complexity.

As multi-antenna transmission and reception is a fundamental part of the WINNER radio interface concept, assessment results related to it are dispersed over the link- and system-level assessment appendices, i.e. Appendix F and Appendix G. The results verify that multi-antenna processing is one of the key technologies in reaching the stringent targets set for the WINNER system.

Transmit beamforming and receive diversity are essential techniques to ensure coverage and high system throughput in the downlink. Especially in wide-area scenarios with high number of active users fixed beam techniques offer high performance gains with low complexity and control overhead. Average sector throughput increases by up to a factor of 3 for 8 transmit antennas (Appendices G.1.5 and G.2.4). The increased complexity of adaptive beams is easily justified in cases of few active users and SDMA, where substantial sector throughput gain can be observed (Appendix G.2.2), or for delay-sensitive flows (Appendix G.2.1). Given an identical number of antenna elements, spatial multiplexing can be used to increase the user peak data rates (Appendix F.1) at approximately identical sector throughput, i.e. at the expense of reduced inherent fairness (Appendix G.2.4). The use of spatial diversity must always be considered in the context of other sources of diversity already exploited and therefore might provide only marginal additional gain (Appendix G.2.4). Local area scenarios allow applying advanced spatial processing techniques based on short-term CSI and multi-user precoding, like the SMMSE technique developed within WINNER. Initial results in Appendix G.2.5 shows that such techniques have the potential to meet the requirements of 4 bits/s/Hz user throughput mentioned in Appendix A.1.4. From multi-antenna receiver complexity point of view OFDMA is preferred over MC-CDMA (Appendix G.2.3).

In downlinks (Appendix G.2.3, Appendix G.2.4) as well as uplinks, one can note significant gains in throughput when going from one to two antennas at the user terminals. MMSE combination in receivers can be seen to outperform MRC significantly (Appendix G.2.3). The corresponding gain in sector throughput compared to the single receive antenna case is in the order of 35 % for MRC and an additional 15% for MMSE/IRC (Appendix G.2.4).

The receiver complexity increase is considerable when compared to single antenna systems (factor of about 30 for a 4x4 system, when spatial multiplexing is used), but still acceptable when compared to the decoding complexity of error control codes, especially if higher order modulation is considered. The evaluations show that the multi-antenna methods studied are feasible and practical, with some restrictions on in which environments and specific system modes these methods should be used.

For the uplink, base station receive diversity significantly improves sector throughput and enhances user data rates. Performance improves with larger antenna separation and IRC with a lower number of antennas may give similar performance as MRC with a larger number of antennas (Appendix G.5.1). In most of the cases SDMA using single-stream beamforming per user is the best solution to benefit from the spatial degrees of freedom (Appendix G.5.2).

On the total system design there are still several open questions. In particular, the impact of simultaneous use of several complex techniques has not been analysed thoroughly. For example, the concurrent use of different multi-antenna technologies, advanced coding methods, fast link adaptation and scheduling can result in a challenging overall computational complexity, even considering the expected advances in digital processing technologies.

5.3.3 Multiple access

Starting from the initial assessment of multiple access schemes in [WIND26], a further refined assessment has been performed for the most promising candidates by means of multi-link and system simulations. In contrast to previous multiple access oriented simulation campaigns, inter-cell interference, one of the most important aspects when aiming at a frequency reuse one deployment, is now modelled more properly. However, it should be stressed that still many simplifying simulation assumptions had to applied to keep simulation setup and run-time manageable. Some aspects of the results have been highlighted in Section 3.1.6.

Simulation results with focus on comparative or absolute performance assessments of multiple access schemes can be found in Appendix G.1 and Appendix G.4 for downlink and uplink respectively. Regarding the downlink emphasis has been placed in comparing interleaved OFDMA/TDMA and MC-CDMA/TDMA as the most promising multiple access candidates for non-frequency-adaptively scheduled flows. Results obtained in Appendix G.1.1 indicate that OFDMA/TDMA performs slightly worse than MC-CDMA/TDMA if spreading is applied within one chunk only. Spreading within a chunk enables low complex user separation at the UTs without performance penalties due to the flat fading characteristic of each chunk. The decreased chunk granularity allows for a larger frequency diversity gain than with OFDMA/TDMA that explains its performance advantage. If spreading is applied across several chunks as analysed in Appendices G.1.2 and G.1.3, MC-CDMA suffers from imperfect user separation at the UT with increasing load and OFDMA performs similar or slightly better in that case. In addition, equalisation considerably increases the complexity of MC-CDMA for the UT.

Performance assessment of adaptive chunk based OFDMA/TDMA revealed the high multi-user diversity gains obtainable by frequency adaptive resource scheduling. Considering a score-based scheduler that already takes fairness constraints into account, the average cell throughput was increased by a factor of 1.6, see Appendix G.1.1, compared to non-frequency adaptive scheduling. However, no traffic-model specific delay constraints have been taken into account yet since full queues were used as a baseline assumption throughout all simulations.

In a wide-area scenario OFDMA/TDMA/SDMA has been proven to provide large system capacity gains by a factor of 2 compared to pure OFDMA/TDMA with beamforming using eight antennas in both cases, see Appendix G.1.5. Larger gains with more antennas are likely to be achieved. From a complexity point of view adaptive OFDMA/TDMA/SDMA with beamforming supports simple UT receiver processing, without the need for multiple antennas and/or complex multi-user detection.

Regarding the uplink, similar studies were performed including pure TDMA. MC-CDMA was not considered as viable multiple access scheme for the uplink due to the resulting high BS complexity. From the UT perspective TDMA is attractive since it supports the use of single carrier transmission with lower peak to average power ratio and thus higher power efficiency than multi-carrier transmission. In Appendix G.4.1 it is shown, that even TDMA allows for a multi-user diversity gain by adaptively scheduling in time, albeit with much lower performance potential than adaptive scheduling in frequency.

Frequency offset errors among UTs can be suppressed to around 1% of the subcarrier spacing by the UL-DL synchronisation scheme outlined in Appendix B.4.1 and investigated in [WIND23]. Therefore, chunk based OFDMA/TDMA was chosen to be the main multiple access candidate for adaptively scheduled flows in the uplink as well as in the downlink. Moreover, it is highlighted in Appendix G.4.3 that – although theoretically optimal – sharing the subcarriers does not yield any perceivable capacity gain. Hence, adding an additional CDMA component to OFDMA would only increase the system complexity.

Even the synchronisation of a self-organised OFDM network is technically feasible, with a reasonable overhead. If relaying techniques are an integral part of the system design, a single hop network can be extended to a multi-hop network without too high impact on implementation complexity at the user

terminals. On deployment costs no final conclusions can be made yet, since the density of base stations and relay nodes depend crucially on the actual frequency allocation. The restrictions due to the delay introduced by RN's forwarding process, the additional signalling overhead or the combination of duplex schemes at the two links at a RN require a more detailed analysis.

The interference from other cells should be taken into account in the design of multiple access schemes and in the resource partitioning of the super-frame. In frequency reuse 1 networks, schemes for interference avoidance or reuse partitioning between cells (WP3 deliverables, e.g. [WIND32] and [WIND35]), which in effect increase the reuse factor to between 1 and 2, are important for optimising the spectral efficiency. The effect of introducing interference avoidance (RRM) is illustrated in the results of Appendix G.1.2. It should be noted that the delay differences between cells are likely to exceed the OFDM symbol guard intervals. Therefore, reuse partitioning that allocates different sets of frequencies to different cells, e.g. in their outer regions [WIND32], should not be performed without guard intervals in frequency. As illustrated by Appendix G.7.3, the overhead due to such guard intervals can be held at reasonable levels.

5.3.4 Radio protocols

As noted in Chapter 1, system design and protocol specification is an iterative procedure; an initial design is needed in order to select an adequate protocol architecture, which in turn may lead to a refined system design. In Phase I of WINNER, key protocol technologies have been identified and assessed, but the final performance evaluations and subsequent choices for the WINNER RI can only be made when the consolidated and refined system concept is available. Therefore, in the following, we focus on a brief but more general discussion about complexity and overhead aspects of different protocol technologies.[6]

The complexity increase in the design of radio protocols is mainly due to the required measurements, signalling overhead and due to the implementation of baseband processing at the base station. It has been shown that the enhanced MAC protocols can provide high throughput and low delays at a feasible amount of complexity and overhead.

The coordination between base stations is needed particularly in heavy traffic load situations, and will increase performance in medium load situations. A promising framework for inter-cell interference management and integrated load sharing with reasonable balance between performance and complexity is to perform the coordination hierarchically at different time scales, with the lowest level working on the fastest time scale, by assigning constraints on resources to distributed schedulers in the cells. In addition, self-organised radio resource management techniques, which do not require signalling overheads or cause delays, can be used, and are particularly well suited for multi-hop networks where delays can be a problem.

The multi-mode system concept introduces additional complexity both in the design of protocols and associated algorithms, as well as hardware implementation. In general, modularity of system design helps to reduce the computational complexity, but many of the implementation specific issues can be assessed only after the spectrum allocation is known.

5.4 Comparison of performance results with requirements and design targets

In Section 1.1 and Appendix A, a number of requirements and design targets were listed. This section assesses to what extent the present radio-interface concept can meet these targets. This assessment is based on results from all appendices and also from previous WP2 deliverables, but in particular on the multi-link and system-level assessments summarised in Appendix G.

This kind of assessment faces several types of difficulties. First, several of the requirements have to be made more precise before they can be compared in a meaningful way with performance results. Second, one should be very careful when using the present simulations to assess absolute network performance figures. The used models and assumptions are crucial for the outcome. Moreover, at this stage most evaluations/simulations are neglecting many imperfections, e.g., estimations errors and delays. Accounting for these imperfections may have a large impact on absolute performance figures. Still, the results may be used to indicate the performance potential of the technology.

The assessments are based on the following assumptions, summarised from Appendix A and Appendix E.

[6] See WP3 deliverables for first assessments in different deployment concepts.

- **Deployment:** Sites with three sectors (cells), as described in Appendix E, deployed without use of relay nodes. Max. 8 antenna elements per base station sector and (mostly) two antenna element per UT.
- **Duplexing and bandwidths**. Three types of radio bandwidths are considered: FDD with paired 20 MHz and 40 MHz bands and TDD on one 100 MHz band. Data rates per link refer to downlinks in TDD or *half-duplex* FDD, both with activity factor 2 (reception half of the time).
- **Overhead**. The overhead due to guard bands and cyclic prefixes has been taken into account in all simulations. Overhead due to pilots and downlink control signalling has been specified to around 20% in multi-link and system-level simulations, see Appendix E.3.1, and is taken into account in these results. In the link-level results, this overhead is not taken into account and has to be added separately. The MAC layer adds some overhead due to CRC codes, sequence numbers for retransmission units and non-perfectly filled chunks. That MAC overhead has not been investigated and is therefore *not* taken into account below.
- **Restrictions**. Perfect channel estimation will be assumed unless otherwise indicated and the results refer to downlinks. Full queue models are used for the downlink flows.

Requirements stated in Section 1.1.

R3.3: A consistent and ubiquitous data rate per link of 5 Mbit/s above Layer 2.

Assume a single user in the cell of interest and fully loaded neighbouring cells that generate interference. Due to the activity factor for TDD or half-duplex FDD, the requirement corresponds to 10 Mbit/s downlink cell throughput with one user at the cell edge. This requirement is attained without problems in the considered 40 MHz FDD and 100 MHz TDD modes.

For 20 MHz FDD downlinks, relevant investigations are found in Appendix G.2.4 for 700 m cell radius. In the lower left Figure G.16, the CDF value for 10 Mbit/s active radio link rate is around 0.15 for *one BS antenna* and a UT that uses two antennas with IRC. This means that some, but not all, users at the cell edge would attain the performance. Using fixed beamforming with *4 or 8 antennas* at the BS, the target would be attained with high probability, see the lower left Figure G.18. Results for larger cell sizes (not shown) indicate that the requirement can be fulfilled for cell radii above 2500 m, with 8 BS antennas and 2 UT antennas. At least two users at the cell edge (one in each slot of the FDD frame) can thus be provided at least 5 Mbit/s in rural deployment, using the 20 MHz FDD mode.

R3.2: A sustainable average "high end" data rate per link of 50 Mbit/s above Layer 2.

With the same reasoning as above, this requirement corresponds to an active radio link rate of 100 Mbit/s for a user, on average over all locations in the sector.

For 100 MHz TDD, the requirement is fulfilled in short-range scenarios. Considering 40 MHz FDD, by scaling up the results for 20 MHz of Figure G.17 we see that the result becomes attainable by using 8 BS antennas with grid-of-beams or adaptive beamforming and two UT antennas, up to a cell radius of 1400 m, by using non-frequency adaptive transmission based on turbo coding.

For 20 MHz FDD, the goal seems unattainable with non-frequency adaptive transmission. With many users in the cell, adaptive transmission and multi-user scheduling would boost the aggregate sector throughput but this would *not* enable an individual user to attain 50 Mbit/s on average over its location. Thus the larger bandwidths of 40 MHz FDD or 100 MHz TDD seem to be required.

R3.6: Peak spectral efficiency in connected sites of 10 bits/s/Hz in wide area deploym. for high load.

The “peak” spectral efficiency normally refers to the *maximum* sector throughput allowed by the modulation, coding and antenna design. It is therefore not a function of the load of the system. With 3-sector sites, this requirement means 3.33 bits/s/Hz/sector. The 20% downlink overhead margin raises the requirement to 4.16 bits/s/Hz/sector. This figure is attained since 64-QAM transmission is allowed.

R3.7: Peak spectral efficiency in isolated (non-contiguous) sites of 25 bits/s/Hz.

It is noted in Appendix F.1, from the results in Figure F.4 that this goal is attainable with diversity-based 4x4 MIMO in 3-sector sites, but only at high SINRs of at least 30 dB.

R3.12: User speeds ranging from 0–500 km/h should be supported.

The short OFDM symbol length used for evaluation provides reasonable robustness against the effect of channel variability within symbols, but the performance for the highest vehicular velocities and relay links to moving relays in trains remains to be investigated.

The OFDM pilot grid for non-frequency adaptive SISO transmission has been scaled to be appropriate up to 250 km/h (Appendix B.4.2). Speeds up to 500 km/h and the use of beamforming (e.g. following a moving train) would require extra pilot overhead, but no dramatic effects are expected.

R3.4: A maximum delay over the radio interface of 1 ms at Layer 2

The delay over the radio interface is interpreted as the delay from arrival of a packet to the MAC layer to the earliest instance the packet can be received and decoded. With the tightly designed MAC feedback loops, delays of 0.7–1.7 ms are attained, see Appendix C.1.5. The target round-trip delay of 2 ms (Table A.6) can be fulfilled since the decoding time for reasonably sized encoding blocks and retransmission units (at or below 1520 bytes) should be 0.1 ms or below, according to Table B.2.

ITU-R: 100 Mbps peak aggregate useful data rate for mobile access.

This is a data rate as seen from the base station, not the individual terminals. It is here interpreted as the cell/sector throughput. Thus, the terminal activity factor does not affect the assessment.

This data rate is difficult to attain using 20 MHz FDD. It could be attained in a rural site with many users in the cell by using max. throughput scheduling and SDMA with four beams, see upper left part of Figure G.10. However, that strategy would starve users not located close to the BS. A better indication of the attainable performance for 20 MHz FDD downlinks are the 75 Mbps attained in Figure G.10 when using proportional fair scheduling and SDMA with four beams.

With many users in the cell, experiments with adaptive beamforming in Appendix G.2.1 (that use all 512 subcarriers) provide CDF curves in Figure G.11. They show that the goal is almost attained when using the Tracking/PSF mean-approach. The average data rate with 416 subcarriers would be (416/512)*110 Mbps = 89 Mbps with 60 users per 1-km cell, 8 BS antennas, 1 UT antenna. Note that with many users per sector, the average throughput per user would of course be much lower (right-hand Figure G.11).

ITU-R: 1 Gbps peak aggregate useful data rate for local area.

The results in Appendix G.2.5 indicate that this target is attainable even when channel estimation errors are considered, but only in short-range cells (50 m range) with MIMO links that use large numbers of transmit antennas and four receiver antennas.

Design targets stated in Appendix A.

Throughput per link targets for rural and metropolitan area deployment.

The target 1 bit/s/Hz corresponds to 40 Mbps on active links on 20 MHz half-duplex. It can be regarded as fulfilled when using 20 MHz FDD up to 2.5 km cell radius, if we have only one user per sector. See Appendix G.2.4, Figure G.17. The target 0.5 bit/s/Hz (at 70 km/h) was found to be attainable in Appendix F.1.

Results in Appendix G.1.1, G.1.5, G.2.1 and G.2.2 show that the requirements for low and medium terminal velocities are well fulfilled with multiple users per cell, in particular when using multiple antennas. Terminal velocities of 250 km/h have not been evaluated.

Throughput per link targets for local area deployment.

The target high-end throughput per link of 4 bit/s/Hz per sector is attained for the A1 LOS and A1 NLOS channel models at 50 m distance, according to Appendix G.4.3. It is also attained for the B1 LOS channel model for 10 users all being at 150 m distance with OFDMA maximum throughput scheduling. It is not attained at 150 m with a B1 NLOS model. These results are for adaptive uplinks.

6. Conclusions and Outlook

An overview of the current status of the WINNER radio interface concept was presented in Chapters 1–4, with an emphasis on novelties compared to existing systems. Throughout the work, design and functionalities that allow or facilitate operation in shared spectrum and interoperation between WINNER networks and different RATs deserved special focus.

The design view was consistently used in this deliverable, motivated by its focus on the lower layers and the need to enable direct assessments in terms of performance simulations and implementation impact analysis. Service and protocol views and more information on higher layers can be found in the final deliverables of WP7 and WP3. An overview of simulations investigating different system components as well as the whole system was given in Chapter 5. Also, comparisons were made with requirements from [WIND71] and other design targets defined within WP2. It was concluded that with reasonable assumptions about missing information (yet to be determined by political, legal, economic, and other factors and decisions), and within the uncertainties of the simulations, these requirements and design targets could be fulfilled. The analyses of implementation impact in this and previous deliverables revealed no major critical issues that would prevent a cost-efficient implementation of the system at the time of deployment in 8–10 years. More technical detail, both regarding concept and assessments, is provided in the appendices and in earlier deliverables.

An important objective of Phase II is to further enhance and refine this initial concept to a level of detail needed to build a prototype within the project, and to serve as input to the standardisation process that is expected to follow after World Radiocommunication Conference 2007 (WRC-07).

Appendix A. Requirements and Design Targets

This appendix presents design targets for different scenarios as discussed in Section 1.1. A few scenario-independent targets and general assumptions about spectrum etc are also listed at the end.

A.1 Targets for different scenarios

A.1.1 Scenarios

Depending on the scenario being considered, different subsets of the system requirements will be relevant. In the following discussion we therefore distinguish between the three application scenarios that have been identified for WINNER (respective characteristics listed in sub-bullets):

- Rural area
  - medium traffic demand
  - cellular; large cells
  - range (coverage) issues
- Metropolitan area
  - high traffic demand
  - cellular; midsize cells
  - range (coverage) issues (to some extent)
- Local area
  - high data rate demand, high traffic demand
  - cellular/isolated cells/peer-to-peer; small cells
  - indoor/outdoor

Rural area and metropolitan area will sometimes be referred to collectively as examples of "wide-area" scenarios. Similarly, local area will sometimes be referred to as "short range". For each scenario, technical targets will be summarised in the following sections.

A.1.2 Rural area

In the rural-area scenario, coverage and high UT speeds are the main challenges for the radio interface. Cell radii of 2 km and more will likely be desirable. The system requirements state an average cell throughput of 50 Mbit/s in 100 MHz bandwidth, and a cell border (ubiquitous) throughput of 5 Mbit/s. Either FDD paired bands or TDD may be used; half-duplex is assumed for terminals also in the former case for complexity reasons. For maximum efficiency, frequency 1-reuse is generally assumed, but techniques discussed in e.g. Section 5.2 in [WIND32] may be used to create a higher effective reuse for users at the cell border. The bit rates mentioned here will only be possible to guarantee at low and moderate speeds, cf. [WIND24] and Appendix B.5.2.

Requirements on downlink are summarised in Table A.1. All bit rates refer to throughput above the MAC layer, and full queues are assumed. The cell range is only introduced as a reference point for the throughput values, and the actual coverage areas might be different (at the expense of reduced throughput per link). For the uplink, the lower output power of the terminal will reduce the possible bit rates, see Table A.2. Dual-antenna terminals are considered to be the baseline case. Relaying may be needed to reach the tabulated targets; the feeder links connecting base station and relay node are then normally assumed to use the same spectrum.

Table A.1: Targets for Rural Area (Downlink)

Reference cell range	UT velocity	Throughput per link (cell average, single user in cell)
2 km	0 km/h 70 km/h 120 km/h 250 km/h	1 bit/s/Hz 0.5 bit/s/Hz 0.5 bit/s/Hz 0.1 bit/s/Hz

Table A.2: Targets for Rural Area (Uplink)

Reference cell range	UT velocity	Throughput per link (cell average, single user in cell)
2 km	0 km/h 70 km/h	0.1 bit/s/Hz 0.05 bit/s/Hz

A.1.3 Metropolitan area

For metropolitan area, spectral efficiency and inter-cell interference become more important considerations, whereas extremely high UT speeds are less common. Coverage may sometimes still be an issue, but the maximum cell size is smaller than for the rural-area scenario, and the performance difference between UL and DL is typically expected to be less significant. Relays may be needed also in this scenario. In order to maximise spectral efficiency, MIMO, preferably with fast feedback, will likely be an important feature. Requirements are summarised in Table A.3. The throughput is given per link, and with 3-sector sites and half-duplex for the UT it should be multiplied with 3×2=6 to obtain the corresponding value per site.

Table A.3: Targets for Metropolitan Area (Downlink)

Reference cell range	UT velocity	Throughput per link (cell average, single user in cell)
1000 m	0 km/h 70 km/h	1 bit/s/Hz 0.5 bit/s/Hz

A.1.4 Local area

Local area communication includes cellular systems as well as non-contiguous (isolated) sites and peer-to-peer communication. In the cellular case, the short-range requirements in Table A.4 apply. For non-contiguous cells, inter-cell interference is not an issue, and the highest spectral efficiency, 25 bits/s/Hz/site should be achievable. With 3 sectors and half-duplex this corresponds to approximately 4 bits/s/Hz/link (see Table A.5).

Table A.4: Targets for Local Area (Cellular)

Environment	Reference cell range	UT velocity	Throughput per link (cell average, single user in cell)
Outdoor	100 m	<10 km/h 50 km/h	1 bit/s/Hz 0.5 bit/s/Hz
Indoor	30 m	<10 km/h	1 bit/s/Hz

Table A.5: Targets for Local Area (Isolated Cells and Peer-to-Peer)

Environment	Reference cell range	UT velocity	Throughput per link (cell average, single user in cell)
Outdoor	100 m	<10 km/h	4 bit/s/Hz
Indoor	30 m	<10 km/h	4 bit/s/Hz

A.2 Additional targets

To be able to handle new delay sensitive applications and link adaptation efficiently it is essential to have a low delay over the radio interface. The targets of Table A.6 are assumed.

Table A.6: Delay targets

Basic radio interface delays (physical layer, single hop) –Round-trip time	< 2 ms
Packet channel establishment (minimum) – UT originated – BS originated	< 5 ms < 2 ms
RAN-UT-RAN delay	4 ms

A.3 System assumptions

The preferred spectrum range for WINNER systems is below 6 GHz, and for research purpose the target band is 3.4–5.0 GHz. A bandwidth allocation of 100 MHz per carrier should be seen as an upper limit. Such wide bands are not feasible in the current mobile bands; therefore new bands should be identified. The defined target bands are among the current candidate bands in ITU.

Operation in spectrum shared with other operators that use the same physical layer WINNER mode will be an integral part of the design. Operation in dedicated bands is seen as a special case of this situation. Operation in isolated cells will be seen as a special case of cellular transmission (see also Appendix A.1.4).

Appendix B. Physical Layer

The purpose of this chapter is to provide more detail on the assessment of different physical layer candidate technologies, which eventually lead to the design decisions presented in Chapter 2 of this report. It also gives the rationale behind the parameterisation of different system components, if not yet provided in previous deliverables [WIND23].

Appendix B.1 contains a detailed description of the generic WINNER spatial processing framework, along with some example configurations of it. The provided figures illustrate in more detail the structure of the space-time-frequency processing sub-block of the generic transceiver architecture depicted in Figure 2.1 of Chapter 2. Extending on the framework for the assessment of coding techniques from [WIND23], Appendix B.2 provides a detailed comparison of the most promising FEC schemes considered for the use in WINNER: Duo-Binary Turbo Codes and Block-LDPC Codes. Appendix B.3 presents a short comparison of the different modulation techniques investigated during WINNER Phase I [WIND21, WIND22, WIND23]; as well as a short summary of their merits and drawbacks. Afterwards, Appendix B.4 covers the topic of pilot design for channel estimation and synchronisation. The WINNER plot grid is presented, including a discussion of different core requirements for channel estimation (chunk based channel estimation, extension to the MIMO case, etc.). Finally, Appendix B.5 contains information related to link adaptation: a comparison of different bit- and power loading algorithms, details on the prediction horizons for channel quality prediction; and methods for the compression of feedback for channel state information.

B.1 Spatial processing and space-time-frequency mapping

Figure B.1 shows a generic transmitter chain implementing the WINNER multi-antenna concept[7]. The segmentation stage shown corresponds to the *MAC-3 sub-layer* introduced in Section 3.1.5, which allows splitting one RTU into k encoding blocks that undergo individual forward error correction FEC_k and interleaving Π_k. Spatial reuse of a chunk adds a third dimension, referred to as a *chunk layer* and presented along the vertical axis of Figure B.1. The (maximum) number of layers l in chunk c, denoted Q_c, can be different for different chunks. The mapping of FEC blocks to chunk layers is performed by the ***resource scheduler***. In adaptive transmission, each chunk layer carries data from one flow only. In non-frequency adaptive transmission, code-multiplexing may be used in downlinks. The chunk layers may stem from the different RTUs of different flows in the case of SDMA, or from the same flow in case of per stream rate control and multi-level coding. Note that the number of layers in a chunk may be arbitrary in relation to the number of physical antennas, denoted M_T.

The bits of chunk layer c,l are first modulated onto S_c *modulated layers*. The number of modulated layers is inferior or equal to the number of chunk layers, $S_c \leq Q_c$. Typically they are equal; that is, each chunk layer is modulated independently. However, for the case of multi-level coding, several chunk layers are modulated onto the same modulated layer. The modulated layers are then subject to an optional non-linear precoding[8]. The precoded modulated layers are then dispersed onto *virtual antenna chunks* with a dispersion code. A *virtual antenna chunk* is a three-dimensional entity which spans M_T virtual transmit antennas in space, n_{symb} OFDM symbols in time, and n_{sub} subcarriers in frequency. To simplify the presentation it is assumed that the number of virtual antennas is equal to the actual number of physical antennas. If the underlying dispersion code encodes the signal over less or more dimensions, appropriate zero padding and puncturing in the spatial dimension is assumed. Typically, a linear dispersion code is assumed, but by allowing non-linear dispersion codes, also schemes such as various forms of space-time/frequency trellis-coded modulation may be represented in the generic processing [WIND21, WIND23, WIND26, WIND27].[9]

[7] Figure 2.1 shows the overall transmitter structure. Here, a detailed view of the spatial processing (SP) block in Figure 2.1is given (GMC and pilot insertion aspects are neglected for readability).

[8] The non-linear precoding proposed in [WIND27] is based on Tomlinson-Harashima precoding; however, the non-linear precoding block can also include more general lattice coding techniques. Such techniques allow approaching the optimal dirty paper coding, and can be used to improve the performance of a MIMO single link.

[9] If some form of coding and modulation is performed by the dispersion code, the outer code is probably relatively weak and the modulator essentially bypasses the encoded bits.

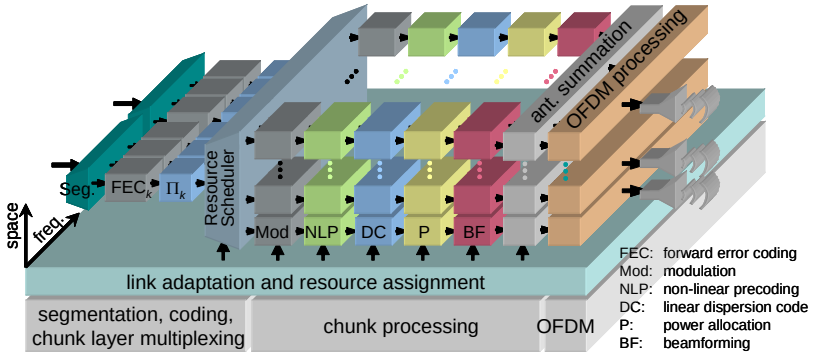

Figure B.1: Overview of the generic PHY processing chain.

The virtual antenna chunk of each layer is then subject to power allocation and linear precoding which means that each virtual antenna chunk of each layer is mapped onto a physical *antenna chunk*. Each element of the three-dimensional antenna chunk is a linear combination of the elements of the layer's virtual antenna chunk. The term linear precoding covers techniques such as closed-loop transmit diversity, linear multi-user precoding and long-term beamforming, and also antenna or beam selection and hopping as well as random beamforming that may be employed by opportunistic beamforming approaches. For cases with multi-user optimisation, the linear precoding and the power of virtual antenna chunks are optimised jointly. Finally, the layers' antenna chunks are summed over the antennas to form a three-dimensional antenna chunk, which is passed to assembly and OFDM modulation per antenna.

The MAC function ***spatial scheme selection*** and ***link adaptation*** will select and configure the blocks of this generic chain to implement the most favourable spatial processing scheme for each flow. A few illustrative example configurations are given in the following. In case of open-loop space-time coding (using an LDC, e.g. the well-known Alamouti-code) all data undergo identical FEC and modulation. The LDC then maps the symbols onto the antenna chunk (Figure B.2). For PARC, however, segmentation is performed first to allow for individual FEC and modulation of the sub-flows which are mapped to different chunk layers (Figure B.3). Figure B.4 shows the processing for SMMSE, where the LDC implements purely a multiplexing onto virtual antenna chunks. The power allocation and linear precoding (BF) is then optimised across all SDMA users according to the SMMSE algorithm [WIND27].

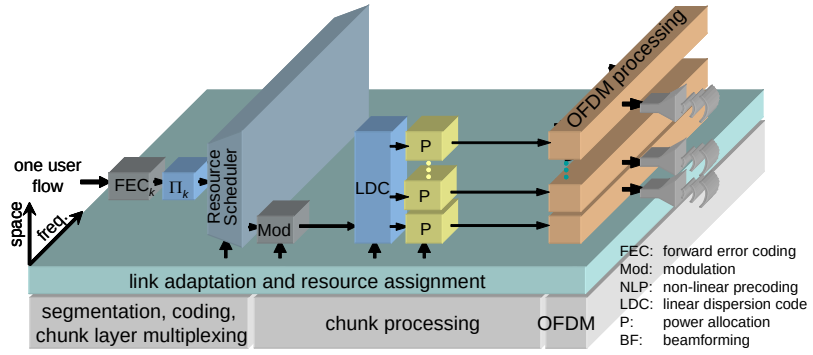

Figure B.2: Example configuration for open-loop space-time coding.

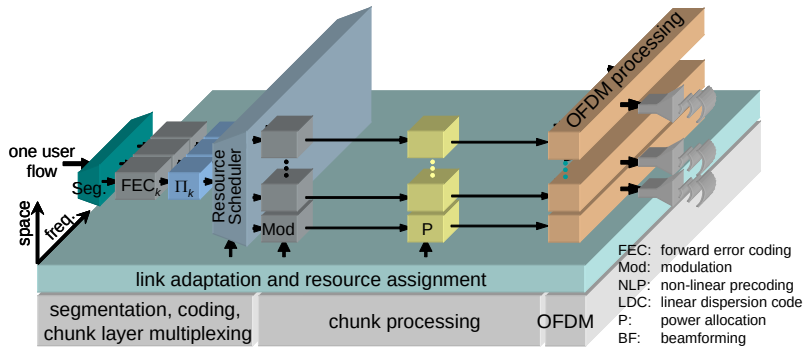

Figure B.3: Example configuration for PARC.

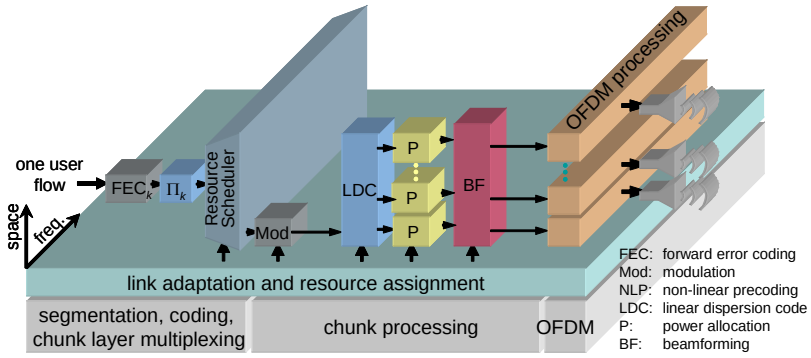

Figure B.4: Example configuration for SMMSE.

Apart from the generic processing chain and example configurations, a lean baseline configuration is defined, which serves as basic implementation guideline and benchmark. It is based on the following simplifications:

- no segmentation (*MAC-3 sub-layer*), i.e. one RTU is encoded as a single FEC block,
- independent processing of each chunk layer, i.e. each modulated layer stems from a single chunk layer,
- no non-linear precoding,
- linear dispersion codes, that generate a set of virtual antenna streams out of each chunk layer,
- pure spatial linear precoding (beamforming), i.e. for a given chunk layer c,*l,* symbol *t,* and subcarrier *f* the elements $\mathbf{x}_{c,l}(t,f)$ of the antenna chunk are obtained by

$$\mathbf{x}_{c,l}(t,f) = \mathbf{F}_{c,l}\mathbf{a}_{c,l}(t,f),$$

where $\mathbf{a}_{c,l}(t,f)$ is an $M_T \times 1$ column vector holding the corresponding element of the virtual antenna. Note that $\mathbf{F}_{c,l}$ is identical for all symbols within one chunk layer and each column of $\mathbf{F}_{c,l}$ can be viewed as transmit weight vector.

Relaying is an integrated part of the WINNER system. Investigations that combine relaying and spatial processing have been performed in [WIND27]. It has been shown that FRN based on decode-and-forward can benefit from different kinds of spatial processing. In-depth investigations and system design that tighly integrates relaying and spatial processing are foreseen in Phase II including more sophisticated concepts, like cooperative relays [AY05].

B.2 Forward error correction

A large number of possible options for forward error correction have been identified and discussed in [WIND21]. With the advent of iterative decoding, very powerful concatenated error correction schemes have been devised which exhibit a decoding complexity that is linear in the block length – a key requirement for inclusion into any practical wireless communications system. Of the plurality of possible concatenated codes, parallel concatenated convolutional codes and low-density parity-check codes have been selected as main candidate technologies, as they showed the best trade-off between performance and implementation complexity. Of these two general classes of codes, Duo-Binary Turbo Codes and (Quasi-Cyclic) Block LDPCC (QC-BLDPCC) are considered for the use in the WINNER system, since they provide the necessary amount of flexibility in terms of block lengths and code rates. However, iterative decoding schemes suffer from quite low performance at short block lengths. Therefore, convolutional codes are used with short block lengths below 200 information bits. The domain of suitability (for a target BLER of 1%) of all candidates is summarised in Figure B.5 below (cf. Appendix F.2 for details):

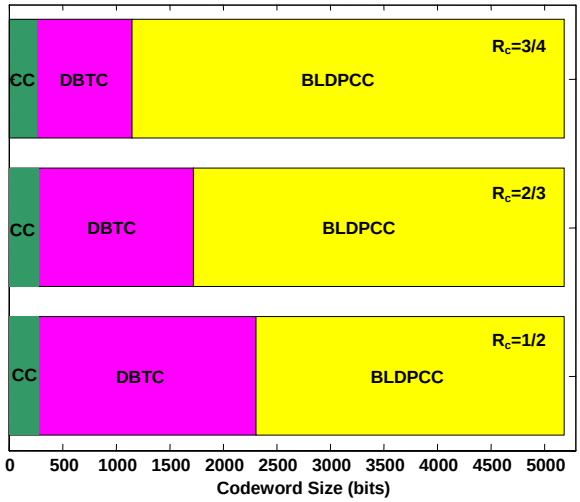

Figure B.5: Domain of suitability of DBTC and BLDPCC for a target BLER of 1%.

Table B.1 summarises the assessment of these three candidate technologies:

Table B.1: Assessment of the most promising FEC techniques

		CC[10]	DBTC	BLDPCC
Performance[11]	Short blocks	-	<0.5 dB	<1 dB
	Medium blocks	<1–1.5 dB	-	<0.2–0.4 dB
	Large blocks	<2–2.5 dB	<0.2 dB	-
Memory Requirements	Code structure	Very low	Low	Medium
	Decoding	Low	Medium	Medium
Encoding complexity		< 10 ops/info bit		
Decoding complexity		~ 2500 ops/info bit	<1700 ops/info bit	<1200 ops/info bit
Maturity		High	Medium	Medium

[10] Memory 8 convolutional code, soft Viterbi decoding

[11] Loss with respect to the best technique at codeword sizes 50, 576, 4308 bits (AWGN, BPSK, target BLER 1%)

DBTC show very good performance already at quite low block sizes (around 128 information bits) and may eventually be used instead of CC in such scenarios. LDPCC are favoured over DBTC for large block sizes due to their superior error correction performance in this regime (lower required bit SNR to achieve BLER of 1% [WIND23]). All codes show the same high degree of flexibility in terms of block sizes and code rates (cf. Appendix B.2.1) and support the construction of rate compatible code sets (cf. Appendix B.2.2). It should be emphasised that the impact of selection of one or another of the proposed FEC technique on the overall system concept is rather limited, as soft-input soft-output versions of decoder algorithms exist for all investigated techniques – the en-/decoding sub-blocks can hence be regarded as a "black box" by the rest of the system.

B.2.1 Implementation issues: flexibility, parallelisation, throughput

An important practical issue when dealing with coding schemes for adaptive radio interfaces is the flexibility in terms of block sizes and code rates. One typical way of constructing good LDPCC is to first optimise the error correction performance of the *code ensemble* for the target code rate (e.g. optimise the degree distribution using EXIT chart analysis) and then generate one *specific code* using construction algorithms that ensure low error floors (e.g. the progressive edge growth algorithms) . The disadvantage of this approach (for practical implementation) is that a new code needs to be designed for each block length and rate. Structured LDPC codes, and especially Quasi-Cyclic and Block LDPC Codes [MY05, MYK05] on the other hand have been shown to have good performance and high flexibility in terms of code rates and block sizes at the same time. The general idea is to base the construction of the LDPCC on different basic elements, usually shifted and/or rotated versions of the identity matrix. Adaptation to different block lengths is easily done by expanding elements of the basic matrix (e.g. by replacing each "1" in the parity check matrix with an identity matrix and each "0" with an all-zeros matrix). Different code rates are obtained by appending more elements to the matrix in only one dimension (i.e., add more variable nodes, but no check nodes). The decoder must obviously be designed to support such changes of the code structure. The inherent parallelism of LDPCC is then exploited by allocating Variable Node Units (VNU) and Check Node Units (CNU) to groups of variable and check nodes, respectively, for processing of the decoding algorithm. The degree of parallelism is dictated by the number of elements in each unit. The throughput of such a semi-parallel decoder architecture can be expressed as follows:

$$D = n_b \cdot R_c \cdot \frac{P}{IT + P/z} \cdot F_{ck} \tag{B.1}$$

where F_{ck} denotes the clock frequency, $(n_b.m_b)$ are the dimensions of the base model matrix, R_c is the code rate and IT is the iteration number. The degree of parallelism P is bounded as $1<=P<=z$, where z is the expansion factor. Note that in this architecture, the total number of VNUs and CNUs is $P \cdot n_b$ and $P \cdot m_b$, respectively [LZ05]. Current technology does not allow yet exploiting this degree of parallelism in full at reasonable cost. Nevertheless, the flexibility of such architectures is quite attractive from a design point of view, as it allows to scale and to tune the hardware cost very easily depending on the target throughput. Such semi-parallel architectures are currently being investigated throughout the whole industry (some first complexity estimates can be found in [ZZ05]). As always when dealing with LDPCC, the number of iterations IT can vary between an average number required for convergence, and a maximum number which represents the worst case decoding delay (and strongly influences the error-correction performance).

Duo-Binary Turbo Codes [WIND21, WIND23] differ from classical PCCC by the fact that the information bits are encoded pair wise. The internal inter-leaver is based on an algorithmic permutation, defined by a single equation. This PCCC can hence be adjusted to any frame size by modifying only four values which parameterise the internal interleaver, implying a high flexibility of this type of PCCC. As the mother code rate of the Duo-Binary Turbo Code is ½ (instead of 1/3 for classical PCCC) it is inherently more robust to puncturing. Duo-Binary PCCC not only achieve very good performance for long block lengths, but also perform well at smaller block sizes and have been standardised in DVB with block lengths as small as 128 bits. The performance has also been improved at low error rates, thanks to the improved internal interleaver. The decoder can be designed to decode 2 information bits per clock cycle and its throughput can hence be obtained by means of the following relation:

$$D = \frac{P}{IT} \cdot F_{ck} \tag{B.2}$$

The throughput is independent of the code rate, as code rates higher than 0.5 are obtained by puncturing.

For the throughput analysis we consider a clock frequency F_{ck} of 200 MHz to be achievable, which corresponds to a technology of 0.13 µm and beyond [THB04]. By tuning the degree of parallelism P and the (maximum) number of iterations IT, we can match the requested decoder's throughput to the system requirements. Table B.2 below summarises the achievable throughput exemplarily for the case of a code raet R_c=0.5:

Table B.2: Achievable throughput for rate 0.5 DBTC and BLDPCC (200 MHz clock frequency)

Code	Parallelism level	Number of iterations	Bit rate (decoded Mbits/s)
DBTC	6	8	150
	12	8	300
	4	5	160
	8	5	320
BLDPCC	2	50 (flooding schedule)	192
	4	50	384
	1	20 (shuffled decoding)	240
	2	20	480

It can thus be concluded that a parallelism level of 12 for DBTC (when using 8 internal decoder iterations) and 4 for BLDPCC (using a standard flooding schedule and corresponding to 192 VNUs and 96 CNUs) is sufficient to achieve a throughput of 300 Mbps (and beyond). We conclude that both coding candidates can offer a suitable throughput. It is, however, known that the inherent parallelism of BLDPCC can be attractive from a designer point of view, as it allows tuning whole hardware/software implementation to the cost and performance constraints. Although very high data rates are theoretically achievable by BLDPC decoders, technology constraints still limit the degree of parallelism affordable, and thus the data rates. To give the full picture, the respective gate count (and thus area estimation) for DBTC and BLDPCC need to be considered. As these figures depend very much on the target architecture and a number of other parameters, this assessment will be done in the next phase of WINNER.

B.2.2 Rate compatible code sets for HARQ-II

Hybrid automatic repeat request (HARQ) schemes combine the reliability of FEC with the throughput of ARQ. Especially type II HARQ schemes, also denoted as *incremental redundancy* (IR), provide an improved throughput and have for example been successfully employed in HSDPA. To construct an efficient IR scheme, a set of *rate-compatible* (RC) codes is needed. This is a sequence of nested codes providing a range of different code rates. It can be constructed, e.g., by puncturing a low rate mother code. A special case of IR is *chase combining,* where the FEC codeword is repeated and soft combining is applied to the received code bits. This is equivalent to using an outer repetition code (e.g. by additional spreading, cf. [WIND23]), which can be used when the channel SNR is insufficient to support successful decoding even at the lowest (mother) code rate.

For the detection of a decoding failure an error detecting code is required. This can either be implemented by an additional outer cyclic redundancy check (CRC), or is already inherently included in the code itself – like in the case of LDPCC. The length of the CRC is determined by the desired probability of an undetected error, which converges asymptotically as 2^{-b}, where b is the number of the CRC parity bits (cf. [3GPP-TR25.212] where a maximum CRC length of 24 bits is used).

Rate compatible punctured code sets are well known for CC and PCCC [RM00], but can also be created both for DBTC and BLDPCC. For the performance of punctured LDPCC it is decisive that the number of punctured variable bits connected to each check node is minimised. If a check node is connected to two punctured bits, there will be only zero messages in the first iteration and the information of this parity check equation is lost. Therefore, best results can be achieved by puncturing only degree 2 variable nodes. In most LDPC construction methods the redundancy part consists (almost) only of degree 2 variables. Often it has a dual diagonal form. Therefore it is possible to puncture only redundancy bits. Figure F.8 illustrates that the performance of rate compatible punctured DBTC and BLDPCCs is quite similar. We

hence conclude that rate compatible punctured codes can be constructed for all FEC techniques that are currently considered for use in the WINNER system.

B.2.3 Low-density parity-check codes: decoding options

The standard algorithm for decoding of LDPC codes is the so-called "belief propagation algorithm" (BPA), of which several good approximations exist. In fact, it has been shown in [CF02] that close-to-optimal error correction performance can be achieved by a corrected version of the so-called Min-Sum algorithm (MSA). The basic idea of the MSA is essentially the application of the maxLog approximation to BPA decoding. Similar to the case when using maxLogMAP decoding of PCCC, this comes at a performance loss in the order of 0.5 dB (on AWGN channels, cf. [WIND23]). This loss can be dramatically reduced by appropriate scaling of the extrinsic messages, to compensate for the over-estimation of extrinsic information (this approach has been also applied in Turbo decoding [VF00]). This corrected version of the MinSum algorithm will in the following be denoted as "Min-Sum*". Calculating variable and check node messages during decoding then only involves simple sum and minimum operations, respectively, plus a scaling of the check node messages. In theory, the scaling factor α needs to be optimised for each code and SNR by means of Density Evolution (DE), or Monte-Carlo simulation to achieve optimal results. However, Monte-Carlo simulations showed that choosing α=0.8, as proposed in [CF02] results in very good performance independent of the SNR operation point for the BLDPCC considered for use in WINNER. The "MinSum*" algorithm is therefore considered to give the best performance-complexity trade-off for LDPC decoders.

However, in the case of irregular LDPCC even using the MinSum* with optimal correction still not fills the gap w.r.t. true belief propagation decoding. Therefore, further investigations have been carried out recently, leading to new sub-optimal decoding algorithms [GBD03, JVS+03] that could be good candidates in terms of complexity/performance trade-off and memory savings. *Bit-Flipping Algorithms* [BR04, ZF04, ZB04, KLF01, ZF04] on the other hand might be considered an option for very low-end terminals, where a loss in performance might be acceptable when large savings in decoding complexity can be achieved. A drawback of such approaches is the absence of reliability information at the output of the decoder. However, since low-end terminals will most probably not use iterative equalisation and/or channel estimation techniques, this appears to be no significant limitation.

B.2.4 Scheduling of the decoder

The decoder for LDPCC is a message-passing algorithm operating on the Tanner graph [WIND21] which is equivalent to the structure of the parity-check matrix of the code. In the standard schedule of the BPA, which is often denoted as *flooding schedule*, first all check node are updated and then all variable nodes are updated. An alternative is *shuffled scheduling* [KF98, MB01, ZF05, YNA01, MS02] also known as *layered decoding*. Here, the BP decoder uses not only the messages from the last iteration, but uses also the information of the updates from the current iteration. This leads to a considerable increase in convergence speed. One can discern horizontal and vertical shuffling. The vertical shuffling schedule operates along the variable nodes: all check nodes connected to the current variable node are updated and the current variable node is updated. The horizontal schedule operates along the check nodes: the current check node is updated and all the variable nodes connected this check node are also updated. Simulations show that both methods increase the convergence speed roughly by a factor of two for both maximum and average number of iterations. However, the operation count of a single iteration of the BP decoder is increased, compared to the flooding schedule. In vertical shuffling each check node is updated d_c times per iteration while in horizontal shuffling each variable node is updated d_v times per iteration (d_v and d_c is the degree of the respective node). As the check node update is more complex than the variable node update, horizontal scheduling should be preferred. It is possible to perform group-wise shuffling, i.e. updates are performed on a group of nodes before the nodes of the other type are updated. This is especially suited for quasi-cyclic block LDPC codes as nodes within one block do not exchange messages anyway. Group-wise shuffling also enables semi-parallel decoding and reduces the required memory [MS02]. For the LDPCC considered in the WINNER framework, investigations showed that the performance of group-wise horizontal shuffling with 20 iterations is equivalent to that of the flooding schedule with 50 iterations (consistent with the speedup factors reported in [ZF05]). In the assessment of complexity/performance trade-off (cf. Appendix F.2) results will be given in terms of flooding scheduling, as reference point for any other comparison.

B.3 Modulation

B.3.1 Assessment of modulation techniques

As outlined in Section 2.2, supporting bandwidths of up to 100 MHz and enabling the "always best" principle translates into the following main requirements for the selected modulation technique: efficient equalisation of frequency selective channels, high granularity and the possibility to adapt transmission parameters to different environment conditions (delay spread, Doppler spread, available spectrum), user requirements (data rate, delay), and user terminal capabilities (maximum transmit power, antenna configuration etc.). Frequency domain signal processing, and more specifically the *generalised multi-carrier* concept are very elegant means of providing the required flexibility. Among the large number of modulation techniques that can be accommodated in the GMC framework (cf. Section 2.2), the following have been assessed in more detail during WINNER Phase I: different "flavours" of OFDM (CP-OFDM, IOTA-OFDM, PRP-OFDM), MC-CDMA, and FMT, as well as serial modulation, and IFDMA (or FDOSS). Table B.3 summarises the assessment of these modulation techniques. Although several transmission technologies are also related to multiple access, the discussion here focuses solely on the modulation aspect. The benefits and drawbacks of the main candidate technologies CP-OFDM and CP based frequency domain generated serial modulation are discussed in the following section.

Table B.3: Assessment of most promising modulation techniques

	Serial modulation	**IFDMA**	**CP-OFDM**	**PRP-OFDM**	**MC-CDMA**	**FMT-FDMA[12] (NB/WB)**	**IOTA-OFDM**
Required IBO	Typically 2–3dB lower than for multi-carrier techniques		High (6–9 dB,[WIND22])				
Tx complexity	IFFT FFT	Low	IFFT (addt. spreading for MC-CDMA)				
Rx complexity	FFT IFFT		FFT	FFT postfix suppr.	FFT addt. de-spreading[13]	FFT	FFT
Filtering complexity	Low		Low[14]			High (poly-phase filtering)	
Equalisation Issues	May require DFE/TEQ for higher order modulation[15]			acquisition delay			
Spectrum flexibility	+	-	+	+	o/+	-/+	+
Robustness w.r.t. ICI	+	-	-	-	-	+/-	+
Required guard bands/periods	Similar requirements (~10% for GI, ~20% for guard bands under the current assumptions)					+[16]	+[16]
Maturity	O	O	+	O	O	O	O

[12] The specific merits of FMT-FDMA depend very much on the modulation format chosen within the sub-bands.

[13] May also require multi-user detection in environments where the delay spread is large.

[14] It is possible to run multi-carrier based transmission without any additional filtering, resulting in substantial spectral side-lobes. Additional filtering is often required to meet spectral mask requirements.

[15] Noise enhancement in linear (MMSE) FDE may cause error floors for higher order modulation (16QAM) when using high code rates [WIND23], the issue can be overcome by using decision feedback/Turbo equalisation.

[16] Cyclic prefix can be omitted. However, additional pilots would then be required to achieve coarse synchronisation.

Interleaved Frequency Division Multiple Access (IFDMA) [WIND23, Section 5.2.1.4] can be interpreted both as a serial modulation (FDOSS) [WIND21, Section 4.15][ChC00, DFL+04] and a multi carrier modulation scheme [GRC02], thus combining many of the advantages of the two approaches. As a special case of frequency domain based serial modulation (using interleaved assignment of subcarriers), it enables the same high frequency diversity and low peak to average power ratio. It also facilitates low complexity signal generation [FCS04] and user separation (as for OFDMA). On the other hand, IFDMA and OFDMA exhibit a similar sensitivity to frequency offsets.

Multi-Carrier Code Division Multiple Access (MC-CDMA) has been considered extensively in [WIND21 Section 4.5][WIND23, Section 5.2.1.3][WIND26]. Since it provides high frequency diversity and good granularity also for low data rate transmission, MC-CDMA is proposed for the use with frequency non-adaptive transmission. Detection complexity will be low when using MC-CDMA only within one chunk (i.e., under time and frequency non-selective fading). Complexity can, however, become an issue in environments with high delay spreads (high frequency diversity) and in conjunction with spatial processing. Low-complexity techniques such as Pre-Detection SUD have been proposed, together with linear (ZF, MMSE) and non-linear multi-user detection that achieve good performance at the cost of higher receiver complexity.

IOTA-OFDM [WIND21, Section 4.12][WIND23, Section 5.2.1.2] [LGA01][JDL+04] and Filtered Multi Tone (FMT) [WIND21, Section 4.11][CFO+03][CEO02] modulation use prototype functions/filters to guarantee good localisation of the subcarrier spectra in the frequency (and time) domain. Thus, high robustness to inter-carrier interference (e.g. arising due to time and frequency errors as well as to Doppler effects) is achieved without requiring the insertion of a cyclic prefix – leading to a higher spectral efficiency. However, the cyclic prefix is used in WINNER to achieve coarse synchronisation, and the introduced overhead is below 10% for both the TDD and the FDD mode. When using IOTA-OFDM or FMT, an overhead would have to be invested for synchronisation pilots – thus reducing the potential gains in spectral efficiency.

Wideband FMT with high subcarrier spacing (and hence frequency selective fading per sub-channel) is a valid alternative to traditional (*time domain* based) single carrier transmission *over the whole bandwidth*, allowing a higher flexibility and granularity in the usage of the broadband channel. The same (or higher) flexibility can be achieved by using *frequency domain* based serial modulation – wideband FMT is a special case of this scheme, with block subcarrier assignment and a specific type of filtering.

Using a Pseudo Random Postfix (PRP) as guard interval [WIND21, Section 4.6–4.10] [WIND23, Section 5.2.1.1][MDC+04, MBL+05][MCD05] provides means to estimate and/or track the channel impulse response without adding any overhead in terms of learning symbols and/or pilot tones – allowing for increased spectral efficiency. However, in order to achieve a high precision (low MSE) of the channel estimates, a delay of several OFDM symbols in the radio interface may have to be accepted. This is especially the case for higher order modulation with high requirements on the channel estimation (cf. results in Appendix F.3.5). Moreover, the scheme is less applicable for uplink scenarios, where postfixes of different users superimpose at the base station. Since low delay is a very important requirement for the WINNER radio interface and the overhead required for a scattered pilot grid is quite low (cf. Appendix B.4.2), this solution has been selected for channel estimation and tracking in WINNER instead.

To summarise, CP-OFDM is the preferred solution for the downlink (and the uplink when terminal power consumption is not an issue) as the spectral efficiency gains from using other techniques are currently considered not to justify the increase in implementation complexity (e.g. poly-phase filtering) and/or delay (for the case of PRP-OFDM). Frequency domain based serial modulation is preferred for uplink transmission, due to its low PAPR and as it enables to flexibly switch between interleaved (IFDMA) and block subcarrier assignment (wideband FMT) according to need.

B.3.2 OFDM vs. single carrier

Serial and parallel modulations have generally similar BER performance on frequency-selective channels, when used with coding and other enhancements like iterative detection or adaptive loading. Note, however, that linear FDE receivers become limited by noise enhancement, at high SNR. OFDM systems therefore yield better performance than serially modulated systems, when considering transmission with higher order modulation and only *linear* equalisers, OFDM has been (and is) in use in a number of wireless communications standards (e.g., IEEE 802.11 and DVB systems). The main advantage of this technique is its implementation simplicity, at least from a baseband perspective: very low complexity equalisation algorithms are available and channel estimation and tracking is straightforward and of low arithmetical complexity if pilot/learning symbols based approaches (or derivates) are applied.

Concerning the trade-offs between OFDM and serial modulation, the main issues are the following ones:

i) the OFDM time domain signal is characterised by an inherent high peak-to-average-power ratio (PAPR) which is challenging for the RF implementation of HPAs (high power amplifiers) [FK05, WIND22, WIND23]. The power backoff required by OFDM or other multi-carrier modulation approaches is typically 2 to 3 dB higher than for serial modulation, even when PAPR-reduction methods are applied (for both systems, cf. [WIND23]). Serial modulation thus allows the use of cheaper power amplifiers. Furthermore, if a serial modulation system and a parallel system are required to use the same type of HPA and have the same maximum spectrum sidelobe levels, the parallel system's average allowed transmit power will be lower resulting in lower received power and correspondingly higher bit error rate and lower coverage [WIND23]. This constitutes the main motivation for the use of serial modulation in the uplink where terminal battery duration, terminal cost and coverage are critical issues. Furthermore, generation of serial modulation by the generalised multi-carrier approach is equivalent to generation of OFDM or OFDMA that has been precoded by a FFT operation. Thus serial (single carrier) modulation itself can be considered as just a form of OFDM to which a very effective PAPR reduction method has been applied.

ii) OFDM is sensitive to time and frequency synchronisation offsets. However, efficient algorithms (of relatively low computational complexity) are available which assure a sufficiently precise synchronisation in both, time and frequency. From a practical point of view, synchronisation issues are not a main limiting factor of OFDM.

iii) OFDM is in general sensitive to higher levels of inter-carrier-interference (ICI) (resulting, e.g. from high Doppler environments, phase noise, frequency offset etc.), which lead to a degradation of the system performance. A suitable design of the OFDM parameters (in particular the subcarrier spacing) is required in order to avoid this problem. Assuming reasonable design parameters, OFDM is also applicable to high mobility scenarios. Phase noise on the other hand can be a limiting factor, especially when high carrier frequencies and/or low cost implementations are targeted. Serial modulation is less sensitive to such self-interference effects [WIND23].

B.3.3 Guard interval design

The main purpose of the guard interval is obviously to limit inter-symbol-interference (ISI) for all block transmission based GMC schemes [WIND23]. Therefore, the amount of signal energy contained in the channel taps that exceed the guard interval length (resulting from a long channel impulse response, potential inter-cell interference, time synchronisation errors, and filter impulse responses) should be low enough to avoid error floors in the transmission (i.e. be some dB below the thermal/ADC noise floor). There are efficient methods to minimise the ICI (e.g. timing-advanced transmission in up-link) which can be used to considerably reduce the guard interval length and thus increase spectral efficiency. The guard interval length is often chosen to be a fraction $1/2^n$ of the raw symbol length, although this is not strictly necessary from the implementation perspective. It should, however, be an integer multiple of the sampling interval [WIND23]. Additionally to avoiding ISI, the cyclic prefix in CP-OFDM turns the linear convolution into a set of parallel attenuations in the discrete frequency domain, thus enabling simple single tap equalisation and contributing significantly to the receiver simplicity of OFDM systems.

B.3.4 Modulation alphabets and bit mapping

Non-differential M-PSK and M-QAM modulation will be used in the WINNER system, as channel state information can be made available to the receiver at relatively low pilot overhead in all scenarios (cf. Sections 2.3 and B.4). For the wide-area scenario, modulation formats up to 64-QAM are proposed, while for short-range transmission even 256-QAM appears to be feasible.

As a baseline case, Gray mapping is assumed. It provides the highest amount of mutual information when no a-priori knowledge is available, however, it shows little gain when additional a-priori knowledge becomes available. Since decoder and detector/channel estimator EXIT transfer curves must be matched in order to achieve good performance, it should evidently be used with a strong outer code, mostly in non-iterative setups. Note that the use of Gray mapping facilitates the calculation of soft output at the detector at low complexity, if the standard maxLog approximation is used. The selection of other mappings is useful in with the context of iterative equalisation/channel estimation, mostly in conjunction with a weaker outer code. Ideally, the mapping and the channel encoder should be chosen jointly in order to maximise the gain achieved after several iterations. In practice, rapid changes of the propagation environment may render this optimisation unfeasible. A robust solution shall then be preferred, at the price of a loss of optimality. Optimised bit labellings (used with a low memory CC) in Appendix F in the context of iterative channel estimation.

B.4 Pilot design for channel estimation and synchronisation

B.4.1 Intra- and inter-cell synchronisation using dedicated training symbols

A synchronisation approach is proposed that enables both intra- and inter-cell synchronisation in a self-organised way, without relying on any external reference, e.g. GPS. The approach assumes a cellular OFDM network, where the terminals in every cell, BSs or UTs, are allowed to receive and transmit over the whole system frequency band at the same time during synchronisation.

The approach proposed in this section is based on the acquisition of the coarse intra-cell time synchronisation by means of a DL synchronisation pilot, referred to as T-pilot. The T-pilot is sent in DL by all BSs inside the network at the beginning of each super-frame. It is proposed to build the T-pilot for each cell as a specific Gold code. This pilot structure has been proved to be robust against both inter-cell interference and multi-path fading [CSB05]. However, the correlation of T-pilots is sensitive to carrier frequency offsets, as shown in Appendix F.4.1.

In order to improve the achieved accuracy the DL T-pilot is followed by at least two F-pilots, that is two OFDM symbols. The frequency and time offsets can be estimated simultaneously in the frequency domain (post FFT) as the phase rotation between two adjacent OFDM symbols on the same subcarrier in the same OFDM symbol, and as the phase difference between two adjacent subcarriers, respectively. The phase rotation method requires the time and frequency offsets to be within one half of the OFDM symbol period and within one half of the subcarrier spacing, respectively. This condition is assumed to have been guaranteed at the beginning of the fine synchronisation by the initial coarse synchronisation.

In order to achieve inter-cell synchronisation, two methods can be considered which are described in the following.

The first, referred to as DL-UL synchronisation, assumes that all UTs within a certain cell, which have become mutually synchronised during the DL phase, transmit UL sync signals which are in turn received and analysed by all BSs within range. A synchronisation signal structure was proposed in [WIND23] that can be used in UL for the inter-cell synchronisation as well as alternative to the one described above for the DL fine intra-cell synchronisation. This signal consists of three adjacent OFDM symbols, during which each BS, in DL, transmits only on a single pair of adjacent subcarriers with the maximum power, as described in [WIND21], Section 9.5.4. The DL-UL method has been shown to provide very high accuracy in [WIND23] for both intra- and inter-cell synchronisation. More precisely, in 20 super-frames, both frequency and time synchronisation between all BSs within the cellular network can be achieved with remaining frequency offset of about 1% of the subcarrier spacing and time offset of about 10% of the guard interval, respectively.

According to the second method, referred to as DL-only, the inter-cell synchronisation is obtained without relying on UL sync signals. Each UT continues to listen to the sync signals sent in DL by all other BSs, measures itself the relative time and frequency offsets with respect to its own BS and feed back this information to its own BS. Each BS adjusts then its clock and its oscillator according to the offset measurements signalled by the UTs within its cell. An advantage of this method is that it can rely also on UTs in sleep mode, since it does not require continual transmission of pilots on the UL but only the occasional feedback signalling. Also for the DL-only method a very accurate convergence of the inter-cell synchronisation can be achieved under the assumption of ideal UL feedback. Performance is similar to that of the DL-UL method reported in [WIND23]. A proper design of such feedback signalling and the comparison of the involved overhead with respect to the DL-UL method described above should be subject of further investigation.

Since the DL only synchronisation uses relative measurements the influence of the propagation delay might become smaller. One additional advantage of the DL only synchronisation is that it relies on DL pilots. There is an additional degree of flexibility: adjacent BSs can also receive this pilots it they are able to receive DL signals and do not transmit during the pilot OFDM symbol. Without changing the pilot structure the system is able to switch dynamically between UT-aided synchronisation and synchronisation based on measurements at the BS. BS based synchronisation is useful in some deployment scenarios when the B2B link will give better receive signal level than the receive level at the UT (e.g. LOS conditions between BS). This flexibility can be conveniently exploited in TDD systems, while the complexity would increase in FDD since the BS has to be able to receive DL signals. Therefore, it is suggested as an option in the system concept.

For the above described inter-cell synchronisation schemes there exists a drift of the achieved common time offset due to the propagation delay. In the following, a *differentiated timing adaptation* is proposed, which can completely avoid the timing drift of stations.

The idea of this method has been first proposed in [ER01] and [WER03]. The systematic timing drift results from the fact that with each acquired time offset not only the actual difference of the node timings is acquired but also the distance-dependant propagation delay.

In contrast to other timing adaptation methods, the differentiated method only initiates a timing adaptation if a negative time offset is acquired. If a positive observed time offset is acquired, no timing adaptation is initiated, except the case that the positive time offset is over a threshold, which causes loss of synchronisation. Since a positive time offset at a first station corresponds to a negative time offset at a second station, the time offset will be compensated by the second station.

Estimation of the propagation delays in intra-cell synchronisation

Especially in the wide-area scenario, large propagation delays may be observed. A time-aligned arrival of signals from different UTs, which is required for a joint spatio-temporal processing at the BS, can be enabled if the UTs estimate their propagation delays during a so called 'ranging process' and use this information afterwards to transmit their data alligned to a common timing reference.

The proposed ranging process requires two different pilot signals (T- and F-pilots) and consists of three phases: an initial downlink phase, a succeeding uplink phase and another final downlink phase, depicted in Figure B.1, where one BS and two UTs are considered. The letters r and t denote the reception and the transmission status of each communication device. The process is described as follows: Initially, the BS transmits a beacon signal, which enables the UTs to perform a coarse synchronisation. For this beacon signal, a signal like the T-pilot introduced within the proposal above may be employed. After the reception of the beacon signal, each UT transmits its individual pilot, which consists of a single frequency tone selected from a predefined set of equally spaced tones. Each UT uses a different pilot tone. At the BS, the single user pilots are separated by filtering the received signal in he time domain.

After a specific user pilot has been detected, it is immediately retransmitted by the BS. This retransmitted pilot then is detected at the dedicated UT in the same way as it is done at the BS. From the temporal difference between the transmission of the UT's pilot and the reception of its retransmission, the UT may deduce the propagation delay.

Within the simulations at an SNR of 0 dB, hardly any values lying outside the range of the CIR length occurred, hence the ranging process can be regarded as being robust and reliable.

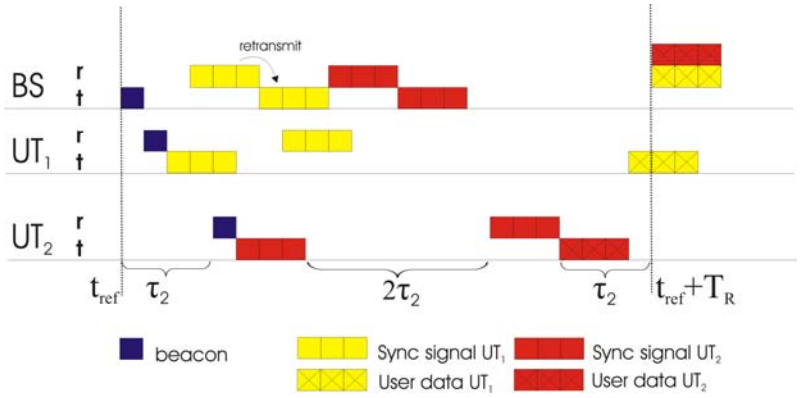

Figure B.1: Detailed scheme of the ranging process.

If the UTs retransmit their individual synchronisation tones (F-pilots) in advance by the estimated propagation delay after the ranging process has been finished, a fine estimation of the carrier frequency offset may be carried out at the BS: The single synchronisation tones, which arrive aligned in time at the

BS now, are again separated by applying the filtering process from above, and by averaging the slope of the phase of each separated tone, information on each user's carrier frequency offset may be obtained.

B.4.2 Pilot grid for generalised multi-carrier (GMC)

Channel estimation by interpolation in time and frequency is considered to be an efficient solution for an OFDM-based radio interface [WIND21, WIND23]. Generally, a scattered pilot grid can be implemented for any GMC signal in the frequency domain, on both the downlink and the uplink. While blind channel estimation schemes require little or no pilot overhead, their application may critically depends on the assumptions on the chosen transmission scheme. With a large variety of adaptive algorithms in time, frequency and space to choose from, the flexibility of the WINNER radio interface might be severely compromised by exclusively relying on blind schemes. Moreover, as the pilot overhead of the considered pilot aided techniques is in the range of 2 to 5% per spatial stream, the potential benefit of blind channel estimation techniques is limited. On the other hand, for highly dispersive channels and/or high-end terminals, blind or semi-blind schemes might provide a performance improvement and could therefore be considered as optional enhancements.

In the following a generic framework for the pilot design of GMC signals is described. Two types of frequency domain pilots and one type of time domain pilots are options, the frequency expanding technique (FET) and Frequency domain superimposed pilots (FDSP). FET preserves and rearranges data-carrying subcarriers to accommodate pilots, while FDSP obliterates data-carrying subcarriers where pilots are to be inserted. Applied to OFDM, FET is equivalent to a scattered pilot grid, where data symbols are inserted at subcarriers where no pilots are present. FDSP on the other hand, can be viewed as a puncturing of the data symbols. So, data symbols are inserted on all subcarriers, and subsequently pilots are superimposed. This effectively results in an increased code rate.

Frequency domain pilots for the WINNER radio interface

Pilots are used for implementing certain physical layer support functions, e.g. connection setup, synchronisation, mobility support, power control, CQI measurements and most importantly channel estimation. Two types of channel estimation must be distinguished: channel estimation for data reception (where the pilots are send at the same time), and channel estimation for adaptive transmit processing based on return link feedback or measurements (where an additional extrapolation/prediction in time is required, see also Appendix B.5.2). In order to realise an efficient system, the same pilots should be reused for different support functions. Spatial processing, however, limits the potential reuse of pilots and brings along additional requirements [WIND27]. In particular we need to distinguish:

- ***Dedicated pilots*** may be required if user-specific transmit processing (i.e. a user-specific adaptation of amplitude and phase) is applied to the data symbols. These pilots are subject to the same transmit processing as the data symbols and therefore allow the receiver to estimate the effective channel $\mathbf{H}_U \cdot \mathbf{f}_U$ of user U. The use of dedicated pilots for other purposes, like CQI measurements, is limited, since they contain a power allocation specific (in most of the cases) to another user. In time, the interpolation is constrained by TDMA, i.e. to the chunk duration in adaptive downlink transmission. Regarding the interpolation in frequency, two different types of dedicated pilots can be distinguished:
    - ***Full-band dedicated pilots*** having identical weights for all chunks in frequency dimension dedicated to a particular user. Therefore interpolation over these chunks is possible.
    - ***Chunk-specific dedicated pilots*** where different weights are applied to each chunk and no interpolation in frequency domain is possible. This is usually the case for user-specific transmit processing based on short-term CSI and /or in case FDMA on chunk basis is used.
- ***Common pilots*** have the property not to include user-specific transmit processing and thus the interpolation in frequency is restricted by the specific channel estimation algorithm (i.e., related to the estimator complexity) and not by chunk specific constraints. In case of user-specific transmit processing, the amplitude and phase of common pilot deviates from those of the data symbols, and therefore the receiver cannot detect those based on common pilots. Different variants of common pilots exist, e.g.,
    - ***A common pilot per cell/sector***, which is transmitted omnidirectionally (i.e. not subject to beamforming) and normally used to support mobility-related functions. It allows obtaining an unweighted channel coefficient **h**.

- ***Common pilots per antenna*** are used to obtain the unweighted channel matrix **H** which describes the propagation channel between any combination of transmit and receive antennas in the MIMO case.
- ***Common pilots per beam*** are useful to estimate the effective channel (including the beamforming weights) and perform CQI measurements for the associated beam for fixed beamforming approaches. Note, that measurements on such pilots in neighbouring beams could then be used for beam handover. Also, the common pilots per beam benefit from the beamforming gain, which reduces the transmit power required for a target channel estimation error and coverage area.

Due to the fact that common pilots can be used by several users, they are appealing for the downlink processing, since the overall energy to perform the associated functions has only to be spent once and the pilot symbols can be spread over all resources. Also they provide a basis for un-biased CQI measurements. However, certain user-specific spatial processing techniques require dedicated pilots.

Multi-user precoding techniques are assumed to impose the most stringent requirement on channel estimation, since high accuracy prediction of the downlink channel need to be obtained based on uplink measurements. A performance degradation of 2 dB due to imperfect channel estimation requires a pilot SINR of 20 dB and channel estimator gains between 13 dB and 17 dB [WIND27]. In Appendix F.3.3 results for the channel estimator gains of the WINNER pilot specifications are presented. It is shown that with pilot aided techniques the required gains of 13 to 17 dB can only be achieved with sophisticated post-processing, for instance by an iterative channel estimation scheme.

A careful radio interface design must balance the number of users that can be scheduled in the downlink with the number of users that can be estimated based on the uplink pilots in the TDD PLM. The competition bands and the active/semi-active flow states that are discussed in Appendix C.1 are tools for performing this trade-off. Simulations for the linear precoding technique (SMMSE) have shown that in order to obtain sufficient SDMA and spatial multiplexing gain, around 9 orthogonal pilots[17] would be required per competition band.

Since the requirements regarding pilot type, number of pilots and pilot SNR are varying considerably, a modular and scalable MIMO-pilot design should be adopted. For example, a combination of common pilots and additional dedicated pilots per chunk according to the requirements of the spatial processing scheme is conceivable.

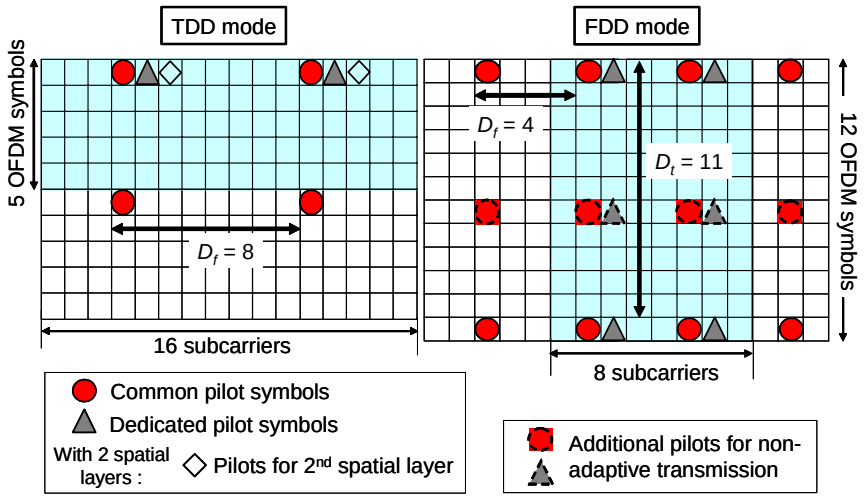

Figure B.6: Frequency domain pilot grids for GMC signals.

[17] Corresponding to an average of 3.4 users according to the assumed user population (20% with 1 antenna, 40% with 2 antenna, and 40% with 4 antenna.

Figure B.6 shows the pilot grid arrangement for the WINNER TDD and FDD modes. The placement of pilot symbol within a chunk is based on the following rules (based on the framework from [WIND21, WIND23]):

- For *common pilots* a reasonable over-sampling factor in frequency direction would be 20—100%. On the other hand, the chunk dimension also imposes constraints on the pilot spacing. To this end, a constant number of common pilots per chunk is desirable. For the TDD and FDD modes this translates to a pilot spacing of D_f=8 and D_f=4, respectively.
- For *dedicated pilots* the over-sampling factor should be at least 100%, which also results in a pilot spacing of D_f=8 and D_f=4 for the TDD and FDD modes, respectively.
- For channel estimation in time direction, the number of available pilots is limited by the fact that half duplex FDD or TDD a mobile terminal is not able to transmit and receive at the same time. Therefore, the same guidelines for common and dedicated pilots apply.
    - For adaptive transmission, the mobility of UTs must follow certain constraints, which gives upper bounds on the maximum Doppler frequency. This results in a total of 2 and 4 pilots per chunk for the TDD and FDD modes.
    - For non-frequency-adaptive transmission in the FDD mode, two additional pilots are inserted in time direction, to support mobile velocities up to 250 km/h, totalling to 6 pilots per chunk. For the TDD mode, no additional pilots are necessary if at least 2 chunks per frame are used.

In order to be able to estimate the channel from different antennas orthogonal pilots are required and the following principle design guidelines are possible:

- transmit pilots in frequency-multiplex (different subcarriers of one chunk), as indicated in Figure B.6,
- transmit pilots in time-multiplex (consecutively on one subcarrier),

Additional code multiplexing of pilots in time as well as frequency multiplex is possible. In existing MIMO-OFDM real-time test-beds, code-multiplexing using Hadamard sequences on consecutive pilot symbols of one subcarrier has been extensively used and verified [MKK+05, JFH+05, JHF04]. A similar design has also been proposed for fixed grid of beam techniques in WINNER (see Section 3.2.2.2 of [WIND27]. There each antenna is identified by an orthogonal sequence reused on all pilot subcarriers but additionally scrambled in the frequency domain. Such overlapping pilot-based techniques have also been studied for adaptive uplink transmission, see Appendix B.5.2 and [WIND24], Section 3.1.1. Advantages are that the power on pilot carriers is not enhanced compared to the power of data, i.e. the transmit spectrum is flat. Moreover, the reconstructed pilots can be reused for the carrier phase tracking at the receiver, if the sequence is additionally stretched along the time direction over the chunk. The pilot overheads of the pilot arrangements in Figure B.6, per spatial stream per chunk are summarised in Table B.4. The pilot overhead is defined as the ratio of the number of *pilot* symbols per chunk, N_{pilot}, to the number of *data* symbols per chunk N_{data}. The chunk sizes are 96 and 80 symbols for the FDD and TDD modes.

Table B.4: Pilot symbol overheads per spatial stream per chunk

Tx mode / Pilots data	**FDD mode**		**TDD mode**	
	Non adaptive	Adaptive	Non adaptive	Adaptive
# pilots per chunk	6	4	2	2
Pilot overhead N_{pilots}/N_{data}	7.5%	5%	2.5%	2.5%

The pro and cons of the pilot design principles in the WINNER framework are for further study. This is particularly true for the various proposed MIMO schemes. The assessment of channel estimation schemes for uplink single carrier signals is studied in Appendix F.3.1. The performance of OFDM channel estimation schemes for common and dedicated pilots, using the pilot grids in Figure B.6 is evaluated in Appendix F.3.2.

B.5 Adaptive transmission

B.5.1 Bit and power loading algorithms

If channel quality information is available on each subcarrier (or chunk) is it possible to increase the performance of the radio link and/or save power by performing bit and/or power loading for each subcarrier (chunk). This single-user link adaptation can be used as an element in the solution of the complete multi-user adaptation and scheduling problem. There are many different algorithms that realise so called water-filling concept in a multi-carrier transmission. Most of them originate from the *asymmetric digital subscriber line* (ADSL) technology.

Depending on their application, existing bit and power loading algorithms can be divided into two groups:

1. Algorithms that maximise the number of transmitted bits with a given total power and required BER constraints (variable bit rate).
2. Algorithms that minimise the BER with a given throughput and transmitted power constraints (fixed bit rate).

For most algorithms, the average computational complexity of the analysed algorithms is proportional to $O(N \log(N))$, where N represents the number of subcarriers (or chunks) being adaptively loaded. The assessment presented in [WIND24] focused mainly on the Hughes-Hartogs (HH) algorithm [Hug91, Bin90]. However, from the complexity point of view, this algorithm seems to be unsuitable for practical implementations (see Appendix B.5.1.1). The complexity of Campello's implementation [Cam98][Cam99], on the other hand, is proportional only to $O(N)$. Therefore, this algorithm might be considered as a favourite one from the complexity point of view. In practice, however, also other algorithms are much faster than the HH algorithm, e.g. the one by Chow, Cioffi and Bingham [CCB95], or the Fischer and Huber [FH96] algorithm. The computational complexity may depend on the application and the channel transfer function as well. Note that of the discussed algorithms only the Hughes-Hartogs and the Campello algorithm are optimum in the data rate maximisation sense. For additional details, please see the following discussion on complexity and implementation issues, and the details given in Appendix F.5.

B.5.1.1 Hughes-Hartogs optimum algorithm

The Hughes-Hartogs bit and power loading algorithm is a part of the ADSL modem U.S. patent [Hug91]. A detailed description of the steps of the algorithm is included in [WIND24] in the form described in [Bin90]. The HH algorithm does not realise the water-pouring principle in its classical sense, but it is an optimum solution for a multi-carrier transmission using QAM constellations and symbol-by-symbol detection, since it spends the transmitted power in the most effective way. However, this procedure has high computational requirements because an extensive sorting and searching has to be performed in each step of the loop. Since the average running time of the algorithm is proportional to the product of the total number of loaded bits loaded (fractional bits for coded transmission), and the number of subcarriers (chunks), it seems to be unsuitable to be implemented in systems with high data rates, high granularity and a high number of subcarriers (chunks) to be adapted.

B.5.1.2 Chow, Cioffi and Bingham algorithm

This algorithm, proposed by Chow, Cioffi and Bingham in [CCB95], offers significant implementation advantages over the previously mentioned Hughes-Hartogs algorithm, whilst the performance degradation is negligible as compared to the optimal solution. Although this algorithm might be slightly sub-optimal, it converges much faster, as compared to the HH algorithm. This is due to a limited number of internal iterations needed. The authors have found that 10 iterations are sufficient to ensure the convergence of the algorithm. The worst case running time of this procedure is proportional to:

$$O(MaxIters \cdot N_c + 2N_c), \tag{B.3}$$

where: *MaxIters* is the maximum number of iterations, and N_c is the number of subcarriers (chunks). This figure is much lower than the average running time of the HH algorithm (see Appendix B.5.1.1). Moreover, the worst case running time of the CCB algorithm does not depend on the granularity of loaded bits, so it is suitable for a joint code and modulation adaptation.

B.5.1.3 Fischer and Huber algorithm

In this algorithm, presented in [FH96], the data rate and power are assigned to each subcarrier to minimise the error probability. The Fisher and Huber algorithm has a very low complexity, even lower than that of the Chow, Cioffi and Bingham algorithm. According to what the authors claim, the achievable performance is higher or at least comparable to the performance of the CCB algorithm. However, in the WINNER system case, this seems to be a bit too optimistic assumption (see Appendix F.5). One of the advantages of the algorithm from the implementation point of view is that the logarithms of the subcariers' (chunks') noise variances are calculated only once in the beginning and stored in a memory. In the main loop only additions and one division by an integer have to be performed for each subcarrier (chunk).

B.5.1.4 Chunk-based single-user link adaptation in the adaptive resource scheduling framework

Adaptive transmission and scheduling in the WINNER AI concept is assumed to take place within the framework outlined in Appendix C.1.6. For each chunk (layer), each candidate user terminal predicts the channel quality (SINR). Modulation levels, inner code rates (typically using convolutional coding) and possibly power adjustments together comprise the link adaptation. They are pre-computed for all chunks and all candidate flows/user terminals. This adjustment should take not only the predicted channel gain into account, but also its accuracy. That problem can be solved by averaging over the pdf of the power prediction error, when adjusting the rate limits [FSE+04], [SF04] and Section 2.2 of [WIND24]. Furthermore, the interference level must be predicted. Interference prediction remains a major research problem for WINNER II and it involves both the SDMA interference within the cell and the interference from other cells and operators.

The link adaptation will in general work together with an outer code (turbo or LDPC).An appropriate criterion for the link adaptation would then be to target a constant SINR per bit. This would essentially convert the fading channel into something closer to an AWGN channel, as seen from the outer code.

The pre-calculated chunk capacities (bits per payload symbol) that result from the link adaptation for each chunk layer and each flow form one set of inputs to the adaptive resource scheduler. The scheduler uses them, together with information on the queue levels and the flow priorities, to allocate the next slot.

B.5.2 Channel quality prediction for adaptive transmission

Adaptive transmission always involves a closed feedback loop, and thus incurs a delay. The allocation decision will be based on outdated channel quality information. While most WINNER terminals are expected to be stationary or slowly moving, this will create a problem for faster moving terminals. It would be advantageous with a scheme that allows the vast majority of WINNER terminals, including many of those moving at vehicular velocities, to utilise adaptive transmission. The situation can be improved markedly by introducing a channel predictor. In [WIND24], it is shown that this enables prediction of the channel power at sufficient quality over time delays consistent with realisable feedback loops, at vehicular velocities and 5 GHz carrier frequencies. Adaptive transmission at vehicular velocities would *not* be possible if the present channel state is just extrapolated. A special problem is prediction in the uplink. Since several terminals will then be in competition for the whole or a part of the bandwidth, they have to send pilots over the whole of this band. The overhead due to these pilots would increase proportionally with the number of active terminals. To prevent this overhead from becoming too large, a simultaneous transmission of the pilots, *overlapping pilots*, is preferred. This technique requires the terminals to be sufficiently well synchronised in time and frequency. It also requires estimation of a multiple-input single-output channel based on these overlapping pilots. Orthogonal symbol sequences would be used as pilots, spread out over different frequencies in several chunks. It should be noted that after propagation through different frequency-selective channels, the received signals would no longer be orthogonal.

Channel prediction can be performed in the time-domain for the impulse response [Ekm02], [SEA01] or in the frequency domain for the channel gains. In [WIND24], frequency domain prediction is investigated. It utilises the correlation between neighbouring subcarriers, and the time-domain correlation between subsequent OFDM symbols in a state space model [SA03]. Control symbols are used in the decision directed mode for improving the estimates. Figure B.7 below shows the results, expressed in normalised prediction error MSE, as a function of the SNR and the prediction horizon scaled in wavelengths. The result is for downlink predictions for the FDD mode in cellular deployment, assuming a full duplex FDD terminal that listens continuously on the downlink pilots. The Urban Macro channel model has been used. Note the large dependence of the performance on the SINR.

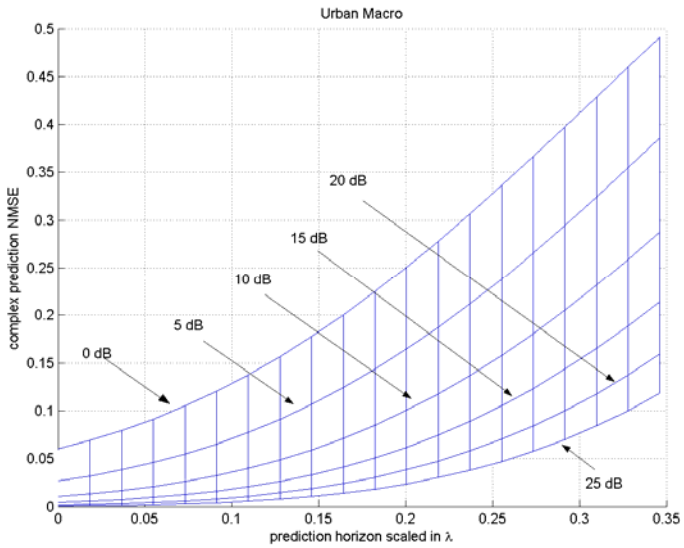

Figure B.7: FDD downlink prediction accuracy in terms of the normalised channel prediction MSE, as a function of the prediction horizon scaled in carrier wavelengths and the SNR. Results for FDD downlink over Urban Macro channels, using a Kalman algorithm that utilises 8 subcarriers.

Adaptive transmission to/from a terminal will be feasible up to a maximal velocity for a given SINR, or equivalently, down to a limiting SINR at a given velocity. For combinations of velocities and SINRs beyond such a boundary, non-frequency-adaptive transmission must be used. In [WIND24], a preliminary finding is that the normalised prediction error level 0.15 indicates the location of this boundary rather well, when using adaptive convolutional coding combined with BPSK or M-QAM. Based on this, one may calculate the approximate SNR boundaries for different velocities, different predictor designs and different designs of the adaptation feedback loops. The results in Figure B.7 are for the adaptation loop designs presented in Section 3.1 of [WIND24]. For the FDD mode, it is based on downlink channel prediction 2.5 slots ahead at the terminals. In uplinks channel prediction is based on overlapping pilots, at the base station. For the short-range TDD modes, the prediction is assumed to be performed by the user terminals. (A scheme that moves the predictor to the base station is of course also possible). The required prediction horizons to the far end of the predicted chunk, scaled in the carrier wavelength λ_c at 5 GHz, are also shown in Table B.5. For further results please see Section 3.1 of [WIND24] or [SFS+05].

Table B.5: SINR limits for cases where the accuracy limit $\tilde{\sigma}^2 = 0.15$ allows the use of adaptive transmission, exemplified for three terminal velocities for a 5 GHz carrier frequency. Also shown are required prediction horizons in carrier wavelengths. From [WIND24], Table 3.2

	30 km/h	50 km/h	70 km/h
TDD downlink (prediction horizon 2 slots)	< 0 dB (0.094 λ_c)	5 dB (0.156 λ_c)	10 dB (0.219 λ_c)
TDD uplink (prediction horizon 3 slots)	5 dB (0.150 λ_c)	15 dB (0.25 λ_c)	> 25 dB (0.35 λ_c)
FDD downlink (Figure B.7)	< 0 dB (0.117 λ_c)	6 dB (0.195 λ_c)	12.5 dB (0.273 λ_c)
FDD uplink, 2 users in competition band	0 dB (0.117 λ_c)	7 dB (0.195 λ_c)	15 dB (0.273 λ_c)
FDD uplink, 8 users in competition band	3.5 dB (0.117 λ_c)	11 dB (0.195 λ_c)	20 dB (0.273 λ_c)

In these examples, adaptive transmission can be expected to work in the widest variety of situations in the proposed wide-area FDD downlinks and short-range TDD downlinks, while it works in the narrowest range of circumstances in the proposed short-range TDD uplink that requires the longest prediction hori-

zon. The case of wide-area FDD uplinks, using overlapping pilots, falls somewhere in-between. The performance deteriorates with the number of simultaneous users that transmit overlapping pilots, but this deterioration is not severe.

B.5.3 Compression of channel state feedback for adaptive transmission

This section contains a brief summary of results from Section 3.1.4 in [WIND24] and and additional results on multi-antenna systems. Assume that one or several clients within a terminal are in competition for a sub-bandwidth of the total band comprising N chunks (one-antenna SISO transmission is assumed here). K active terminals compete for this competition band. Assume that each terminal feeds back a proposed code and modulation rate for each chunk. For a scheme with r rates, each terminal then needs to feed back $N \log_2(r)$ bits per chunk duration T_{chunk}. For K users, the required total feedback data rate is then

$$R_f = KN \log_2(r) / T_{chunk} \quad \text{[bit/s]}$$

For a 40 MHz FDD downlink with $N = 104$ chunks and with $r = 8$ code and modulation rates, we would have a feedback overhead of 925 kbit/s per active user! Expressed in another way, for each chunk for which K downlink users compete, $K \log_2(r)$ feedback bits would have to be transmitted in the following uplink chunk. The FDD mode chunks of Appendix C.3 contain 96 symbols. With around 80 non-pilot symbols per uplink chunk, $K = 8$ active terminals with $r = 8$ would consume 24/80 = 30% of the uplink bandwidth for control signalling, if one feedback bit/feedback symbol can be used on average. The situation described here is clearly unacceptable. Fortunately, there are several ways in which the required feedback rate can be reduced significantly.

The channel gains and SNRs at adjacent chunks will be highly correlated. (If they were not, the chunk widths would have been selected too wide, and we would have severe problems with channel variability within the chunks.) This correlation can be utilised to reduce the feedback rate. The channels are also correlated in time. Furthermore, it is likely that in most cells except those situated close to major roads, the large majority of terminals will not travel at vehicular speeds, but rather be stationary. For those terminals, very little feedback is required.

In Section 3.1.4 of [WIND24], several principles for compression are introduces and evaluated. Lossless compression of the modulation-coding rates could, for the considered ITU Vehicular A and Pedestrian A channels be performed at rates close to 0.91 bits/chunk and 0.35 bits/chunks, respectively.

Significantly lower feedback rates can be attained by using lossy compression of the SINR. This method provides the added benefits that SINR-values, not only suggested rates, are fed back. This enables the scheduler to select intelligently among users who would have suggested the same rates for a given chunk. The net effect is that lossy compression of SINR values is superior to lossless compression of suggested modulation-coding rates. It enables us to attain *both* lower feedback data rates *and* a higher performance, in terms of the attained spectral efficiency when performing multi-user scheduling. The suggested coder uses transform coding (discrete cosine transform, DCT) to compress the SINR data in the frequency direction. It combines this with sub-sampling in the time direction to obtain a further compression due to the temporal correlation. Motivations for these design choices are discussed in [WIND24]. The resulting algorithm is summarised by Figure B.8 and Figure B.9 below.

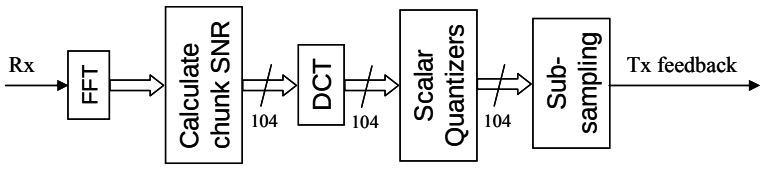

Figure B.8: A block diagram of feedback handling in the terminal

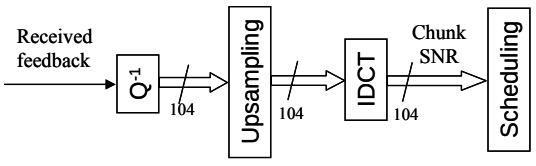

Figure B.9: Block diagram of feedback handling at the base station.

With the discussed compression of SINR predictions, only 0.25 bits/chunk are required for the Vehicular A channels and 0.12 bits/chunk for the Pedestrian A channels when all users travel at 50 km/h and the modulation-coding scheme uses $r = 8$ rates. If the mobile speed is reduced, it will be possible to further sub-sample the coded feedback information. For example, at 5 km/h, it would be possible to reduce the feedback information further by a factor of 10. With a feedback rate of 0.25 bits/chunk over the Vehicular A channel, we would only need 4 bits per chunk to accommodate 16 *vehicular* 50 km/h users per competition band, in addition to many more stationary users. Uplink feedback with only four 4-QAM symbols per chunk that use rate ½ coding is adequate for this.

For multiple antenna systems, the required feedback rate will of course increase proportionally with the number of virtual antenna streams for which the channel quality feedback is required. If not only real-valued channel quality SINR values, but channel state information in the form of complex-valued matrices is required, this will increase the feedback requirements quite substantially. In [KBLS06], a method is described that can significantly reduce the required CQI feedback using vector quantisation techniques.

An example of a system with four transmit antennas and one receive antennas that would need 32 bits if all four complex gains were represented by 8 bits each. Using an optimised quantiser, it is possible to use only one or two bits and still reach a significant portion of the performance for perfect CSI. Especially, for scenarios where long-term CSI is available at the transmitter, this additional information can be efficiently exploited by combining a fixed quantisation scheme for the short-term CSI with a linear transformation that only depends on the long-term CSI. The resulting feedback requirement may still be high for adaptive multi-user transmission. However further reductions can be expected by utilizing the temporal correlation, as was outlined for the SISO case above.

Appendix C. MAC System Layer Functions

This appendix gives more details on the services and functions within the MAC modes that were presented in Chapter 3. Appendix C.1 below gives brief descriptions of the resource and transmission control functions for in the two cellular MACs. The functional architecture of the peer-to-peer MAC is outlined in Appendix C.2.

The functional description of the PHY system layer is important for understanding the transmission, but it has been left out from this report to save space. It can be found in Section 5.5.2 of [WIND76].

C.1 Functional architecture of the WINNER medium access control for FDD and TDD cellular transmission

The presently assumed design of the MAC system layer for FDD and TDD cellular transmission was outlined in Section 3.1, see Figure 3.3 and Figure 3.4. The implementations of these two MAC modes are common to about 90% and their interfaces to higher layers are identical. They will therefore be described together below, with mode-specific differences indicated when they appear.

The description follows the presentation in Section 5.4 of [WIND76]. Since the delivery of [WIND76], the design has been refined and modified on several points. As compared to the presentation in [WIND76], the design has been modified as follows:

1. The PHY control signalling is under current investigation. It has been re-organised so that a major part of the transmit control processing is executed by the MAC system layer. As outlined by Figure 3.3, three special PHY services can be invoked transferring control packets:
    a. Transmission together with the BCH packets in the super-frame preamble,
    b. Use of non-frequency adaptive transmission,
    c. Use of special time-frequency resources earmarked for control transmission, via the service ***Special Transmit Control Signalling*** PHY service.

    In addition, piggybacking of control bits in ordinary packets may also be used.

2. Measurements are as before provided as a PHY layer service. They may also be provided in further processed form as a MAC system layer service. The partitioning of processing of measurements is under current discussion and will continue to be investigated in WINNER II.

3. The transport channel **TCC** for control flows has provisionally been added, to aid investigations on the design of protocols that supports all required control messaging.

4. ***Antenna calibration*** has been added as a function within the ***spatial scheme controller.***

The sections below describe all the main control functions that are introduced in Figure 3.3. Appendix C.1.5 summarises how different transport channels are handled, as illustrated by Figure 3.4. The resource scheduler (Appendix C.1.6) is a crucial system element of the WINNER design; it is, in a sense, the "spider in the net" of the whole design. Appendix C.1.7 provides additional discussion on the problem of SDMA and spatial user partitioning. Finally Appendix C.1.8 summarises the time scales on which the different functions work.

C.1.1 MAC radio resource control: Resource partitioning and constraint combining

The problem that the **resource partitioning** has to solve is the structural preparation of the next super-frame, outlined in Section 3.1.4. The time-frequency *chunk* is the basic unit for subdividing the radio resources. The partitioning of the super-frame between different transport channels will be performed with chunk granularity. Reuse partitioning between cells is supported.[18] It must be performed with guard-bands, due to the non-orthogonality introduced by large time delays. See Appendix G.7.3. It has to be performed in terms of wider frequency resource units, since the guard bands would otherwise represent too large an overhead. The resource partitioning may be changed on a super-frame basis, but most parameters will typically stay unchanged over longer time horizons. In TDD, one single super-frame is to be defined. In FDD, separate uplink and downlink super-frames are to be specified, see Annex A.3.1 of [WIND35]. The uplink and downlink super-frames will normally use differing allocations.

[18] See Section 5.2 in [WIND32].

The resources of the next super-frame are allocated and subdivided in the following sequence:

- First, all constraints on the use of chunks are updated by the ***Constraint combining*** function of the constraint processor at the BS. It receives control inputs from the RLC on restrictions due to spectrum sharing and interference avoidance with neighbouring base stations. At the BS, the spatial properties of the restrictions are re-calculated in terms of BS antenna transmission properties.[19]

The subsequent steps are performed by the ***Resource partitioning*** function that is implemented in the MAC control plane at the base station.

- ***DAC assignment***. A (nonzero) set of consecutive chunks is reserved for DAC (contention-based traffic). In the TDD mode, these resources may also be used for peer-to-peer traffic. This assignment is placed in the frequency region that is assumed available everywhere (Figure 3.2).
- ***RN assignment***. In cells that include relay nodes, sets of chunk beams are reserved exclusively for transmission between these RNs and UTs. Each set is reserved either for single RNs or for a group of RNs that will create little mutual interference. Furthermore, resources may be allocated for use in the relay links between BSs and RNs.
- ***TDC adaptive transmission assignment***. The remaining chunks are divided for use by adaptively and non-frequency adaptively scheduled flows, respectively. This division is based on the history of the previous traffic demand.
- The set of chunks reserved for adaptive transmission may be further divided into *competition bands*, where one stream normally uses only a single band. These competition band allocations are updated, if required.

The super-frame has now been constructed. Control messages that specify the allocation are transmitted from the BS at two instances. In the case of two-hop relaying, the resource partitioning information is thereby distributed to all the participating UTs at the beginning of the following super-frame:

- The RN partitioning is transmitted from the BS to the RNs over the relay link in chunks that are reserved for control signalling within the present super-frame.

The remaining control information is transmitted by the BS to the UTs. This is done during the downlink control part within the preamble of the super-frame being defined. In the here-considered case of two-hop relaying, it is the next super-frame. Simultaneously, each RN transmits the RN assignment to the UTs under its control. For more details, please see Section 6.3.4 of [WIND35].

C.1.2 MAC radio resource control: Flow setup and termination

New uplink and downlink flows are established by the Flow establishment RRM function in the RLC system layer. It requires the detailed setup of a flow context over each involved hop. That flow context establishment is executed by the MAC ***flow setup*** function. Flow context release is initiated by the RLC and is executed by the MAC ***Flow termination*** function. In the case of per stream rate control (PSRC) see Appendix B.1, several queues per flow are used.

When a new downlink flow is established, it is given a local flow address that is unique within the cell. Its destination UT (or UTs in the case of CDC point-to-multipoint flows) is notified and a resource scheduling buffer queue is initialised.

In the FDD mode, flows to/from half-duplex terminals are assigned to one of four groups: *Group 1* transmits in the downlink the first half of the frame, and in the uplink during the latter half. *Group 2* transmits/receives in the opposite way. *Group 3* contains half-duplex terminals that have adaptable and flexible uplink and downlink transmission periods. Full-duplex terminals belong to *Group 4*.

TDC flows are initially assigned either for adaptive or for non-frequency adaptive transmission by the flow setup controller. The choice is based on the capability of the terminal, the average SINR and the velocity of the terminal. The choice is also affected by the potentially available spatial schemes, and their CSI and CQI requirements. The initial assignment may be changed later if the circumstances change. Flow setup in relay-enhanced cells is discussed further in Section 6.3.5 of [WIND35].

[19] In a grid-of-beams implementation, constraints on the transmit power used in each beam may be used. In the general case, constraints on the transmit covariance matrix may be used .

C.1.3 MAC radio resource control: Spatial scheme pre-configuration and selection

A base station or relay node can have one or multiple antennas. These antennas can be localised or may constitute a distributed antenna system, e.g. comprising all antenna elements within a building. A general *spatial processing scheme* for MIMO transmission and spatial domain link adaptation has been defined [WIND27]. It includes multiplexing, diversity-based transmission, fixed beamforming and adaptive beamforming as special cases, see Appendix B.1. The spatial scheme controller performs a baseline spatial scheme selection process. It is invoked to select an appropriate spatial transmit scheme for the newly established flow. This selection is based on the terminal capabilities, the BS antenna capabilities and the choice of adaptive and non-frequency adaptive transmission. In addition, the interference properties of other flows and their demand for spatial channels influence the decision. Also for already established flows, the spatial processing scheme can be changed by the Spatial Scheme Controller. To reduce the complexity of this process a split in two functions and temporal layering is used:

- ***Spatial scheme pre-configuration*** performs static and long-term trigger-based assignments. These assignments serve as inputs and constraints to the next step.
- ***Spatial scheme selection*** determines the dispersion code (degrees of spatial diversity and spatial multiplexing), the possible use of per stream rate control and the possible use of and type of precoding.

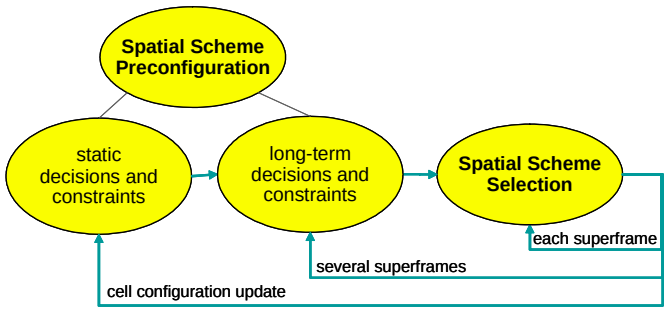

Figure C.1: Overview of temporal layering of the MAC functionalities Spatial scheme pre-configuration and selection within the spatial scheme controller.

The Figure C.1 above illustrates these functions and the different time scales at which they operate. The *static* part of the ***spatial scheme pre-configuration*** evaluates all parameters, decisions and constraints that can only be changed with an update of the basic cell configuration, including the physical layer mode, type of deployment (cellular, isolated hot spot), cell range, and the base station (BS) antenna configuration. Furthermore, mapping tables indicating the possible spatial schemes for each transport channel and terminal capability, as well as a list of possible combinations of dispersion code, PSRC, and precoding type can be generated at this stage.

The long-term part of the spatial scheme pre-configuration evaluates all parameters, decisions and constraints that normally change on time scales greater than one super-frame or issues that cannot be decided on a per-flow basis, like the overall selection of a scheme that applies to all users of a cell (e.g., configuration of a fixed beam approach, or multi-user precoding). Slowly varying parameters include user distribution, user speed, quality of CQI/CSI information, the flows' QoS parameter, and long-term channel characteristics, like average SINR, long-term channel rank and eigenvalues. Also certain flow-specific decision will be long-term oriented, e.g. the decision between long-term and short-term spatial processing.

Spatial scheme selection performs the remaining decisions based on decision criteria that change on a short-term basis include, e.g., number of active users, cell load (due to packet-oriented transmissions), and the short-term channel characteristics. The spatial scheme selection considers these parameters and adapts the spatial scheme per flow under the constraints set by the ***spatial scheme pre-configuration***.

An important additional part of the Spatial Scheme Controller is the ***calibration*** function. Calibration is required to relate a desired spatial distribution of energy in space to specific transmit weights and to allow exploitation of channel reciprocity in the TDD mode despite of RF front-end imperfections. The calibration function checks the calibration status of a link with the particular requirements of the selected spatial processing technique and triggers the corresponding calibration procedure if required. Calibration

is therefore invoked at flow setup and each time either the selected spatial scheme is altered or the calibration status changes (e.g. temporal expiry).

C.1.4 MAC control feedback

The definition of service primitives for the MAC Control Feedback service is driven completely by the demand for such feedback from the RLC system layer and the IP Convergence layer. In principle, all outputs from the main function blocks, and even internal states of these function blocks, could be made visible to upper layers, to enable various forms of inter-layer interaction. The set of required feedback parameters is under discussion. It includes SLC Cache levels (see below) as well as resource use per flow.

C.1.5 Radio packet transfer: Transmission and reception

The transmission control is performed in cooperation with the QoS control of the RLC system layer. A **Service Level Controller (SLC) Cache**, with per-flow queues for all downlink TDC, CDC and DAC flows, is assumed to be implemented within the MAC at each BS and RN. For uplink flows, corresponding buffers are present at each RN and UT.

The RLC layer Service level controller and flow scheduler (Section 4.1 and Appendix D.1.2) controls the inflows to the BS SLC Cache and monitors its state. The outflow from the SLC Cache is under control of a MAC:

- For BS-to-UT downlinks and BS-to-RN relay links, the MAC at the BS controls the transmission.
- For UT-to-RN uplinks, the MAC at the RN controls the transmission.
- For UT-to-BS uplinks, the MAC at the BS controls the transmission.

Packet transmission and reception will be handled differently for the five transport channels. BCH packets and RAC packets are encoded at transmission and decoded at reception, but are not processed further by the MAC layer. TDC, CDC and DAC packets are processed by a more elaborate transmit and receive sequence that is divided into *five protocol sub-layers*, as illustrated by Figure 3.4:

MAC-5: Performs optional segmentation and reassembly of MAC SDUs (i.e. RLC PDUs). MAC-5 also performs flow identification at reception.

MAC-4: Sender adds CRC, resulting in a *retransmission unit (RTU)*. Receiver checks CRC and may ask for retransmission in case of error. The retransmission mechanism is denoted *MAC retransmission*.

MAC-3: Sender performs optional segmentation of RTUs into *encoding blocks.* The receiver then performs reassembly of received blocks into RTUs.

MAC-2: Coding of each encoding block results in an *FEC block* (forward-error-correction coded block) that is saved in the appropriate RSB queue. The receiver decodes each FEC block. It may also perform (soft) combination with retransmitted FEC blocks. This encoding /decoding will in the following be referred to as the *outer code*. Encoding and decoding schemes have been discussed in Appendix B.2.

MAC-1: Performs puncturing of FEC blocks and resource mapping onto assigned chunks. ***Resource mapping*** is a separate main function of the MAC user plane.

The protocol sub-layers MAC-5–MAC-2 may all be transparent, i.e. their functions are optional. Special cases of this transmission sequence accommodate all retransmission schemes and segmentation strategies that are at present under consideration. The design outlined above performs segmentation and encoding before the mapping onto chunks. It thus decouples the segment size used for retransmission from the chunk size. It also decouples the code block size from the chunk size, in a practical way. These factors are also important when the WINNER radio interface concept is used as a test-bed to compare and evaluate different combinations of MAC retransmission strategies and coding schemes.

For BCH, the mapping onto super-frame control symbols is controlled by the ***Resource partitioning*** function For TDC, CDC and DAC, the ***Transfer control*** function supervises both transmission and reception.

The transmission control is focused at fast transfer via the physical layer:

- For adaptively allocated TDC downlink flows, a transmission can be initiated during the downlink part of frame *j* and then be performed during the downlink slot of frame *j+1*.
- For adaptively allocated TDC uplink flows, a transmission can by requested during frame *j*, prepared and scheduled during frame *j+1* and then be performed in the uplink slot of frame *j+2*.

- For non-frequency adaptively allocated TDC and CDC downlink flows, the scheduling can be determined during frame *j*. An allocation table is transmitted in the first DL OFDM symbol of frame *j+1*. The transmission can then be performed either within frame *j+1* or during frame *j+2*.
- For non-frequency adaptively allocated TDC uplink flows, the transmission is initiated during frame *j* and is then performed in the uplink slot of frame *j+1*.

Thus, the delay from initiation of a transmission to its completion is 1.0–2.5 frames (0.7–1.7 ms) over one hop. Multi-hop transmission will add to the total delay. The roundtrip delay until a MAC retransmission can be performed depends on the decoding delay. The computation speed estimates presented in Table B2 in Appendix B.2.1 is around 200 kbit/ms. The additional decoding delay for the outer code should then not exceed 0.1 ms for RTU sizes of interest (up to 1520 bytes).

The transmission of packets belonging to the different transport channels is summarised below.

TDC (downlinks and uplinks): Packets in scheduled Targeted Data Channel flows are optionally segmented and then coded, using the transmission sequence outlined above. The FEC blocks are buffered by per-flow queuing in the resource scheduling buffer. Scheduling and the subsequent mapping is then performed by either the adaptive or the non-frequency adaptive resource scheduling algorithm, depending on the assignment of the flow. Thereafter, transmission proceeds using the PHY Adaptive transfer or Non-frequency adaptive transfer services. At reception, complete FEC blocks are delivered to the MAC. In *downlinks*, the MAC at the BS or RN controls the transmission. In *uplinks*, packet transmissions are initiated by UT requests. The MAC at the BS/RN with which the UT communicates controls the subsequent scheduling, transmission and retransmission.

CDC (downlinks only): The point-to-multipoint transmission has to deal with a wide variety of channels and directions to the destination users. This complicates the adjustment of the transmission parameters and the use of beamforming. To reduce the problems, a CDC flow may be partitioned into separate copies, *targeted flows*, which are destined to specific groups (clusters) of users in different directions/within different beams. A CDC flow is processed through the MAC-5–MAC-2 protocol layers. The resulting FEC blocks are copied into one or several queues in the RSB, one queue for each targeted flow. Scheduling and mapping of each targeted flow then proceed by non-frequency adaptive transmission, with transmission parameters that are adjusted in a conservative way. The transmission uses the PHY Non-frequency adaptive transfer service. At reception, complete FEC blocks are delivered to the MAC, where they are decoded. Packets (MAC SDUs) are finally recombined if segmentation was used. A reliable multicast service may utilise retransmission. The retransmissions could be triggered by NACKs from any of the destination users of a targeted flow. Schemes that combine this mechanism with ACKs from the terminal with worst channel are also possible.

DAC (uplinks only): Contention-based transmission is potentially the best way of transmitting uplink flows that have small packets with a low packet arrival rate. The main current proposal for contention-based transmission is a scheme that uses carrier-sense multiple access and therefore requires a constant set of frequencies to be assigned exclusively during the whole super-frame. When an uplink packet destined for contention-based transmission is drained from the SLC Cache at the UT, it is prepared for possible retransmission and then coded. The same function blocks/sub-layers as for TDC and CDC transmission are used, but the parameter settings may be different. The FEC blocks are transmitted by using the PHY contention-based transfer service. Received DAC FEC blocks are decoded and the RTUs are possibly retransmitted if an error is detected.

BCH (downlinks only): The BCH packets contain control signalling from higher layers. The range of their reliable reception places an upper bound on the size of the cell. These downlink broadcast channel packets are combined with super-frame control information. The combined packets are low-rate encoded in the MAC combined with space-time-frequency (inner) encoding performed at the PHY layer. Transmission and reception proceeds via the PHY BCH and SF control transfer service. Retransmission cannot be used. Adjacent BS and RN should use orthogonal time-frequency sets within this timeslot for their downlink preamble control transmission, to limit their mutual interference

RAC (uplinks and, for TDD, BS-to-BS/RN): The Random access channel can be used for initial access to a BS or RN by the UTs, e.g. after handover. RAC packets are coded and then transmitted in the reserved time-slot of the super-frame preamble in a contention-based manner. Transmission and reception proceeds via the PHY RAC transfer service. The MAC protocol and transmission strategy for this channel has not yet been defined.

The RAC time-slot can in TDD systems can also be used for *BS-to-BS and RN-to-BS over-the-air control signalling*. A BS or RN involved in this transmission would use the RAC for transmission in a few super-frames, while it listens for reception in the others.

C.1.6 Resource scheduling

The ***Resource scheduler*** determines the resource mapping for TDC and CDC flows. It utilises two scheduling algorithms:

- The ***Adaptive resource scheduler***, used for high-performance TDC transmission.
- The ***Non-frequency adaptive resource scheduler***, used for all CDC flows and as a fallback alternative for TDC flows. It is also foreseen to be used for parts of the control signalling.

These algorithms take priorities from the RLC Service Level Controller into account, as well as the queue levels in the RSB and the SLC Cache.

In addition, the resource scheduler contains several support functions: ***Spatial link adaptation***, ***Uplink slow power control, Active set selection, RS parameterisation and Allocation Statistics***, that will not be discussed further here.

- The ***adaptive resource scheduling*** and transmission uses predictions of channel quality information (CQI) to *utilise the small-scale and frequency-selective variations of the channel* for different terminals. The scheduler assigns a set of chunk layers (see Section 1.3.2) within the frame to each flow. After scheduling, the RSB queues are drained with bit-level resolution. The bits from each flow are mapped onto the assigned chunk layers. This mapping is exclusive, i.e. several flows do not share a chunk layer. The transmission parameters within each chunk layer are adjusted individually through link adaptation to the frequency-selective channel of the selected user. This link adaptation may use combinations of adaptive modulation, (inner) coding that is adjusted to each chunk, and power control. The link adaptation can be designed to provide a target SINR per bit for the FEC blocs that are coded with the (outer) FEC code. It then converts the fading channel into something approximating an AWGN channel, as seen by the outer code. Link adaptation may be combined with spatial multiplexing, for example in the form of per-stream rate control, where different FEC blocks of one flow are mapped to different chunk layers. By selecting the best resources for each flow, multi-user scheduling gains can be realised. The scheduling algorithm should take into account the *channel quality information* of each user in each chunk layer, the RLC flow *transmission requirements/priorities* and the *queue levels*. Timely channel quality information requires the SINR within each chunk layer and for each candidate terminal to be predicted with relatively high accuracy. The most advanced multi-antenna transmit schemes furthermore require the whole MIMO channel gain matrix to be known at the transmitter. This is denoted full *channel state information (CSI)*.
- ***Non-frequency adaptive resource scheduling*** and transmission is instead based on *averaging strategies*. Such transmission schemes are designed to combat and reduce the effect of the variability of the SINR, by interleaving, space-time-frequency coding and diversity combining. Non-frequency adaptive transmission is required when fast channel feedback is unreliable due to e.g. a high terminal velocity or a low SINR [WIND24], or when the terminal does not support adaptive transmission. It is also required for point-to-multipoint communication belonging to the common data channel (CDC) flows. The non-frequency adaptive transmission slowly adapts to the shadow fading, but it averages over the frequency selective (small-scale) fading. It requires the FEC blocks to be mapped on a set of chunks that are widely dispersed in frequency and if possible on different antennas to maximise the effectiveness of the coding and interleaving.

Figure C.2 below gives an overview of the downlink transmission of scheduled flows. Among other things, this figure illustrates that two scheduling entities control the flows, and have to cooperate. The Flow scheduler at the RLC system layer is part of the Service level controller (Section 4.1 and Appendix D.1.2). The Resource scheduler at the MAC system layer works on a faster time scale and takes the channel properties into account. The adaptive RS uses detailed knowledge of the available resources, the non-frequency adaptive RS has to work with more crude measurements of the average channel qualities In the present design, these SLC and the RS interact in a very simple way: The SLC fills the SCL Cache, while the RS is responsible for draining it. The SCL furthermore reports priorities of each flow to the RS. Only a few priority levels are used. The RS drains the queues and allocates the transmission resources in a way that optimises a criterion that takes the queue levels and the priorities into account. Existing algorithms with *very low computational complexity* can be used to solve the resource scheduling problem, when formulated in this way. See e.g. Chapters 6 and 7 in [Eri04]. These algorithms have computational complexity that grows linearly with the number of scheduled resources and linearly with the number of scheduled flows. Execution times below 0.1 ms can be attained, which is consistent with the very fast transmission strategies outlined in Appendix C.1.5 above.

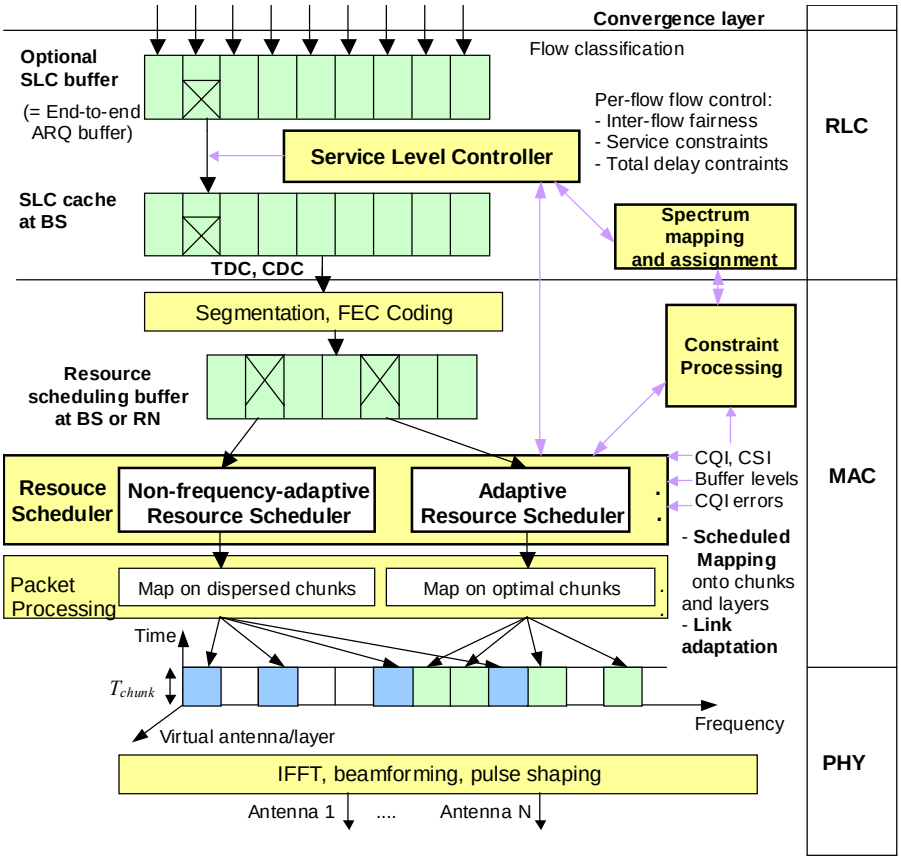

Figure C.2: Data flows and some control functions in downlinks of the scheduled data channels.

Adaptive transmission requires prediction of the channel quality due to the transmission control loop delay. In [WIND24], summarised in Appendix B.5.2, the predictability and attainable prediction accuracy is investigated as a function of the SINR and the terminal velocity. The effect of the prediction errors on the attainable adaptive transmission performance and on attainable multi-user scheduling gain was investigated. Fast adaptation control loops are a part of the WINNER design. With correspondingly low delays, adaptive transmission was found feasible at vehicular velocities at 5 GHz carrier frequencies. A SINR and velocity-dependent boundary delineates when adaptive or non-frequency adaptive transmission is the best alternative (Appendix B.5.2). This decision is taken at flow setup, and may be changed later.

Both downlink and uplink power control is supervised by the Resource scheduler and is integrated into the optimisation of the transmission parameters.

A novel framework had been developed for handling the spatial dimension of the multi-user scheduling and link adaptation problem. It integrates various SDMA (spatial division multiple access) strategies into the total solution.

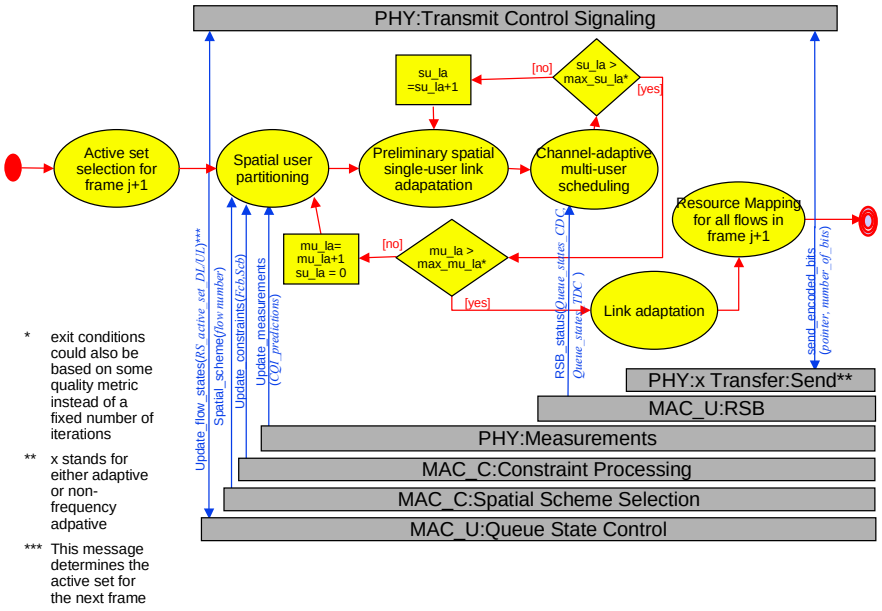

Figure C.3: Resource scheduling sequence overview (adaptive and non-frequency adaptive).

As outlined by Figure C.3 above, adaptive multi-antenna link adaptation and scheduling is separated into four steps, to limit the computational complexity so that a fast feedback loop is obtained:

1) **Spatial user partitioning**, i.e. separation of users into spatially well separated sets.
2) **Preliminary single-user link adaptation** for each potential user and potential resource.
3) **Channel-adaptive multi-user scheduling** within the sets of spatially highly-interfering terminals, using the chunk capacities calculated in step 2. (In case of non-frequency adaptive transmission, only slow adaptation to the shadow fading is used.)
4) **Final link adaptation**, resource mapping and transmission of the selected flows, using either the link adaptation parameters that were determined in step 2, or iteratively refined schemes.

The sequence can be iterated a few times to improve the estimate of the spatial inter-set interference

Step 1, the spatial user partitioning will be discussed in more detail in Appendix C.1.7 below. Step 2, the single-user link adaptation, was discussed briefly in Appendix B.5.1.4.

The channel-adaptive multi-user scheduling should in general be designed to take queue levels into account, as discussed above. In the simulation evaluation investigations presented in Appendix G below, the simplification of a *full queue model* was used. The following simple resource scheduling strategies were used in most of the investigations on adaptive transmission:

- Round robin, i.e. periodic allocation to all flows,
- Max rate scheduling, i.e. giving the resource to the flow that can have the highest throughput,
- Score-based scheduling [Bon04], a modified proportional fair strategy.

To reflect the bursty nature of packet flows and to limit the transmission overhead, each adaptively allocated TDC flow shifts between the following states:

- **Passive**. The flow has an empty RSB queue and no packet in the SLC Cache. Minimal transmission control signalling is required. Terminals may be in micro-sleep mode except during specified control transmission time-slots.
- **Semi-active**. This state is only used for adaptively allocated TDC flows. The flow has segments in queue, but is not eligible for scheduling during the present frame.
- **Active**. The flow is eligible for scheduling during the present frame. The full transmission control loop is up and running.

The transition between these three states and the corresponding PHY control messaging is governed by the ***Queue state control*** function within the Flow state controller and the ***active set selection*** in the RS. The queue state is updated every slot (half-frame).

In cells with few flows, all flows with packets to transmit will be in the active state. In cells with many flows assigned for adaptive transmission, the access to the active state can be restricted, to limit several types of complexity and overhead: The *scheduling computational complexity*, the *downlink control overhead*, the *channel prediction complexity* and the *CQI and CSI feedback signalling overhead*.

C.1.7 SDMA and spatial user partitioning.

The task of ***spatial user partitioning*** is to separate the user terminals into *spatial sets* with low mutual interference. The aim is to group the user terminals so that their correlation matrix (power at receiver i, resulting from a downlink transmission to terminal j) becomes approximately block diagonal. *Highly* interfering terminals are placed into the *same* spatial sets; members of pairs with mutual interference below a pre-defined threshold can be placed in *different* sets. Once such spatial sets are established, we can use SDMA for flows of *different* sets. Such groups of flows that share a chunk are called (spatial user) *groupings*. Other multiple access schemes (such as TDMA, FDMA) are used to avoid interference when transmitting to/from users within the same set. The sets can be thought of as (generalised) beams. They are reached by using specific spatial precoding (beamforming) weights.

The spatial user partitioning allows controlling the interference generated by SDMA by setting appropriate interference thresholds during the generation of the spatial sets. Therefore the allowed SDMA interference can be considered in the overall interference prediction used for in resource scheduling in the individual spatial sets. To a first approximation, we can therefore *assume that the subsequent multi-user scheduling can be performed independently within each spatial set of terminals*. This reduces the computational complexity drastically; spatial user partitioning reduces the problem of multi-user multi-antenna scheduling to that of performing chunk-adaptive multi-user scheduling within the individual sets.

The procedure to obtain such spatial sets depends on the amount of channel knowledge at the transmitter. If channel state information (CSI) is available at the transmitter, the spatial sets can be generated by calculating the mutual correlation between users. If only a channel quality indicator (CQI) is available, so-called opportunistic or grid-of-beams beamforming approaches are used.

As the number of users increases, it becomes increasingly complex to find spatial sets with good separation properties and testing all possible terminal combinations must be avoided[20]. We may then partition the time-frequency resources into two or more groups, and assign subsets of users to each group. These subsets of user terminals are called *orthogonal groups***.** If this grouping is performed properly, it simplifies the task of forming well-separated spatial sets within each orthogonal group. Different criteria to form orthogonal groups are conceivable, e.g.

- For fixed beamforming the users associated to beams that can be transmitted concurrently with inter-beam interference below a pre-defined threshold can form one orthogonal group.
- For adaptive precoding, terminals can be grouped according to their SINR requirements (i.e., according to their target data rates and interference suppression capabilities). This allows using different SDMA interference thresholds in the different groups. It therefore improves the overall opportunities for SDMA (which would otherwise be limited over all resources by the weakest terminal).

The SDMA decision must be integrated in the overall resource allocation process, i.e. the decision must integrate the priorities due to QoS contracts and the opportunities and constraints due to the spatial channel characteristics. The numbers of users served concurrently by SDMA is a parameter which has a significant impact on the performance: the throughput gain offered by serving multiple users at the same time comes at the expense of serving each user with a smaller fraction of the available transmit power.

An example of the use of SDMA and spatial user partitioning is given in Appendix G.2.2. Furthermore, a specific algorithm for creating spatial groupings is discussed in more detail below.

[20] The complexity is especially severe in cases where CSI is used at the TX for precoding, because the precoding solution depends on the combination (and possibly also on the user ordering) to be tested and again differs for every chunk.

Low Complexity Space-Time-Frequency User Partitioning for MIMO Systems with SDMA

The algorithm was originally derived for a precoding technique that forces the interference to be zero between all users that are served simultaneous via SDMA. Even if no interference is present, spatial scheduling is of crucial importance. If users with spatially correlated channel subspaces are served jointly, this leads to inefficient precoding matrices and a drop in the strength of the equivalent channel after precoding. The goal of the algorithm is therefore to group together users with uncorrelated channels. The precoding technique under investigation allowed the use of an efficient approximation technique based on orthogonal projection matrices to calculate the capacity after precoding, which serves as a scheduling metric. The capacity estimate also allows to inherently consider the effect of different group sizes, since it includes the transmit power. In the case of precoding where interference is not fully suppressed, the problem of correlated subspaces will lead to a slight reduction in link quality and to an increase in interference. Since the latter is dual to the drop in link quality in the zero forcing case, the proposed solution is also applicable in the non-ZF case as shown in [FDGH05b].

An iterative method for forming these groupings, presented in [FDGH05a], will be described briefly.

For any users g out of G users, a rough estimate $\eta_g^{(S)}$ is calculated that represents the spectral efficiency that *would* result if that user *were* allowed to transmit in the selected way. It approximates the inter-layer interference effect and can be calculated by a simplified projection scheme, see [FDGH05a], [FDGH05b]. The equivalent channel of user g is represented by its channel matrix after an orthogonal projection into the null-space of a joint channel matrix containing all G users' channels, *except* that of the g'th. The resulting chunk throughput when transmitting to all users in the grouping is simply estimated as the sum of the G individual terms $\eta_g^{(S)}$.

The iterative tree-based scheme for forming appropriate groupings can now be explained as follows. Let us start with a situation where all users are part of one spatial set, i.e. each use forms a separate grouping with only one member (lowest row in Figure C.4). SDMA would then not be used at all within the cell. First, the user with the best metric is identified. In the figure, it is user number 1. Then, one user at a time is added to it and the metric sum of the combination is calculated. The combination with the highest metric sum is kept as candidate user groupings with size 2. The algorithm is repeated to test and form a grouping of size 3. It proceeds in this way up to the maximum allowed group size. When done, the grouping of size G with the highest metric sum $\hat{C}_G$ (or highest capacity if higher accuracy is desired) out of all candidate groupings (marked in red for $G = 3$ in the example in Figure C.4) is chosen. To reduce complexity even further, the solution can be tracked in time. Instead of calculating the entire tree, the sorting starts with the previously found solution and proceeds, e.g., one level up in the tree and two levels down again, updating also the previous solution. The sub-grouping is then selected only from three new candidates. Going top-down in the tree is achieved by testing one by one which user to delete from the grouping in order for the remaining group to have maximum sum metric.

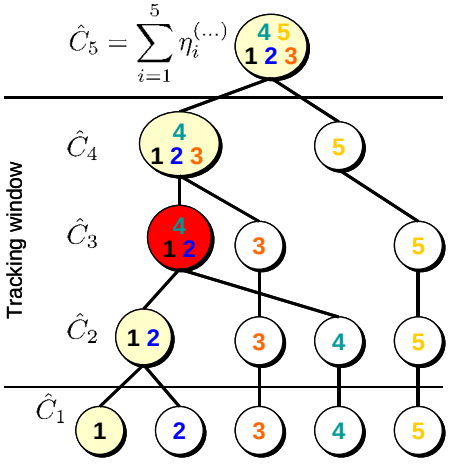

Figure C.4: In a system with 5 users, candidate user grouping are built by adding one user at a time and keeping the grouping with highest sum metric. Finally, the grouping with highest sum metric (e.g., the one marked in red) out of all candidate groupings (marked in yellow) is used.

C.1.8 Timing of the execution of the main MAC functions

The main functions of the control plane (C) and the user plane (U) are executed on the following time scales:

Executed once every super-frame:

- Constraint combining (C).
- Resource partitioning (C).
- Spatial scheme selection (C).
- Coding, resource mapping and PHY transmission of RAC and BCH flows (U).
- Reception from PHY and decoding of RAC and BCH FEC blocks (U).

The execution of the following functions is trigger-based, when required:

- Flow setup control (C).
- Flow release control (C).
- Spatial scheme pre-configuration (long-term decisions and constraints) (C).
- Calibration in the spatial scheme controller (C).
- Support functions within the resource scheduler (U).

Executed every slot (half-frame in FDD, UL / DL period of frame in TDD):

- Queue state control (U).
- Resource scheduling (U).
- Coding, segmentation, resource mapping and PHY transmission of TDC and CDC flows (U).
- Reception from PHY, decoding and reassembly of TDC and CDC FEC blocks (U).

C.2 Functional architecture for peer-to-peer MAC

C.2.1 MAC services provided for peer-to-peer transmission

The *Radio_Resource_Control* service for P2P transmission is used to start, maintain, and stop the operation of a P2P-DAC in the BS. User terminals, which intend transmitting peer-to-peer, have to attach to the channel before transferring data using this service. Detaching terminals from the DAC is another service that is provided. If a UT intends to transmit data packets synchronously, the service provides functions to create and terminate a synchronous data flow. The primitives, of type req: *request*, ind: *indication*, rsp: *response* and cnf: *confirm*, that are provided to use this service at higher layers, are summarised in Table C.1.

Table C.1: Overview on MAC_P2P_CONTROL primitives for P2P transmission

Name	req	ind	rsp	cnf
MAC_P2P_CONTROL_START_DAC	✓	-	-	✓
MAC_P2P_CONTROL_STOP_DAC	✓	-	-	-
MAC_P2P_CONTROL_ATTACH_TO_DAC	✓	✓	✓	✓
MAC_P2P_CONTROL_ATTACH_INFO	-	✓	-	-
MAC_P2P_CONTROL_DETACH_FROM_DAC	✓	✓	-	✓
MAC_P2P_CONTROL_CREATE_SYNC_FLOW	✓	-	-	✓
MAC_P2P_CONTROL_TERMINATE_SYNC_FLOW	✓	-	-	✓

After the P2P-DAC has been configured appropriately and the UTs involved in P2P/PMP transmission have been attached, the *Radio_Packet_Transfer* service for P2P transmission can be used to exchange

segmented packets either asynchronously or synchronously between peer terminals. The primitives, which are provided to use this service at higher layers, are summarised in Table C.2.

Table C.2: Overview on MAC_P2P_USER primitives for P2P transmission

Name	req	ind	rsp	cnf
MAC_P2P_USER_SYNC_DATA	✓	✓	-	✓
MAC_P2P_USER_ASYNC_DATA	✓	✓	-	✓

C.2.2 MAC functions provided for peer-to-peer transmission

DAC-P2P flow setup, data transfer, and flow termination

Figure C.5 shows the state-transition diagram implemented in the P2P-DAC flow setup and termination unit of the base station (see Figure 3.7). After radio resources have been allocated for the DAC, the service primitive START_DAC.req triggers the execution of the *P2P-DAC initialisation function* and the transition to state P2P-DAC_ACTIVE. In this state, the *P2P-DAC beacon/resource control function* is continuously executed to control the operation of the DAC by broadcasting beacons with the appropriate information about the available DAC service and the current DAC frame structure. This control function is terminated by executing the *P2P-DAC terminate function* after receiving a STOP_DAC.req.

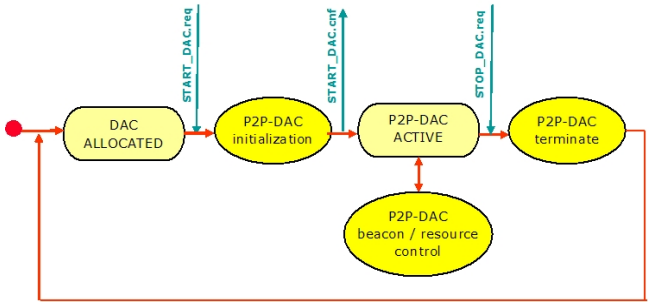

Figure C.5: State-transition diagram of P2P-DAC flow setup and termination in the base station.

The state-transition diagram in Figure C.6 illustrates how the various protocol functions of the P2P-MAC interact with each other in the UT to setup a P2P-DAC flow, control the data transfer, and terminate the flow.

After being synchronised to the BS, the user starts the *P2P-DAC attach function* by sending an ATTACH_TO_DAC.req primitive to the flow setup and termination unit. This function conveys to the BS information about the UT, and the BS assigns to the UT a unique identifier for efficient addressing. After its successful completion, a confirmation is sent to the user before the finite-state machine transits to state ATTACHED. A UT can detach from the DAC at any time by executing the *P2P-DAC detach function*.

In the state ATTACHED, the user can request an asynchronous transfer of a radio packet in the CAP or GAP to the peer UT by sending a USER_ASYNC_DATA.req. This initiates the execution of the *P2P-DAC asynchronous transfer control function*. If the packet should be transmitted in the GAP, the UT informs the BS with an UL command of the pending transmission request. If resources are available, the BS schedules time slots for the transfer request and announces the availability of the time slots for the requested P2P transfer in the beacon. The transfer control function then controls segmentation, retransmission, and multiplexing of the segmented radio packet onto the assigned time slots. If the packet should be transmitted in the CAP, the request is forwarded to the *P2P-DAC channel access control function*. After completing the data transfer, the successful transfer is confirmed and the finite-state machine returns to state ATTACHED.

Before radio packets can be synchronously transferred between peer UTs, a service user has to request the execution of *P2P-flow setup function* by sending a CREATE_P2P_FLOW.req. This procedure establishes a synchronous P2P-flow by exchanging protocol messages between the UTs and the BS. If time slots are

periodically available for the requested data transfer, the BS assigns a unique index to the newly created flow. After the successful completion of the procedure, a confirmation is sent to the user and the finite-state machine transits to state P2P-FLOW_ESTABLISHED. A UT can terminate a P2P-flow by executing the *P2P-flow termination function.*

In the state P2P-FLOW_ESTABLISHED, the user can request a synchronous transfer of radio packet on the pre-established P2P-flow by sending the USER_SYNC_DATA.req primitive. This primitive initiates the execution the *P2P-DAC synchronous transfer control function*, which controls segmentation, retransmission, and the multiplexing of the segmented data to the pre-allocated time slots of the DAC frame. After the completion of the data transfer, the transfer is confirmed and the finite-state machine returns to state P2P-FLOW_ESTABLISHED.

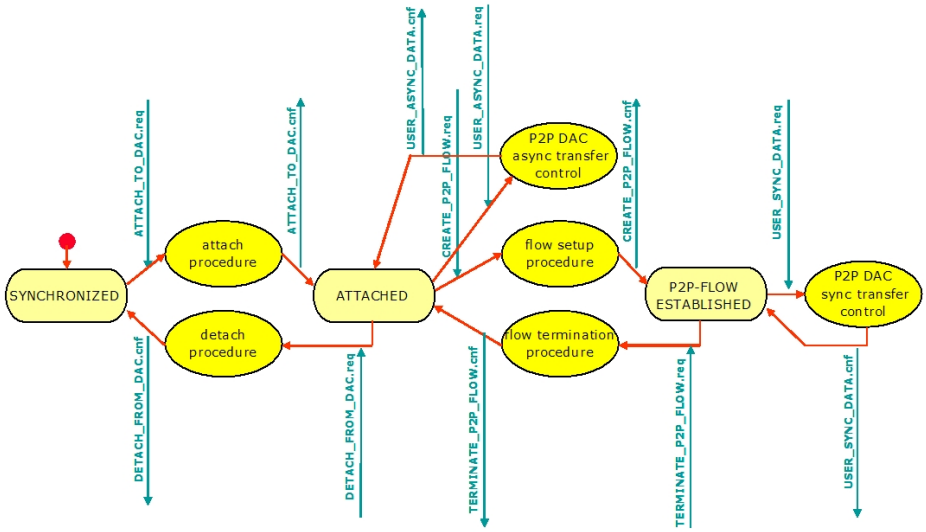

Figure C.6: State-transition diagram of P2P-DAC flow setup, transfer control, and flow termination in the user terminal.

P2P-DAC channel access control functions

The *P2P-DAC channel access control functions* give UTs random access to the P2P-DAC for transmitting control messages to the BS, and exchanging protocol messages or small amount of user data between peers.

A UT, which is synchronised to the P2P-DAC, can transmit command frames to the BS in the UL command time slot by using a slotted ALOHA access protocol. The access to the time slot is controlled by a contention window that is maintained by each UT. The size of the window is defined as $cw(a)=min\{2^{a+1},256\}$, where a represents the number of retransmission attempts already made by the UT. The UT chooses a uniformly distributed random value r within the interval $[1,cw(a)]$ and starts the access after r DAC frames. After receiving a response from the BS indicating successful command reception, the parameter is reset to zero.

A UT, which is attached to the P2P-DAC, can asynchronously transmit control messages or a small amount of data to a peer UT in the contention-access period. Since no establishment of a synchronous P2P flow is required, this method leads to a faster access and data transfer. The basic medium access mechanism used in the CAP is the well-known carrier-sense multiple access scheme with collision avoidance. A UT with a pending data transmit-request senses the state of the wireless medium before it can transmit. If the medium is idle longer than a pre-defined time interval, it can proceed with the transmission. Otherwise, it first waits until the medium becomes free, then generates a random backoff time before it tries to transmit in order to minimise the risk of collisions with transmit request issued by other terminals.

C.3 Chunk definition

The scaling of chunks in the WINNER system is based on the following general considerations:

- The appropriate frequency extent of a chunk should be determined by analysing the balance between two factors: 1) The performance loss due to channel variability within the chunk, which is decreased with narrow chunks. This factor depends on the typical channel power delay profile, which is in turn related to the cell size and the deployment scenario. 2) The required control overhead and feedback rate with adaptive transmission, which is decreased with wide chunks.
- The appropriate time duration of a chunk is determined by the following factors: 1) Short chunks lead to a small overall radio interface delay. 2) Short chunks enable the design of feedback loops for adaptive transmission also for fast fading channels. 3) Short chunks may contain so few payload symbols that the overhead due to pilots and in-band control symbols becomes prohibitive. 4) Long chunks may contain too many payload symbols. Transmission of small FEC blocks will then become problematic, since flows are in general mapped exclusively to flows in adaptive transmission, without chunk-sharing.

The chunk definitions found below are specified for the (frequency) adaptive transmission mode, which will be used whenever precise channel quality information is available at the transmitter, to steer link adaptation on a fine granularity level. Within chunks allocated for non-frequency adaptive transmission, there is a potential need for a more fine-grained rate matching. Solutions to solve this problem are outlined in Section 3.1.6.

The chunk width is set to *8 subcarriers, or 312.5 KHz* in the FDD mode and to *16 subcarriers, or 781.2 KHz* in the TDD mode. The motivation for this difference in chunk widths is that the FDD mode has in WINNER phase I been evaluated in rural area and metropolitan area deployments, with rather high delay spread and frequency selectivity in the channels, see Table F.1 in Appendix F. The TDD mode has been evaluated primarily in short-range deployments with less delay spread in the channel models and thus less frequency selectivity.

Thus, the usable 416 subcarriers in the FDD mode are partitioned into 52 chunks, the usable 1664 subcarriers in the TDD mode are partitioned into 104 chunks. The radio interface delay requirement of 1 ms [WIND71] can be interpreted as a requirement on the slot duration of the FDD transmission, and the uplink and downlink slot lengths of the TDD transmission, by the following reasoning: The shortest control loop for a transmission consists of a request, response, and transmission. Each such sequence should have duration of approximately 1 ms. The chunk durations T_{chunk} of the FDD mode will therefore be set to 12 OFDM symbols plus guard times, or 345.6 μs. The ***frame*** of the half-duplex FDD system consists of a downlink chunk followed by an uplink chunk, with duration $T_{frame} = 2\ T_{chunk} = 691.2$ μs. The frame of the TDD mode consists of a downlink period + duplex guard time + uplink period + duplex guard time. This frame duration is set equal to the FDD frame duration of 691.2 μs, to simplify inter-mode cooperation. The TDD chunk duration is set to 5 OFDM symbols plus guard times = 108.8 μs. The duplex guard time is set to 19.2 μs. Each TDD frame contains 6 chunks plus two duplex guard times. With asymmetry 1:1, each frame contains three uplink chunks and three downlink chunks.

A chunk thus contains 96 symbols in the FDD cellular mode when used for CP-OFDM transmission and 80 symbols in the TDD cellular mode. See Figure 3.1.

Appendix D. Radio Resource Management (RRM) and Radio Resource Control (RRC)

D.1 RRM functions

D.1.1 Spectrum control

Spectrum Sharing

Spectrum Sharing controls the access to the spectrum in frequency bands which are shared with other RATs, which are probably the ones used by legacy systems. Depending on the regulatory rules governing the shared bands, different scenarios for spectrum sharing are possible:

Horizontal sharing: The involved systems in the shared frequency band have equal regulatory status, i.e. no system has priority over the other(s) in accessing the spectrum.

- *Horizontal sharing without coordination*: No signalling is required between the involved systems, as e.g. nowadays on the ISM band. Since QoS cannot be guaranteed for any system, this possibility is not considered in further detail.
- *Horizontal sharing with coordination*: The involved systems coordinate their spectrum access based on a set of predefined rules (spectrum etiquette) that all systems adhere to. This requires capabilities for signalling or at least detection of the other systems.

Vertical sharing: In this modality, sharing is performed with clearly established priorities. The primary system has preference in accessing the spectrum and the secondary system(s) may only use the spectrum as long as they do not cause harmful interference towards the primary.

The most important as well as complex service component is the one where WINNER is the secondary system, which controls the emissions from the WINNER system to avoid harmful interference towards legacy systems. This function first has to reliably identify the "white spaces", i.e. unused spectrum and then determines the transmit constraints of the WINNER system. The identification of the *white spaces* can be based on measurements, and it can be significantly assisted with information provided by a spectrum database or a central radio controller. Based on the available and measured information, constraints for the transmit parameters are determined and signalled to the constraint processing function in the MAC layer.

Spectrum Assignment

Spectrum Assignment periodically reassigns a portion of the available spectral resources between multiple WINNER RANs. In contrast to the conventional fixed spectrum assignment, herein it allows dynamical balancing of spectral resources between networks. As a result, spectral resources available for a network can be adjusted according to, e.g., changes on the operators' customer base (or market shares). Spectrum assignment also facilitates introduction of operators with relatively small customer base or network coverage area. In addition, spectral resources can be re-assigned according to the variations on the aggregate loads on the networks, hence, enhancing the overall use of spectrum over all networks.

Long-term Spectrum Assignment. The spectral resources assigned to the networks are defined in terms of chunks and, hence, separation between networks can be done either in frequency (e.g. in FDD mode) or both in time and frequency. One principle for the re-assignment assumed in the following is to keep the spectral resources assigned to the networks as orthogonal as possible. In other words, the resources are separated in time, frequency or space so that interference between networks is minimised. This prevents the need for extensive coordination (or tight coupling) between networks, for complicated interference management over multiple networks, as well as for strict limitations to the operation of RRM within networks. The principle likely favours TDD bands where orthogonal resource allocations are efficiently obtained in time. This is due to the synchronisation between networks required also with the conventional fixed spectrum assignment due to the adjacent channel interference. Other principles assumed in the following are:

- The spectrum assignment functionality is distributed to all networks, and re-assignments any negotiated between networks without any central controller.

- Central database containing relevant information on spectrum priorities as well as on fairness and cost metrics, enables higher layer control on the spectrum assignment through the priorities and fairness/cost metrics. It also enables simple introduction of new networks.
- Spectral resources are divided into two categories: resources assigned with a priority and common pool resources.
  - The purpose of resources assigned with a priority to a certain network is to guarantee basic operation of the network under all circumstances. A network can release some of the priority assigned resources for other networks, but it can retrieve the resource in the next negotiation phase. In other words, it has incontestable priority to the resource.
  - Common pool resources can be reserved by any network.
- Fairness and cost metrics are used in the negotiation of assignments to achieve fair and efficient allocation solution.
- Spectral resource assignments vary geographically, although spatially contiguous assignments are preferred to avoid unnecessary interference between networks. To facilitate smooth spatial transition in the assignments, it is envisaged that long-term assignment specifies for large geographical areas with spatial granularity of several cells (sets of cells), and short-term assignment optimises the border regions further with cell-wise resource assignments.
- Spectral resource re-assignment is done periodically and at a slow rate (i.e. several minutes).

It may be preferable that resources in the common pool are assigned to a network for multiple spectrum assignment periods at a time. In other words, not all common pool resources are re-assigned at each period. This results in a smoother spectrum assignment adaptation, and probably reduced need for the priority assigned spectral resources. A simple solution may be that assignments have a common duration of multiple assignment periods, and a resource can be released during the assignment.

*Short-term Spectrum Assignment***.** The short-term spectrum assignment complements the main spectrum assignment by providing short-term and local, i.e., cell-specific variations to the spectrum assignments covering large geographical areas. Hence it enables 1) faster adaptation to the local traffic load variations and 2) geographically more accurate spectrum assignments. In the part of faster adaptation to load variations, it provides complementary method for inter-network load sharing. The assessment of the true benefits of this approach in comparison to plain load sharing remains to be done in WINNER II.

The re-assignments of spectral resources are performed in the time scale of several seconds. To limit the induced complexity, the functionality resorts to only simple inter-network signalling. Functionality requests resources from other WINNER RANs after triggered by the long-term spectrum assignment or preventive load control. In the case of a resource request from other RANs, the functionality rejects, accepts or partially accepts the request based on information from load prediction and MAC control feedback on the overlapping and neighbouring cells. Inter-network signalling is performed either over the air or through the core network. For the over the air signalling, RAC is used through the MAC radio packet transfer service. The constraint information is updated based on the decisions and sent to appropriate MAC layer.

D.1.2 Service level control (SLC)

The SLC has the overall responsibility of adjusting inter-flow fairness and assuring the fulfilment of service level contract agreements and total delay constraints. In particular:

- it may perform by requesting resources from several BSs that may utilise different WINNER modes
- it works on a slow time scale characterised by the packet arrival rates
- it may allocate resources belonging to several modes/base stations.

The SLC forwards packets to SLC cache (Figure C.2) based on a predicted sum rate and QoS requirements which could be derived by the queue levels, feedbacked by the SLC cache. The SLC cache is kept rather small, corresponding to few frames while separate queues are allocated for each flow. Furthermore, the SLC assigns static priorities per flow and RS schedules based on priority, queuing time and channel state.

The service differentiation is exercised through the following service components, while an example is given in Figure D.1:

- *Flow Conditioning*: The traffic of each flow is conditioned to ensure that it complies with the corresponding profile definition; in particular the defined maximum traffic rate.
- *Flow Queuing*: In WINNER, it is assumed that separate queues are allocated for each flow. Packets in respective queue may get dropped during transient phases of congestion.
- *Flow Scheduling*: Flow scheduling may be considered as management between flows and determines the order in which PDUs will be forwarded to the SLC cache buffer residing at the MAC layer and works on a time scale characterised by the packet arrival rates.
- *Flow Monitoring*: The main aim for flow monitoring is to (as the name suggests) monitor the flow and provide feedback on flow traffic predictions to any other function that may require this information.

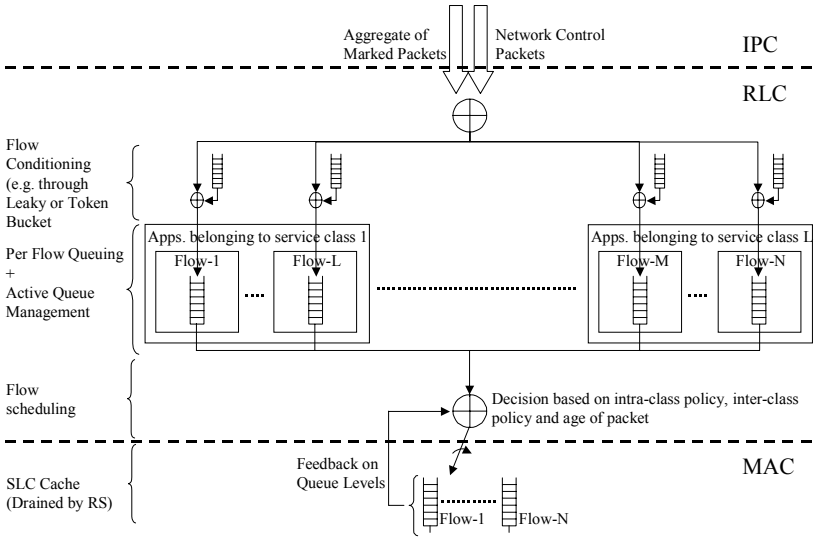

Figure D.1: Example of flow conditioning, flow queuing and flow scheduling.

D.1.3 Mode/RAN selection

The different architecture alternatives may be expected to differ in what decision variables are available and according to the way different available modes are used. We have above defined:

1. fast selection - which is a quasi-simultaneous operation of modes and will have to be performed in both the BS and the UT, the decision variables and boundary conditions are expected to be set by RRM but the selection decision has to be taken by MAC (Figure D.2)
2. slow selection - which is an RRM function to control alternative operation of modes, the process perhaps bearing many similarities to the RAN selection.
3. re-selection - which is an RRM/RRC function to handle changing radio conditions / availability of modes.

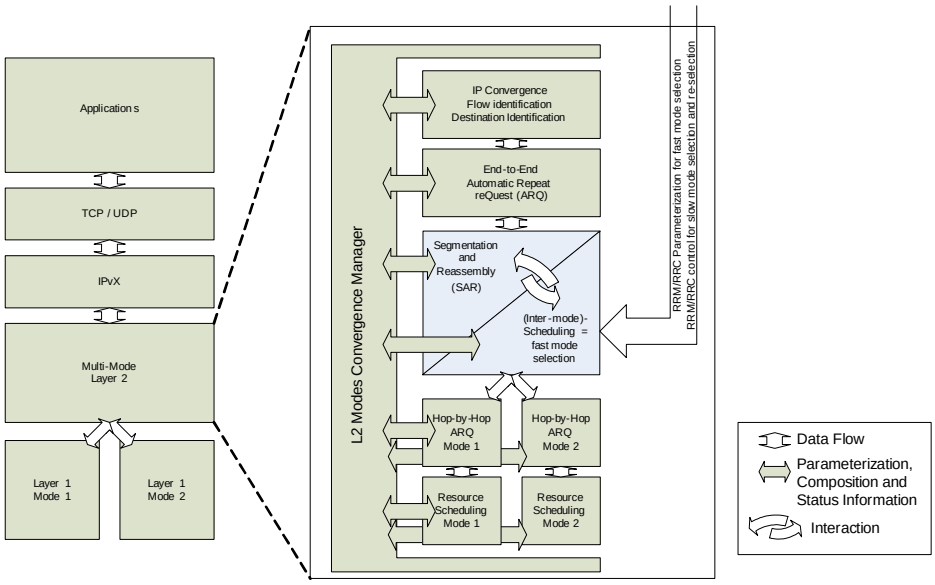

Figure D.2: User plane data flow and fast mode selection (not shown: slow mode selection and re-selection performed by RRM/RRC).

According to the variant of mode selection applied, a subset of the decision variables can be used:

- Mode availability - which subset of the modes that a terminal can support is in fact available at the current location.
- Service – the mode, which is most efficient for the service in question, is selected.
- Signal strength – the mode from which the strongest signal is received is selected. This is a simple version of the more sophisticated selection parameter radio resource cost discussed below.
- Radio resource consumption – the mode for which the least relative amount of radio resources (e.g. power, codes, timeslots, etc.) is required to support the users is selected.
- System load – the mode with the least relative load is selected. This does not necessarily improve capacity, but improves user quality at loads below the capacity limit, and avoids reallocations as the load approaches the capacity limit.
- Packet size – the mode which is most efficient for the packet size in question is selected.
- Price – the mode for which the price for supporting the user is lowest is selected. This is especially interesting in case the different modes are run by different operators, and the decision is taken by the end-user or the terminal.

The RAN selection algorithm selects the most suitable RAT for attending the service requests of UTs. Of importance here are the RAT's preferences for the requested service according to the QoS offered by each RAT and the balance among the radio resources occupation of the different RATs achieved by a suitable traffic load balance among them. The algorithm is based on the availability of a list for all the available RATs capable to provide the service. This list is made based on QoS information. A decisive factor for prioritising a RAT over another RAT will be the user preference [WIND41] [WIND42].

D.1.4 Handover

The general rules for handover between the WINNER modes are expected to be mode availability and terminal mobility. For example, UTs with high mobility are expected to always be connected with the wide area cell even if they are in the vicinity of the short range cell. Also, the triggers for handover and their thresholds between the two modes will depend on the deployment scenario i.e. extension of coverage and increase of spectral efficiency, as well as on the relaying concept. In case of an inter-system handover this is expected to take place either when there is loss of coverage of the current system or in the case of overlapping coverage due to user/operator preferences or traffic congestion. Example of handover triggers are given in [WIND41] [WIND42].

Intra-system handover

Since the wide area cell is going to exist as an umbrella over the short range cell, there is a need for making the UT aware that it has the option of changing to TDD mode. In order to allow for a seamless handover within the WINNER RAN, BSs and RNs of the same or different mode can announce their presence to the UTs by broadcasting control messages using orthogonal resources. This scheme is especially helpful for the handover between WINNER FDD and TDD as it allows the UTs to be aware of the presence of BSs and RNs that operate at a different mode without disrupting their normal operation to "sniff" other parts of the spectrum. Further information can be found at [WIND43] [WIND44].

Inter-system handover

Location-based Vertical Handover (VHO)

In a homogeneous system the scanning of other possible connections is triggered by the condition of the link, since an ongoing connection with good performance makes such a procedure dispensable. For a vertical handover continuous surveillance is mandatory. At the moment this can only be handled by the terminal itself because no entity exists for the integration and information exchange of different networks. Therefore the mobile must scan all other possible RATs. The autonomous gathering of information by means of scanning may impact both the own and other transmissions. Therefore it makes sense to look for alternative ways of gaining respective measurement results. Since the need for own measurements shall be reduced as much as possible, another way of gathering the relevant information is to employ measurement reports, which have been collected by other active UTs, within the same or within other systems. Information gathering within the same system thereby is required for horizontal handover (HHO) preparation, whereas for VHO information gathering between different types of systems is needed. However, information may also be used to control other mechanisms such as appropriate physical mode selection for link adaptation (LA) or (joint) Radio Resource Management (RRM). In all cases, the location-based VHO in combination with the Hybrid Information System (HIS) offers a great economic potential since participating devices can minimise or even avoid self-driven scanning procedures. The principle of the HIS presumes that each system collects data about the current link state within the covered cell and provides this information on request to mobiles that are willing to change their connection within the same system (HHO) or different systems (VHO) [WIND41] [WIND42] [WIND43] [WIND44].

CRRM based VHO

Another approach for an inter-system handover is based on the CRRM framework defined in the 3GPP [3GPP-TR25.891], which allows the exchange of load information between UMTS and GSM networks. The proposed algorithm takes in a first step only load criteria into account, but in a second step will include also service criteria [WIND41] [WIND42]. These algorithms can be extended to WINNER inter-mode handovers [WIND43] [WIND44].

D.1.5 Admission control

Admission control schemes are the decision making part of networks with the objective of providing to users services with guaranteed quality in order to reduce the network congestion and call dropping probabilities and achieve as much as possible resource utilisation. An example of an admission control algorithm for the selection of the appropriate RAT in the case of RAN cooperation is summarised below [WIND41] [WIND42] [WIND43] [WIND44]:

- The algorithm makes a list of the candidate serving networks and candidate cells for each network. The lists contain the candidate networks and cells capable of providing the requested flow service and they are ordered in such a way that better fulfils its requirements in each network.
- If there is only one RAT available in the flow's location area and the flow can be served by that RAT then it is selected, otherwise (if the flow cannot be served by that RAT) the flow will be rejected.

After selecting the target RAT the algorithm checks if the flow is new or from handover (which means that the flow was already going on in a RAT and for some reason it was decided to change its RAT). If it is a new flow, then if there are other flows waiting in the queue it will be rejected (or it will select another RAT if there is one in its list), otherwise it goes to the next step. The next step of the algorithm is to check (no matter if it is a handover or new flow) if there are sufficient resources in that network for the flow to be served. If there are sufficient resources, the flow will be admitted to the target RAT/mode. If the resources of the target RAN are insufficient it will be first checked if the flow can be served by another RAT/mode. If the flow is new and has low priority then it is rejected in this RAN and it's checked if another one can serve it and if none is available the flow is rejected. If the flow is from handover or a new - high prioritised, it is not rejected in the target RAT, but it is first checked if it can be served by another

RAT (suitable for it). If not, it is checked if there is a possibility that other ongoing flows can perform a handover to another suitable network. If this action does not also gain the needed resources for the flow, then it is checked if degrading the QoS of some ongoing flows (in this RAT) with low priority (where "low" is relative to the priority that the flow has) is possible and enough to admit the flow:

If the flow is new and has high priority, it will be checked if degrading the QoS (i.e. lowering the bit rate at a tolerant level) of some low priority flows will gain the needed resources and if yes, then the flow is admitted, otherwise it is rejected.

If it is a handover flow then it is also checked if low priority flows can degrade their QoS as much as it needs to admit the flow. If this can't be done, the handover flow will enter the handover queue in a position related to its priority that means that it will enter in front of flows with lower priority. The flow will remain in the queue until:

- The needed resources become available (i.e. by completion of other flows);
- The flow leaves the cell, i.e. the user moves to another cell, or the flow is completed;
- The flow is terminated due to timeout.

The admission control algorithm for the cooperation between B3G and legacy RANs aims to maximise the number of admitted or in-flow traffic sources supported over the RANs, while guaranteeing their QoS requirements and ensuring that the new connection does not affect the QoS of the ongoing connections. The decisions to accept or reject a new connection are based on different criteria, taking into account each RAT's nature.

D.1.6 Load control

Reactive load control is used to face a situation where the networks are in a overload situation and the users' QoS is at risk due to increase of the interference, mobility aspects, low bandwidth availability etc. When already admitted users cannot satisfy their guaranteed QoS to their services, for a specific percentage of time, then the network is considered to be in an overload/congestion situation. Herein, we describe am example of a reactive load control mechanism that is monitoring WINNER as well as legacy RANs and if an overload situation occurs it tries to decrease the load of the network performing several actions and especially trying to make the RANs cooperate i.e. by forcing users to perform handovers. The reactive load control algorithm is divided into three phases [WIND41] [WIND42] [WIND43] [WIND44]:

1) *Detection phase*: The algorithm continuously monitors the networks and periodically checks the load of the networks in order to detect a overload situation in anyone of them. It is considered that a network is overloaded if the load factor is over a certain pre-defined threshold during a certain amount of time.

2) *Resolution phase*: This is the phase that the algorithm is trying to resolve the problem that causes the overload situation. At first, as it is obvious, we must drop all the incoming flows (new and handover) as they will increase more the load of the network, so admission control is forced to reject the flow requests for that network. Then in case flow conditioning is not used the algorithm checks if the overload situation is caused due to users that violate their QoS restrictions in terms of bit rate, which means that it tries to find if there are flows that transmit with more bit rate than they should, according to the service agreements made between the network and the user. If such flows exist then the algorithm drops their bit rate to the value that exists in the service agreements. After restoring the bit rate of the users to the agreed, there is a check if the network is still in a congestion situation and if so the algorithm performs a number of actions which include handover of flows, decreasing of their bit rate or even selective dropping of flows.

3) Then the algorithm enters the *recovery phase*, where we try to restore the transmission rate to the flows, which rate was decreased in the second step of the resolution phase. A recovery algorithm is necessary, because we cannot leave the flows with a bit rate that violates the QoS service agreements. The problem here is that if we restore the flows' bit rate incautiously, the network could fall once again in a overload situation and that's why we must be very careful to that. For all the flows that we have decreased their bit rate, we check (separately) if we can restore their transmission rate without causing congestion again, by computing the amount of load needed in order to restore the transmission rate.

D.1.7 Routing

The overall picture of the routing in multi-hop cellular networks (MCNs) is depicted in Figure D.3. From the architecture perspective, two basic routing strategies are envisioned in multi-hop systems: centralised or distributed. Under the centralised strategy, route determination is performed in a central controller, which normally possesses powerful processing capability and has knowledge on global network status, so that sophisticated routing algorithms could be adopted to optimise the system performance. With the

distributed strategy, individual network nodes from the source to the destination jointly perform route determination. This strategy could function when no central controller is reachable, but its performance is normally limited by network nodes' processing capability and knowledge on network status.

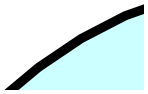

Figure D.3: Routing in MCNs.

In terms of protocol nature, the routing algorithms in conventional multi-hop networks, such as ad-hoc networks, can be mainly broken down into two categories: proactive routing and reactive routing. With proactive routing schemes, network nodes continuously evaluate the topology of the network, so that when a packet needs to be forwarded, the route is already known and can be immediately used. Reactive schemes, on the other hand, invoke a route determination procedure on demand only. Thus, when a route is needed, some sort of global search procedure is employed in order to find a suitable route to the destination. The protocol nature of the routings in MCNs could be both proactive and reactive but being applied at different circumstances, for instance, reactive routing is be used for idle users, whereas proactive routing is applied for active user. Nevertheless, further studies will be carried out on this issue.

For both proactive and reactive routing schemes for ad-hoc networks, topology/route information is normally preserved in routing tables. The difference is, for proactive routing, the table contains up-to-date and complete topology information, whereas, for reactive routing, a route is only created in the table when needed. For the routing in MCNs, likewise, routing tables are also supposed existing at BSs, RNs and UTs to keep the necessary routing information for respective nodes. This will be further explained in the later part of this section. The routing in MCNs is responsible for a number of basic tasks, such as route/topology discovery (N.B. route discovery is normally for reactive routing schemes, whereas topology discovery is for proactive ones.), and route table updating/maintenance etc.

Decision criteria: In the literature, various criteria have been proposed for the routing criteria in MCNs such as distance, pathloss, and transmission power etc. For each user, these routing algorithms intend to find and choose the route with the least distance, pathloss or transmission power etc. In our recent work [LHYT01] and [LHYT02], a novel routing criterion, named the *Load Cost Indicator (LCI)*, is proposed:

$$\zeta_{route\ i} = C_{route\ i} / R_{route\ i},$$

Where $\zeta_{route\ i}$ is the *LCI* of route *i*, $C_{route\ i}$ represents the consumed capacity of the transmission on route *i*, and $R_{route\ i}$ is the transmission data rate on route *i*. Apparently, such a criterion reflects the consumed system capacity when delivering unit amount of traffic on a particular route. Given a certain system capacity constraint, if every user employs the route with the least LCI among all its possible routes, the system throughput can be maximised.

Routing tables: As mentioned earlier, like in ad-hoc networks, in MCNs, routing tables are also supposed existing at individual network nodes, including BSs, RNs and UTs. Nevertheless, due to the fact that the BS is the common source for all the downstream [WIND25] flows, and meanwhile the common destination for all the upstream flows in one radio cell, the routing tables in MCNs are much simpler than their counterparts in ad-hoc network, moreover, for packet delivering purposes, an BS only needs to keep downstream routing table/tables, a UT only needs to have upstream routing table/tables, whereas a RN needs to have both downstream and upstream routing tables. Nevertheless, as mentioned earlier, the routing is envisioned to be centralised (BS-based) in MCNs, in another word, the route table calculation

for all the nodes within one cell is to be performed by the BS, hence, BS actually has the knowledge of the up-to-date route tables at individual nodes within the cell.

D.2 RRM architecture

Intuitively, the problem of optimising resources is better posed when doing it in a common fashion rather than regarding separately cells/modes. When information about interference induced by surrounding cells and about the amount of spectrum resources in other modes is available (CRRM approach), algorithms perform better and the usage efficiency is increased. This also applies when considering not only surrounding cells but also different radio networks operating simultaneously, i.e. JRRM approach.

Benefits of centralised RRM are achieved at the expense of a higher computational complexity since the algorithms have to deal with a higher number of degrees of freedom, and involve a larger interchange of information among network agents, thus increasing the signalling. Time restrictions on signalling are also to be considered. Centralised RRM algorithms have been proven to perform worse than distributed ones when delay introduced by signalling is larger than few seconds (5 s).

D.2.1 Location of WINNER functions

A first approach regarding the WINNER RRM architecture is shown in Figure D.4. According to this approach the mode specific functions are located at the BS and RN while the mode generic user plane ones are located at the RANG logical node. All the control plane functionalities are located at the Access Control Server (ACS) logical node. A disadvantage of such an RRM architecture would be the possible overload of the system due to increased signalling directed to the ACS node leading to delays.

The service level controller (SLC) regarding the downlink is foreseen to be located at some distance from the BSs, such as at RANG. It has the overall responsibility for adjusting inter-flow fairness, assuring the fulfilment of service level contract agreements and total delay constraints. It may perform by requesting resources from several BSs that may utilise different WINNER modes working on a slower time scale and may allocate resources belonging to several modes/base stations. As buffer management and traffic policing could impose constrains on the service load controller, they could be located at the same node. After flow classification, the service level controller will direct packets of a flow to one specific queue within a buffer residing in an BS or RN. On the other hand, the flow scheduling of the SLC for the uplink direction will be located at the BS or even the RN. The resource schedulers, link adaptation and power control should always be located close to the BSs to minimise delays.

However, all mode generic control plane and cooperative functionalities are located at the ACS logical node. In this almost centralised approach the problem of optimising resources is better posed as it is done in a common fashion rather than regarding separately cells/modes/RANs. The main disadvantage of such an RRM architecture is the higher computational complexity since the algorithms have to deal with a higher number of degrees of freedom, and involve a larger interchange of information leading to the possible overload of the system due to increased signalling directed to the ACS node leading to delays.

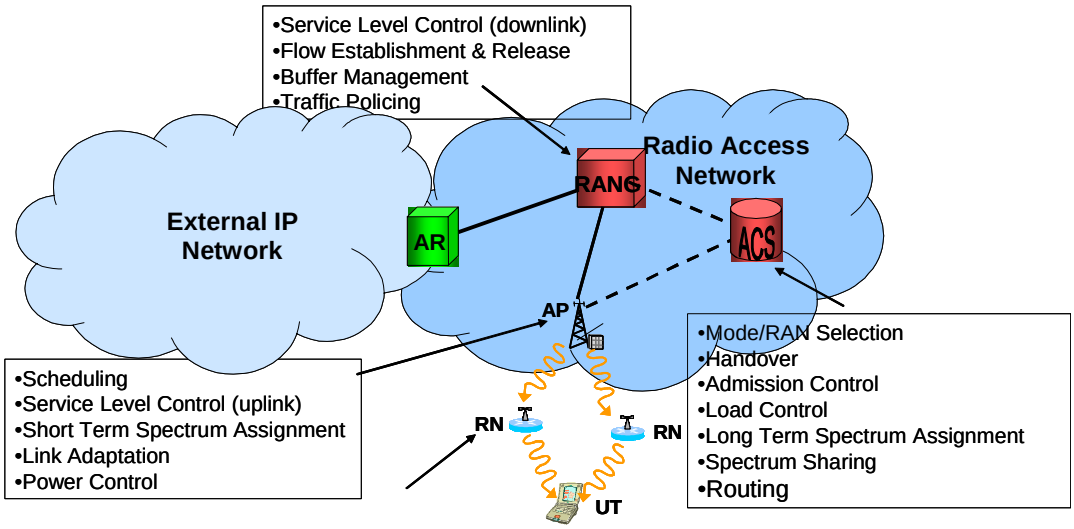

Figure D.4: WINNER RRM Architecture.

It is envisaged that for the WINNER system with the multiple operating modes, the hybrid approach would be suitable. In particular, in order to avoid extensive delays in the decision making and signalling overload a solution could be to bring some of the control plane functions closer to the BS physical nodes, adding more complexity to the BS physical nodes and therefore increasing their cost. However, assuming different types of BSs for the wide-area and short-range scenarios, we could restrict the extra functionality to the wide-area BSs (BSwa). In particular, the ACS node would comprise mainly the RRM functions needed for the cooperation of the WINNER system with legacy RANs (handling user admission / control to the WINNER system) and the coordination of the BSwa (if necessary) where a more comprehensive status of the system is required. On the other hand, the mode generic related control functions would be located at the BSwa (handling flow admission / control), reducing the amount of signalling information required and allowing for faster decisions since the resources are controlled at a cell level. For the BSwa to be able to make decisions on mode selection / re-selection, handover, admission control, congestion control and spectrum mapping between the BSsr that fall within its cell as well as between it and the BSsr, several information are required to be transmitted periodically or upon request from the BSsr to the BSwa. These include: BSsr id and cell id, current load, max load, power information, handover statistics per RN and BSsr (successful, drop rate etc), number of RNs attached to BSsr (in case of mobile RNs), CELLsr range (this can be change in case of mobile relays leaving/joining).Furthermore, some of the mode specific RRM functions such as scheduling might reside at the RNs performing at different time scales as it is envisioned to have RNs with different functionality layers (layers 1/2/3).

D.3 RRC functionalities

D.3.1 Measurements and reports

To choose the most suitable mode/RAT, a fundamental aspect is to assess the quality that different modes/RATs will provide to the users. This quality indication is basically obtained from measurements on the current and target networks. RRM mechanisms in B3G systems will be able to use more metrics and information as inputs than the current RRM algorithms, since information will be exchanged between networks and new metrics are becoming available.

Current handover mechanisms are only based on received power either in cellular systems or in WLAN networks. Congestion control algorithms in UMTS use mainly power measurements and service attributes to control access and load. On the contrary, in B3G systems *various* metrics coming *from all the networks* available can be used as inputs of *any type* of RRM algorithms.

Some of these new metrics or information foreseen as useful to improve the RRM performance are listed below:

- Cell load, free capacity,
- Location,

- Velocity, direction,
- User's environment (indoor, outdoor, etc.),
- Terminal capabilities,
- Handover statistics.

Other information concerning the link connection includes: Price of per bit in the link; Security setup and encryption used in the link; ARQ status of the link etc.

Measurements can be performed either in the base stations or in the user terminal. Usually RRM decisions are taken by the network, therefore mechanisms must exist to report measurements from base station or terminal to the network. The reporting may be periodic, event-triggered or on demand.

The WINNER system should at least provide to the RRM (or/and cooperative RRM) entity:

- Signal strength measurements, performed by either terminals or base stations, on the WINNER RAN, but also on legacy RANs when necessary,
- Transmitted power measurements, performed by either UTs or BSs,
- Quality measurements,
- "Cell" load measurements (e.g. power measurements, L2 buffer load: indeed the exact definition of load for the WINNER system must be investigated and will depend on the chosen radio interface),
- A beacon that terminals on other systems can listen to and measure, e.g. in order to prepare for a handover to WINNER.

The possibility for a terminal in a WINNER system to measure the received signal strength of base stations/base stations of legacy systems should be foreseen when defining the WINNER system. Alternatively, the RRM entity in WINNER should have access to these measurements on legacy systems. Moreover the possibility to exchange load information between WINNER and legacy systems should also be anticipated (e.g. exchanged between cooperative RRM entities).

WINNER inter-system handover should be consistent with the inter-system HO already defined in legacy systems. In particular, the inter-system handover procedure between UMTS and another RAT is already specified by the 3GPP. Some of the specifications are applicable to any RAT while others are RAT specific (e.g. specified measurements on GSM are applicable to GSM only). Therefore, the WINNER design must fulfil all the requirements that are mentioned in the 3GPP specifications for every RAT and the 3GPP will need to do some specifications dedicated to the WINNER system [WIND41] [WIND42] [WIND43].

D.3.2 Other functions

Feature discovery

Both the antenna configuration and relaying issues can be perceived jointly in context of the space-time coded cooperative transmission, where virtual antenna arrays are created for the purposes of enhancing the overall WINNER system performance. However the question arises how to configure the virtual antenna array and which space time code to select in order to meet the requested *Quality of Service*. Answering this question, renders it necessary to investigate the problem of efficient exploitation of the additional information about links, provided by the routing protocol. Since the target WINNER routing protocol is not established, the *Multi-Constrained Optimised Link State Routing protocol (MC-OLSR)* candidate solution will be used during simulations. This protocol, which was proposed in [WIND31] and [WIND32], will be expanded with the cooperative relaying functionality, which in turn was investigated in [WIND24], where the *Adaptive approach to antenna selection and space-time coding* was analysed.

RRC/RRM and cooperative transmission

RRM is connected with RNs assignment, transmit power control etc. Proper RNs assignment in for the purposes of cooperative relaying in WINNER is very important because it directly affects the transmission parameters and therefore the attainable *QoS* level. When at least coarse channel parameters between the transmitting node and the relaying ones are known, it is possible to create the virtual antenna array VAA in a more optimum way. To this end the selected RRC functionalities were identified, which along the flow of control information are presented in Figure D.5.

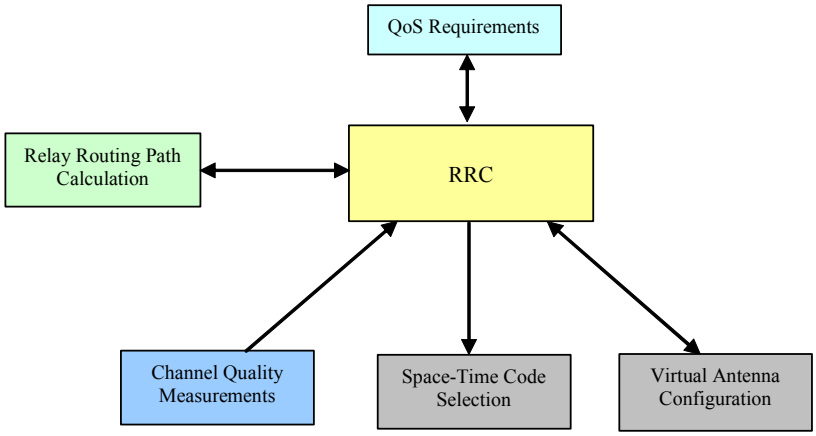

Figure D.5: RRC and cooperative relaying.

Here the *Radio Resource Control* service exploits the *Channel Quality Measurements* and *Relay Routing Path Calculation* functionalities in order to perform the space-time coded cooperative relaying in an optimum way. It is then of prime importance to identify:

- how to efficiently exploit the routing information, provided by the routing protocol (e.g. the *MC-OLSR* protocol),
- how to perform routing so that cooperative relaying could be efficiently exploited,
- how to configure the virtual antenna arrays and which space time code to select so that the requested *Quality of Service* could be met.

There is also a question on how the resource partitioning between BS and RNs should be performed. In case of the *MC-OLSR* enhanced with cooperative relaying it is assumed the control is BS-centralised, which means that resources are managed and assigned by BSs.

Appendix E. Assessments Assumptions

E.1 Overview

This chapter summarises baseline simulations assumptions and parameters applied in link, multi-link and system-level oriented simulations. Four prioritised deployment scenarios A1, B1, C2 and D1, identified in [WIND72], are addressed. Additionally, the B3 scenario is considered for link level investigations. For scenarios A1, B1 and B3 (collectively referred to as "short-range" scenarios), evaluations are performed using the TDD cellular system mode, and for scenarios C2 and D1, evaluations are performed using the FDD cellular system mode. A rough characterisation of these scenarios is given in Table E.1 below:

Table E.1: Basis scenarios considered

Scenario identifier	Deployment	PHY mode	Mobility [km/h]	BS height [m]	UT height [m]	Traffic density
A1 In building	small office/ residential	TDD 100 MHz	0–5	2	1	high
B1 Hotspot	Typical urban micro cell	TDD 100 MHz	0–70	e.g. 10 (below RT[21])	1.5	high
B3 Hotspot	Indoor	TDD 100 MHz	0–5			
C2 Metropolitan	Typical urban macro cell	FDD 2×20 MHz	0–70	e.g. 32 (above RT)	1.5	medium to high
D1 Rural	Rural Macro cell	FDD 2×20 MHz	0-200	e.g. 45 (above RT)	1.5	low

It should be stressed that the selected assumptions, models and parameters reflect a compromise taking into account the latest system design aspects, the realisable simulator capabilities as well as the open issues to be addressed. They only served as baseline assumption slightly different settings may have been used in the end. Moreover, not every detail is covered especially with respect to system level simulations in order to keep the simulator setup feasible for many partners.

E.2 Basic parameters for link level evaluations

For performance evaluation of different link level parts (mainly modulation schemes, channel estimation and synchronisation), the system parameters fixed in Table 2.1 have been used for simulation. As channel models, one "representative" example (i.e., a channel having a reasonable delay spread) has been selected for each the FDD and TDD case, based on the tapped delay line models provided in [WIND54]. The model C2 NLOS has been selected for simulations with the FDD system parameters, while the B3 NLOS model was the baseline comparison case for the TDD system parameters. Additionally, the A1 NLOS model was used in some simulations, as an example for a channel providing a high degree of spatial diversity (i.e., suitable for achieving high spectral efficiency when using spatial multiplexing techniques). For channel coding, the memory 6 convolutional code was used as a baseline case (gains of around 2 dB are expected when using better codes for large block lenghts, cf. Appendix F.2). More advanced coding schemes were used in Appendix F.1, in order to demonstrate the potential performance of the coding within the WINNER physical and MAC layers. For the (relative) performance assessment of different coding techniques, simple BPSK transmission over an AWGN channel was used (without OFDM modulation/demodulation), as the relative merits of different coding techniques proved to be relatively independent of the channel and modulation technique [WIND23].

[21] RT = rooftop

E.3 Basic parameters for multi-link and system level evaluations

E.3.1 Mode specific parameters

FDD mode (used in wide area simulations)		
Parameter	**DL**	**UL**
Centre frequency	5.0 GHz	4.2 GHz
Bandwidth/channelisation	20 MHz paired UL/DL	
Duplex scheme	(T+F)DD	
Transmission technique	OFDM Δf=20 MHz/512 = 39062.5 Hz $\rightarrow T_N$ =25.6 μs f_c=kΔf, k∈[-208:208], k≠0 T_G=3.2 μs $\rightarrow T$=T_N+ T_G =28.8 μs	a) single carrier (continuous) Pulse period T = 25.6 μs/416 = 61.54 ns pulse shaping: square root raised cosine with roll-off β=0.231 b) single carrier (block oriented) same pulse as in a) block length: 416 symbols $\rightarrow T_N$ = 25.6 μs guard length: T_G=3.2 μs
Number of sectors	3	1
Antenna configuration WA_1	BS: |	A_1: |
Antenna configuration WA_2 (ULA)	BS: | | | | | | | (0.5λ)	A_1: | A_2: | | (0.5λ) A_3: | | | | (0.5λ)
Antenna gain	15 dBi	0 dBi
Frame length	691.2 μs (=2 DL chunks)	
chunk size	8 subcarriers × 12 OFDM symbols	unspecified
overhead (parameter estimation, signalling)	19 out of 96 resource elements of each chunk	unspecified

TDD mode (used inshort range simulations)		
Parameter	**DL**	**UL**
Centre frequency	5.0 GHz	
Bandwidth/channelisation	100 MHz	
Duplex scheme	TDD	
Transmission technique	OFDM Δf=100 MHz/2048 = 48828.125 Hz $\rightarrow T_N$ =20.48 μs f_c=kΔf, k∈[-832:832], k≠0 T_G=1.28 μs $\rightarrow T$=T_N+ T_G =21.76 μs	
Number of sectors	1	1
Antenna configuration SA_1	BS: |	A_1: |
Antenna configuration SA_2 (ULA)	BS: | | | | | | | | (0.5λ)	A_1: | A_2: | | (0.5λ) A_3: | | | | (0.5λ)
Antenna gain	8 dBi	0 dBi
Frame length	691.2 μs (3 DL chunks + 3 UL chunks + 2 × duplex guard time), duplex guard time = 19.2 μs	
chunk size	16 subcarriers × 5 OFDM symbols	
virtual overhead for parameter estimation	15 out of 80 resource elements of each chunk	unspecified

E.3.2 Common to all modes

Parameter	DL	UL
Coder	convolutional coder	
Interleaver	random bit interleaver	
Modulation formats	BPSK, QPSK, 16-QAM, 64-QAM	
Spreading codes	Walsh-Hadamard (WH)	WH (synchronous UL) Gold (asynchronous UL)
Medium access scheme	frequency adapative scheduling → OFDMA/TDMA frequency non adaptive scheduling → OFDMA/TDMAMC-CDMA	
Channel estimation at Rx	perfect	
Synchronisation	perfect	
channel measurement accuracy for adaptive processing	perfect	
delay between CQI measurement and its application	1 Frame	
Equalisation (if required)	MMSE	
Demodulation	ML based soft output demodulation If equaliser is present, apply ML criterion to equaliser output signal	
noise spectral density	-174 dBm/Hz	
noise figure	7 dB (at MT)	5 dB (at BS)
Resource assignment strategies	non-adaptive mode: round robin adaptive mode: score-based opportunistic scheduling	
Link adaptation strategies	non-adaptive mode: adaptive coding and modulation based on average CSI (across all sub-channels) adaptive mode: adaptive modulation and coding per chunk based on instantaneous CSI	
(H)ARQ	none	
power control	no	perfect
azimuth pattern of antenna elements	$A(\theta) = -\min\left[12\left(\frac{\theta}{70}\right)^2, 25\right]$ [dB] θ_{3dB}= 70°	omni directional
correlation of shadow fading between sectors	same site: full, i.e. use same value different site: no	
correlation of fast fading between sectors	same site: use same bulk parameters but redraw delays, AoAs, AoDs, … different site: no	

E.4 Scenario parameters

Parameter	A1	B1	C2	D1
channel modelling	WINNER-I interim channel models, see WP5 deliverables			
Average BS transmit power	1 W	4 W	20 W per sector	
Average UT transmit power	200 mW			
Cell radius R	unspecified		1 km	
Cellular structure	isolated cell only		hexagonal grid, see Figure E.1	
Number of cells to be simulated			19 three sector sites	
frequency reuse distance			unspecified	
number of users	variable parameter but constant for any simulation run and snapshot			
user distribution	uniform within cell area		uniform within 19-cell area	
user location update	random drop of users in every snapshot within each snapshot users virtually remain at fixed positions even in case of velocity $\|v\| > 0$ km/h			
Traffic model	full queue assumption (holds for any user)			
Mobility model (only affects fast fading)	angle$\{v\} \sim U(0,2\pi)$, $v_x \sim \eta(m,\sigma^2)$, $v_y \sim \eta(m,\sigma^2)$, $\|v\| = (v_x^2+v_y^2)^{0.5}$			
mobility model parameter	M_1: m_1= 1 km/h, σ_1= 1.6 km/h	M_1: m_1= 1 km/h, σ_1= 1.6 km/h M_2: m_2= 5 km/h, σ_2= 12 km/h	M_1: m_1= 1 km/h, σ_1= 1.6 km/h M_2: m_2= 25 km/h, σ_2= 15 km/h	M_1: m_1= 1 km/h, σ_1= 1.6 km/h M_2: m_2= 55 km/h, σ_2= 29 km/h
Distribution of user characteristics considering cases SA_1/WA_1 (SISO)[22]	M_1: 100 % A_1: 100 %	M_1: 80 % M_2: 20 % A_1: 100 %	M_1: 50 % M_2: 50 % A_1: 100 %	M_1: 40 % M_2: 60 % A_1: 100 %
Distribution of user characteristics considering cases SA_2/WA_2 (MIMO)[7]	M_1: 100 % A_1: 20 % A_2: 40 % A_3: 30 %	M_1: 80 % M_2: 20 % A_1: 20 % A_2: 40 % A_3: 30 %	M_1: 50 % M_2: 50 % A_1: 50 % A_2: 30 % A_3: 20 %	M_1: 40 % M_2: 60 % A_1: 50 % A_2: 30 % A_3: 20 %

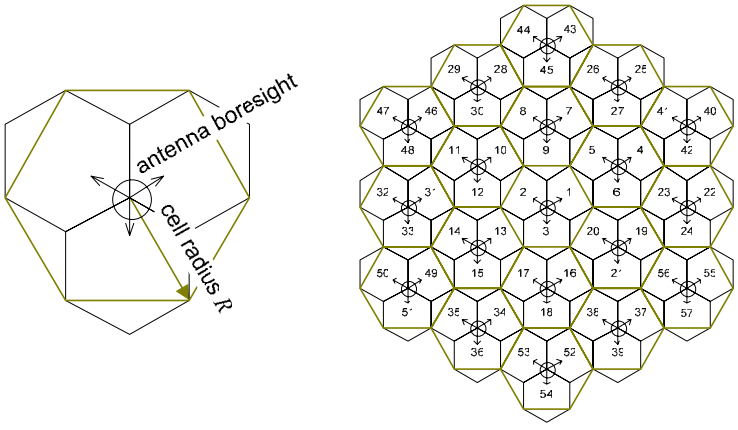

Figure E.1: Example sketch of cellular scenario with 19 three-sector sites.

[22] No correlation between mobility, transmit power and antenna parameters is taken into account so far

Appendix F. Link-Level Assessments

The merits of different coding, modulation, channel estimation and link adaptation techniques have already been assessed in a number of previous WINNER deliverables, most notably [WIND22, WIND23,WIND24,WIND26,WIND27]. Therefore, this chapter contains mainly assessment results necessary to justify the WINNER system design decisions reported in Chapter 2 of this report. Thus, Appendix F.2 presents a detailed comparison of the complexity and performance of Duo-Binary Turbo Codes and Block-LDPC codes; as these have been identified as the most promising FEC candidate technologies. More detail on the assessment methodology and other coding techniques (CC, standard PCCC and PEG-based LDPCC) can be found in [WIND23]. Appendices F.3 and F.4 provide detail on the performance of different channel estimation and synchronisation techniques, to back up the results from Appendix B.4 in terms of the amount of pilots required to achieve a CSI of sufficient quality at the receiver. Finally, in Appendix F.5 results for the performance of different bit-and power-loading algorithms are presented. Another purpose of this chapter is to present results that give insight into the overall performance of the WINNER physical layer – Appendix F.1 serves that purpose.

F.1 Link layer performance: Throughput

In order to assess whether the performance of the WINNER physical layer is sufficient to live up to the requirements stated in Section 1.1 and in order to provide first results that allow for an estimation of the SNRs required to achieve different spectral efficiencies, the performance of a single user CP-OFDM system using advanved coding (3GPP Turbo Code, 8 iterations maxLogMAP decoding) has been evaluated. This setup can be considered as an example of a single user served in the non-frequency-adaptive mode (where MC-CDMA with spreading factor 1 reduces to CP-OFDM). Note that the protocol overhead (super-frame structure, in-band signalling, pilot subcarriers), as well as SNR penalties due to imperfect channel estimation / synchronisation are not included in this assessment. The overhead due to guard bands, on the other hand, is included. The overall throughput of a single link will hence be slightly lower than the figures given in the following plots, and the required SNR will be slightly higher. The activity factor for FDD is not included in the throughput figures, an appropriate scaling must be included for all cases where the activity factor is smaller than 1.

Table F.1: Summary of parameters for WINNER channel models

Scenario identifier	Deployment	PHY mode	UT speed [km/h]	Delay Spread [ns]	Composite angular Spread at BS/MT [degrees]
A1 In building	small office/ residential	TDD 100 MHz	3	24	23.2/39.1
B1 Hotspot	Typical urban micro cell	TDD 100 MHz	3	90	12.4/36.4
B3 Hotspot	Indoor	TDD 100 MHz	3	30	3/18.7
C2 Metropolitan	Typical urban macro cell	FDD 2x20 MHz	70	310	8/53
D1 Rural	Rural Macro cell	FDD 2x20 MHz	70	28	22.4/17.9

Table F.1 summarises some relevant parameters for the used WINNER tapped delay line models. Scenario A1 and B3 provide roughly the same amount of frequency diversity. However, the angular spread at the BS is very small for the B3 and C2 models – in contrast to most other results presented in this chapter, the scenario A1 has therefore been selected for TDD mode evaluations. Although both wide area cases (metropolitan and rural) have been simulated, the focus in the present section is on the

metropolitan area, where the larger traffic demands can be expected. In this scenario, the high correlation between BS antennas is expected to significantly affect the gains achievable by using spatial multiplexing techniques, as is confirmed by the results in Figure F.3.

Figure F.1 below shows the performance of a SISO system with the parameters from Table 2.1 for FDD mode operation (20 MHz bandwidth, the used channel model is the clustered delay line model C2 NLOS from [WIND54]). A SNR beyond 20 dB is required to achieve a spectral efficiency of 3 bit/s/Hz. Taking a duplex activity factor of 0.5 and an overhead of 20% into account, the spectral efficiency design target of 0.5 bit/s/Hz/link in the downlink (see 70 km/h in Appendix A.1.3) corresponds to about 25 Mbit/s, which with dual-antenna terminals as baseline (roughly 3 dB gain in this scenario) and assuming a loss of 1 dB from non-ideal channel estimation requires a SINR of around 9 dB. A simple link budget (using pathloss models and other parameters listed in Appendix E[23]) based on this SINR requirement gives a maximum cell range very close to 1000 m without indoor-to-outdoor coverage. This indicates that the above-mentioned cell-average of 0.5 bits/s/Hz/link with single user should be possible to obtain with some margin even without relays.

Turning to the rural area scenario, simulations (not shown) together with a link budget[24] show that the spectral efficiency target of 0.5 bit/s/Hz/link at 70 km/h can be reached with good margin (up to a cell range of well above 3 km). For the uplink, the targets are somewhat tougher, but should still be reachable (in particular with relays).

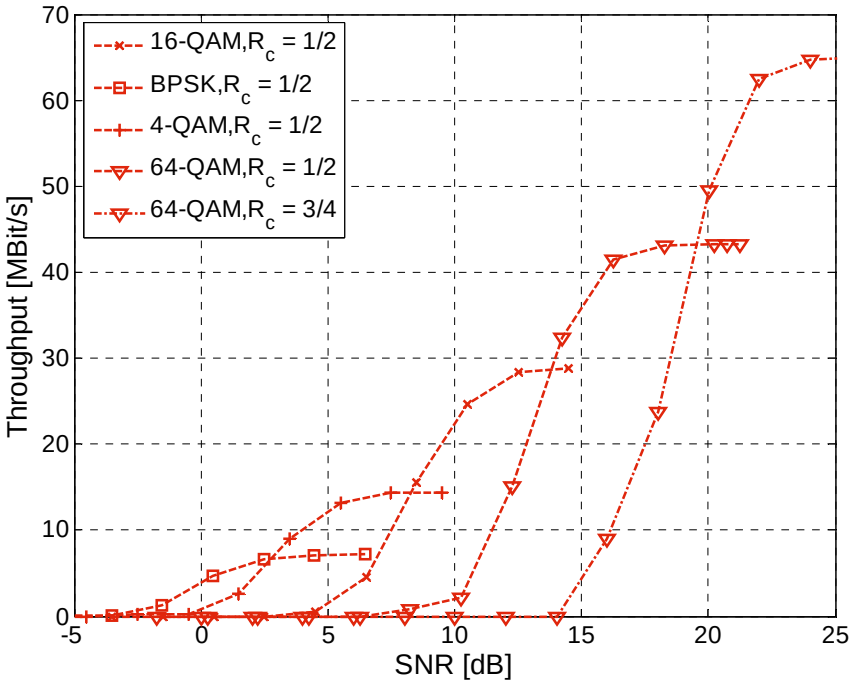

Figure F.1: Throughput of CP-OFDM-based FDD mode system (20 MHz, SISO, C2 NLOS).

Figure F.2 depicts the TDD mode case (100 MHz bandwidth, again for a SISO setup) – data rates are evidently higher while spectral efficiency figures are comparable, as could be expected from the system definition in Table 2.1. The channel model used is A1 NLOS from [WIND54]. Achieving the target spectral efficiency of 4 bit/s/Hz (cf. Appendix A.1.4), with half-duplex and 20% overhead corresponding to about 1000 Mbit/s, seems to be difficult without the use of some form of spatial multiplexing/spatial diversity techniques, to be further discussed in the following.

[23] Noise bandwidth 16 MHz, noise figure 7 dB on DL (5 dB on UL), transmit antenna gain 15 dB, output power 20 W. Based on the shadow fading standard deviation of 5.7 dB, a shadow fading margin of 3.5 dB was assumed by scaling the results in [SGF95].

[24] Here the shadow fading standard deviation is 8 dB, and a margin of 5 dB was used, cf. [SGF95].

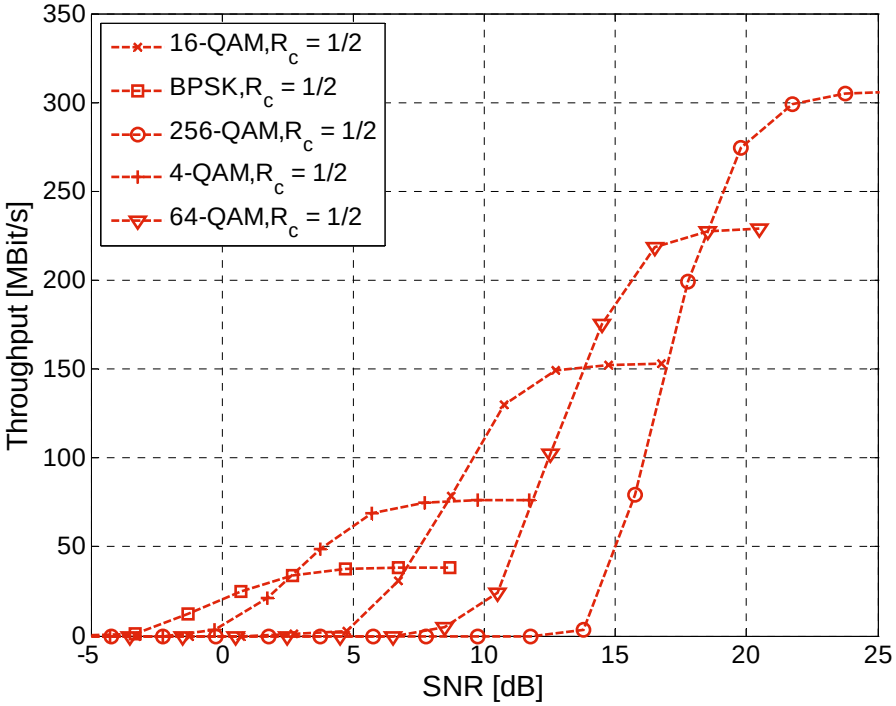

Figure F.2: Throughput of CP-OFDM-based TDD mode system (100 MHz, SISO, A1 NLOS).

Figure F.3 and Figure F.4 show the performance for the spatial multiplexing case, for both FDD and TDD mode operation. For the FDD system, a 2x2 MIMO setup was selected, while a 4x4 MIMO setup was used for the TDD case, where more spatial diversity is expected to be available (cf. the higher angular spread at the base station in Table F.1).

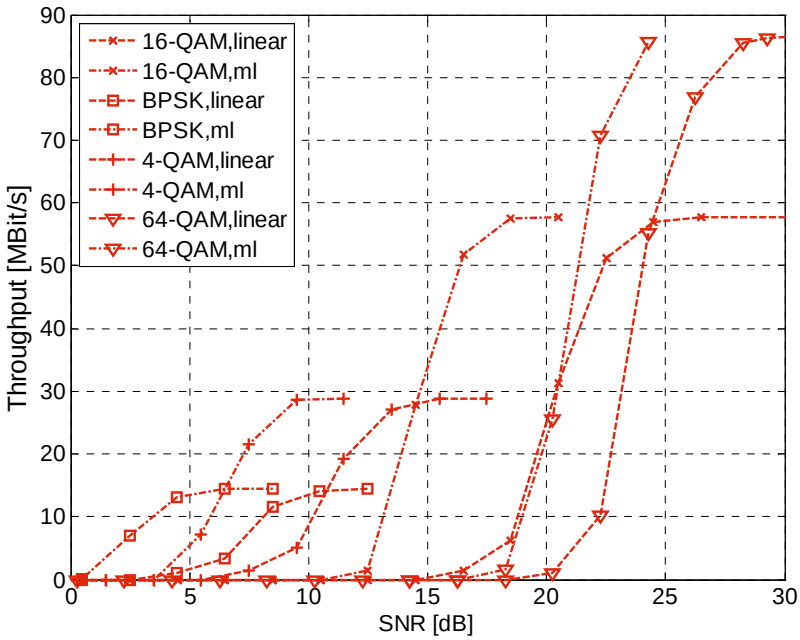

Figure F.3: Throughput of CP-OFDM-based FDD mode system (20 MHz, 2x2 MIMO, C2 NLOS).

For both setups, the performance was evaluated when using a simple linear MMSE equaliser, and also when using a high performance equaliser (ML detection where possible, otherwise Sphere Detection with a sufficient number of full length candidates). Taking the results for the latter receiver architecture and comparing then the MIMO with the SISO case allows for identifying the performance losses due to antenna correlation (the throughput would roughly scale with the number of transmit/receive antennas in a completely uncorrelated scenario). Comparing the results of the linear and the ML/Sphere detector allows for identifying how much gains can be achieved by using advanced receiver architectures, as compared to the simplest one. As is evident, a SNR in excess of 30 dB would be required to run the maximum modulation/coding schemes investigated for the SISO case in Figure F.1 and Figure F.2. Consequently, the maximum spectral efficiency does not scale fully with the number of antennas, which can be attributed to the limited amount of spatial diversity. A spectral efficiency of around 4 bit/s/Hz is achieved at SNR=25 dB for the 2x2 MIMO FDD case, when using a high performance detector. The gains at lower SNRs, which are expected in multi-cell environments, are substantially lower. More specifically, at a SNR of 4 dB, the spectral efficiency is not increased with respect to the SISO case.

For the 4x4 MIMO TDD case, a spectral efficiency of 12 bit/s/Hz is achieved at SNR=30 dB. At a bandwidth of 100 MHz, this would, with an activity factor close to 1 allow achieving the target peak data rate of 1 Gpbs cited in Section 1.1. With half-duplex and 20% overhead, the design target spectral efficiency of 4 bit/s/Hz (cf. Appendix A.1.4) can also be achieved at about 30 dB.

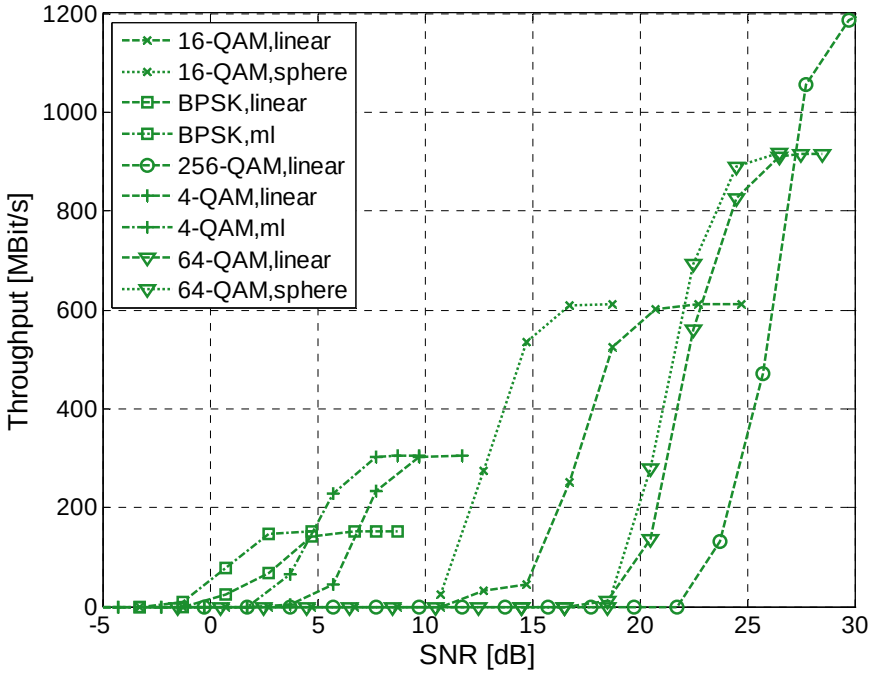

Figure F.4: Throughput of CP-OFDM-based TDD mode system (100 MHz, 4x4 MIMO, A1 NLOS).

F.2 Forward error correction

In this part, the two main channel coding candidates Duo-Binary Turbo-Codes and Quasi-Cyclic Block-LDPCC are investigated, their performance compared, and finally first results on the complexity/performance trade-off are given. In order to cover a wide range of applications, 5 different block lengths have been selected: 576, 1152, 1728, 2304 and 4308 coded bits, together with 3 different code rates R_c = 1/2, 2/3 and 3/4. The assessment in this section follows the framework from [WIND23]. For details on cycle count and energy consumption figures, please refer to [WIND23]. The performance comparison is done for BSPK transmission over the AWGN channel. The (relative) assessment, however, is expected to be similar for a wide range of channels, as was confirmed by the assessment done in [WIND23] for different types of Rayleigh fading channels.

F.2.1 Performance comparison

The performance comparison (cf. Figure F.5) underlines the fact that the selection of an appropriate coding technique depends crucially on the target block length. For code rate 0.5, DBTC outperform BLDPCC for block lengths up to 1728 (0.2 dB gain over BLDPCC for N = 576). Then LDPCC start progressively to outperform DBTC (0.1 dB better for N = 4308). In general, the performance loss by going from large to small block sizes is lower for DBTC than for BLDPCC. The threshold (in terms of block length) that separates these two regimes, however, depends on the code rate. When increasing the code rate to R_c = 3/4, a block length of 1152 is sufficient for the BDLPCC to achieve the same performance as the DBTC, and the difference observed for N = 576 is very small (cf. Figure F.7).

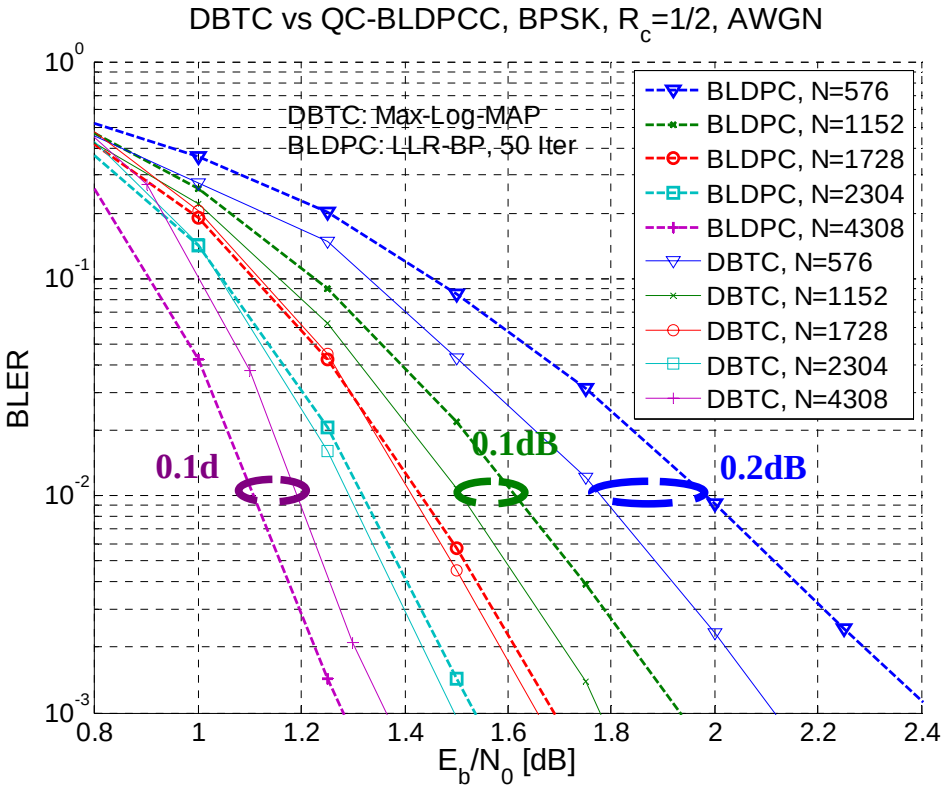

Figure F.5: Performance comparison between DBTC and QC-BLDPCC, Rc=1/2.

F.2.2 Complexity-performance trade-off

Relying on the computational complexity assessment introduced in [WIND23] and [3GPP-WG1#42], together with the relative cost of operations given by Table 5.1 from [WIND23], the energy consumption and cycle counts were computed for both DBTC and BLDPCC. For the sake of clarity, we restricted the presentation of results to two extreme block length cases N = 2304, and N = 576, respectively. In the case of DBTC, only the Max-Log-MAP decoder with scaling of extrinsic information (factor 0.5 in the first,

0.75 in the 2nd to 7th and 1 in the last iteration) is used, as it has been proven to give performance similar to Log-MAP decoding, at attractive reduction in complexity. Similarly, the MinSum* algorithm (MSA*) provides the best trade-off for LDPC decoding, as illustrated by the results in Appendix F.2.4. Additionally, alternative schedulings (*shuffled decoding*) should be used, as they lead to faster convergence of the decoding algorithm and (same performance at roughly half the iterations; cf. results in Appendix F.2.5).

In the sequel, we tried to keep similar notations already introduced into [WIND23]. Due to comparison between different packet lengths, minor modifications have been proposed. Packet length of $N = 2304$ bits are represented by purple coloured markers, and those of $N = 576$ bits by blue coloured markers. Concerning DBTC, the triplet "(mx, iy, lgMPz)" indicates the memory size 'x' of constituent encoders, the number of maximum iterations 'y', and maxLogMAP ('z=0') or logMAP ('z=1') decoding algorithm, respectively. In the present investigation, only the maxLogMAP decoding algorithm will be considered for Duo-Binary Turbo-Code, and its marker will be a diamond. Due to simple operations only, the edge colour will be green (energy cost=cycle count). The marker face colour represents the considered packet length. In the case of block LDPC codes, we have to differentiate also the number of iterations. A circle marker denotes the *maximum* complexity (maximum number of iterations 20 in the considered setup). A triangle marker is used for the *average* complexity (average number of iterations). Energy and Cycles are distinguished then by the use of non-filled or filled marker, respectively.

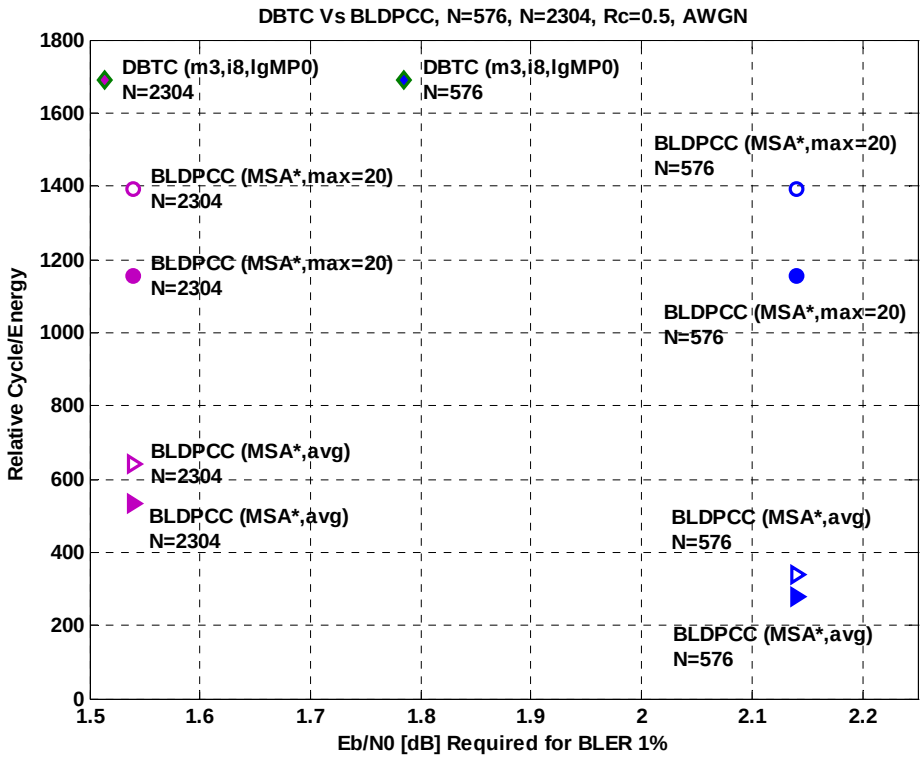

Figure F.6: Complexity-performance trade-off for QC-LDPCC and DBTC, Rc=1/2.

For the case of R_c=1/2, depicted in Figure F.6 above, Duo-Binary Turbo-Codes offer a better complexity-performance trade-off than block LDPC codes with low block size ($N = 576$), as they perform better at only slightly more energy consumption (w.r.t. the maximum iteration case for BLDPCC). However, for a higher block length ($N = 2304$), BLDPCC become more suitable, since their energy consumption saving is achieved at the expense of only minor performance degradation. These two trends are reinforced throughout the remaining results, cf. Figure F.7 below. Indeed, the higher the coding rate the less energy/cycles are required by BLDPCC (provided that the high code rate is achieved by using a code of a different rate rather than puncturing the rate 1/2 code). It might be worth mentioning that DBTC still outperform BLDPCC for lower block length, but their higher energy consumption in the present case of 8 internal decoder iterations seems to be the price to be paid for such performance.

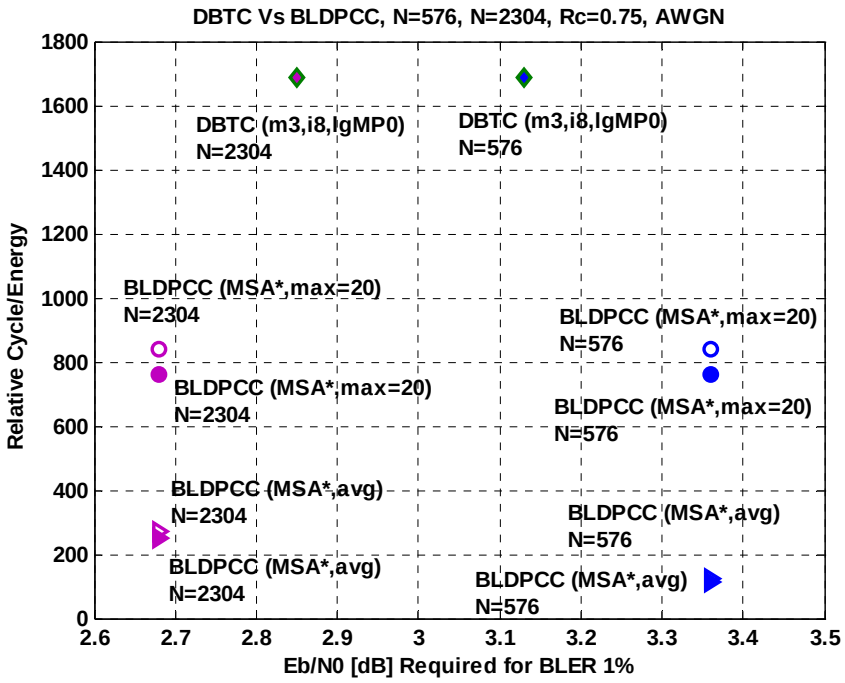

Figure F.7: Complexity-performance trade-off for QC-LDPCC and DBTC, R_c=3/4.

This complexity/performance trade-off is a necessary step towards fair comparison of these two main channel coding candidates DBTC and BLDPCC. Although these results are quite informative, they are not yet sufficient for any further technological decision. Indeed, the number of gates and the memory size requirements, together with performance robustness to quantisation (fixed point simulations) still have to be investigated still. Based on current assessment and know-how, these two channel coding techniques look more like complementary than concurrent solutions (w.r.t. block length). The next phase of WINNER (Phase II) should give additional answers and lead to in-depth understanding and comparison of both technologies by focusing more and more onto architecture and implementation aspect.

F.2.3 Performance comparison of rate compatible punctured codes

The performance of rate compatible punctured *standard* PCCCs and LDPCCs can be considered to be equal. LDPCC show better performance at high SNR, which, however, is less relevant for HARQ, as negligible number of retransmissions are needed in this SNR regime. Figure F.8 shows exemplary the performance of constructed BLDPCC, punctured BLDPCC and DBTC for two block lengths (the mother code rate of the punctured codes was R_c = 1/2). Note that the average number of iterations of punctured LDPCC is about twice as large as that of the constructed LDPCC.

F.2.4 BLDPCC performance comparison of major decoding algorithms

In recent years, a lot of different LDPC decoding algorithms have been proposed in literature. Our target in this part is thus to compare the most important ones – Belief Propagation [Gal63], A-Min [JVS+03], Lambda-Min [GBD03], Min-Sum and its corrected version [CF02]. To do so, we have assessed their performance for different block lengths and code rates. As a summary of the performance-complexity trade-off, Figure F.9 depicts the decoding complexity over the bit SNR required to achieve BLER 1%, for the example code rate 0.5 and two different code block lengths (again purple for N=2304 and blue for N=576). The advantage of the MinSum* can be emphasised quite clearly as it leads to good performance at low cost expense.

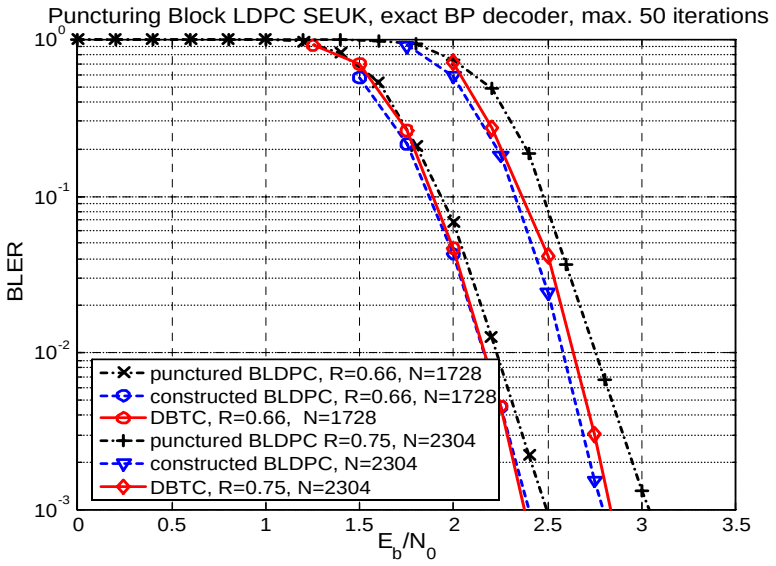

Figure F.8: Rate-compatible puncturing of block LDPC.

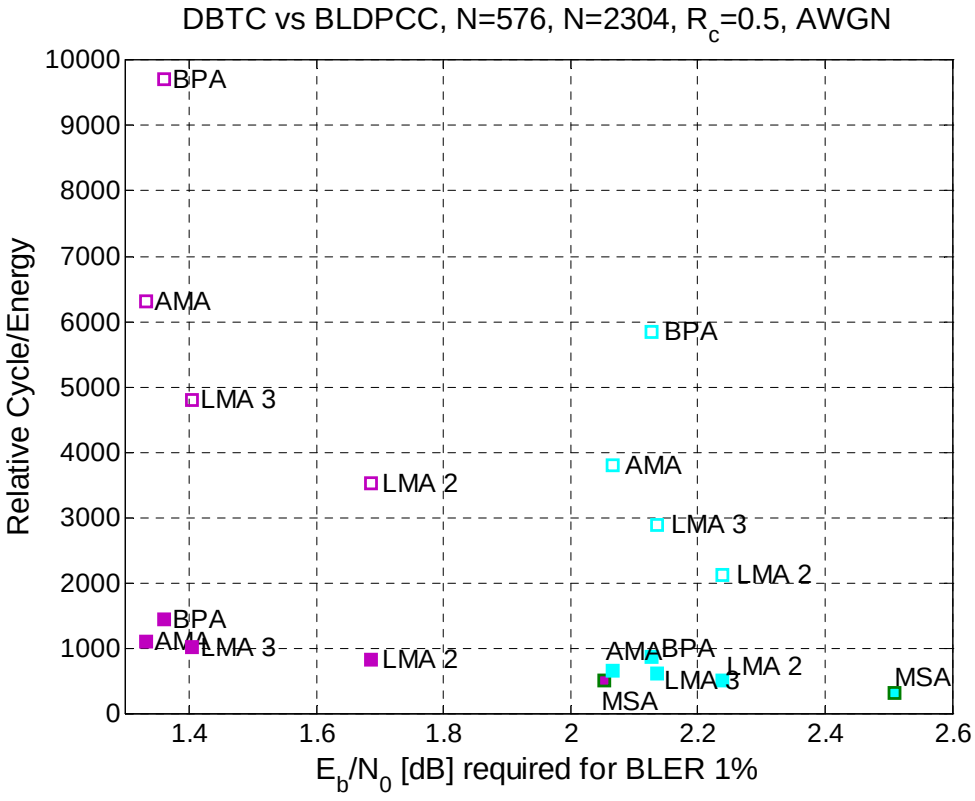

Figure F.9: Complexity-performance trade-off for different LDPC decoding algorithms, R_c=1/2.

F.2.5 Performance when using different decoding schedules

Figure F.10 illustrates that the same performance can be achieved by using either a maximum of 50 iterations and flooding decoding or a maximum of 20 iterations and shuffled decoding (cf. Appendix B.2.4).

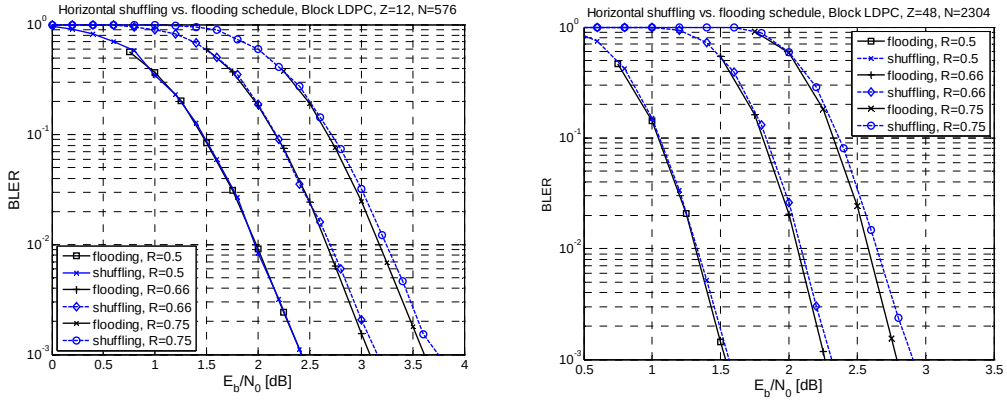

Figure F.10: Scheduling of BPA decoder for block LDPC of lengths N=576, N=2304: Horizontal (group 48) shuffling with max. 20 iterations vs. flooding schedule with max. 50 iterations.

F.2.6 Base model matrices for BLDPC codes

The BLDPCC investigated in this document are relying on the following base model matrices, in conjunction with the appropriate expansion process. They constitute the current state-of-the-art when it comes to (LDPC) code construction in the WINNER project and will be the starting point of investigations in WINNER Phase II. The three base model matrices in Figure F.11 - Figure F.13 correspond to the three code rates R_c=1/2, R_c=2/3 and R_c=3/4, respectively.

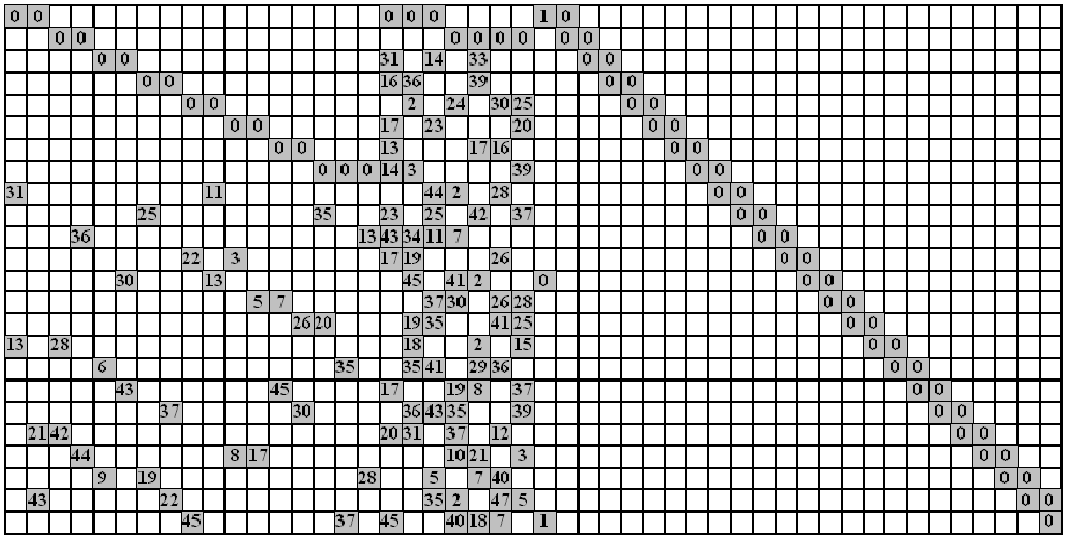

Figure F.11: (24, 48) Base model matrix, R_c=1/2.

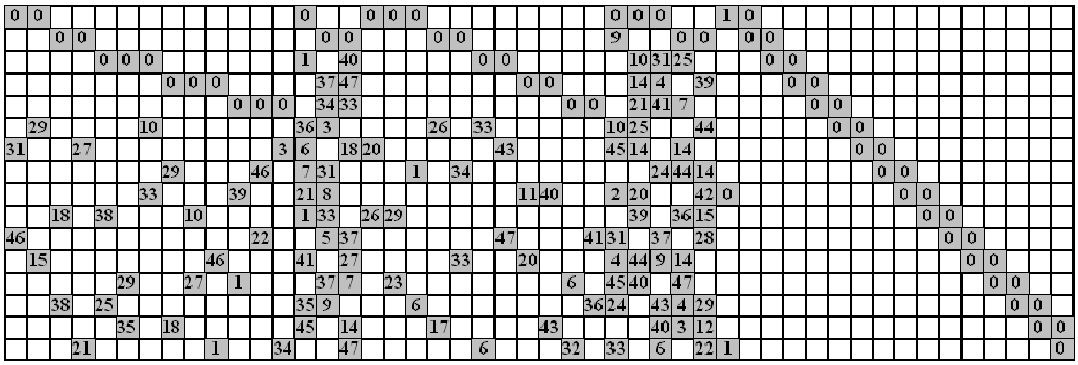

Figure F.12: (16, 48) Base model matrix, R_c=2/3.

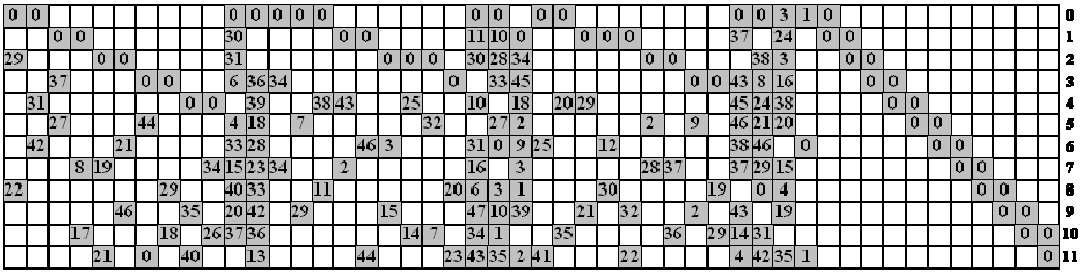

Figure F.13: (12, 48) Base model matrix, R_c=3/4.

F.3 Channel estimation

F.3.1 Uplink single carrier

As mentioned in Appendix B.4.2, time domain or two types of frequency domain pilots are options for channel estimation for uplink single carrier. In comparative simulations, the C2 urban macro channel was used, with parameters from Table 2.1 for frequency domain generation of a single carrier signal. A classical Doppler spectrum was assumed to generate channel realisations with UT speed of 50 km/h. The coding used was a rate 1/2 convolutional code with memory 6. Random bit interleaving was also included. In the receiver, a linear MMSE symbol based equaliser and an iterative soft decision feedback equaliser [TB04] were tested. The soft Viterbi algorithm was used in the decoder. The time domain multiplexed pilot signal was a 64-symbol Chu sequence, which has a uniform envelope and power spectrum. The FET frequency domain pilots were formed from the FFT of a 52-point Chu sequence; the FFT components were mapped to the pilot grid: every 8^{th} frequency of every 5^{th} block. This grid was found to be more effective for the SC system than the FDD grid of Figure B.6 used for the OFDM-PACE system, and had approximately the same overhead. For FDSP, since no extra subcarriers are used for pilots, a more liberal grid was used, with pilot subcarrier spacing of 8, and pilot block spacing of 2. For blocks with pilots, least square (LS) estimator was used for 'raw' channel estimation, followed by an FFT interpolator in frequency domain. Linear LS line fitting was used for channel estimates for blocks without pilots[25]. This approach is suboptimal, but relatively simple. Simulation results were obtained by averaging the block error rate (BLER) over 10000 frames. There were 12 blocks (and thus 12 correlated channel realisations) per half-frame (slot).

The iterative soft decision feedback equaliser (SDFE) is a simplified version of a frequency domain turbo equaliser [TB04]. Its iterative process does not include decoding or channel estimation. One or two iterations are generally sufficient to yield a significant performance improvement over linear equalisation on severely dispersive channels. It is more effective than a conventional hard decision DFE, and avoids its error propagation problem, at the expense of slightly higher complexity. SDFE brings the performance of the FDSP technique closer to that of the linearly-equalised FET and TDM techniques at the expense of some extra receiver complexity.

Other considerations also influence the choice of a channel estimation pilot scheme for serial modulation. The prime advantage of serial modulation over OFDM is its lower PAPR and hence lower transmit power backoff requirement. The PAPR is not affected by the addition of a Chu sequence time domain pilot signal, but the addition of frequency domain pilots amounts to the transmission of several parallel waveforms, and thus increases the PAPR somewhat. Furthermore, it can be shown that the PAPR is also increased in the FET approach due to the rearrangement and expansion of the signal spectrum to accommodate the added pilots. Measurements of the power backoff required to confine the transmitted spectrum to a given spectral mask indicate that the backoff is still less than that of a comparable OFDM signal, but the margin is slightly reduced for FDSP, and more so for FET. Another consideration is overhead; the FET and TDM techniques both incur higher overhead than the FDSP technique.

Figure F.14 shows block error rate performance curves for TDM, FET and FDSP pilot techniques, as well as for the case of no pilots and perfect channel state information. Figure F.14 (a) shows the results for linear equalisation, and Figure F.14 (b) shows results for the soft iterative DFE with two iterations. The 1's and zeroes in the legend indicate which blocks have pilots, and P indicates the number of pilots per block; e.g. [100000000001] indicates pilots in every 11^{th} block, and P=104 indicates 104 pilots in a set of 416 used subcarriers – equivalent to the pilot grid scheme of Figure B.6.

[25] For MS speed <=70 km/h, we assume the channel varies linearly within one frame.

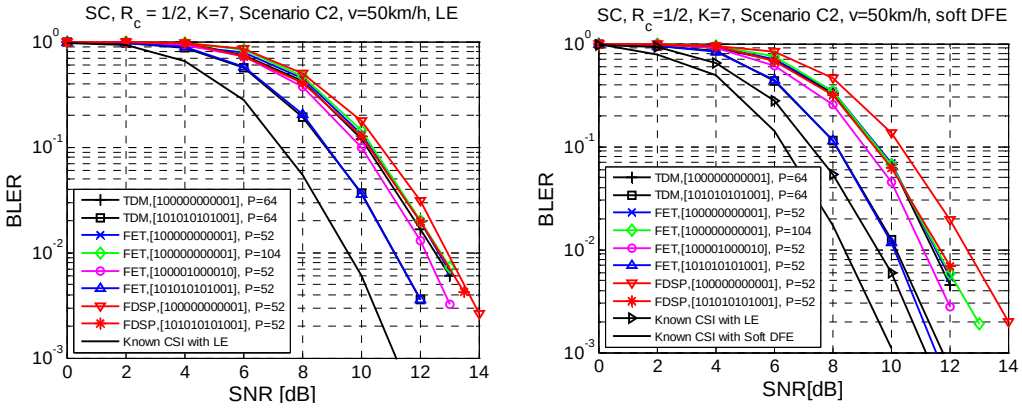

(a) (b)

Figure F.14: Block error rates for linear (a) and soft DFE equalisers (b).

Table F.2 summarises the SNR degradations relative to known channel for OFDM from Figure F.15, and also the total overhead. The total overhead includes pilots, cyclic prefix, and unused subcarriers in the FFT blocks. The extra backoff is with respect to the power backoff required for the OFDM system. The power backoff in each case was determined so to accommodate the transmitted spectrum emerging from a power amplifier modelled by a Rapp model [Rap91] with parameter p=2. The table also includes the OFDM-PACE and the iterative channel estimation OFDM-ICE scheme. Iterative channel estimation schemes could also be applied for single carrier, but were not evaluated here.

Table F.2: Comparison of performance, pilot overhead, and required power backoff for three different pilot schemes, for linear equalisation and soft decision feedback equalisation, and for OFDM. Channel is C2 with wide area FDD signal parameters.

Pilot schemes	SNR degradation @BLER=10^{-2} relative to SNR=8.6 dB for OFDM with perfect CSI (dB)		Total overhead[26] (%)	Power backoff to satisfy spectral mask relative to OFDM (dB)	Power penalty relative to OFDM with perfect CSI (dB) and no pilots (col. 2+col. 4)	
	LE[27]	SDFE[28]			LE	SDFE
SC-TDM[29]	3.7	2.7	28.5	-3.0	0.7	-0.3
SC-FET[30]	3.6	2.4	29.6	-1.1	2.5	1.3
SC-FDSP[31]	3.9	2.9	27.8	-1.5	2.4	1.4
OFDM - PACE[32]	1.7		29.4	0	1.7	
OFDM - ICE(8)[33]	0		29.4	0	0	

The calculated overheads, which are a direct measure of modulation inefficiency for the various schemes, are similar. Most of the overhead is contributed by cyclic prefix and unused subcarriers rather than by pilots. The table's last column shows the power penalty due to the combination of SNR degradation and required transmitter power backoff for a given power amplifier. We see that single carrier with time division pilots give the least power penalty. The single carrier frequency domain pilots and OFDM schemes are about 1 to 2 dB worse (due to their increased backoff requirements). The single carrier frequency domain pilot schemes have roughly the same power penalties as those of OFDM-PACE, when the receiver uses the soft iterative DFE, and would likely have similar penalties as OFDM-ICE if iterative channel estimation were added. The major power backoff advantage of single carrier is best realised when time domain pilots are used for channel estimation.

F.3.2 Pilot-aided and iterative channel estimation for OFDM

In this section, pilot-aided (PACE) and iterative channel estimation (ICE) is evaluated for non-adaptive OFDM transmission in both FDD and TDD mode [WIND21, WIND23]. The pilot-aided technique relies

[26] Total overhead =

$$\alpha_p \cdot \frac{N_{CP} + N_{pilot} + N_{GI}}{N_{FFT} + N_{CP} + N_{pilot,t}} + (1-\alpha_p)\frac{N_{CP} + N_{GI}}{N_{FFT} + N_{CP}}$$

Where NCP : cyclic prefix length=64, Npilot : number of pilot symbols per block=52, 64 or 104, NGI : number of unused subcarriers in each FFT block=96, NFFT : FFT block length=512, Npilot,t : number of time domain pilot symbols (if any)=0 or 128, αp : fraction of blocks with overhead-causing pilots=1/11.

[27] Linear frequency domain equaliser.

[28] Soft iterative decision feedback equaliser, with 2 iterations.

[29] Single carrier with 64-symbol time domain-multiplexed pilot sequences. Pilot sequence inserted every 11th block.

[30] Single carrier with frequency domain pilots inserted every 8th frequency in every 5th block.

[31] Single carrier with frequency domain pilots, replacing data at every 8th frequency in every second block.

[32] OFDM with frequency domain pilots inserted every 4th frequency in every 11th block. Results from Figure F.15,

[33] Iterative channel estimation using 2 turbo iterations.

on common pilots proposed in Appendix B.4.2 scattered over the whole available bandwidth, or solely from dedicated pilots of one chunk.

The pilot grid used for simulations is in line with the general pilot grid pattern suggested in Appendix B.4.2. For Wiener filtering, a robust filter design is selected for each mode, according to the specifications of the "mismatched Wiener interpolation filter (WIF) in Appendix F.3.3. While the actual velocity for the typical urban macro channel model C2 is set to 50 km/h, a UT velocity of 100 km/h was assumed to generate the filter coefficients in time direction. For the correlation in frequency direction, a mismatched filter assuming a maximum delay of the channel τ_{max}, equal to the CP duration is used.

For the case of QPSK modulation, we consider channel estimation with common pilots, using the full bandwidth, and with dedicated pilots for chunk-based channel estimation. The allocation of chunks to users is performed in a round-robin manner. In the numerical simulations, the channel encoder is a memory 6 CC with generator polynomials (133,171) in octal form. At the base station, each data stream corresponding to a given user is iteratively decoded. Figure F.15 shows the BLER performance achieved with PACE or ICE respectively in the TDD and the FDD mode, when channel estimation is carried out at the chunk level or using the full available bandwidth. The results are summarised in Table F.3. For ICE with common pilots no performance loss relative to perfect channel knowledge is observed. For chunk based channel estimation with dedicated pilots ICE turns out to be particularly effective. Generally, the performance loss relative to perfect channel knowledge is greater in the FDD mode. In this transmission scenario, the user mobility and a higher frequency selectivity of the channel render channel estimation more difficult than for the TDD case.

Table F.3: SNR degradation of several channel estimation techniques with respect to the case of perfect channel knowledge at the receiver.

Transmission mode	**Channel model / mobility**	**SNR Degradation @ BLER = 10^{-2}**			
		Chunk-based - PACE	Chunk-based - ICE	Full BW - PACE	Full BW – ICE
TDD	B3 / no mobility	2.8 dB	0.9 dB	1.2 dB	0 dB
FDD	C2 / 100 km/h	3.4 dB	1.1 dB	1.7 dB	0 dB

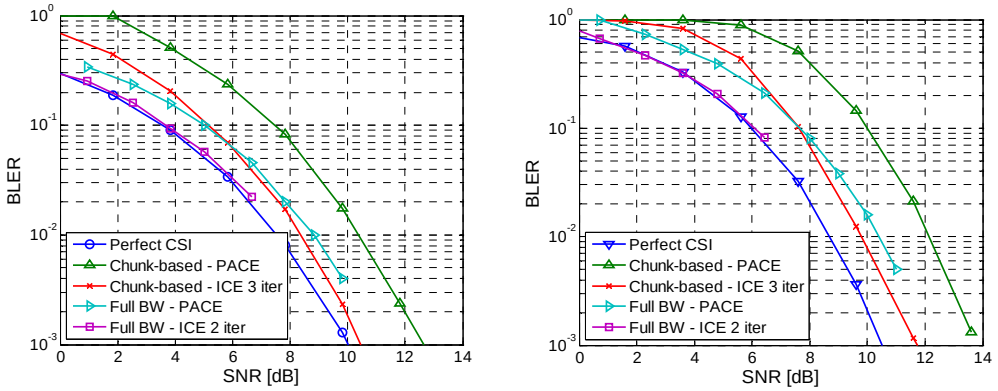

Figure F.15: BLER performance for PACE or ICE at the chunk level or using the full data bandwidth with QPSK modulation. Left: SISO, TDD mode, channel B3 NLOS, no mobility; right: SISO, FDD mode, channel C2 NLOS, UT velocity 50 km/h.

Figure F.16 depicts the BLER performance achieved with PACE or ICE with higher-order modulation alphabets (16-/64-QAM). Apart the parameters for common pilots using the full bandwidth from the previous figures apply. For both 16 and 64-QAM, ICE approaches the performance of a receiver with perfect channel knowledge. For 16-QAM, the SNR loss with PACE at BLER = 10^{-2} varies from 1.3 dB to 1.7 dB respectively for the TDD and the FDD mode. With 64-QAM, the performance degradation caused by channel estimation errors induced by PACE ranges from 1.2 dB in the TDD mode to 2.2 dB in the FD mode. The SNR degradation for PACE remains almost constant over the range of BLER considered for the evaluation of the channel estimation performance.

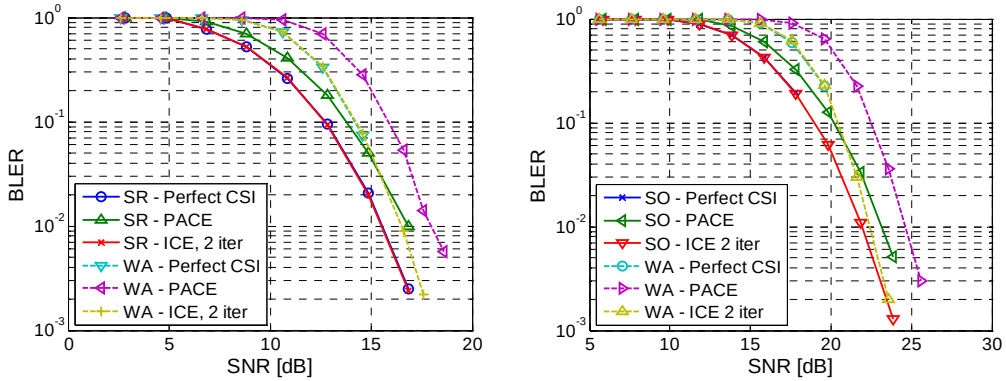

Figure F.16: BLER performance of PACE and ICE after 2 turbo iterations with 16-QAM modulation (left) and 64-QAM modulation (right) for the short-range (SR), TDD mode and the wide-area (WA), FDD mode.

F.3.3 Design of the channel estimation unit

For pilot aided channel estimation (PACE) two cascaded FIR interpolation filters are used, one operating in frequency direction for interpolation over subcarriers of one OFDM symbol; and the other operating in time for interpolation over OFDM symbols of a certain subcarrier, as described in [WIND21], section 6.2.1. The performance of the interpolation filter depends on the amount of knowledge of the channel statistics, these are:

- A Wiener interpolation filter (WIF) which is perfectly matched to the channel statistics. The power delay profile (PDP) and the Doppler power spectrum (DPS) are assumed to be perfectly known.
- A WIF with "matched pass-band". Knowledge about the maximum delay of the channel $\tau_{\max}$ and the maximum Doppler frequency $f_{D,\max}$ are assumed. However, within [0, $\tau_{\max}$] and [$-f_{D,\max}$, $f_{D,\max}$], the PDP and DPS are assumed to be unknown and uniformly distributed. For the results the WINNER B3 and C2 channel models were used for the TDD and FDD mode, respectively.
- A mismatched WIF, where the maximum channel delay is assumed to be equal to the CP duration, and the maximum Doppler frequency is set to the maximum value of expected mobile velocities. For the TDD mode pedestrian velocities of 10 km/h, while for the FDD mode velocities up to 100 km/h are assumed, corresponding to a normalised Doppler frequency of $f'_{D,\max} = 10^{-4}$ and $f_{D,\max} = 0.013$, respectively.

In all cases perfect knowledge of the SINR at the receiver was assumed, as it is expected that this information is needed also by other parts of the WINNER system.

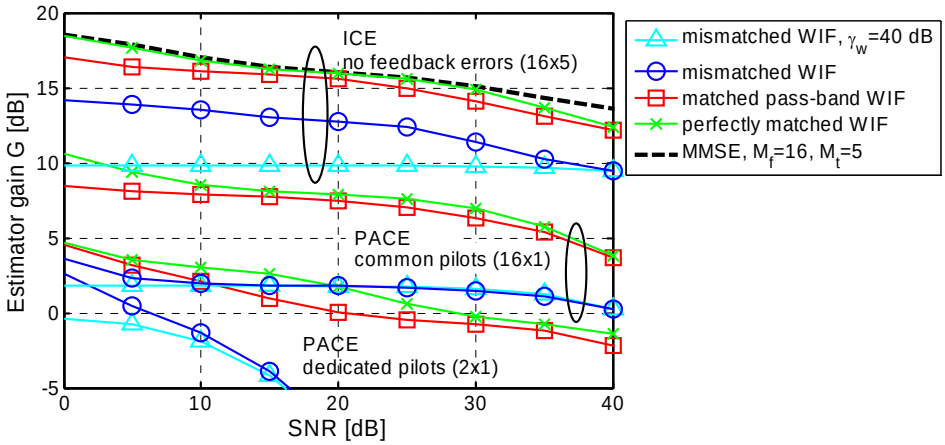

Figure F.17: Estimator gain vs SNR for dedicated and common pilots of various channel estimation techniques. Also shown is the estimator gain in case all symbols per chunk can be used as pilots, which can be viewed as a lower bound for ICE if decision feedback errors are negligible.

For certain MIMO techniques utilizing short term channel knowledge at the transmitter the degradation due to channel estimation errors is very severe (see Appendix B.4.2). There estimator gains in the range of 13 to 17 dB are required. The estimator gain is a measure for the quality of the channel estimate, and is defined as *1/(MSE·SNR)*. Figure F.17 shows the estimator gains for dedicated and common pilots of the three considered channel estimation techniques. PACE with dedicated pilots cannot achieve the required gains, even for a perfectly matched filter. If all symbols within a chunk can be utilised as pilots, estimator gains exceeding 13 dB are possible. This may be achieved by ICE, in case decision feedback errors are negligible, a realistic assumptions in the high SNR regime.

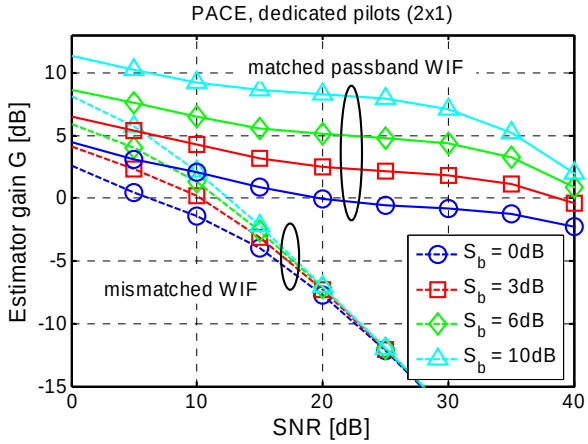

Figure F.18: Estimator gain vs SNR for dedicated pilots for various pilot boosts.

Unfortunately, even with excessive pilot boosts the estimator gains for dedicated pilots are not sufficient, as shown in Figure F.18. So, some post processing of the PACE channel estimates appears necessary.

F.3.4 Unbiased channel interpolation

Unbiased interpolation is used in the bootstrap phase of the communication. It is based on the relation between the delay and frequency-domain channel coefficients in OFDM systems (see [JFH+05]). Solutions are needed for full-spectrum (down-link) and at chunk level, for up-link and dedicated pilots. Here we report on the full-spectrum approach while chunk-level concepts are still under development.

It is assumed that all subcarriers can be used for pilot or data transmission and that a sparse regular pilot grid is used. Figure F.19 (left) shows the reconstructed frequency response using a pilot spacing of 16 subcarriers in the short-range scenario (SNR = 20 dB). If the channel delays approach the CP length, this is

the theoretical maximum pilot spacing according to the sampling theorem. Figure F.19 (right) shows the estimator gain achieved with linear unbiased interpolation. It depends on both SNR and delay spread (measured in taps, 1 tap = 10 ns). The lower the SNR and the smaller the delay spread are the less taps are detected and, hence, the more noisy taps can be removed.

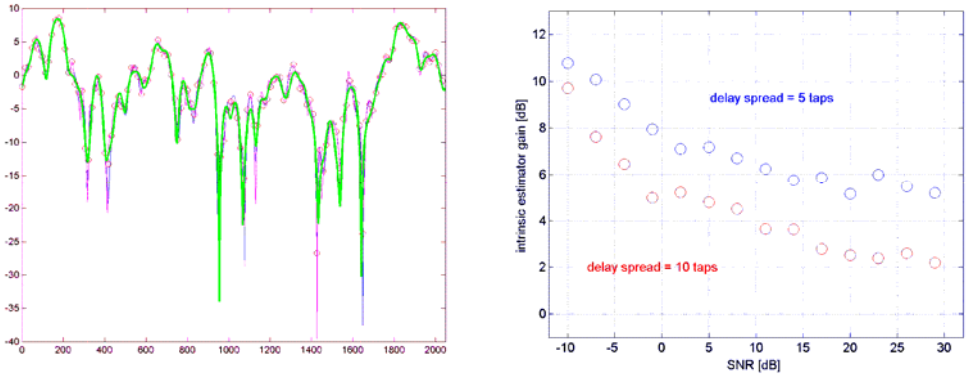

Figure F.19: Left: Results for unbiased interpolation over the full spectrum (blue: true channel, red: channel with noise, open dots: estimates on sparse pilot grid, green: interpolated frequency response). Right: Estimator gain with noise reduction in time domain.

F.3.5 Channel estimation using the guard interval — pseudo-random-postfix OFDM

PRP-OFDM simulations were performed for the FDD parameter set presented in Table 2.1. Channel propagation conditions are used as defined in scenario C2 NLOS. PRP-OFDM requires a significant number of OFDM symbols per frame in order to provide high SNR CIR estimates. Since the parameter set defines a relatively short frame of 12 OFDM symbols only, the simulation results focus on QPSK constellations. PRP-OFDM will be shown to enable the system to work efficiently in a high mobility context (up to 144 km/h is considered here) if QPSK constellations are applied. Due to the short frame length, a significant error floor can be observed for 16-QAM transmission (which requires good channel estimates) which is improved (but not completely removed) by iterative interference suppressions (IIS). Any scenario with a frame-length smaller than 12 OFDM symbols is not considered for the use with PRP-OFDM (due to the insufficient CIR estimation MSE).

Simulations are performed taking 11 OFDM symbols into account for CIR estimation. The frame to be decoded is assumed to be preceded by (dummy) PRP-OFDM symbols that are not decoded, but whose postfix sequences are exploited for CIR estimation. The results of PRP-OFDM are compared to a standard CP-OFDM system where the CIR estimation is assumed to be performed on 2 OFDM learning symbols at the beginning of the frame, just after synchronisation. No channel tracking is performed in this case. The simulation results in Figure F.20 show that a considerable error floor is present for standard CP-OFDM system for the mobility scenarios. For PRP-OFDM, this error floor disappears in the BLER range of interest and only an offset in SNR remains (approx. 2 dB offset comparing 0 km/h vs 144 km/h). As a conclusion, it can be stated that in combination with the chosen system and simulation parameters PRP-OFDM is useful in high mobility scenarios applying lower order constellations (QPSK in this example). Higher order constellations (QAM16 and higher) require larger observation window sizes for the CIR estimation and thus longer frames. In the QPSK context, PRP-OFDM leads to very acceptable system performance results at UT velocities as high as 144 km/h and beyond: the performance loss at 144 km/h is limited to approximately 2 dB, compared to the static case.

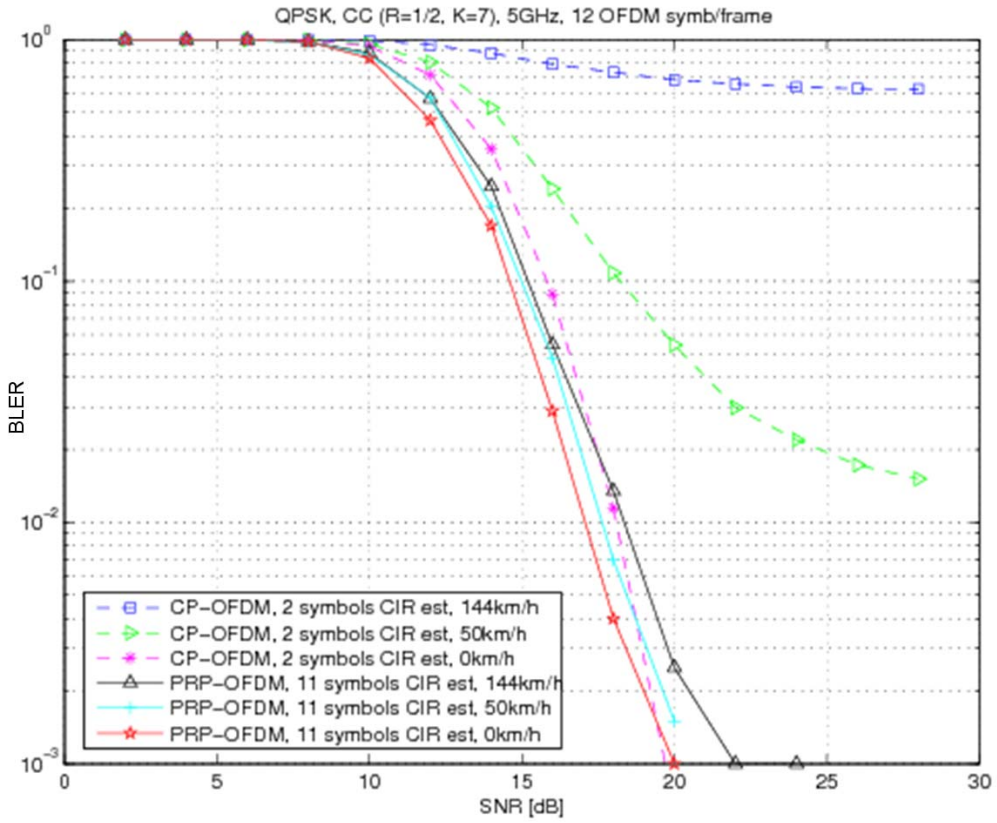

Figure F.20: PRP-OFDM, 11 Symbols CIR Estimation, QPSK, BLER simulation results.

The simulation results show that PRP-OFDM can be used in the downlink to reduce the overhead required for channel estimation, by using the guard interval for this purpose. However, the drawbacks, namely the introduced delay (especially for higher order modulation) and the inability to extend this scheme to the uplink case are currently considered to outweigh the benefits. Therefore, CP-OFDM relying on a scattered pilot grid is currently the preferred solution.

F.4 Synchronisation

F.4.1 Synchronisation without utilizing an explicit training symbol

In [BSB97] a blind algorithm for symbol timing and frequency offset estimation was proposed, which utilises the guard interval, having the great advantage that it does not require any overhead in form of training data. The basic idea is that the cyclic prefix is identical to the original part of the GMC block from which it is copied. Correlation of the cyclic prefix with its original part results in a correlation peak. The magnitude of the correlator output peaks at the beginning of an OFDM symbol, while its phase at this time instant is proportional to the carrier frequency offset Δf. The algorithm detailed in [BSB97] is the maximum likelihood (ML) estimate in an AWGN channel. For the ML estimate, knowledge of the SNR is necessary, which is impractical for acquisition, when usually no information about the received signal is available. The ML metric consists of the correlation metric ρ of the cyclic prefix with its original part, as well as a metric which accounts for the signal power ϕ.

Three different variants of the CP based synchronisation are compared:

- The ML estimator proposed in [BSB97]
- An estimator which only uses the correlation metric ρ labelled “COR”. Utilizing only ρ approaches the ML estimate at low SNR [LC02].
- An estimator which uses the difference $\rho - \phi$ approaches the ML estimate at high SNR [LC02]. This approach is named “norm COR”, since it is normalised by the power of the received signal.

Unfortunately, the performance of this approach degrades in a frequency selective channel, since the time dispersive channel impulse response reduces the ISI free part of the guard interval. Computer simulations have been carried out for the WINNER FDD mode, with channel model C2 and system parameters taken from Table 2.1. For the TDD mode the performance is expected to be better, since CP correlation typically performs better if the number of subcarriers is large.

Since the time and frequency offset will be constant during some OFDM symbols, averaging over several estimates considerably improves the performance [BBB+99]. *This simple averaging of the correlation metric is a highly effective means to increase the robustness as well as accuracy of the CP based acquisition.* In the simulations, averaging was performed over 12 OFDM symbols, i.e. one OFDM frame.

For channel model C2 the mean estimated timing offset is $E\{\Delta T\} \approx 6\,T_{spl}$, which implies that the timing estimator is biased. Unfortunately, a positive mean will cause ISI and should therefore be avoided. The bias may be compensated by a fine timing synchronisation unit operating in the frequency domain.

The standard deviation of the time and frequency offsets is shown in Figure F.21. Averaging the correlation metric of the CP based algorithm significantly improves the accuracy of the time and frequency estimates, as shown in Figure F.21. For cross-correlation based synchronisation averaging is only possible over the two OFDM symbols which carry pilot symbols. Thus, this technique cannot benefit from averaging to the same extend as CP based synchronisation. While the combination of the CP based and the cross-correlation approach are possible [LWB+02], the cross-correlation approach cannot substantially improve the synchronisation accuracy. Hence, cross-correlation based synchronisation is applicable mainly in case that BSs are not synchronised.

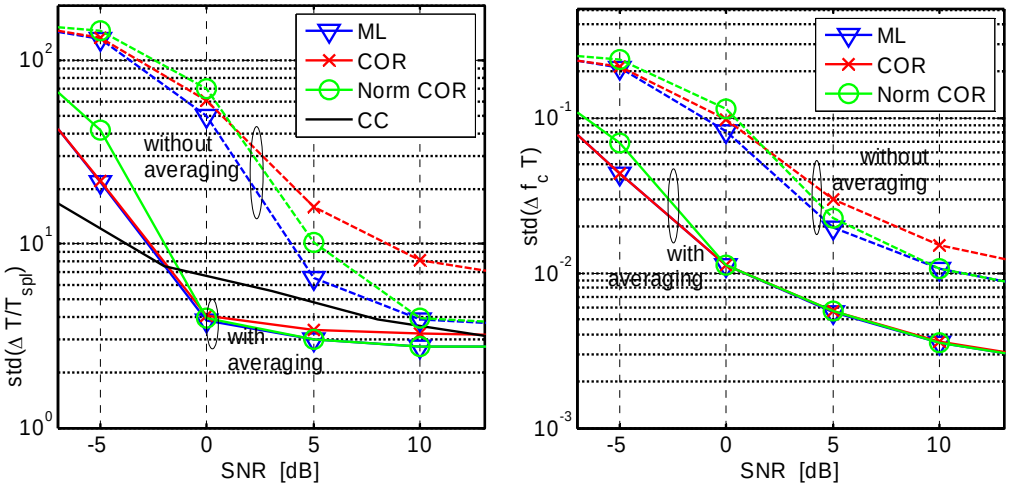

Figure F.21: Standard deviation of the estimated time and frequency offset against the SNR; (a) standard deviation of the time offset (left side, CC = cross-correlator) and (b) standard deviation of the frequency offset (right side).

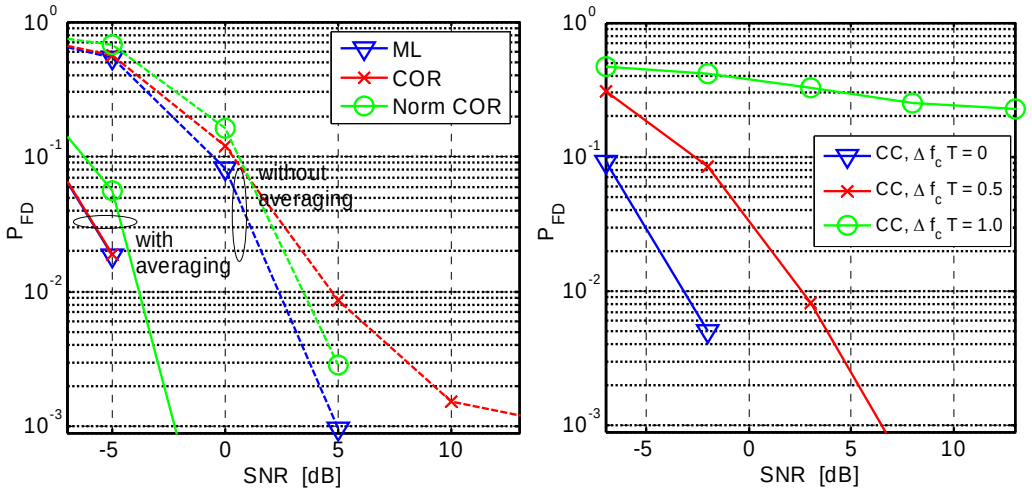

Figure F.22: Probability of false detection, P_{FD}, against the SNR, for (a) the CP correlator (left side) and (b) the cross-correlator (CC) using the scattered pilot grid of Figure B.6 (right side).

Of particular interest is the performance of the algorithm at low SNR. We define a false detection if the timing estimate is outside the window [$-N_{CP}/2$, $N_{CP}/2$]. In Figure F.22 the probability of false detection, P_{FD}, of the CP correlator is plotted against the SNR (left side). It is seen that P_{FD} is significantly reduced by averaging over 12 OFDM symbols. The probability of false detection can be further reduced by averaging over more OFDM symbols. For the simple COR synchronisation scheme the improvement through averaging is most significant.

On the right hand side of Figure F.22, P_{FD} is shown for the cross-correlation (CC) based synchronisation scheme using the scattered pilot grid of the WINNER FDD mode. It is seen that the detection probability of the OFDM symbol timing severely degrades if a carrier frequency offset is present. For synchronisation in a wireless network, time synchronisation for non-synchronised BSs is possible, if adjacent BS use different pilot sequences. However, since the cross-correlator is sensitive to frequency offsets, BSs should be either time or frequency synchronised. Comparing the CP-based auto-correlation with the cross-correlation technique, the CP correlation with averaging appears favourable. Only for not time synchronised BSs the CC technique is a valid option. It should be noted, however, that this statement depends on the chosen pilot grid. For a smaller pilot spacing, the performance of the CC technique is expected to improve.

To conclude, synchronisation by correlating the cyclic prefix (CP) with its original part is robust even at very low SNR provided that the correlation metric is sufficiently averaged. Averaging over 12 OFDM symbols mitigates false detection for SNR≥0 dB. Since COR is the technique with the least complexity, it can be concluded that averaging combined with COR is an appropriate choice, due to its simplicity, low overhead, high accuracy and reliability. Cross-correlation synchronisation utilizing a scattered pilot grid, predominantly used for channel estimation, can be used for synchronisation of a network where BSs are not time synchronised. However, BSs need to be frequency synchronised for this algorithm to work.

F.5 Performance of selected bit and power loading algorithms

In [WIND24] a set of various aspects of the adaptive link-level transmission using Hughes-Hartogs optimum bit-loading algorithm was assessed. However, as mentioned in Appendix B.5.1, the HH approach is not ideal from the complexity point of view. Therefore, the following simulation results present a performance comparison between the HH algorithm and two others suboptimum, less complex implementations by Chow, Cioffi and Bingham and by Fischer and Huber.

The presented bit error rate results have been obtained using a Monte-Carlo method by transmitting 100 million information bits per one particular SNR value. This gives a sufficient precision to estimate bit error rates in the order of 10^{-5}.

A limited power constraint, equal to the value of 1 [W] times the number of used subcarriers $N_u = 1664$, has been assumed in all evaluations. Moreover, a constant number of information bits have been loaded in each OFDM symbol, i.e.:

$$B_i = N_u \cdot R \cdot \log_2(M) \tag{F.1}$$

where: N_u means number of used subcarriers, R represents the code rate, and M is the constellation size.

In order to compare the performance of the evaluated loading algorithms, the actual power loaded on each subcarrier has been normalised, so the following criterion is fulfilled:

$$\sum_{i=0}^{N_u-1} P_i = P_{target},$$

where P_i is the power loaded on the i^{th} subcarrier after normalisation and P_{target} is the total power limit.

Figure F.23 presents the simulation results for indoor scenario A1 NLOS channel model for a velocity $v = 5$ km/h. The suboptimum, less complex CCB and FH bit and power loading algorithms are compared to the Hughes-Hartogs approach. All three algorithms have used the target BER setting equal to 10^{-4}. The mean number of information bits transmitted in each OFDM symbol has been set to $2\,N_u = 3328$. The maximum number of iterations of the CCB algorithm has been limited to 10 (see Appendix B.5.1.2). For comparison purposes an extra curve for non-adaptive transmission with fixed code rate and constellation size is depicted. The overall bit rate of this fixed transmission is the same as in the adaptive cases.

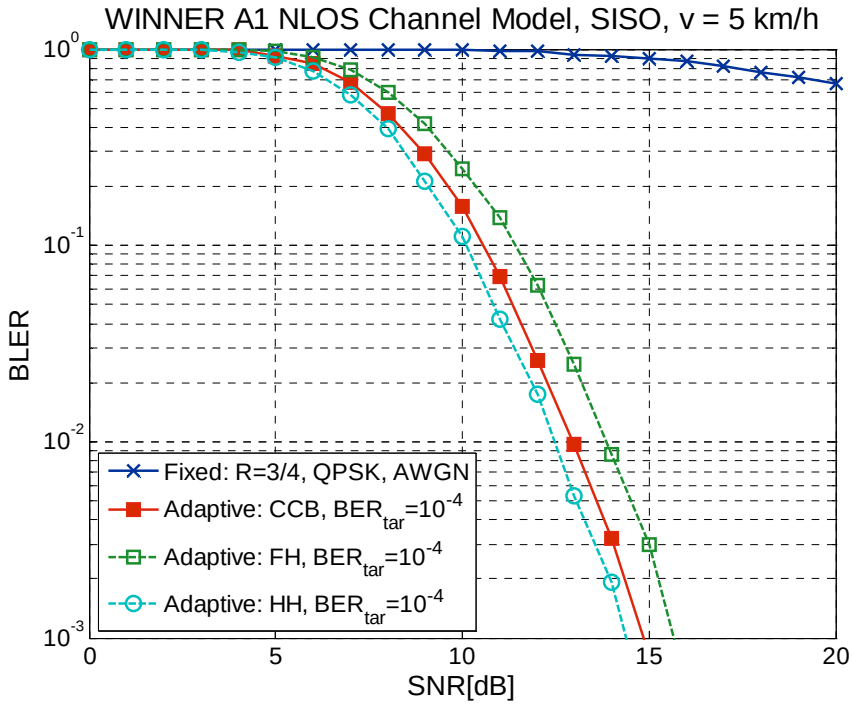

Figure F.23: Performance comparison of the HH, CCB, and FH bit and power loading algorithms (short-range scenario, A1 NLOS channel model, SISO case, v = 5 km/h).

Similar simulation results are shown in Figure F.24. Here, slight different parameters have been chosen for comparison. The channel model is B3 NLOS (short-range hotspot scenario), however, the velocity has been set to the same value $v = 5$ km/h. The mean number of information bits transmitted in one OFDM symbol is equal to $1.5\ N_u = 2496$, which is adequate for a transmission of a whole OFDM symbol using the code rate $R = ¾$ and QPSK constellation on each used subcarrier.

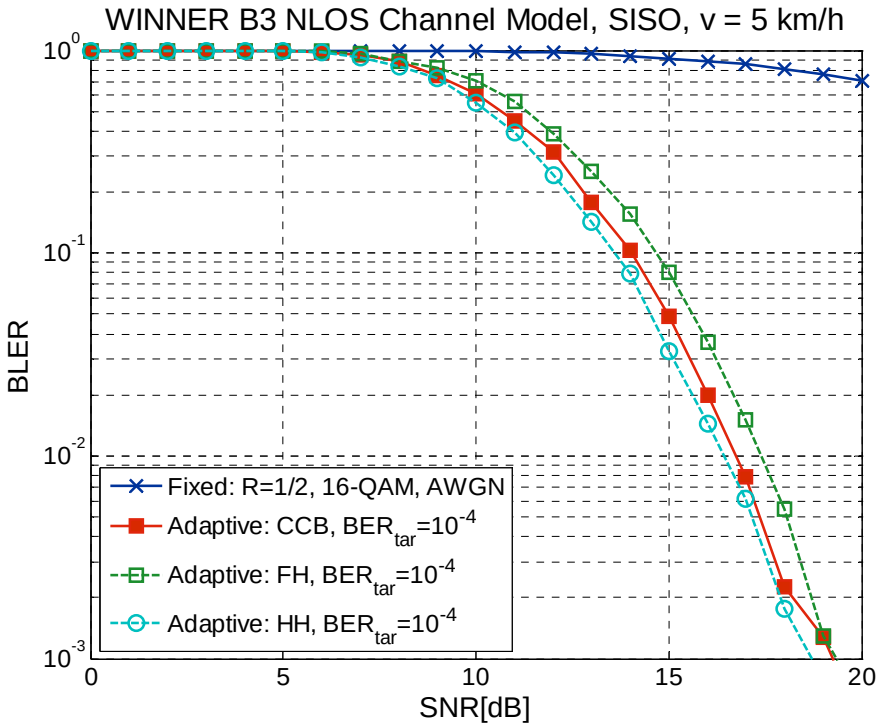

Figure F.24: Performance comparison of the HH, CCB, and FH bit and power loading algorithms (short-range scenario, B3 LOS channel model, SISO case, v = 5 km/h).

Having looked at the results presented above one can conclude that the Fischer and Huber approach has only slightly worse performance than the Chow, Cioffi and Bingham solution, in a coded transmission over wireless channel models. As expected, Hughes-Hartogs bit and power loading algorithm performs best, but it has the highest computational complexity. In general, the observed performance degradation of the suboptimum algorithms is so small that it can be neglected in this case.

Appendix G. Multi-Link and System-Level Assessments

Multi-link and system level simulations have been set up in order to study those techniques which directly or indirectly influence the level of interference at the receivers. Basically, these are multiple access, radio resource management, spatial processing at transmitter, synchronisation of multiple transmitters (in case of a synchronised network) and power allocation/control. Another class of techniques which has to be studied by means of system or multi-link simulations is related to receiver processing and the ability to cope with or to combat interference. This class typically comprises the large set of single user and multi-user detection algorithm with or without the aid of multiple antennas and iterative processing. Even synchronisation belongs to this class of receiver techniques provided there is a potential crosstalk from other simultaneously transmitting stations.

This discussion reveals the huge amount of different topics which can and have to be assessed by means of multi-link or system level simulations. Within WINNER Phase I emphasis has been placed on the evaluation of different multiple access schemes for up- and downlink partly in combination with various spatial processing options. It is a continuation of the work being done in [WIND26] and [WIND27] focusing now on the most promising candidates and using more elaborated simulation environments. For non-frequency-adaptively scheduled flows in the downlink, the multiple access candidates are chunk based OFDMA/TDMA and MC-CDMA/TDMA and a comparison can be found in Appendix G.1.1. The subcarrier interleaved variants of these two multiple access schemes are considered in Appendix G.1.2. Regarding frequency-adaptively scheduled flows, chunk based OFDMA/TDMA was identified as the most promising approach due the highest flexibility in allocating resources to users. The additional SDMA gain using grid of fixed beams in a wide-area scenario is addressed in Appendix G.1.4. In the same context, spatial processing gains using more sophisticated adaptive beamforming approaches are analysed in Appendix G.2.1 and Appendix G.2.2. For non-adaptively scheduled flows, a comparison of beamforming, diversity and multiplexing is performed in Appendix G.2.4. Moreover, as in Appendix G.2.3, the impact of multiple antennas at the UT and associated combining techniques on system performance is studied. The absolute performance of linear multi-user SMMSE precoding is assessed in Appendix G.2.5 for the short-range scenario considering again non-frequency-adaptively scheduled flows. Taking realistic system impairments into account the required number of antennas to achieve an average sector throughput of 1 Gbit/s is identified.

The preferred medium access candidates considered for the uplink are pretty much the same as for the downlink including additionally symbol based TDMA. Compared to OFDMA/TDMA, pure TDMA is beneficial from terminal power consumption point of view and it is less susceptible to frequency offsets among terminals. However, the impact of synchronisation errors is not yet included when comparing OFDMA/TDMA and OFDM/TDMA in Appendix G.4.4. The absolute performance of OFDM/TDMA and ODFMA/TDMA with adaptive scheduling is assessed in Appendix G.4.1 and Appendix G.4.3, respectively. Considering a short-range scenario in Appendix G.4.3, the optimum resource allocation and bit loading scheme for OFDMA/TDMA with respect to sum capacity is compared to low complexity solutions.

The impact of spatial diversity at the BS for various antenna configurations is analysed in Appendix G.5.1. An information theoretic approach with respect to optimum spatial processing at the UT using two transmit antennas can be found Appendix G.5.2.

Other main results are related to multi-user detection/separation at the receiver. This holds not only for base stations but also for user terminals if MC-CDMA is applied. Corresponding results considering different receiver structures without and with multiple antennas at the UT can be found in Appendix G.3.1 and Appendix G.3.2, respectively. From the base station perspective, receiver structures for SISO DS-CDMA and MIMO single carrier are presented and compared in Appendix G.6.1 and Appendix G.6.2.

Other investigations which are not directly related to up/downlink multiple access, spatial processing or detection are part of Appendix G.7. In Appendix G.7.1, a comparison of OFDM and single carrier (with cyclic prefix) based uplinks is performed taking the increased power backoff constraint of OFDM into account. Appendix G.7.2 deals with low rate channel coding as a means to enable service to users at cell edge even in case of frequency reuse 1. Appendix G.7.3 focuses on the crosstalk which is induced in an OFDM receiver if signals from different base station suffer from transmission delay differences larger than the guard interval. Two resource partitioning schemes among base stations are compared with this respect: TDMA and FDMA. In Appendix G.7.4 conventional and self-organised RRM is compared with respect to system throughput considering several options how to cope with varying interference

conditions from newly arriving users. Finally, Performance results of a protocol which utilises and exploits the benefits of distributed antennas are presented in Appendix G.7.5.

It should be stressed that simulation results are provided by different partners using uncalibrated implementations and to a certain extent differing simulation assumptions. Consequently, results are not directly comparable unless otherwise noted (i.e. when they are from the same partner). Every contribution starts with a summary of the applied simulation assumptions different from those defined in Appendix E followed by a discussion of the simulation results and corresponding conclusions.

For illustrative purposes, the main set of medium access schemes which have been studied in greater detail by means of multi-link or system level simulation is depicted in Figure G.1. Note that in the section headings, the term TDMA has been omitted in most cases for the sake of brevity.

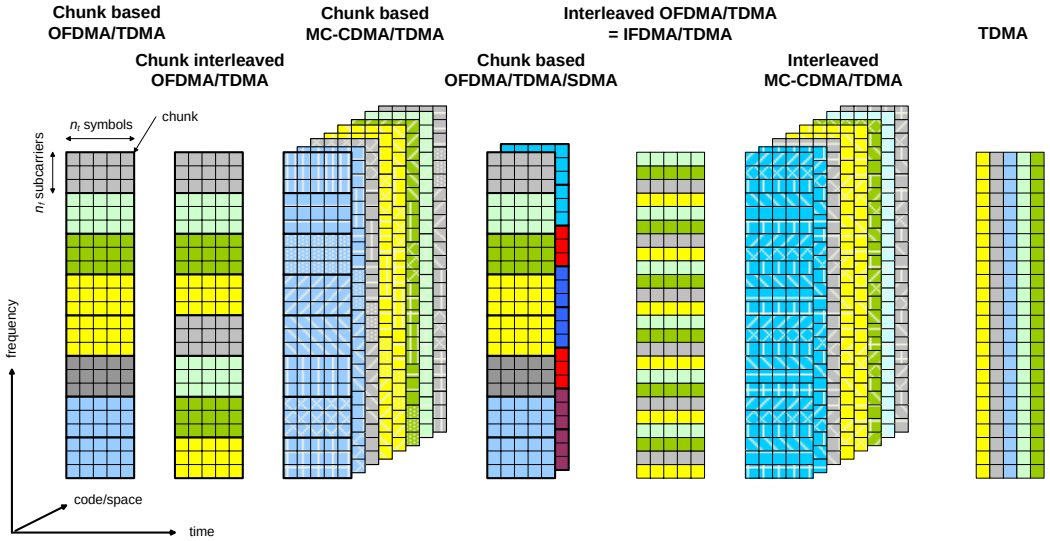

Figure G.1: Illustration of considered GMC-based medium access schemes.

G.1 Downlink multiple access

G.1.1 Comparison of non-adaptive OFDMA, MC-CDMA and adaptive OFDMA

Simulation Assumptions	
Simulator	System simulator using AWGN look-up tables and effective SINR mapping. Combined snap-shot dynamic mode, >100 runs of 1.4 s each simulated
Scenario	wide area cellular, frequency reuse: 1, single antenna BS and UT
Channel modelling	C2, NLOS, clustered delay line
Interference modelling	Central cell mode, with simplified inter-cell interference model (two tiers of fully loaded sectors)
Cell radius	900 m
MCS	6: QPSK,r=1/3;QPSK,r1/2;QPSK, r2/3;16-QAM, r=1/2, 16-QAM, r3/4; 64-QAM,r=2/3; BLER target: <0.1
FEC	Punctured convolutional coding $(561,753)_{oct}$ with memory 8 Codeword length: fixed size of 480 data symbols corresponding to 320–1920 payload bits depending on MCS used.
HARQ	Chase combining, maximum 6 retransmissions
Type of feedback	Non-freq. adaptive: Best MCS fed back by each terminal Freq. adaptive: One SINR per chunk, Ack/Nack messages explicitly fed back in all cases. Delay: 1 chunk duration
Overhead	Total overhead of 23% taken into account in TX-power and resources.
Mobile speed	30 km/h, same for all mobiles - results in almost perfect link adaptation

With the OFDMA variant considered here, each user scheduled for transmission is assigned a subset of 6 chunks (out of 48) thus serving 8 users per chunk duration. TDMA is applied in each of the two successive chunks forming a frame. Thus, 16 users are served in total in one FDD frame. In the frequency non-adaptive case, the 6 chunks of the 8 selected users are simply interleaved in frequency to provide a diversity gain for the channel decoder. Note that in this case the link adaptation could also be pre-calculated at the terminal and best MCS feedback would be sufficient. In the frequency-adaptive case, the 8 users select their preferred 6 chunks in a fair way. This requires an increased feedback using one SINR value per chunk for each user. Link adaptation is then performed explicitly by the base station after chunk allocation.

In case of MC-CDMA spreading is performed within the chunks only using a spreading factor of 8. Hence, the whole available bandwidth is shared by 8 users simultaneously. MC-CDMA requires only a feedback of the best MCS for each user in the cell assuming that link adaptation is pre-calculated at the terminals. Based on this feedback time-domain scheduling (selecting 16 simultaneous users) and link adaptation is performed at the base-station.

The simulation results in Figure G.2 and Figure G.3 firstly show a comparison of different scheduling algorithms in the non-frequency adaptive case using MC-CDMA. An evaluation of these scheduling algorithms for pure TDMA and lower system bandwidth (5 MHz) was already presented in earlier WINNER deliverables. The major difference compared to earlier results is the fact that with MC-CDMA, using a spreading factor of 8 and half-duplex FDD, 16 users are scheduled in parallel instead of just a single user. Since the gains obtained from multi-user diversity depend on the number of users competing for the resource, it is not surprising that the channel dependent schedulers Score Based and Maximum SINR achieve much lower gains in cell throughput compared to Round Robin (Figure G.2) than was found in the earlier studies for a comparable number of users.

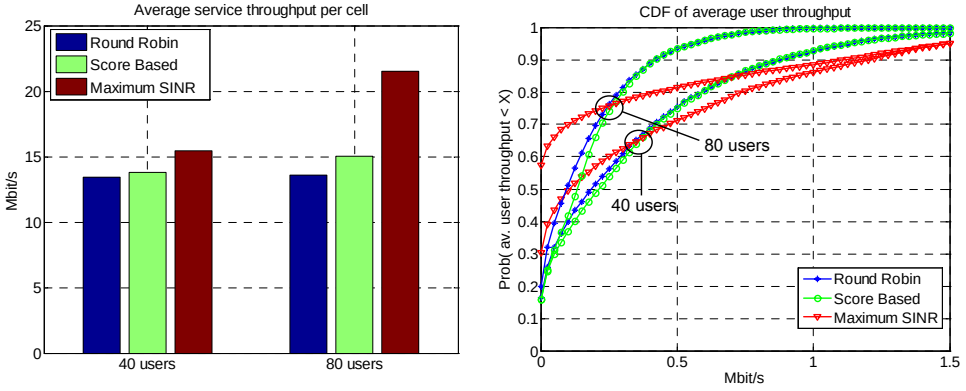

Figure G.2: Throughput for MC-CDMA vs. number of users/cell.

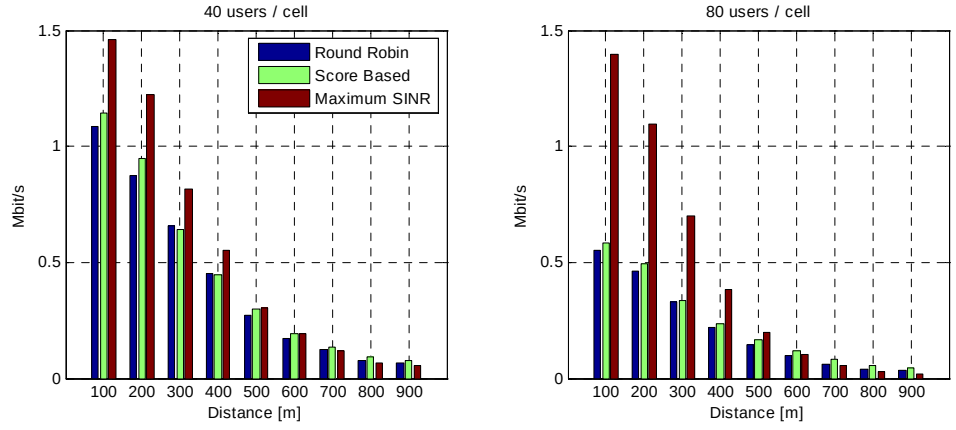

Figure G.3: Av. user throughput vs. distance (only scheduled users considered).

Note also that the cell throughput for the fair score-based scheduler is limited by the low rate users at the cell border (Figure G.3) similar to Round Robin. In contrast, the Maximum SINR scheduler artificially reduces the coverage by serving only users close to the cell centre. Note from Figure G.2 that for Maximum SINR scheduling around 30% (58%) of the 40 (80) users in the cell are not served. For Round Robin and score-based scheduling this number is slightly lower than 20% for both system loads. Hence, the single antenna configuration and the MCS's used for these first results do not provide satisfactory coverage and the use of multiple antennas and advanced coding strategies (e.g. Turbo Coding) does appear mandatory.

In Figure G.4 and Figure G.5, MC-CDMA and OFDMA are compared for the frequency adaptive and the frequency non-adaptive case. In the frequency non-adaptive case, MC-CDMA outperforms OFDMA in terms of cell and user throughput for all considered loads and scheduling algorithms. This is due to the frequency diversity advantage of MC-CDMA achieved by spreading the coded block over the whole bandwidth.

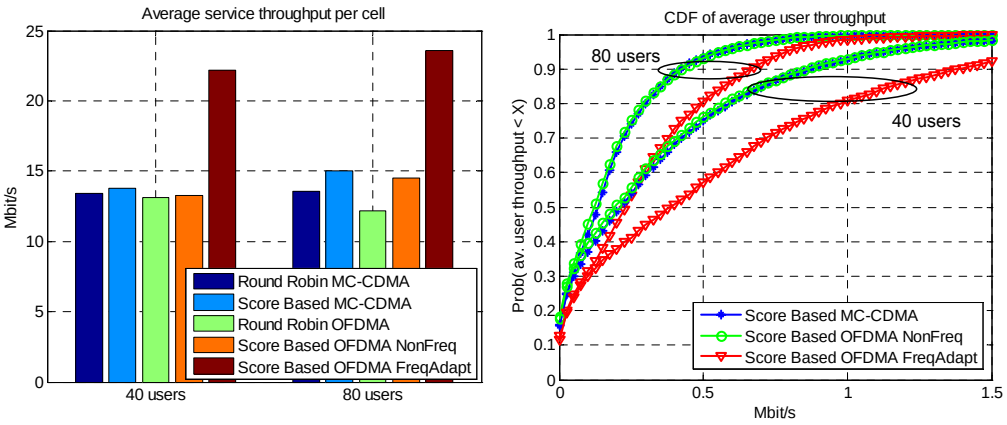

Figure G.4: Throughput for MC-CDMA and OFDMA vs. nb of users/cell.

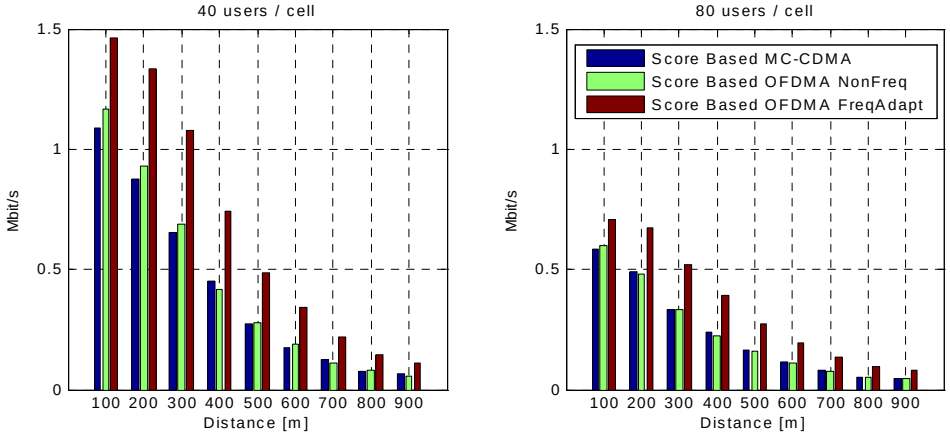

Figure G.5: Av. user throughput vs. distance (only scheduled users considered).

In the frequency-adaptive case, where the base station can use feedback on chunk level for adaptive chunk allocation, OFDMA achieves high gains in user and cell throughput. However, the gain is to a certain extent limited by the constraint that a fixed amount of chunks (6 in this case) is assigned to each user scheduled for transmission. The percentage of un-served users decreases by adaptive transmission to around 12% (Figure G.4) and the user throughput increases within the whole cell range (Figure G.5). However, the observation that overall coverage is unsatisfactory still holds in the frequency adaptive case

The following main conclusions can be drawn from the results:

- Multi-user diversity gains from fast scheduling can only be obtained when a **strong TDMA component on sub-frame level** is kept in the multiple access scheme. Only a limited number of users should be served simultaneously depending on delay constraints and required throughputs.
- In the considered single antenna system configuration, the cell coverage is unsatisfactory. The use of advanced antenna techniques (MIMO) and improved coding schemes (e.g. Turbo Coding) is mandatory to achieve satisfactory wide area coverage.
- **OFDMA** achieves high performance gains in the **frequency adaptive mode**, when a reliable feedback of the channel quality per chunk, e.g. SINR, is available for all users competing for the resource.
- In the **non-frequency adaptive case, MC-CDMA** outperforms OFDMA, thanks to the better frequency diversity obtained by spreading the symbols over the whole bandwidth. However, the differences are rather small and will probably vanish if other sources of diversity are available.[34]

G.1.2 Comparison of non-adaptive, subcarrier interleaved OFDMA and MC-CDMA

Simulation Assumptions	
Simulator	multi-link level
Scenario	Short range cellular, single antenna BS and UT
Channel modelling	IEEE 802.11n including path loss and shadowing
Interference modelling	Whole tier of interfering cells around desired cell, each cell generates own transmit signal and signal is transmitted through independent channel
Cell radius	300 m
Link adaptation	QPSK, r=1/2
FEC	Convolutional coding: $(561,753)_{oct}$ with memory 8 Codeword length: 3328
spreading	type: Walsh-Hadamard ; spreading length: 8 Despreading: MMSE based
Mobile speed	3 km/h

The simulation results in Figure G.6, left plot, show a direct comparison between subcarrier interleaved OFDMA and subcarrier interleaved MC-CDMA in a cellular environment in terms of BER. In case of OFDMA each user gets exclusively 208 subcarriers out of 1664 allowing a maximum number of 8 users to be served simultaneously. With MC-CDMA the data of each user is spread over 8 subcarriers leading to multiple access interference. Since the number of active users, the maximum number of users, the data symbols per user, and the frame size are equal, the comparison of the medium access variants is regarded as fair. The resource load of OFDMA is defined by the ratio of the number of allocated subcarriers relating to the number of available subcarriers. In MC-CDMA, the resource load is given by the ratio of the number of active users relating to maximum number of users which could be served using all available codes. In the case of OFDMA, an RRM over three cells can avoid a double allocation of subcarriers up to a resource load of 1/3. Otherwise, the subcarriers are randomly allocated. Three scenarios are investigated determined by the distance of the UTs to the base station: d_0=(150, 200, 300). In the inner part of the cell (d_0=150 m), MC-CDMA outperforms OFDMA for resource loads smaller than 0.75 due to enhanced frequency diversity but the difference is rather small if translated into throughput. The benefit of MC-CDMA reduces with increasing resource load because the multiple access interference increases. Since the inter-cellular interference is small in the inner part of the cell, the RRM for OFDMA does not enhance the performance dramatically. In contrast, the RRM improves drastically the performances for OFDMA in the outer parts of the cell (d_0 >200 m) for lower resource loads indicating that RRM is an important means for throughput enhancements at the cell edge especially if the system is not fully loaded (which is mostly the case in a real system). MC-CDMA always outperforms pure ODFMA in all three scenarios for resource loads lower than 0.6.

[34] The actual WINNER system concept offers additional sources of diversity in the spatial domain. A comparison of the additional benefit of MC-CDMA against the increased complexity in particular in conjunction with MIMO techniques is for further study.

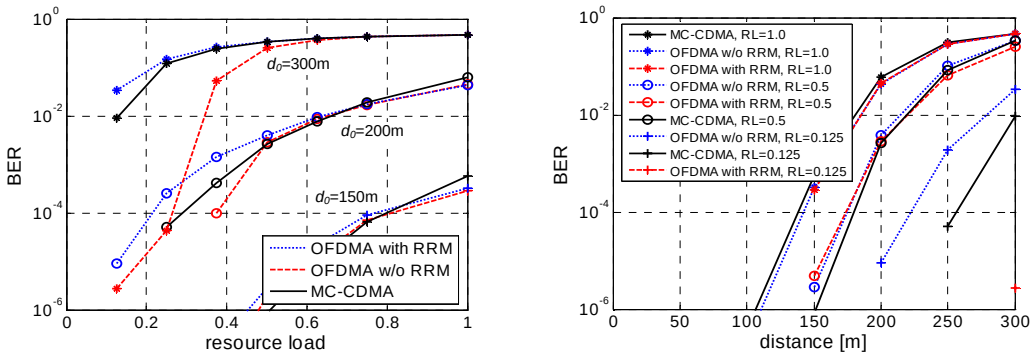

Figure G.6: BER versus resource load for different UT distances (left plot) and BER versus UT distance for different resource loads (right plot) considering interleaved MC-CDMA and OFDMA.

The right plot of Figure G.6 shows the BER versus the mobile distance to the desired base station. Three different resource loads for an OFDMA and MC-CDMA system are investigated. Due to the avoidance of inter-cellular interference by using the RRM for OFDMA, the BER with a resource load of 0.125 is nearly zero in the whole cell. MC-CDMA can utilise the whole frequency diversity, and therefore, MC-CDMA outperforms pure OFDMA in the scenarios with resource load 0.125 and 0.5 in the whole cell area. OFDMA slightly exceeds the MC-CDMA performance in the fully-loaded scenario because the multiple access interference is the major degradation factor of MC-CDMA.

To sum up, at low resource loads (smaller than 0.6) MC-CDMA performs always better than pure OFDMA due to the higher frequency diversity but the differences are small and will probably disappear if further sources of diversity are exploited, see footnote 34 on page 138. However, the enhanced interference suppression opportunities with smart RRM allow a large performance gain for lower bounds. The RRM shows a lower bound for the OFDMA system without any channel knowledge at the transmitter side. At high loads, both techniques show similar performances.

G.1.3 Comparison of non-adaptive OFDMA, MC-CDMA and TDMA

Simulation Assumptions	
Simulator	Multi-cell link level
Scenario	Wide area, single-antenna BS and UT; cell radius 1000 m
Channel modelling	C2 generic channel model (D5.4) including path loss + shadowing
Interference modelling	Whole tier of interfering cells around desired cell.
MCS	2: 4-QAM, r=1/2; 16-QAM, r=1/2
FEC	Convolutional coding: $(561,753)_{oct}$ with memory 8 Codeword length: 1664
Spreading	Type: Walsh-Hadamard ; spreading length: 8
Channel allocation for each codeword	TDMA – 4-QAM: 416 carriers × 2 symbols; TDMA – 16-QAM: 416 carriers × 1 symbol OFDMA – 4-QAM: 32 adjacent carriers × 26 symbols; OFDMA – 16-QAM: 32 adjacent carriers × 13 symbols MC-CDMA – 4-QAM: 416 carriers × 16 symbols MC-CDMA – 16-QAM: 416 carriers × 8 symbols Spreading is performed across 8 adjacent subcarriers

Simulations have been conducted in order to compare the performance of OFDMA/TDMA, MC-CDMA/TDMA and pure TDMA which can be regarded as a special case of MC-CDMA with spreading factor 1. Figure G.7 presents the throughput results for a fully loaded scenario, i.e. where all resources are used for data transmission, and 1/4 loaded scenario. Resources are allocated to UTs of different cells randomly, that is, no interference avoidance scheme is used. The results show that all considered multiple access schemes have very similar performances. In fully loaded case, OFDMA is slightly better than MC-CDMA due to inter-code interference in CDMA. In 1/4 load case, MC-CDMA is slightly better than the others, confirming the results obtained in G.1.2. It can also be seen that OFDMA is a little better than TDMA in both cases. This is due to OFDMA taking more advantage of the time diversity provided by the channel conditions used in the simulation. However, no spatial diversity has been taken into account yet

which may further reduce the performance differences between OFDM/TDMA, OFDMA and MC-CDMA (see also footnote 34 on page 138).

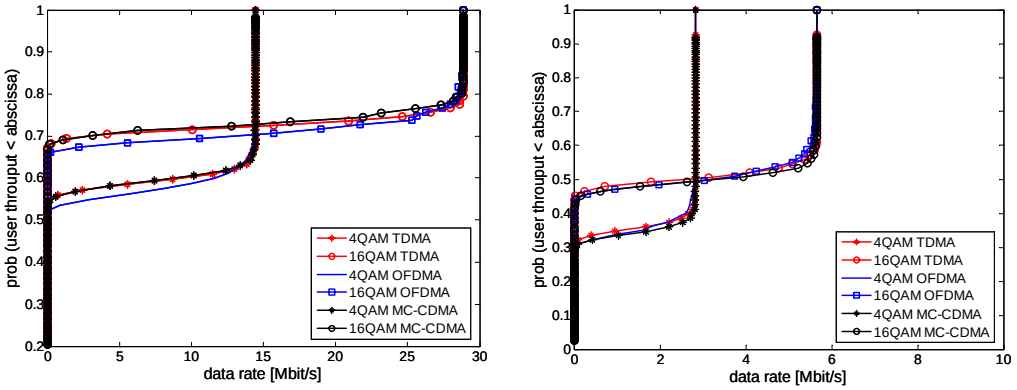

Figure G.7: Performance comparison of OFDMA, MC-CDMA and TDMA in fully loaded case (right plot) and non-fully loaded case (left plot).

Figure G.8 presents throughput results obtained for various reuse factors using OFDM/TDMA although the general conclusions stand for other MA schemes. Four tiers of interfering cells are used for the simulation. The results show that only about 77% of the cell has been sufficiently covered, therefore stronger MCS are required to cover users at the cell edge. These results support the suggestion in [WIND32] to cover different areas of the cell with different reuse factors. Approximately 37% of the cell can be covered by reuse 1. A further 28% of the cell can be covered by reuse 3. Reuse 7 can be used in approximately 12% of the cell.

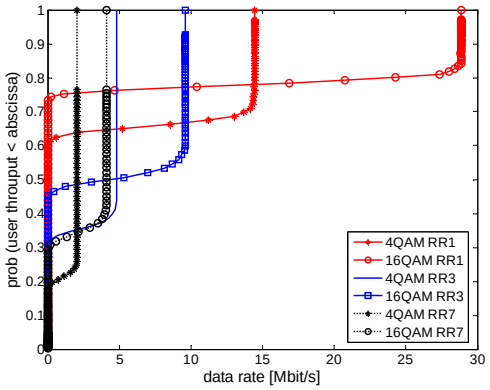

Figure G.8: Throughput for different reuse factors for OFDM/TDMA.

G.1.4 Impact of chunk sharing on the performance of adaptive OFDMA/TDMA

Simulation Assumptions	
Simulator	Link level
Scenario	wide area, $M_T = 1$; $M_R = 1$; mobility: 50 km/h for all mobiles
Channel modelling	C2 clustered delay line
Interference modelling	no inter-cell interference
MCS	4: 4-QAM, 16-QAM, 64-QAM, 256-QAM adaptive bit and power loading
FEC	no

An algorithm to perform adaptive user-to-subcarrier allocation with bit and power loading has been proposed in [WIND26] for the downlink of a multi-carrier CDMA systems with spreading both in time and in frequency. The algorithm yields an optimisation of the subcarrier sharing that enables a considerable performance gain with respect to OFDMA systems, where each subcarrier is exclusively

assigned to one user [WIND23]. In order to implement subcarrier sharing other sharing techniques like TDMA or FDMA can be used as well. Although chunk-wise resource allocation already implicitly provides time sharing in an OFDMA system, we show that a considerable performance gain can be achieved through further chunk sharing in case that the number of users competing for resources is quite high (K=32 in this case) and the time constraints for serving all these users is very stringent (one chunk duration=334.6μs). Sharing of a chunk by different data flows can be implemented in many different ways, in particular:

CDMA – all $n_{sub}\, n_{symb}$ time-frequency bins of a chunk or a subset thereof are simultaneously utilised by a number of data flows. To decrease message delays, it would be advantageous to perform pure frequency-domain spreading, by which, in frequency-selective fading, CDMA can provide diversity gain even with single-user detection. However, in an adaptive system, no room for diversity is left.

TDMA – each flow utilises all subcarriers of a chunk during $\rho_{kq} n_{symb}$ OFDM symbol periods.

FDMA – flow k utilises $\rho_{kq} n_{sub}$ subcarriers during the n_{symb} OFDM symbol periods of a chunk. Some kind of frequency hopping per chunk can be advantageous in severe frequency selective channels.

Figure G.9 illustrates the impact of chunk sharing and chunk size variations on BER performance. Here, S_f denotes the spreading factor and S the number of users sharing a chunk. Under the specific conditions considered, chunk sharing with n_{sub}=4 and S_f=S=4 yields a significant performance improvement with respect to exclusive user-to-chunk assignment, i.e. n_{sub}=4 and S_f=S=1.

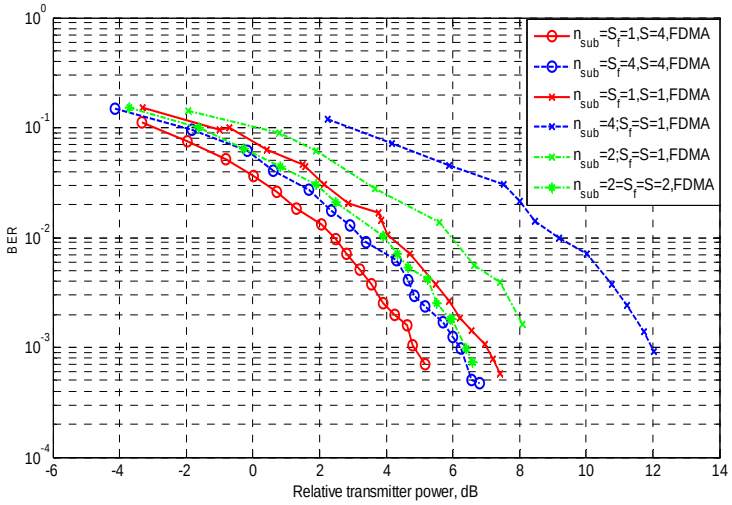

Figure G.9: Gain of chunk sharing/chunk size considering 32 users competing for 416 subcarriers with a granularity n_{sub}= 1 to 4 and n_{symb}=12. [35]

It is reasonable to expect that the achievable gain decreases by relaxing the constraint on the number of users to be served within one chunk duration, i.e. by decreasing the demand on granularity, as it had been previously shown in [WIND26] with reference to single subcarrier sharing. Moreover, from the figure, it can be inferred that the gain of chunk sharing increases with the number of subcarriers constituting the chunk: at BER=10^{-3}, a gain of 2 dB is achieved for n_{sub}=2 and 6 dB for n_{sub}=4, respectively. Furthermore, it can be observed that by optimizing the transmission scheme over sub-bands of size n_{sub}>1 the transmitter power needed to achieve a given BER increases (by 1 dB for n_{sub}=4). Indeed, increasing the chunk size reduces the performance of link adaptation due to the effect of channel-to-noise ratio averaging. But on the other hand it also reduces the amount of feedback information which was not taken into account here.

We note that results for $S \leq 4$ have been plotted, since preliminary results had shown that increasing S further does not provide any improvement. Finally, all curves refer to the case of FDMA sharing, since it had also been proven that the performance of TDMA and CDMA chunk-sharing is essentially the same,

[35] It should be noted that the fairly large gains seen here apply only to specific situations with very strict delay requirements as e.g. control signalling for scheduling and retransmissions for highly prioritised services.

from which it can be inferred that CDMA is not affected by the loss of orthogonality among codes within one chunk.

G.1.5 Comparison of adaptive OFDMA and OFDMA/SDMA using GoBs

Simulation Assumptions	
Simulator	System level simulator, 30 Frames per snapshot, 20 snapshots per simulation
Scenario	wide area; $M_T = 8$, $M_R = 1$; cell radius 1000 m, all UTs move at 3 km/h frequency reuse 1: 336 carrier per sector frequency reuse 3: 112 carrier per sector frequency reuse 7: 48 carrier per sector Tx power per carrier is set to 125 mW in all cases
Channel modelling	C2 and D1 generic channel model (according to D5.4)
Interference modelling	Full modelling using wrap around technique
MCS	6: BPSK, r=1/3; BPSK, r=2/3; QPSK, r=2/3; 16-QAM, r=2/3; 64-QAM, r=2/3; 64-QAM, r=8/9
FEC	punctured convolutional coding $(133,171,145)_{oct}$ with memory 6 codeword length: variable – one codeword always fills one chunk
Type of feedback	For each user and chunk: MCS and corresponding throughput value
Feedback delay	0
Beamforming	Chebychev tapering with 25 dB side lobe suppression using either eight grids with one beam each (1 beam case), 4 grids with two beams each (2 beam case) or 2 grids with 4 beams each (4 beam case)

A simple grid of fixed beam (GoB) is considered in order to investigate the potential SDMA gains achievable under wide-area scenario conditions. The basic approach used here is to form beams simultaneously from all BS allowing the UT to measure and feedback some kind of CQI as e.g. SINR per chunk and beam, see [WIND27]. Based on this feedback, resources are allocated to the UTs adaptively (opportunistically). Proportional fair scheduling (PFS) is applied to take fairness constraints into account. Considering synchronised cells and leaving the beam pattern and corresponding power allocation constant at all base stations during measurement phase and payload phase leads to predictable inter-cell interference conditions and hence supports short term adaptivity[36].

System simulation results for channel model D1 comparing average sector throughput for single antenna base stations (SISO) and multi-antenna base stations forming one, two or four beams on each chunk are shown on the left side of Figure G.10. Note that the SISO and the one beam case are associated with chunk based OFDMA/TDMA and the two and four beam case with chunk based OFDMA/TDMA/SDMA, respectively. Two main conclusions can be drawn out of these plots. Firstly, a fixed frequency reuse of one is always beneficial with respect to the cell throughput even if fairness (deducible from the right two plots in Figure G.10) is taken into account. This holds also for the SISO case which may be explained by different (in the simulation uncorrelated) shadow and fast fading characteristics for any BS↔UT link leaving sufficient variability to be exploited by adaptive scheduling. Secondly, increasing the number of beams leads to an increasing sector throughput indicating that SDMA is a viable option.

[36] Predictable SINR conditions are even more challenging for adaptive spatial processing. The measurement phase and the corresponding feedback signalling can be implemented as additional time-multiplexed parts of the super-frame not shown in Figure 3.2. The detailed layout of these phases within the super-frame is for further study.

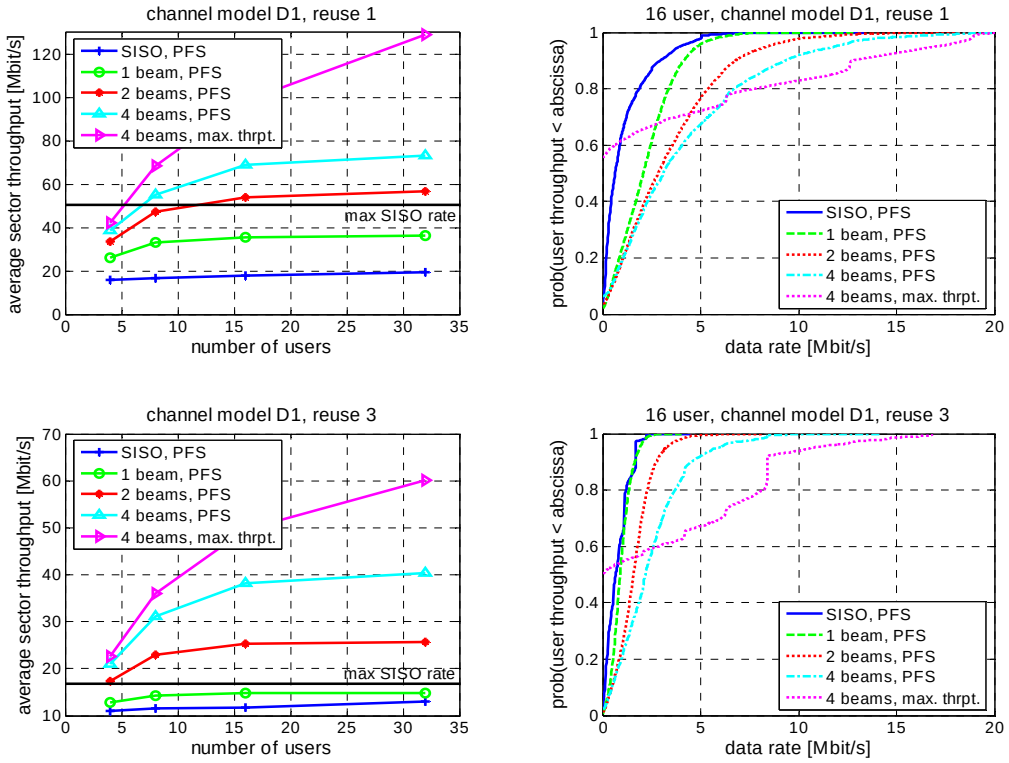

Figure G.10: average sector throughput and CDF of user throughput for channel model D1 with varying number of beams in different reuse scenarios; zero feedback delay.

Further exemplary simulations have been performed in order to assess the impact of various system parameters as feedback delay, amount of feedback and number of antennas at the UT starting from the parameter setting [4beams, channel model D1, reuse 1, prop. fair scheduling, 16 users]. Figures are omitted for the sake of brevity but basically it turns out that in case of channel model D1 the system is quite robust with respect to feedback delays. For example a delay of 64 OFDM symbols between measurement and payload phase in a scenario where all UTs move at 70 km/h (corresponding to a Doppler normalised delay $f_D t_{delay}$=0.6) led to an average sector throughput loss of around 16%. The relatively small loss is mainly due to high LOS probability associated with this channel model. In case of channel model C2 (NLOS only), however, the average sector throughput loss is substantially higher and amounts to 67% under the same conditions.

Regarding the amount of feedback, a considerable performance loss can be observed when CQI information is fed back for less than around 35 percent of all chunks. But this threshold depends to a certain degree on the number of different grids and how they are mapped to the chunks. In this simulation, only two different grids each with four beams were considered causing a certain periodicity in frequency direction.

Increasing the number of antennas at the UT provides significant system performance gains of around 25% (2 antennas) and 50% (4 antennas) using maximal ratio combining (MRC). Even larger gains are expected if the combiner accounts for the interference characteristics (IRC) as described in G.2.4. Of course, further investigations a required to study the interaction of the parameters presented.

Realizing SDMA by GoBs requires a relatively low angle of departure spread to keep intra-cell interference, i.e. intra-beam interference, small. The more beams are formed the more stringent this requirement is. Channel model C2 has a much larger angle of departure spread than D1 and therefore the performance gain achieved by SDMA are considerable smaller. In fact, forming four beams yields approximately the same performance as with two beams.

To sum up, using grids of beams in combination with opportunistic scheduling is a simple but yet efficient and robust solution to realise SDMA gains with low complexity even in reuse case 1 provided

that the angle of departure spread is sufficiently small as for scenario D1. In scenario C2, the SDMA gain with GoBs is limited to a factor of around 1.5 compared to pure beamforming.

G.2 Downlink spatial processing

G.2.1 Comparison of fixed and tracking based beamforming

Simulation Assumptions	
Simulator	System simulator, 200 snapshots, snapshot duration: 250 chunks.
Scenario	Wide area cellular, $M_T = 8$, $M_R = 1$, frequency reuse 1; all 512 carriers used; cell radius 1 km
Channel modelling	C2 WIMI generic channel model
Interference modelling	Full interference modelling
Multiple access	adaptive OFDMA/TDMA
MCS	No MCS: a successful transmission occurs when the predicted transmission rate is lower than the actual capacity of the equivalent channel.
FEC	No FEC
Type of feedback	8 bits feedback per user per chunk, SNR in case of OBF, complex gain in case of adaptive beamforming with channel tracking.
Feedback delay	2 chunk duration
Overhead	19 out of 96 resource elements for each chunk
Mobile speed	Pedestrian (M1) 50% of users, Vehicular (M2) 50% of users.
Beamforming	OBF: 1 varying beam spanning a grid of 40 fixed beams

In an environment where the NLOS (or fading) component of the channel is dominant with respect to the LOS component (typically C2 environment in WIMI), the performances of fixed beamforming and long-term CSI based beamforming techniques degrade due to the large angle of departure spread of the channel. In this case short-term CSI based adaptive beamforming techniques are better suited to exploit the multi-antenna gain. The main limitation when using these techniques in a wide-area scenario is the high signalling overhead needed for the feedback of the CSI from the mobile end to the BS. In order to reduce the signalling overhead and still preserve the multi-antenna gain an adaptive beamforming technique based on channel tracking (TrackBF) is considered.

With this approach, the beamforming vectors are determined according to the maximum ratio combining solution, i.e. $\mathbf{w}(n) = \hat{\mathbf{h}}_{k^*}^{\mathrm{H}}(n) / \left\| \hat{\mathbf{h}}_{k^*}(n) \right\|$, using the estimated (tracked) channel $\hat{\mathbf{h}}_{k^*}(n)$ of the scheduled user k^*. It is assumed that the complex gain $\alpha_k(n)=\mathbf{h}_k(n)\mathbf{w}(n)$ is fed back and used to track the channel at the BS via Kalman filtering [GA93]. In addition to the channel, the Kalman filter gives an estimate of the covariance matrix $\mathbf{C}_k(n) = \mathrm{E}(\mathbf{h}_k(n) - \hat{\mathbf{h}}_k(n))^{\mathrm{H}}(\mathbf{h}_k(n) - \hat{\mathbf{h}}_k(n))$, which is a measure of the quality of the channel estimation and is used to predict the transmission rate for user k. The scheduling decision is then made using the Proportional Fair Scheduler (PFS).

The proposed technique has the same reduced complexity and feedback requirements as the existing Opportunistic Beamforming (OBF) [VTL02] approach, which is implemented here using a varying beam $\mathbf{w}(n)$ that spans a grid of 40 fixed beams and where the resulting gain $\alpha_k(n)=|\mathbf{h}_k(n)\mathbf{w}(n)|$ or the associated SNR is fed back. This technique is used as a benchmark for comparison.

Results show both the TrackBF and OBF enhance the performance over the SISO case by exploiting the multiple transmit antennas advantage (Figure G.11). In terms of mean cell throughput, the TrackBF and OBF improve the performance by 47% and 16% respectively over the SISO case. Moreover, the TrackBF outperforms the OBF in terms of throughput and fairness, the latter is reflected by the lower probability of high inter-packet delays (Figure G.12). As expected, the TrackBF performs much better for pedestrian users than for vehicular users (Figure G.11). The performance degradation in the case of vehicular users is related to the poor channel tracking quality due to high mobility.

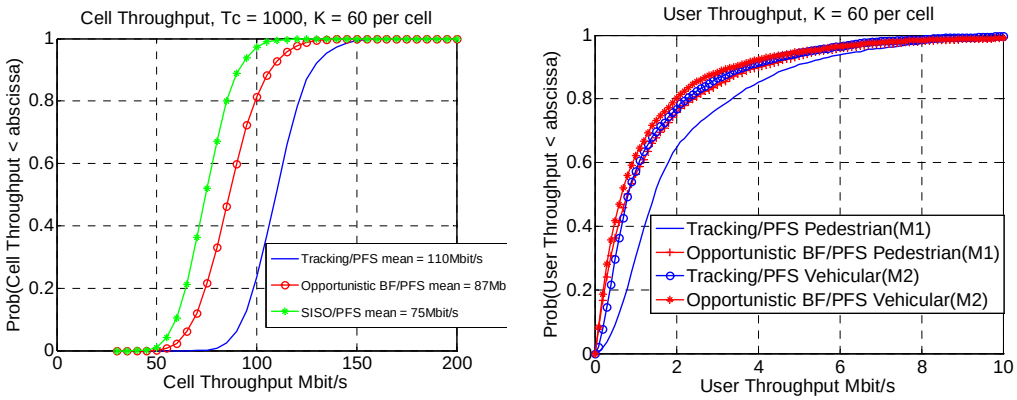

Figure G.11: CDF of cell throughput (left plot) and user throughput (right plot) for SISO, adaptive beamforming with tracking and OBF with fixed grid of beams, 20 users per sector.

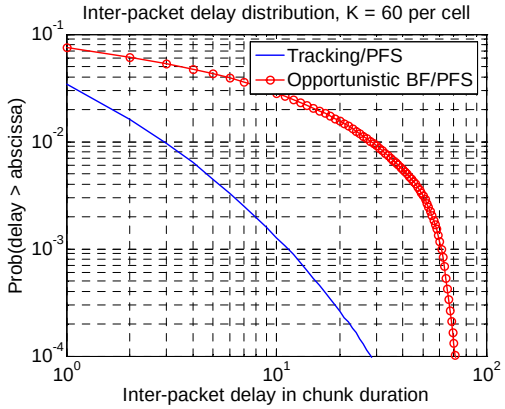

Figure G.12: inter-packet delay distribution, 20 users per sector.

G.2.2 Comparison of various adaptive beamforming techniques

Simulation Assumptions	
Simulator	Multi-link, one sector, 1000 frames simulation time with 100 drops
Scenario	wide area cellular; $M_T = 8$, $M_R = 1$, ULA
Channel modelling	SCME, no path loss, no shadowing
Interference modelling	Only Intra-cell interference by full simulation of all links
Mulitple access	adaptive OFDMA/TDMA/(SDMA)
OFDM parameters	20 MHz bandwidth, 512 subcarriers (406 used)
MCS	1: 16-QAM, r=1/2
FEC	Conv. coding: $(561,753)_{oct}$ with memory 8, Codeword length: 2 chunks
Feedback	delay 1 frame, CQI feedback, either beam selection info or covariance matrix
Overhead	None
Mobile speed	50 km/h, same for all mobiles

In these investigations several beamforming techniques plus SDMA are studied in a wide-area scenario on multi-link level. Scheduling is done chunk based in a score-based proportional fair way, one chunk occupies 8 subcarriers × 12 OFDM symbols. Coding and scheduling is always performed for groups of two consecutive chunks.

The first beamforming technique is a grid of fixed beams (GOB) with 8 beams. Non-neighboured beams share the same time-frequency resources. A feedback of the strongest beam and a corresponding CQI value are assumed. Inside each beam, the CQI value is used for the scheduling score calculation.

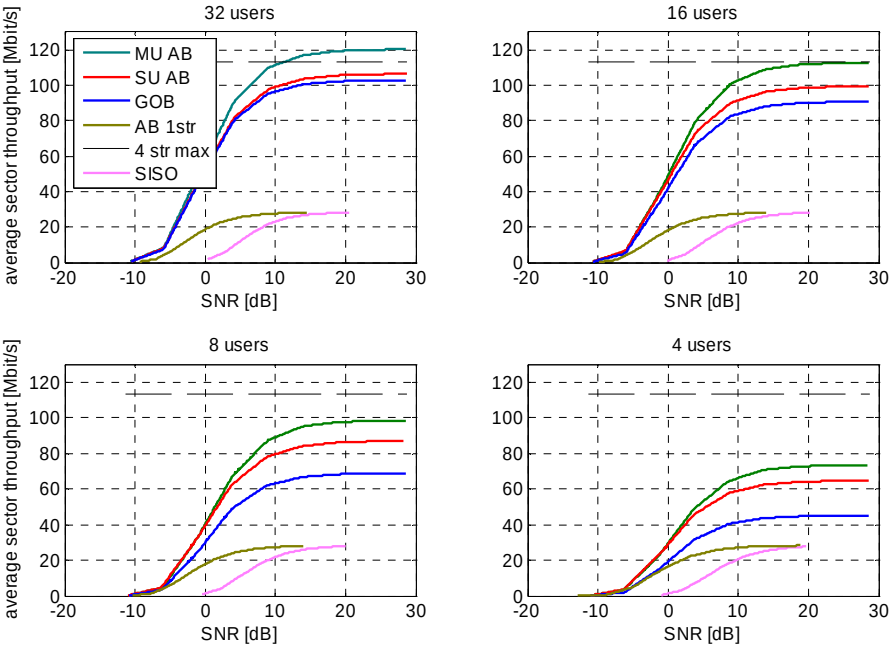

Figure G.13: Score based, suburban macro.

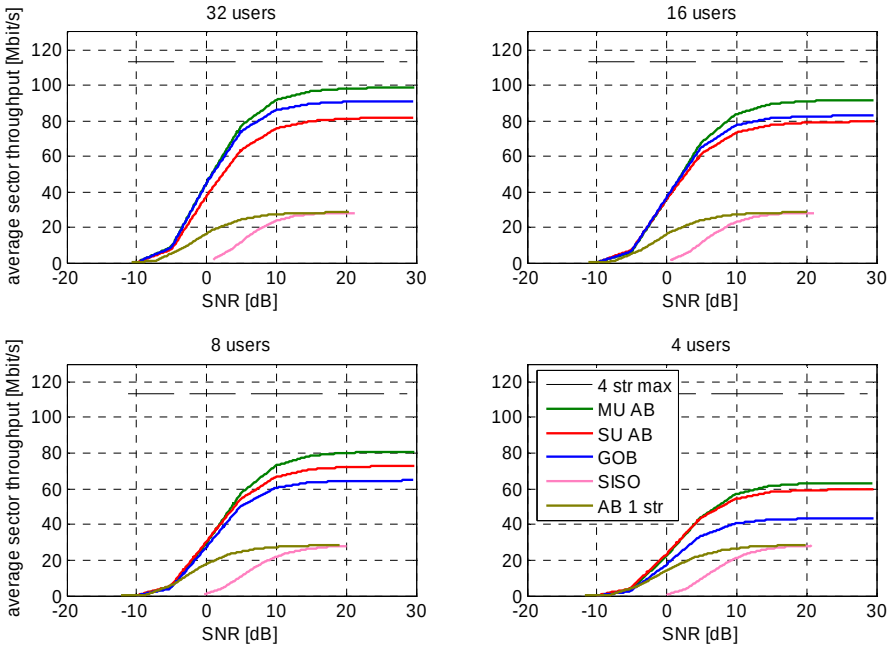

Figure G.14: Score based, urban macro.

The second technique is adaptive beams with single-user optimised antenna weights (AB SU) based on Eigenbeamforming (see [HBD00]). For SDMA the selection of users is done successively. The user with the highest score is selected first. All spatially separable users are candidates for scheduling. From these candidates the user with the highest score is selected. This process is repeated until there are no more spatially separable users or the maximum number of desired spatial streams is reached. The transmitter relies on feedback of CQI information (to calculate the score) and the spatial covariance matrix to calculate the antenna weights and to decide on spatial separation.

The third technique is adaptive beams with multi-user optimised antenna weights (AB MU). The user selection is done as above, additionally the antenna weights are altered to achieve mutual interference suppression by multiplying the Eigenbeam weights by an inverted interference covariance matrix.

As a reference case also results for SISO and adaptive beams without SDMA (AB 1str) are shown. The figures above show the average total sector throughput over the SNR for the different investigated techniques. '4 str max' refers to the maximum which can be achieved by a 4-stream SDMA with the given MCS. GOB is hard limited by these four streams, adaptive beams have a soft limit.

It can be concluded that multi-user optimised adaptive beams always outperform the other two SDMA schemes. The relative sector throughput gain versus GOB increases with decreasing number of users. This is caused by more degrees of freedom in user selection and better mutual interference suppression. But it relies on the knowledge of the long-term covariance matrix (meaning a higher feedback rate is necessary if no UL CSI can be used.). Single user optimised adaptive beams are characterised by a reduced computational complexity compared to AB MU. They always outperform GOB with few users. On the other hand, with high load (more streams) and a larger demand of spatial separation (e.g. Round Robin instead of score based or a scenario with more angular spread) they can even be outperformed by GOB. So in total they are questionable to be used in conjunction with SDMA. GOB inherently carry benefits by their simple feedback and scheduling and their orthogonal design, being a simple form of multi-user optimisation.

SDMA in general shows increasing gains with increasing number of active users (due to increased chances of spatial separability) and decreasing angular spread. SDMA has a large potential for increasing cell throughput and is a promising candidate for a wide-area scenario.

G.2.3 Comparison of maximal ratio and interference rejection combining at UT

Simulation Assumptions	
Simulator	Multi-link
Scenario	wide area, downlink, $M_T = 1$, $M_R = 2$
Channel modelling	WINNER channel model, C2 NLOS, no path loss, no shadowing
Interference modelling	One Inter-cell interference with DIR of 6 dB
Multiple access	Non-adaptive OFDM/TDMA, MC-CDMA/TDMA
OFDM parameters	20 MHz bandwidth, 512 subcarriers (406 used)
MCS	QPSK, r=1/2; 16QAM, r=1/3
FEC	3GPP 1/2 and 1/3 Turbo coding
Mobile speed	50 km/h for all terminals

When frequency reuse one is assumed in downlink at wide area mode, inter-cell interference or co-channel interference will degrade system performance. However, multiple antennas at receiver can be used to mitigate the interference.

Here 1x2 OFDM and 1x2 multi-carrier CDMA systems are considered in downlink for wide area. For multi-carrier CDMA, spreading factor and the number of Walsh-Hadarmard codes are both equal to 8. One inter-cell interference with dominant interference ratio (DIR) of 6 dB is generated. QPSK with 3GPP 1/2 Turbo coding and 16QAM with 1/3 Turbo coding are used. At receiver, two combining methods are considered. One is maximum ratio combining (MRC) and another is interference rejection combining (IRC) which is also referred to here as miminum mean square error combining (MMSEC).

Simulation results are shown in Figure G.15. No matter which MCS and receiver algorithm is used, the performance for 1x2 OFDM and multi-carrier CDMA are very similar. However, receiver complexity of multi-carrier CDMA is larger than that of OFDM system. On the other hand, MMSE combining provides significant gains over MRC combining under interference scenario. Therefore receive antenna processing, e.g. MMSE combining is a very efficient means to suppress inter-cell interference.

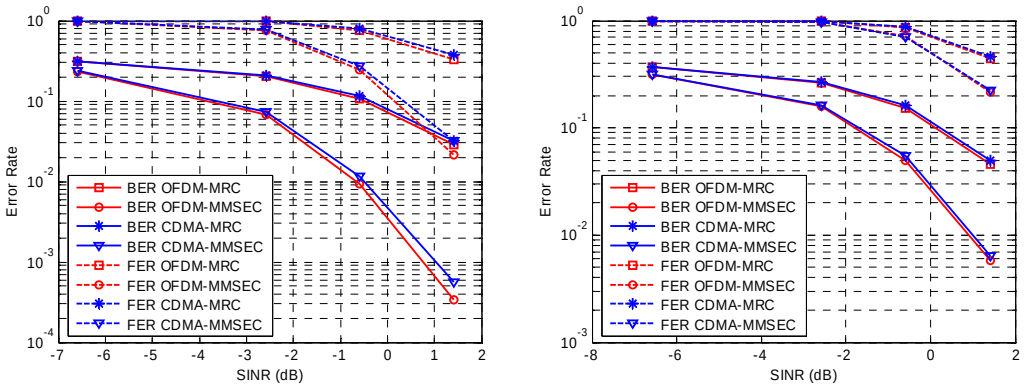

Figure G.15: Performance of 1 × 2 MRC and MMSEC considering OFDM/TDMA and MC-CDMA/TDMA with QPSK modulation and 1/2 turbo coding (left plot) and 16QAM modulation and 1/3 turbo coding (right plot).

G.2.4 Comparison of beamforming, diversity and multiplexing

Simulation Assumptions	
Simulator	System, 19 three-sector sites, full interference modelling using wrap-around
Scenario	Wide area cellular; on average 10 users/sector; frequency reuse: 1; MT ≤ 8, MR ≤ 2; varying cell radius
Channel model	C2, NLOS, WINNER interim channel model (WIMI)
MCS	Modulation schemes: QPSK, 16QAM, and 64QAM Channel code rates: 1/10, 1/3, 1/2, 2/3, 3/4, and 8/9
FEC	Turbo code combined with Layer 1 code block segmentation (up to 5114 bits per block) and rate matching, codeword length: from 998 (QPSK, rate 1/10) to 26624 bits (64QAM, rate 8/9), rate 1/7 mother code (polynomials: feedback 013, feedforward 015, 017, 011)
Feedback/Overhead	Chunk SINR after receiver processing, zero delay, no overhead

A non-frequency adaptive downlink based on OFDM/TDMA is evaluated in a multi-cell wide-area scenario in order to assess the value of different components of the WINNER multiple-antenna concept. Performance is compared for different cell sizes and in terms of average sector throughput and active radio link data rates. The latter measure is the (average) user throughput when scheduled for transmission. Since round robin TDMA scheduling is applied, the active radio link rate may be used to assess the fairness in the network. Furthermore, because many idealised assumptions are made, one should not focus on the absolute performance figures but rather on the relative performance.

The upper left plot in Figure G.16 depicts the average sector throughput in a network using a single downlink transmit antenna. Compared to single antenna reception, terminal receive diversity may improve performance significantly. MRC provides an average throughput gain of 35 % in an interference limited scenario. Interference rejection combining (IRC), referred to as optimum combining in [Win84], which suppresses inter-cell interference by taking the spatial colour into account on a per carrier basis, adds another 10–15 %. The lower left plot shows the distributions of the active radio link rates for a cell radius of 700 m, and as can be seen, performance is improved for all users.

Transmit diversity may be realised by using linear dispersion codes. In here Alamouti's orthogonal design is considered with two transmit antennas separated 20 wavelengths. The terminals use one or two receive antennas and as a reference, single antenna transmission is also considered. In the upper right plot of Figure G.16, the sector throughput is shown and in the lower right plot, the distributions of the data rates are shown for a cell radius of 700 m. With receive diversity terminals suppress inter-cell interference taking the structure of the interference into account. The results indicate that compared to single-antenna transmission, the gain of transmit diversity with Alamouti's design is slightly below 10% with receive diversity and slightly above 10% without receive diversity. It can also be seen that transmit diversity does not improve data rates for the lower percentiles but rather for the high percentiles. We note that there is inherently a substantial amount of frequency diversity available in the channel, which may explain the

marginal improvement, and the present evaluation does not illustrate potential benefits of reduced channel quality variations for non-ideal link adaptation.

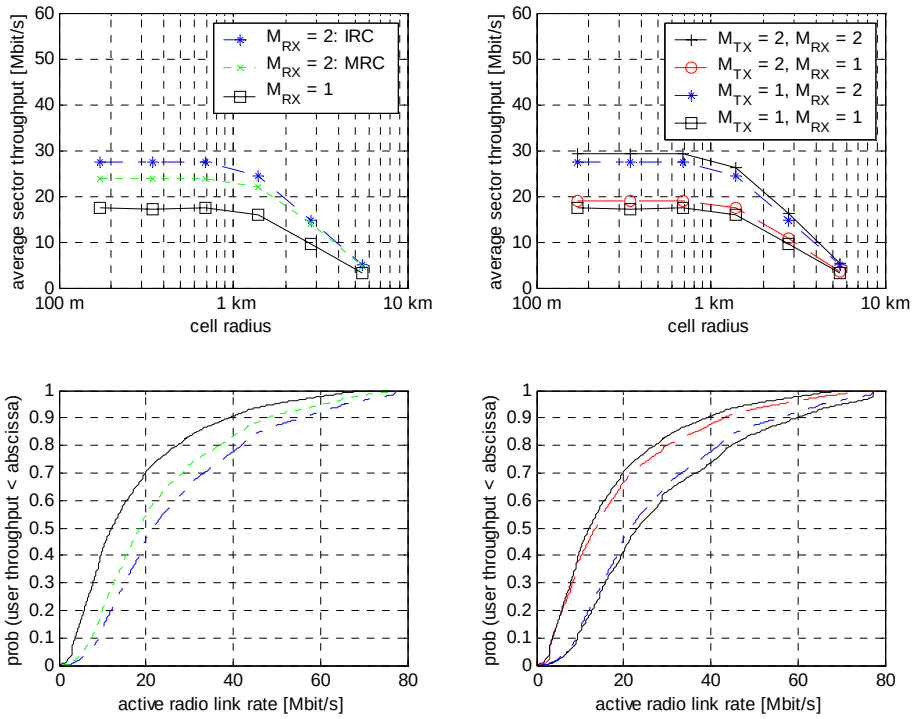

Figure G.16: Average sector throughput and data rate distributions for spatial diversity techniques. The data rate distributions are depicted for a cell radius of 700 m.

Beamforming solutions provide a directivity gain and change the interference situation in the network. Beamforming can be accomplished e.g. by creating a fixed grid of beams (GOB) and using the beam with the lowest pathloss at transmission. An alternative is to form user-specific beams based on the transmit covariance matrix of the channel. In here, the eigenvector associated with the largest eigenvalue of the transmit covariance matrix is used and this is referred to as eigenbeamforming (EBF). The left plot in Figure G.17 depicts the sector throughput with downlink beamforming based on a GOB and EBF, respectively using two, four, and eight base station antennas. With GOB, the antennas are used to form four, eight, and 16 fixed beams, respectively. Terminals have two receive antennas for IRC. The results indicate that in the studied scenario, EBF provides only a marginal performance improvement compared to a solution using a GOB. Thus, heavily quantised knowledge of the transmit covariance matrix, here in terms of a preferred beam, may be enough to capture most of the available gain. Increasing the number of antennas gives throughput improvements in the order of around 30 % when going from two to four antennas and another 20-25 % when increasing the number of base station antennas to eight. The enhancement is generally higher at large cell sizes. To the right in Figure G.17, results with EBF and one and two terminal receive antennas for IRC are shown. The gain of terminal receive diversity in terms of sector throughput is here in the range 35–50 %. The gain typically decreases when the number of base station antennas increases illustrating that benefits not necessarily are additive.

To the left in Figure G.18 performance with beamforming (EBF) at the base station combined with terminal receive diversity is shown. The upper left plot shows the average sector throughput and the lower left plot is the corresponding data rate distributions in a deployment with 700 m cell radius. As can be seen, the combination of beamforming and terminal receive diversity really improves the fairness and the lower percentiles of the data rates. A fraction of the users may even become modulation limited. With eight base station antennas used for beamforming, throughput has increased more than threefold compared to single antenna transmission and reception and more than twofold compared to single antenna transmission combined with dual terminal receive diversity.

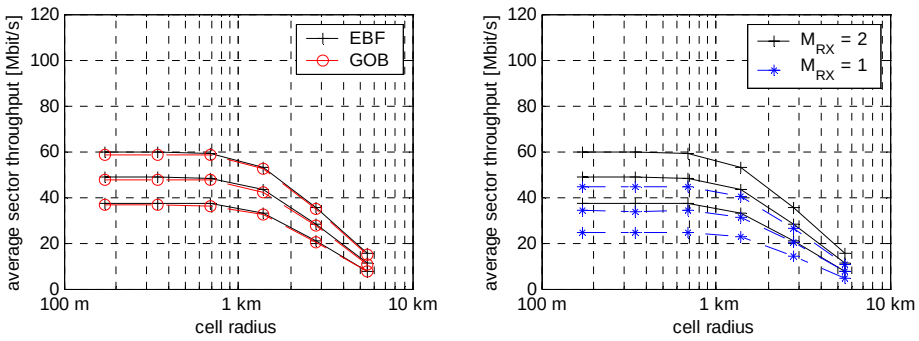

Figure G.17: Average sector throughput with beamforming comparing eigenbeamforming with grid of beams (left) and comparison of terminal receive diversity with single antenna reception (right).

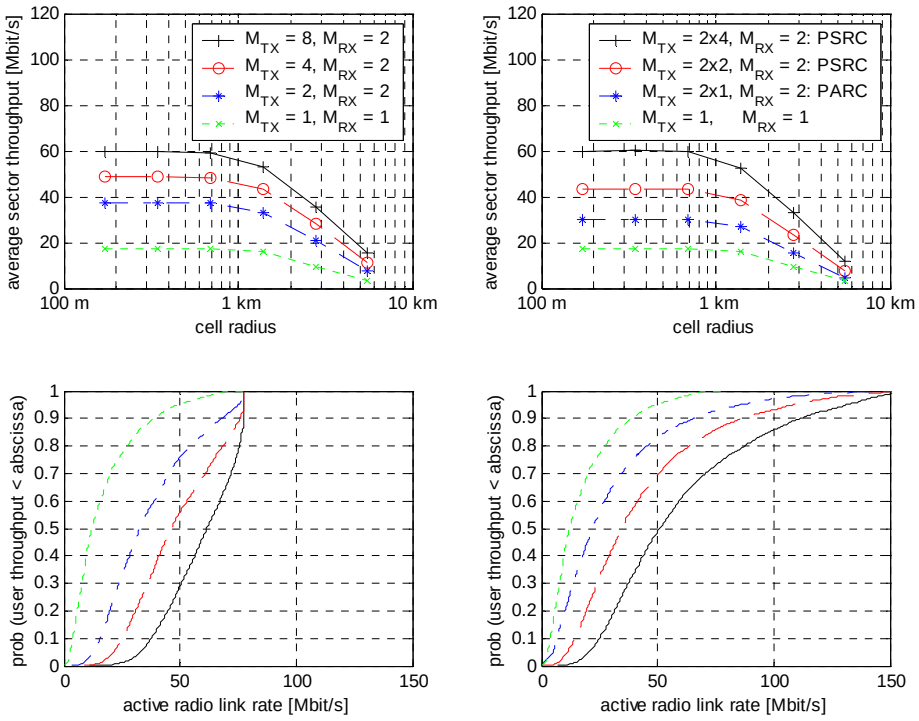

Figure G.18: Performance comparison of conventional beamforming with single stream transmission (left) and dual stream transmission (right). The data rate distributions are for cell radius 700 m.

To achieve very high peak data rates, though, one may have to consider the use of spatial multiplexing. For this purpose, per antenna rate control (PARC) is considered. With two streams, one channel coded block is transmitted from each (virtual) antenna and IRC in combination with successive interference cancellation after channel decoding is employed at the receiver side. The performance of such dual stream transmission is depicted to the right in Figure G.18 together with the corresponding single antenna results. In this case, both PARC with two antennas separated 20 wavelengths as well as the combination with EBF, referred to as per stream rate control (PSRC) for four and eight antennas are considered. For PSRC, antennas are divided into two groups (uniform linear sub-arrays) separated 20 wavelengths, within each group the element separation is half a wavelength, and the two eigenvectors associated with the two largest eigenvalues of the transmit covariance matrix are used to transmit the two streams with the same

power. As can be seen from the lower plots in Figure G.18, which show the data rate distributions for cell radius 700 m, dual stream transmission does indeed increase peak data rates, and for PSRC with eight transmit antennas the fraction of the users benefiting from this is non-negligible. However, on average, dual stream transmission provide a throughput that is slightly below or similar to that of conventional single-stream beamforming with same number of antenna elements. An interpretation of the rate distributions is that the increase of peak data rates comes at the expense of a reduced fairness

In summary, the results indicate that transmit beamforming and terminal receive diversity are essential components to ensure good coverage of high data rates and high system throughput. For beamforming with no SDMA component, eigenbeamforming gives a small performance advantage compared to a grid of beams. In interference limited scenarios, terminal receive diversity with interference suppression gives a non-negligible performance improvement compared to maximum ratio combining. The results further indicate that in the studied scenario transmit diversity using Alamouti's orthogonal design gives only a marginal performance improvement compared to single antenna transmission. One possible explanation of the limited gain is that the wideband channel inherently provides a large amount of frequency diversity. Finally, spatial multiplexing can be used to increase the peak data rates and may be successfully combined with beamforming. Compared to a deployment using conventional beamforming, this increase of peak data rates comes at the cost of reduced fairness although the average throughput is similar.

G.2.5 Performance of SMMSE precoding

Simulation Assumptions	
Simulator	System level simulator, 1000 snapshots, 1 frame per snapshot
Scenario	Short range, M_T = 8, 16, 24; M_R = 1, 2, 4; Round Robin scheduling
Channel modelling	A1, B1 WIMI generic channel model
Multiple access	Non-adaptive OFDMA/TDMA/SDMA
Number of active users	variable parameter, depends on the number of pilots available and the number of antennas at the user terminals
Channel estimation error modelling	Channel estimation error is modelled as a zero mean complex Gaussian variable and the variance is inversely proportional to the average receive SNR. The assumed estimator gain is about G_N=13 dB[37].
Cell radius	30 m in A1 scenario and 550 m in B1 scenario
virtual overhead for parameter estimation	14 or 20 out of 80 resource elements of each chunk
SDMA/SMUX	One spatial stream per user. Maximum number of users multiplexed is fixed

SMMSE precoding is a promising spatial processing candidate for the WINNER system concept [VH04], [VH05a], [VH05b], [WIND27]. In order to assess its performance for varying antenna configurations under realistic impairments, system simulations have been set up for the short range isolated cell scenario.

Modelling of impairments with respect to transmitter/receiver inequalities are performed according to

$$\widetilde{\mathbf{H}}^{(k)DL} = \mathbf{K}_{MS}^{(k)} \left(\widetilde{\mathbf{H}}^{(k)UL} \right)^T \left(\mathbf{K}_{BS}^{(k)} \right)^{-1},$$

where $\widetilde{\mathbf{H}}^{(k)UL}$ and $\widetilde{\mathbf{H}}^{(k)DL}$ denote the uplink and downlink channel matrix, respectively. The terms $\mathbf{K}_{MS}^{(k)}$ and $\mathbf{K}_{BS}^{(k)}$ represent the perturbations introduced by the transmitter and the receiver front-ends. These matrices are diagonal if we assume that the front-ends have only non-linear imperfections, which implies that these matrices can be inverted and that their products are commutative. The amplitude of $\mathbf{K}_{MS}^{(k)}$ and $(\mathbf{K}_{BS}^{(k)})^{-1}$ is modelled as a truncated random Gaussian variable with mean 1.0 and variance 0.007 and 0.0008, respectively. The phase is uniformly distributed in the interval [-8.7°, 8.7°] and [-3.0°, 3.0°], see [BCK03].

The average number of users in the system and the overhead per chunk depends on the number of pilots multiplexed for the channel estimation from the different antennas. In the proposal for the channel estimation it is assumed that we can estimate the channel from 3 antennas in the short-term adaptive mode or 6 in the long-term adaptive mode per one chunk. In our simulations we rely on the assumption that the channel or the second order statistics of the channel are constant over one frame. Since there are 3 time slots in the frame, we multiplex in every time slot pilots from different antennas regardless of whether these antennas are located at the same terminal or not. We assume that one user transmits using only one

[37] Practically the estimator gain may vary depending on the number of users, antennas and on the preamble design and if correlation in frequency domain is corrected or not, see [WIND21]

fourth of the available bandwidth. Thus, the maximum number of different antennas that can be estimated in the short-term adaptive mode is 36 and the average number of users considered in the system simulations was 12.7. In the long-term adaptive mode the maximum number of antennas that can be estimated amounts to 72 and the average number of users considered was 27.

Let us define the average correlation matrix of the i^{th} user in the k^{th} chunk as

$$\mathbf{R}_i^{(k)} = \frac{1}{N_{chunk}} \sum_j \mathbf{H}_i^{(k,j)H} \mathbf{H}_i^{(k,j)}$$

and its singular-value decomposition (SVD) as $\mathbf{R}_i^{(k)} = \mathbf{V}_i^{(k)} \mathbf{Q}_i^{(k)} \mathbf{V}_i^{(k)H}$, where $\mathbf{H}_i^{(k,j)}$ is the i^{th} user channel matrix in the k^{th} chunk. The MU MIMO precoding is now performed on the equivalent channel defined as follows:

$$\breve{\mathbf{H}}_i^{(k)} = \mathbf{Q}_i^{(k)1/2} \mathbf{V}_i^{(k)H} .$$

By using the equivalent channel $\breve{\mathbf{H}}_i^{(k)}$ we facilitate easier adaptation from perfect CSI to the second-order CSI.

The following notation is used to describe the simulated system $\{M_T, K_{\max}, N_{\text{pilots}}\}$, where M_T is the number of antennas at the BS, $K_{\max}$ is the maximum number of spatial streams per chunk and N_{pilots} is the number of different antennas that can be estimated per chunk.

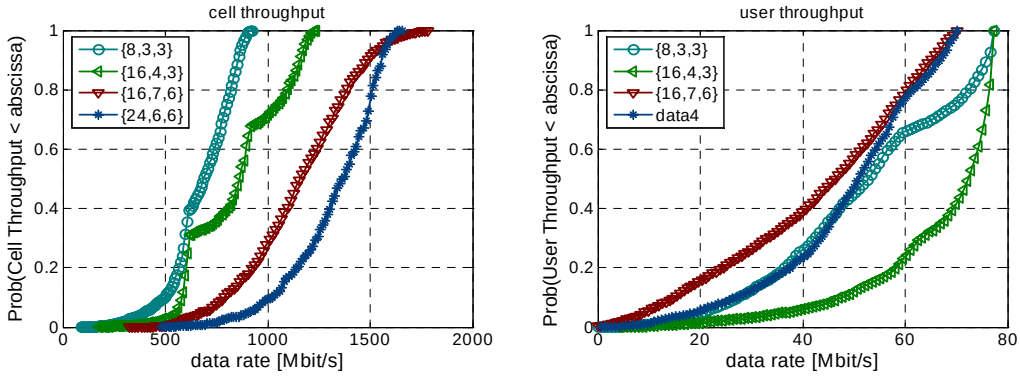

Figure G.19: Cell and user throughput performance of SMMSE in A1 scenario.

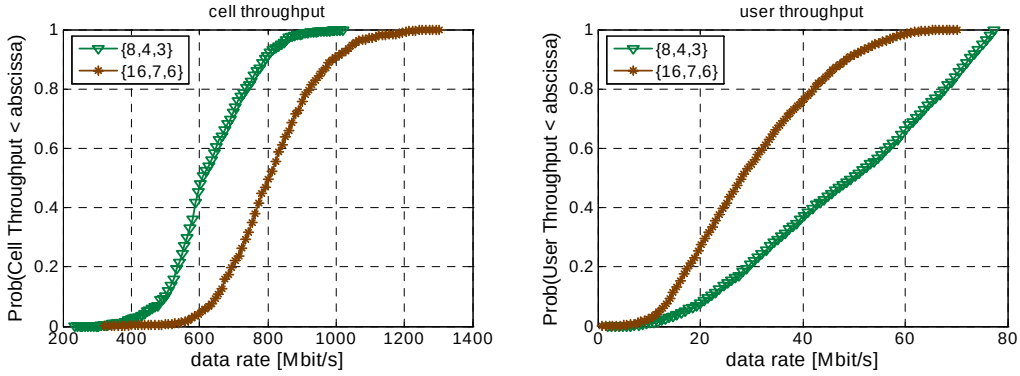

Figure G.20: Cell and user throughput performance of SMMSE in B1 scenario.

Simulation results for the A1 and B1 scenario are plotted in Figure G.19 and Figure G.20. In the A1 scenario, the initial assumption of having 8 antennas at the BS has been shown not to be sufficient to provide 1 Gbps as a target cell throughput. By increasing the pilot overhead we are able to estimate more users' channel matrices. Significant cell throughput improvements can only be achieved by increasing the number of antennas at the BS as well as the number of users that are spatially multiplexed. The 90% user

throughput is almost constant as mobile terminals move away from the BS. The 50% user throughput loss due to the increase of the distance from the BS is less than 10 Mbps.

Similar as in the A1 scenario, in the B1 scenario the target throughput of 600 Mbps is achieved by increasing the number of antennas at the BS and the number of users that are spatially multiplexed. The values necessary to reach the target cell throughput are smaller than in A1 scenario.

Hence, Multi-user MIMO precoding is a powerful tool to provide the required cell/user throughput. It exploits the available CSI at the BS allowing very good use of the available resources in the spatial domain. Benefits are limited by the overhead needed to acquire the necessary information (CSI). It was shown that this trade-off is justified and it results in high throughput gains.

In order to achieve 1 Gbps in an indoor scenario we should multiplex as many users as possible with large number of antennas at the BS. The maximum allowable number of users depends on the number of pilots that are multiplexed per one chunk. The reduction of throughput caused by the increased pilot overhead is compensated for by SDMA/SMUX or higher order constellation sizes.

G.3 Downlink multi-user detection

G.3.1 Comparison of receiver structures for SISO MC-CDMA

Simulation Assumptions	
Simulator	Single-link
Scenario	Short range, isolated cell, single antenna BS and UT
Channel modelling	B1 clustered delay line and Independent Rayleigh
Interference modelling	no
spreading	type: Walsh-Hadamard ; spreading length: 8
MCS	1: 4-QAM
FEC	Convolutional coding $(561,753)_{oct}$ with memory 8 Codeword length: 3328 bit

The physical layer simulation layout follows the generic WINNER transmitter structure, i.e. the user information bits are encoded using a terminated $(561,753)_{oct}$ rate ½ convolutional code (3GPP). The codebits are randomly interleaved and assigned to complex valued 4-QAM data symbols using Gray mapping. These user data symbols are then spread using a 8x8 Walsh-Hadamard spreading matrix, which yields the data chips. The chips are assigned to the used subcarriers of an OFDM symbol. The codeword length, i.e. the frame length of one transmission entity is chosen, such that one terminated convolutional codeword finally forms one OFDM symbol. This means contemporarily, that one OFDM symbol contains exactly one user's data and the user multiplexing is done in time direction, i.e. different OFDM symbols are assigned to different users.

Path loss and shadowing effects are not considered within these investigations. In addition, we assume, that the channel is almost constant during one OFDM symbol's period, i.e. inter-carrier interference is negligible.

Figure G.21 show the bit error rates (BER) and the block error rate (BLER) versus the signal-to-noise ratio (SNR) respectively. The SNR is defined as the ratio of the average user signal power and the variance of the complex valued additive white Gaussian noise (AWGN) in each subcarrier. Solid lines show the error performances for the WINNER B1 NLOS scenario, where the chips of one Walsh-Hadamard spreading entity are distributed over the whole available bandwidth. This is achieved by using a subcarrier block interleaver of size 8x208. Due to multiple access interference (MAI), there is a loss of about 2.3 dB at a BER of 10^{-4} for single user detection (SUD) using MMSE equalisation compared to the interference free (perfect IC) case, where we assume and subtract MAI perfectly. To combat MAI at the receiver, we use a soft parallel interference canceller (SPIC) as described in the WINNER deliverable D2.6 [WIND26]. The BLER performance of the SPIC with 5 iterations almost reaches the perfect IC bound as it can be seen from Figure G.21, right plot. For comparison, we show results for an independent Rayleigh fading channel, which provides maximum (frequency) diversity, and the B1 NLOS without subcarrier interleaving. Due to an increased MAI, the gap between the perfect IC and the SUD performance is even higher compared to B1 NLOS. If, however, we skip the subcarrier interleaver for the B1 NLOS scenario, we observe almost no MAI, since chips are spread over adjacent subcarriers, which, due to strong correlation, maintain orthogonality of the spreading sequences quite well. This results in a negligible difference of SUD and perfect IC error performances. In this case, we cannot benefit from the more complex SPIC receiver.

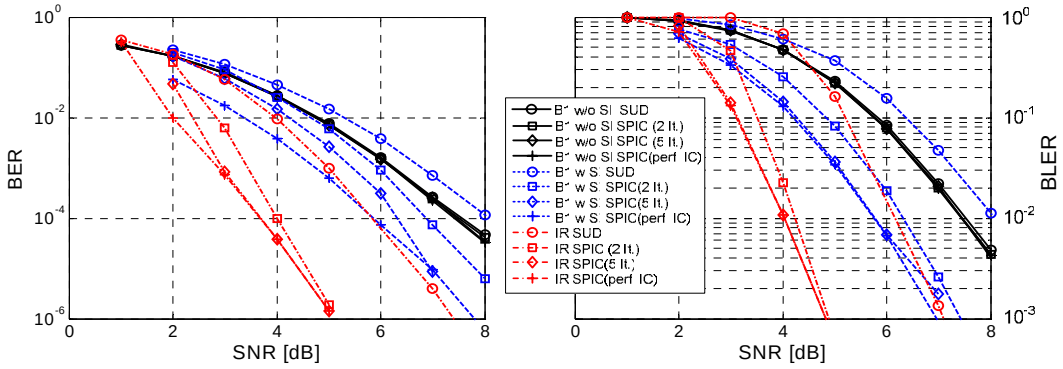

Figure G.21: BER and BLER vs. SNR for B1 NLOS and independent Rayleigh fading.

G.3.2 Comparison of receiver structures for MIMO MC-CDMA

Simulation Assumptions	
Simulator	link-level
Scenario	short range; $M_T = 4$; $M_R = 4$;
Channel modelling	B3,NLOS, WIMI
Multiple access	MC-CDMA/TDMA
MCS	1: QPSK, r=1/2;
FEC	punctured turbo coding $(15,13)_{oct}$ with memory 4 codeword length: fixed size of 6656

A downlink MIMO MC-CDMA system is considered where K users are active in each cell. The desired user is located in the central cell. The spreading factor (in frequency domain) is G (reducing to OFDM iff G=1). The input data bits are encoded by the single antenna turbo code (TC) or by space-frequency turbo-coded modulation (SFTuCM) which is designed for two transmit antennas. We divide the available transmit antennas into independent layers denoted as $J=M_T/J_0$, where J_0 is the number of antennas associated with the encoder. For the single antenna turbo code J_0=1 whereas J_0=2 in the SFTuCM case. A vertical layering structure is applied, where the encoded and modulation mapped symbols are multiplexed for J transmit antenna groups. By doing so, the spatial diversity gain, the space-time coding gain (in case of SFTuCM) and spatial multiplexing gain can be achieved simultaneously. The MMSE based detectors for the multiple antenna MC-CDMA approach considered herein are relying on the techniques presented in [WIND23, WIND26]. In order to achieve better spatial receiver diversity compared to linear receiver, the principle of iterative detection and decoding (IDD) can be employed with the considered symbol level SF-MMSE receiver. The soft interference cancellation with IDD is considered herein.

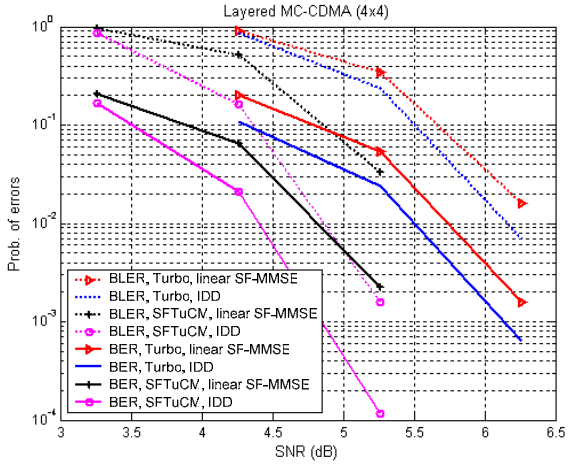

Figure G.22: Performance of layered MIMO MC-CDMA systems.

The simulation performance of the MC-CDMA based downlink with G=K=8 and $M_R = M_T$ =4 is shown in Figure G.22. The scenarios B3 with NLOS clustered delay line model was considered. The system with SFTuCM and group-wise layering outperforms the system with turbo-coded system. The soft co-antenna interference (CAI) cancellation is shown to possess the ability to further improve the performance. Our results indicate that the considered OFDM and MC-CDMA systems are feasible candidates for future cellular high data rate downlink packet transmission. For the SFTuCM coded systems, the complexity is at the same level as the turbo-coded systems.

G.4 Uplink multiple access

G.4.1 Performance of single carrier based adaptive TDMA

Simulation Assumptions	
Simulator	Multi-link
Scenario	Wide area, single-cell, SISO, perfect synch. and long-term power control
Channel modelling	ITU-IV Channel A
MCS	Uncoded: BPSK, 4QAM, 8PSK, 16QAM, 32CrossQAM, 64QAM, 128CrossQAM and 256QAM
Uplink spectrum	4.4 GHz carrier frequency and 25 MHz bandwidth
Single-carrier parameters	Symbol time 49.23 ns, Square-root-raised-cosine roll-off factor 0.231
Data block size	416 symbols and guard period 2.56 μs covers most multi-path delay spread
Frame size	16 Data blocks (time slots), individually allocated to TDMA users

Performance results for an adaptive TDMA block-based single-carrier uplink are provided. This uplink performs multi-user adaptive scheduling to the small scale fading for the individual users and also link adaptation of the scheduled users. Thus, it is time-adaptive towards the small-scale fading, but not frequency-adaptive, since it uses single-carrier transmission. The aim of the investigation is to show the potential multi-user diversity gains that can be obtained. The results are extended simulation results to the work in [WOSS05], where an analytical performance analysis and more details of the design and assumptions behind the investigated uplink can be found. The cyclic prefix of each Data block (time slot) is designed to cover most of the multi-path delay spread. Thus, no inter-Data block ISI is assumed and the FD-DFE [FA02] performs equalisation of the ISI among symbols within each Data block only.

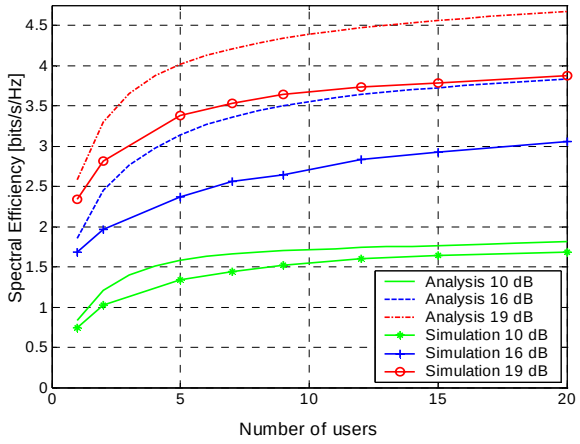

Figure G.23: Multi-user diversity gains for the adaptive TDMA single-carrier uplink.

In the simulations results in Figure G.23, all users have the same average SNR and the user speed is 50 km/h for all users. The scheduler performs max throughput scheduling based on equalised user SNR. Perfect estimation and prediction of the impulse responses of each time-slot of each user are assumed. Thus, the results are upper bounds on the attainable spectral efficiency. Note also that Figure G.23 does not include overhead related to channel estimation and prediction (approx. 15%). In addition, only the signalling bandwidth is taken into account, i.e. the spectral roll-off (23.1%) is not compensated for. As seen, there is a multi-user diversity gain for this uplink. However, compared to the multi-user diversity gains for systems with more narrow bandwidths as investigated in [WOSS05], the gain is smaller. The reason for this is the channel averaging caused by the frequency diversity for the wideband channels. This

makes the variability, of the instantaneous channels from the individual users to be smaller, which in turn limits the obtainable amount of multi-user diversity gain.

A fair comparison between the investigated adaptive TDMA single-carrier uplink and an adaptive TDMA/OFDMA uplink has to take especially the pilot overhead, feedback information rate, subcarrier frequency offset and peak-to-average power ratio (PAPR) mitigation into account. Preliminary results, not shown here, indicate that for a 5 MHz wide uplink channel, there is at least 3 dB gain for the adaptive TDMA/OFDMA uplink with 2% frequency offset of the subcarrier spacing, compared to the adaptive TDMA single-carrier uplink and before PAPR mitigation loss. Thus, an adaptive multi-carrier based TDMA/OFDMA uplink seems more promising as an adaptive uplink for the WINNER system concept.

G.4.2 Comparison of IFDMA and chunk based OFDMA

Simulation Assumptions	
Simulator	Link level
Scenario	wide area, $M_T = 1$; $M_R = 1$; mobility: 70 km/h for all mobiles; single user considerations
Channel modelling	COST 207, TU
Interference modelling	no inter-cell interference
OFDM parameter	Number of used subcarrier = 512, subcarrier distance = 39.0625 kHz, guard period = 7 µs
MCS	1: QPSK, r=1/2
FEC	convolutional coding $(133,171)_{oct}$ with memory 6 Codeword length: fixed size of 1000 bits

The purpose was to investigate the impact of frequency diversity on performance for IFDMA with interleaved subcarrier allocation compared to DFT-precoded OFDMA with block-wise subcarrier allocation. As expected for coded transmission over a very frequency selective mobile radio channel as the one assumed, IFDMA shows significant better performance compared to DFT-precoded block OFDMA for a number of subcarriers per user Q>1. This is due to the fact that, in IFDMA the subcarriers are equidistantly distributed over the total bandwidth of 20 MHz whereas, for DFT-precoded OFDMA only a fraction of the bandwidth is used for transmission. For Q=1, i.e. each user gets only a single subcarrier, both schemes exhibits the same performance and cannot exploit frequency diversity.

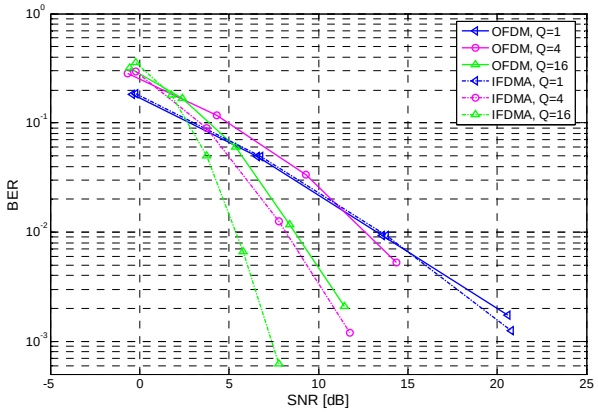

Figure G.24: BER comparison for IFDMA and DFT-precoded block OFDMA for various number of allocated subcarriers per user *Q*.

The SNR gains of IFDMA compared to DFT-precoded block OFDMA at BER=10^{-3} for an interleaving depth of about 250µs is still 5.5 dB at a not too low data-rate, i.e. 625 Kbit/s. It is expected that also for transmission using block codes and for the use of the WINNER channel model the same effect can be shown. However, further studies are required to assess the impact of real channel estimation as well as imperfectly synchronised and power controlled UT's for either case which might reduce the interleaving gain considerably.

G.4.3 Performance of adaptive OFDMA

Simulation Assumptions	
Simulator	Multi-link
Scenario	Short range, isolated cell, single antenna BS and UT
Channel modelling	A1 LOS, NLOS, B1 LOS, NLOS including path loss and shadow fading
Cell radius	50 m for A1, 150 m for B1
MCS	4: BPSK, {4, 16, 64} QAM, generally considered by SNR gap approximation and SNR gap Γ = 5 dB
FEC	convolutional coding $(561,753)_{oct}$ with memory 8, code rate 1/2 Codeword length: 240 × (number of bits per symbol), not relevant for results
User distribution	$d_k = \left(1+9\sqrt{(k-1)/(K-1)}\right)0.1r_{\text{cell}}, \quad k=1,\ldots,K$

The performance of frequency adaptive OFDMA (subcarrier based and chunk based) is evaluated by multi-link simulations. The considered adaptive OFDMA scheme maximises the sum rate of all users under individual transmit power constraints, for which an extremely simple and efficient algorithm for adaptive chunk allocation is found to perform well. The adaptive scheme is appropriate for the uplink in the short-range case where the channel is quasi-static and CSI is available at the transmitter.

We consider the effects of the channel estimation and prediction by a simple Gaussian error model. The largest prediction horizon for the TDD mode is L = 1 ms [WIND24], Table 3.1). In the B1 scenario, the fastest users move at an average speed of v = 5 km/h (see Appendix E.3), the carrier frequency is f_c = 5 GHz, which gives a prediction horizon in fractions of wavelength of $l = vL/\lambda_c = 0.02$. This prediction horizon is rather short in comparison to those considered in [WIND24], Section 3.1.3 and it is thus expected that the CSI feedback delay has no significant effects for the A1 and B1 scenario. The channel predictor estimates the power gain $g_n = |h_n|^2$. Due to channel estimation errors and the inevitable feedback delay, the estimation is slightly degraded. In the following, we consider this effect by the simple model $\hat{g}_n = g_n(1+\eta_n)$ where η_n is N $(0,\sigma_e^2)$ distributed and σ_e^2 denotes the normalised estimation and prediction error. The instantaneous SNR is given by $\gamma_n = |h_n|^2 p_n / N_0 = g_n p_n / N_0$ and the estimated SNR is $\hat{\gamma}_n = \hat{g}_n p_n / N_0 = \gamma_n(1+\eta_n)$. For the simulation of the BER for the selected MCS, first the SNR γ_n is selected and then for each codeword an estimated SNR is generated. The final BER is averaged over many codewords.

In Table G.1, the minimum SNR for a target BER of $P_b = 10^{-4}$ for each MCS is given. The SNR gap Γ denotes the additional required SNR in comparison to the Shannon limit to reach the same bit rate at the target BER: $R = \log_2(1+\gamma_{\min}/\Gamma) \Rightarrow \Gamma = \gamma_{\min}/(2^R-1)$. The average SNR gap for $\sigma_e^2 = 0.01$ is $\Gamma \approx 5\,\text{dB}$, which will be used in the following to consider the effects of realistic adaptive modulation and coding.

Table G.1: Minimum SNR for selected modulation scheme.

		$\sigma_e^2 = 0$		$\sigma_e^2 = 0.01$	
code rate	modulation	SNR $\gamma_{\min}$	SNR gap Γ	SNR $\gamma_{\min}$	SNR gap Γ
0.5	BPSK	0.5 dB	4.3 dB	0.9 dB	4.7 dB
1	QPSK	3.5 dB	3.5 dB	3.9 dB	3.9 dB
2	16-QAM	9.5 dB	4.7 dB	9.9 dB	5.1 dB
3	64-QAM	14.6 dB	6.1 dB	14.8 dB	6.3 dB

Adaptation Problem and Key Design Criteria

The multiple-access scheme has to adapt to the traffic and the QoS requirements as well as to the channel of multiple users. Since joint adaptation to all parameters would result in an impractically complex optimisation problem, it seems wise to separate the problem into two adaptation steps:

1. Scheduling: Adaptation to traffic and QoS requirements like bit rate, delay, queue length and user/service/flow priorities including "fairness"
2. Adaptation to the channel state, i.e. the channel gain to noise ratio.

The priorities of users, services or flows as well as the exact definition of fairness will depend mainly on the operator's adopted strategy and business model. The scheduling strategy, hence, must be flexible and is not only dictated by technical arguments. In the following, we present an adaptive scheme which adapts

to the channel only and offers to the scheduler the possibility to operate near the border of the channel capacity region. The limits of this region are established in [Yu02] and [Tse98], however, no algorithm which is simple enough for practical implementation and achieves *all* border points of the capacity region is known. In [PI05], the scheduling region, which is achievable with a relatively simple algorithm and which may yield a good approximation to the true capacity region, is outlined.

The cell capacity for the uplink can be computed by the *iterative water-filling* (IWF) algorithm [Yu04], which can be adapted easily to OFDMA [Pfl05, PI05]. This algorithm computes the optimum power allocation for all users. The rate obtained with this algorithm corresponds to the Shannon capacity, which can serve as an upper bound. A more realistic rate is obtained by considering an SNR gap of $\Gamma = 5$ dB, which takes into account the considered link adaptation schemes.

Figure G.25 depicts the sum rates achieved with the optimum IWF algorithm for all four short-range scenarios with and without considering the SNR gap. As was also observed in [PI05] – although theoretically optimum – sharing the subcarriers does not yield any perceivable capacity gain. In other words, adding an additional CDMA or TDMA component to OFDMA will only increase the system complexity but not give any capacity gain[38].

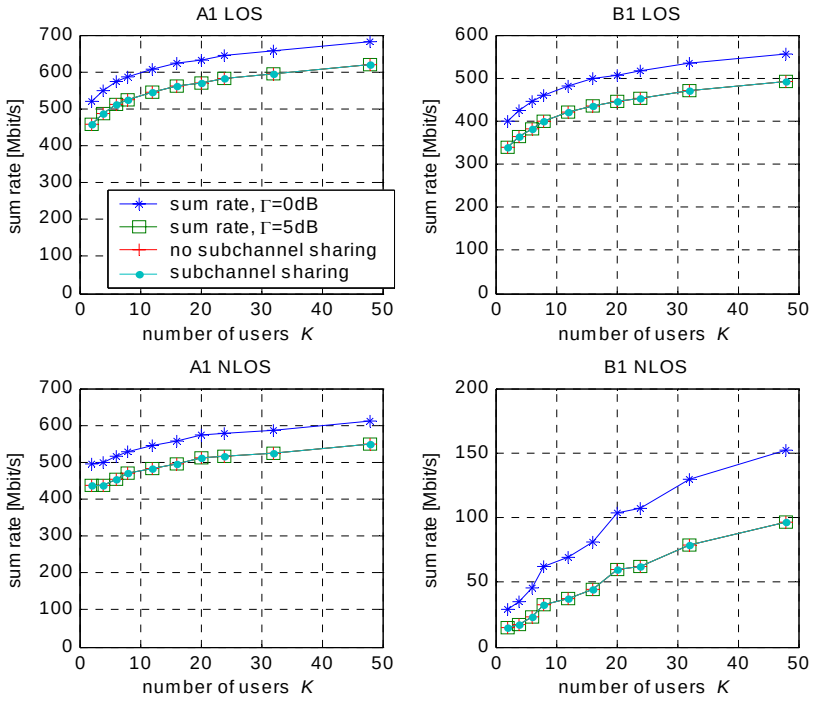

Figure G.25: Uplink cell capacity for OFDMA with N = 1664 subcarriers and constant user density in the cell. The performance loss due to allowing only one user per subcarrier is negligible for all considered cases.

In the TDD mode, n_{sub} = 16 subcarriers are grouped into one chunk. The application of the IWF algorithm to chunks instead of subcarriers is straightforward and the maximum sum rates achieved with a chunk-based (i.e. with subcarrier groups) OFDMA scheme is given in Figure G.26. Naturally, the cell capacity of chunk-based OFDMA is inferior, but the system complexity as well as the algorithm run-times are significantly lower. For practical implementations, the complexity of the IWF algorithm might be an obstacle, but fortunately there is a low-complexity alternative: The XP algorithm [Ace05] (see also [PI05]) is an extremely simple and efficient method for adaptive subcarrier allocation, which attains nearly the same sum rate as the optimum IWF algorithm. In Figure G.26, the sum rate for a fixed subcarrier allocation is given as a reference. The subcarrier allocation for this case is given by

[38] Note that this statement holds for the short-range uplink and for the sum rate optimisation criterion. This does not contradict the results obtained in e.g. [Tri04].

$a_f = \mathrm{mod}_K(f-1)+1$, where a_f denotes the user allocated to subcarrier f. For each user, single-user water-filling is performed on his set of subcarriers to compute the resulting sum rate. Surprisingly, for the 'A1 LOS' scenario, this simple non-adaptive subcarrier allocation performs close to the optimum solution and even better than the XP algorithm while for the 'B1 LOS' case, it comes with a significant capacity penalty

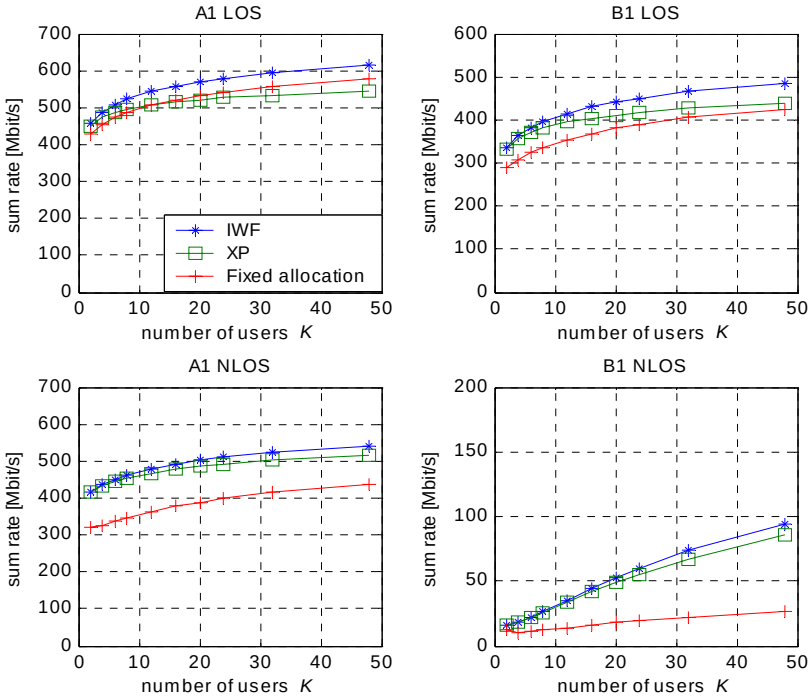

Figure G.26: Sum rate achieved with chunk-based OFDMA (Γ=5 dB). The optimum IWF (iterative water-filling) algorithm achieves the highest rate, while the rate achieved with the low-complexity XP algorithm [Ace05] is only slightly lower.

Conclusions

The considered adaptive OFDMA scheme maximises the sum rate of all users under individual transmit power constraints. It is appropriate for the uplink in the short-range case where the channel is quasi-static and CSI is available at the transmitter. The achievable gain is rather low compared to non-adaptive subcarrier allocation if LOS conditions prevail. However, in NLOS conditions with sufficient frequency-selectivity considerable performance improvements can be obtained.

The considered optimisation criterion consciously excludes fairness issues, since different notions of fairness exist and these may depend on the operators' preferences. "Fairness" and other QoS-related constraints can be included by a traffic-aware scheduler, which selects for each Frame the appropriate subset of active users.

The simulation results show the achievable sum rate per cell or sector in the uplink when both terminal and base station have one antenna. The sum rates for an SNR gap of Γ = 0 dB are strict upper bounds while the rates for Γ = 5 dB consider the effect of realistic modulation and coding schemes.

G.4.4 Comparison of adaptive OFDMA and OFDM-TDMA

Simulation Assumptions	
Simulator	Multi-link, 8 Frames per snapshot, 6000 snapshots
Scenario	Short range, isolated cell, single antenna BS and UT, no power control
Channel modelling	A1, LOS and NLOS, clustered delay line model
Cell radius	100 m and 200 m
MCS	5: BPSK, r=1/3; BPSK, r=2/3; QPSK, r=2/3; 16-QAM, r=2/3; 64-QAM,

	r=8/9
FEC	Punctured convolutional coding $(133,171,145)_{oct}$ with memory 6 codeword length: variable – one codeword always fills one chunk (OFDMA) or one symbol (TDMA)
Type of feedback	Average SINR per chunk (OFDMA) or symbol (OFDM-TDMA)
Feedback delay	1 Frame
Overhead	Chunk's overhead: 17.5%; tail of CC; duplex time.
Mobile speed	angle$\{v\}$ ~ U(0,2π); $v_x \sim \eta(m,\sigma^2)$, $v_y \sim \eta(m,\sigma^2)$, $\|v\| = (v_x^2+v_y^2)^{0.5}$ m = 1 km/h, σ = 1.6 km/h

The performance of OFDMA and TDMA is assessed for the uplink considering several scheduling variants. Common to all these variants is a two step approach: in the first step a decision is taken which 8 users (out of 40 or 80 users) will be served and in the second step it is decided how many and what resources are assigned to the selected users.

In case of Round Robin (RR), both users and resources are sequentially selected and linked. With the MaxSNR1 approach, the 8 users with the highest SNR are selected in the first step. Then, equal amount of resources are allocated to these users in a round robin manner. With MaxSNR2, users are selected via round robin but the resource allocation is performed according to the maximum rate sharing principle. Step one is the same for the fair rate (FR) scheduler but in step two each user gets a fraction of the resources which is inversely proportional to the user's transmission rate. In the second version (FR2), the resource assignment decision is made to maximise the overall frame throughput.

Note that very simple link adaptation based on the average SNR was applied using reference curves from AWGN link level simulations. Since such a model is suboptimum for TDMA (where the codeword suffers from frequency-selectivity), the comparison of both MA schemes is to a certain extent unfair.

Independent encoding of each chunk with tail as considered in case of OFDMA increases the overhead and causes the overall throughput to decrease. This factor is more significant for low quality channels (large distances between the UT and BS), when low order modulations and strong coding schemes are applied. The measured loss with Round Robin scheduling is about 3.7% for 100 meter cells and about 6.9% for 200 meter cells on average, however, users at the cell edge experience a throughput loss higher than 7% and 11% respectively.

The calculated average cell throughput obtained with RR scheduling for 100 meter cell radius and 40 users is equal to 71.38 Mbps for OFDMA and 73.35 for TDMA. The MaxSNR1 scheduling algorithm adaptively selects the users to be served and thus offers an increase of the overall cell throughput to 147.84 Mbps and 153.15 Mbps, respectively. It should be stressed that similar results are obtained for both OFDMA and TDMA since no fully adaptive scheduling has been applied: one part of the chain, i.e. either user selection or resource assignment, is always based on round robin. For the MaxSNR2 algorithm the average cell throughput is about 7 Mbps lower than for MaxSNR1, and for Fair Rate scheduling the average cell throughput for OFDMA is equal to 46.67 Mbps only. Scheduling of users on the equal time sharing base (RR, MaxSNR2, FR) slightly decreases the overall cell throughput for higher number of allocated users (by about 0.2% - 0.4% for 80 allocated users). Increase of the cell radius from 100 m to 200 m decreases the average cell's throughput by about 50% for RR, 19% for MaxSNR1, 17% for MaxSNR2 and 68% for FR scheduling.

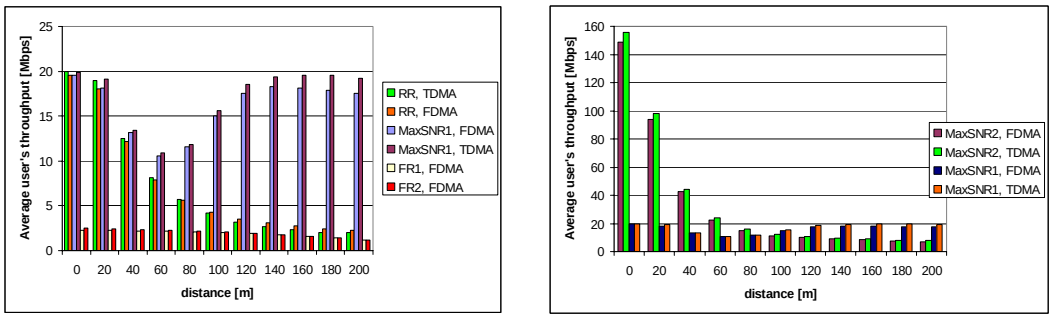

Figure G.27: Average user's throughput vs. distance for different scheduling variants considering 40 users; throughput figures are averaged across served users only.

Simulation results showing the average user throughput versus distance with the different scheduling algorithms discussed are shown in Figure G.27. The average user throughput obtained with FR (left plot) drops very slightly with distance (in contrast to RR), however, the price to be paid is its lower overall throughput. Application of the FR2 increases the overall throughput only slightly compared to FR. In case of MaxSNR1 the average throughput drops for the middle range users but compared to fair rate scheduling a much higher user throughput is achieved. As depicted in the right plot of Figure G.27, MaxSNR2 scheduling achieves dramatically higher throughput values for users located close to the base station than MaxSNR1 albeit at the expense of serving some users not at all (mainly those far away from the BS).

Results presented to far reveal the large impact of scheduling algorithms on cell throughput and fairness. The two step scheduling approach considered here enables a trade-off between both aspects. Further refinement is required to be able to exploit the multi-user-diversity potential of chunk based OFDMA and compare the results to the well known class of proportional fair scheduling algorithms.

G.5 Uplink spatial processing

G.5.1 Performance of spatial diversity

Simulation Assumptions	
Simulator	System, 19 three-sector sites, full interference modelling using wrap-around
Scenario	cellular; on average 10 users/sector; frequency reuse: 1; MT = 1, MR ≤ 8; varying cell radius
Channel model	C2, NLOS, WINNER interim channel model (WIMI)
MCS	Modulation schemes: QPSK, 16QAM, and 64QAM Channel code rates: 1/10, 1/3, 1/2, 2/3, 3/4, and 8/9
FEC	Turbo code combined with Layer 1 code block segmentation (up to 5114 bits per block) and rate matching, codeword length: from 998 (QPSK, rate 1/10) to 26624 bits (64QAM, rate 8/9), rate 1/7 mother code (polynomials: feedback 013, feedforward 015, 017, 011)
Feedback/Overhead	Chunk SINR after receiver processing, zero delay, no overhead

A non-frequency adaptive uplink based on OFDM is considered. The performance of the uplink access method is evaluated using different number of base station antennas in order to demonstrate the importance of antenna diversity. Performance is compared for different cell sizes and in terms of average sector throughput and active radio link data rates. The latter measure is the (average) user throughput when scheduled for transmission. Since round robin TDMA scheduling is applied, the active radio link data rate may be used to assess the fairness in the network. Furthermore, because many idealised assumptions are made, one should not focus on the absolute performance figures but rather on the relative performance.

Figure G.28 shows the average uplink throughput for different number of base station antennas and for different diversity combining schemes, namely MRC and IRC. The antenna element spacing at the base station is half a wavelength (left) and four wavelengths (right). With tightly spaced antennas, the gain of multiple antennas at the base station and MRC is in the order of 35–50 %, 80–110 %, and 130-220 % for two, four and eight antennas, respectively. IRC, which performs inter-cell interference suppression, provides an additional gain of up to 10 %, 20 %, and 25 %. With a wider antenna separation, the diversity gain is enhanced even further and in particular the gain of IRC over MRC is more evident. In interference-limited deployments, the performance with four antennas and IRC is comparable to the performance with eight antennas and MRC.

The lower plots depict uplink data rate distributions in a deployment in which cells have a radius of 700 m. The distributions indicate that in order to provide high uplink data rates to a large fraction of the user population, multiple base stations receive antennas are a very useful means.

In summary, base station receive diversity may significantly improve the uplink performance. Such solutions increase total throughput and enhances data rates for all users. Performance improves, as expected, with larger antenna separation and the results further indicate that IRC with a lower number of antennas may give similar performance as MRC with a larger number of antennas. It should be kept in mind, however, that the inter-cell interference suppression gains of IRC relative to MRC may be smaller when estimation errors are considered.

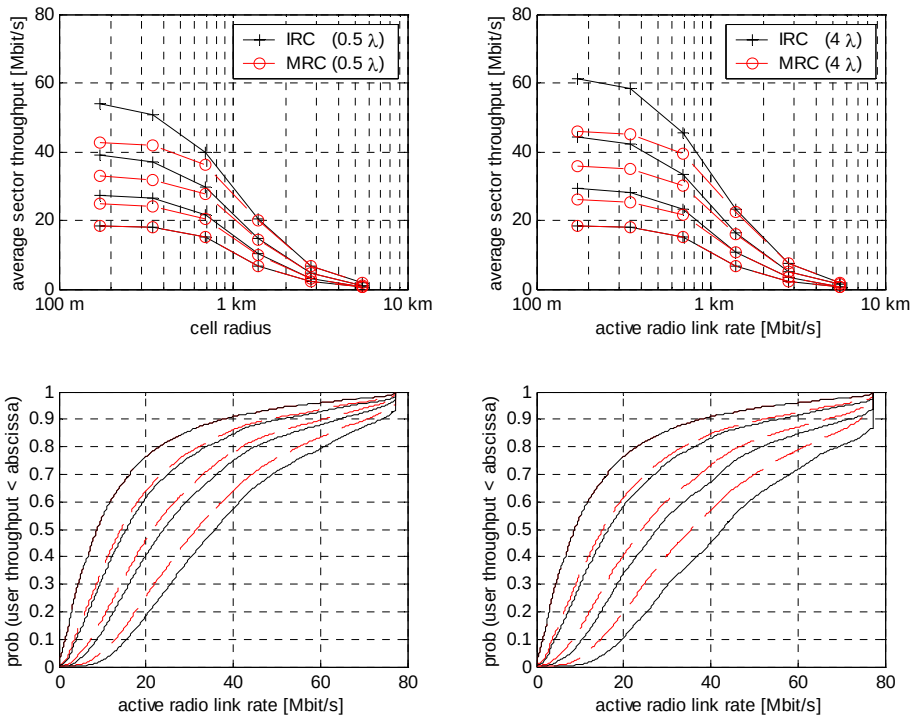

Figure G.28: Average uplink throughput and active radio link distributions for different number of base station receive antennas, combining schemes and antenna element separations.

G.5.2 Linear precoding concepts with long term channel state information

In the wide-area scenario, the instantaneous CSI is not available at the transmitters due to the high mobility. Therefore, linear precoding is performed at the mobiles based on long-term CSI. Long-term CSI are either the channel mean components (first moment of the channels – mean feedback) or the channel correlation matrices (second moment of the channels – covariance feedback). In general, there are two ways to obtain long-term CSI: implicit or explicit feedback.

In TDD mode under the reciprocity assumption, the downlink channel estimation can be reused for uplink transmission. After estimation of the channel during downlink transmission, the instantaneous channel at time $t+\tau$ that is seen by the mobile is modelled by the sum of the estimated channel matrix and a noise matrix. This channel can be interpreted as an MIMO channel with effective LOS component. The K factor corresponds to the quality of the channel estimate. In the explicit form of mean-feedback, the base station performs channel estimation, averages over many blocks and transmits the mean matrix back over a control channel.

In FDD mode, the receiver estimates the correlation matrix on the set of carriers used for downlink transmission [BM04]. There are two key issues regarding the efficiency of estimating the covariance matrix in this way: The covariance must vary slowly enough, i.e. the estimate is still valid, when the base station is sending to user k. There must be enough carriers in the set to well approximate the actual covariance matrix. The explicit covariance feedback scenario is similar to the explicit mean feedback scenario discussed before. The base collects the necessary channel statistics and feeds back the channel covariance matrix to the mobiles.

Let assume the multi-user linear MMSE multi-user receiver is used at the base station. Then the performance criterion is the average total sum MSE [JB03]. The corresponding programming problem is given by minimizing the total sum MSE under individual power constraints. Beamforming of user k on carrier n with the eigenvectors of the transmit covariance matrix, power allocation of user k on carrier n with the eigenvalues of the transmit covariance matrix, and resource allocation is described by the individual MSE of user k on carrier n.

If implicit feedback is used, then the optimal beamforming directions of all users correspond to the eigenvectors of the effective LOS-component for mean feedback or the eigenvectors of the channel transmit correlation matrix for covariance feedback. The resulting power allocation problem is characterised by the range in which a single-beam per user achieves the sum performance. For sum capacity the analysis was performed in [SU05]. The theoretical results and the corresponding SCME channel model results are shown in Figure G.29.

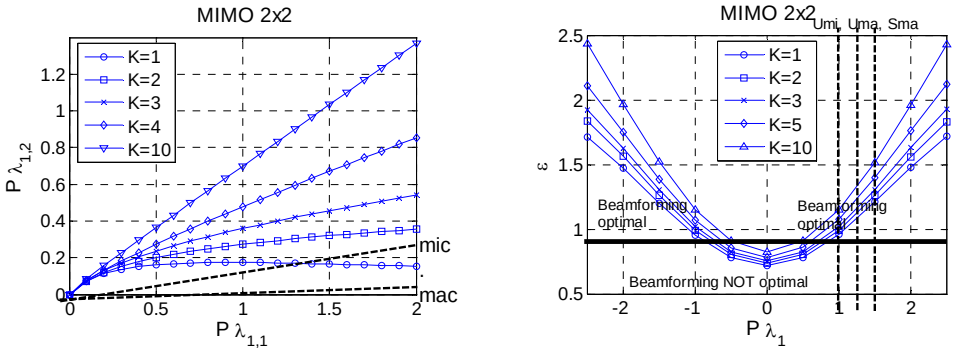

Figure G.29: Beamforming optimality range for covariance and mean feedback in theory and WINNER SCME channel models (micro urban [umi], macro urban [uma], and macro suburban [sma]).

Here, P is the total transmit power, M is the largest mean component, $\lambda_{1,1}$ and $\lambda_{1,2}$ are the largest and second largest eigenvalue of the transmit correlation matrix of user one. The term ε represents the beamforming condition function, i.e. if ε > 1 then beamforming is optimal. Observe that for two transmit and two receive antennas single stream beamforming is optimal for two and more users. Other antenna configurations are to be analyzed.

G.6 Uplink multi-user detection

G.6.1 Comparison of receiver structures for DS-CDMA

Simulation Assumptions	
Simulator	Multi-link
Scenario	wide area cellular, frequency reuse: 1, single antenna BS and UT. average (slow) power control
Channel modelling	C2, NLOS, WIMI
Interference modelling	Interference generated by neighbour cells active users (6 cells surrounding the cell of interest). Assume same number of active users in all cells.
MCS	1: BPSK
FEC	convolutional coding $(561,753)_{oct}$ with memory 8, code rate 1/2 Codeword length: 702 bits
spreading	Walsh-Hadamard, spreading length: 16
Cyclic Prefix length	52 chips (block oriented transmission)
Overhead	Total overhead of 23% taken into account in TX-power and resources.
Mobile speed	50% 1 km/h, 50% 25 km/h
User spatial distribution	$d_k = \left(1+9\sqrt{(k-1)/(K-1)}\right)0.1r_{\text{cell}}, \quad k=1,\ldots,K$

The focus has been placed on evaluating performance of various reduced complexity receivers for the uplink in the wide area non-frequency adaptive WINNER mode, for single carrier DS-CDMA where the multi-carrier approach could encounter important challenges. Two transmission schemes are compared: a time domain processing receiver based on conventional RAKE receiver and a frequency domain processing receiver that makes use of cyclic prefix (CP). In both cases several iterative implementations of the multi-user detector are investigated. Motivated by complexity constraints the focus is on linear multi-user detectors. The complexity of the MMSE receiver is dominated by the calculation of the MMSE filter which requires a large matrix inversion. Rather than direct matrix inversion we use iterative methods for solution of linear systems, concentrating on the Successive Over-relaxation (SOR) method, associated with serial interference cancellation; and the Chebyshev method, associated with parallel

interference cancellation. The details and formulation of multi-user receiver in either domain and the proposed reduced complexity methods for the implementation of a linear multi-user receiver can be found in [IN05][WIND26].

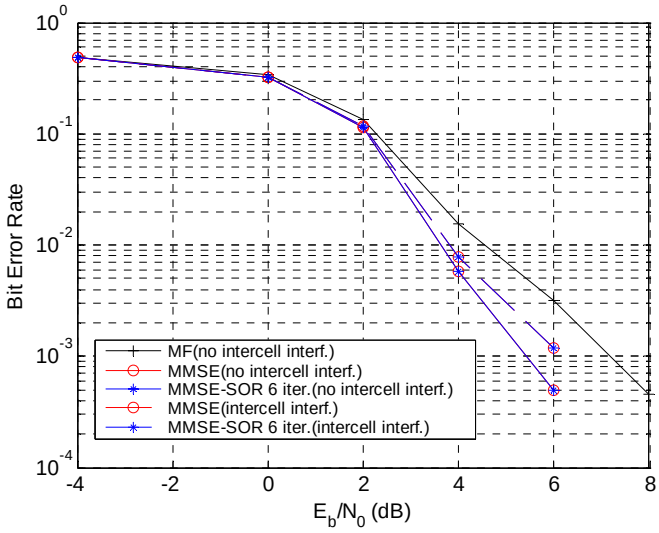

Figure G.30: BER performance of a low complexity frequency domain MMSE receiver in presence of inter-cell interference.

Based on link level simulations results in terms on convergence and performance for single cell scenario where results showed that convergence of the iterative implementation of the TD receiver is substantially slower than for the FD receiver, being in both cases faster for the SOR iterative implementation of the MMSE filter than for the first order Chebyshev iterative implementation, we focus on the FD receiver and SOR implementation of the MMSE detector for the multi-cell multi-link evaluation. Shown in Figure G.30 is the coded BER performance of FD receiver in presence of inter-cell interference compare to no inter-cell interference, for a 50% loaded system, where the performance for the iterative implementation of the MMSE detector is shown for 6 iterations. Similar results have been obtained for other system loads.

To conclude, it is feasible to achieve MMSE performance with a reduced complexity implementation with only a few iterations required. Yet the single carrier DS-CDMA approach will require a multi-user detector.

G.6.2 Comparison of receiver structures for MIMO single carrier

Simulation Assumptions	
Simulator	multi-link
Scenario	wide area, isolated cell, $M_T = 2, 4$; $M_R = 4$; 1–4 users
Channel modelling	C2, NLOS,WIMI
Interference modelling	no inter-cell interference
Multiple access	TDMA/SDMA
MCS	1: QPSK, r=1/2; (SM-MIMO with turbo coding) 1: BPSK; r=1/3 (ST-WNRA)
FEC	punctured turbo coding $(15,13)_{oct}$ with memory 4 space-time weighted non-binary repeat accumulate coding codeword length: fixed size of 1664 bits

Serial modulation for wide area uplink was investigated for the case of single-input-single-output (SISO) transmission with non iterative and iterative frequency domain receivers in [WIND21, WIND23]. In order to further enhance uplink performance, link-adaptation and MIMO techniques are the focus of further study. In this section only MIMO techniques are considered; further information about different link adaptation techniques can be found in [WIND23]. By using at least one of these key technologies, bandwidth efficiency can be enhanced and transmission power of terminal can be reduced. As a result of this, improved uplink performance turns into larger coverage and higher data rates. The goal of this section is to introduce two MIMO techniques for wide area uplink with serially modulated multipoint/point to point transmission. Channel state information is not required at the transmitter and iterative frequency domain processing is performed at the receiver.

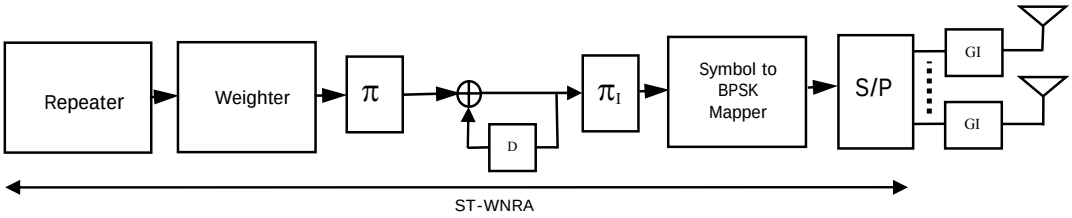

Figure G.31: Transmitter block diagram of space-time weighted nonbinary repeat accumulate (ST-WNRA) coded multipoint/point-to-point MIMO for serially modulated MIMO transmission.

Figure G.31 illustrates the transmitter block diagram of ST-WNRA coded MIMO. The ST-WNRA encoder consists of two main parts; a repeater and the concatenation of a weighter and an accumulator. The function of the repeater is to provide coding gain and the concatenation of the weighter and accumulator is to provide full rank over the whole encoded data. Therefore, ST-WNRA codes can provide full transmit antenna diversity for any number of transmitter antennas in single user flat fading channels with low encoding and decoding complexity. The full transmit antenna diversity can be only obtained by using BPSK as underlying modulation method, because the full rank property is only retained in the binary field. The interested reader is referred to [OY03] for more in-depth information about ST-WNRA codes. The maximum achievable diversity order with ST-WNRA codes using the proposed iterative frequency domain reception is given as $M_T \times L \times M_R$, where M_T, L, and M_R are the number transmit antennas, the number of multi-paths and the number of receiver antennas, respectively. Since ST-WNRA is a pure diversity based MIMO technique, the maximum transmission rate is constrained to one. However, the transmission rate can be enhanced by using a multilevel approach that is briefly described in the next subsection. Finally, it should be noticed that ST-WNRA codes are more flexible compared to other space-time codes that provide both coding and diversity gain e.g. space-time trellis and space-time turbo codes. Flexibility is an important factor when capability to support for any number of transmitter antennas and short frame lengths is required.

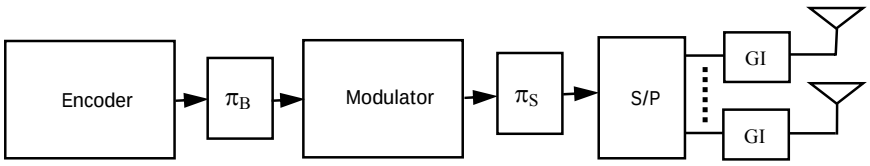

Figure G.32: Transmitter block diagram of spatially multiplexed, vertically encoded multipoint/point-to-point MIMO for serially modulated transmission.

Figure G.32 presents the transmitter block diagram for the well-known vertically encoded spatially multiplexed MIMO transmission. In this scheme the input bit stream undergoes temporal encoding, modulation, and interleaving after it is demultiplexed into NT streams transmitted for individual antennas. Obviously, the purpose of this technique is just to maximise multiplexing gain. Therefore, the maximum achievable diversity order by using convolutional/turbo codes and with the proposed iterative frequency domain reception is given as $L \times M_R$. Further details of this scheme can be found from [SD01].

The parameters used in the simulations are as follows for ST-WNRA multi-user MIMO: the channel is typical urban C2, 2 transmit antennas per user, 4 receive antennas, repetition rate 3, 3 decoder iterations, 4 equaliser iterations; the number of users ranges from 1 to 4. Iterative frequency domain joint-over-antenna multi-user MIMO receiver is used. For spatially multiplexed turbo-coded multi-user MIMO the parameters are the same, except for the code rate being ½ (generator polynomials (15,13)), QPSK modulation.

Figure G.33 presents the simulation results of ST-WNRA and spatially multiplexed vertically turbo-coded multi-user MIMO. ST-WNRA outperforms spatially multiplexed vertically coded MIMO. However, the maximum spectral efficiency in the case of ST-WNRA is 2.66 bit/Hz/s whereas with spatially multiplexed case it is 8 bit/Hz/s. The results also show that with joint-over-antenna signal detection technique the same diversity order is maintained for each of the users. Only a parallel shift is observed when the number of users is increased. This is due to fact that joint-over-antenna technique can preserve the degrees of freedom for the joint-detection of interference and the signal of interest.

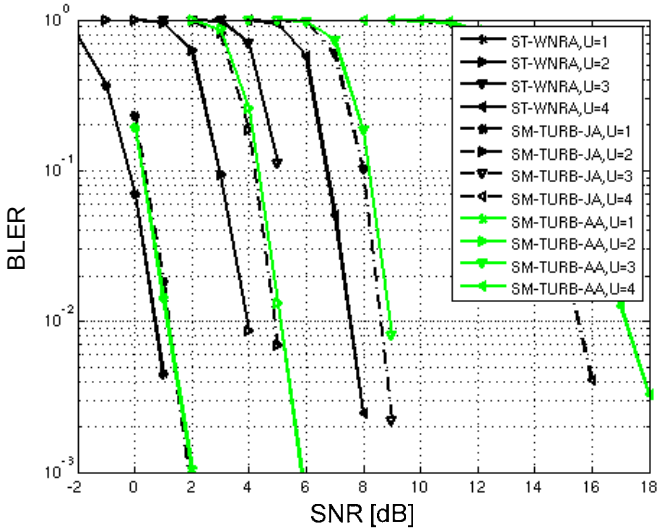

Figure G.33: BLER performance vs. SNR of serially modulated multi-user MIMO transmission in typical urban C2 Scenario. (each user has 2 transmitter antennas and base station has 4 receiver antennas, number of users U = 1,2,3,4).

G.7 Other topics

G.7.1 OFDM versus single carrier based uplinks

Simulation Assumptions	
Simulator	System, 19 three-sector sites, full interference modelling using wrap-around
Scenario	cellular; on average 10 users/sector; frequency reuse: 1; $M_T = 1$, $M_R = 4$; varying cell radius
Channel model	C2, NLOS, WINNER interim channel model (WIMI)
MCS	Modulation schemes: QPSK, 16-QAM, and 64-QAM Channel code rates: 1/10, 1/3, 1/2, 2/3, 3/4, and 8/9
FEC	Turbo code combined with Layer 1 code block segmentation (up to 5114 bits per block) and rate matching, codeword length: from 998 (QPSK, rate 1/10) to 26624 bits (64QAM, rate 8/9), rate 1/7 mother code (polynomials: feedback 013, feedforward 015, 017, 011)
Feedback/Overhead	Chunk SINR after receiver processing, zero delay, no overhead

A non-frequency adaptive uplink based on OFDM or single-carrier transmission is considered. The impact of the high PAPR of the OFDM signal is coarsely modelled by introducing a power backoff factor that reduces the maximum terminal output power. In case single-carrier transmission is considered, a linear MMSE frequency domain equaliser (FDE) is assumed to be used in the base station receiver. Performance is compared for different cell sizes and in terms of average sector throughput and active radio link data rates. The active radio link data rate is the (average) user throughput when scheduled for transmission. Since round robin TDMA scheduling is applied, the active radio link rate may be used to assess the fairness in the network. Because many idealised assumptions are made, one should not focus on the absolute performance figures but rather on the relative performance.

Investigations of single-carrier and multi-carrier modulation techniques in Appendix B indicate that the PAPR of an OFDM signal, and the required power backoff, is typically 2–3 dB higher than that of a single-carrier signal. To capture the high PAPR of the OFDM signal, OFDM transmission is in here modelled with a power backoff (pbo) of 2 dB. As a reference case, OFDM transmission without any power backoff (0 dB) is studied as well. In the left part of Figure G.34 the performance of an uplink access scheme using OFDM transmission is compared to a single-carrier transmission scheme in terms of average sector throughput. Base stations are equipped with four antennas separated four wavelengths and IRC is used to suppress inter-cell interference. The results indicate that in interference limited scenarios,

i.e., for small cells, OFDM has a small performance advantage thanks to the absence of inter-symbol interference. Note further that in such interference limited deployments the OFDM power backoff is of limited importance. In large cell deployments, in which noise rather than interference limits performance, single-carrier transmission provides better performance thanks to the higher output power (compared to OFDM with a 2 dB power backoff). The right plot shows data rate distributions for cell radius 700 m. The plot indicates that compared to OFDM with a 2 dB power backoff, single-carrier transmission provides a small but uniform increase of data rates.

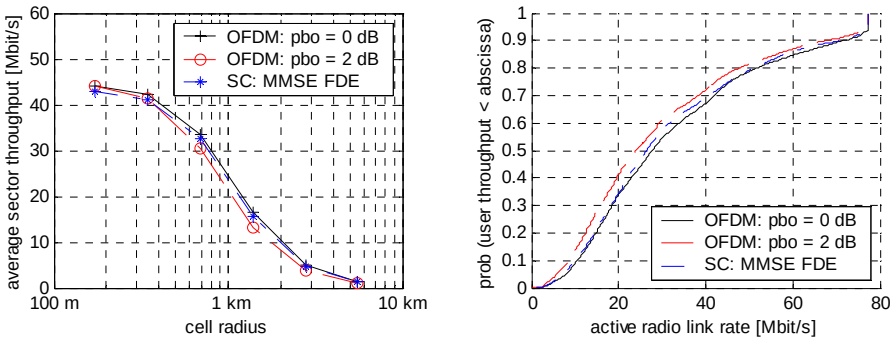

Figure G.34: Average sector throughput for OFDM and single-carrier transmission (left) and an example of the corresponding data rate distributions (right). The distributions are depicted for cell size 700 m.

In summary, the results show that if accounting for the high PAPR of the OFDM signal, here by introducing an OFDM power backoff penalty of 2 dB, OFDM has a small performance advantage in interference limited scenarios while the single-carrier transmission scheme, using a linear MMSE frequency domain equaliser at the receiver, provides better performance in noise limited deployments.

G.7.2 Performance of low rate channel coding for one-cell frequency reuse

Simulation Assumptions		
Simulator	Link level	Inter-cell interference is modelled by Gaussian noise
	System level	19 cells, 3 sectors/cell, full inter-cell interference modelling using wrap-around
Scenario		Wide area cellular, frequency reuse 1, single antenna BS and UT
Channel model		Metropolitan channel model defined in D5.3
Mobile speed		4 km/h for all users
Channel coding		Turbo code
ARQ		Chase combining, Maximum number of retransmissions: $M = 0, 1, 3$
Scheduling (for system level)		Proportional fair scheduling, 4 users/sector, Full buffer model
Channel estimation		Real (Weighted subcarrier coherent averaging)

First, using the link level simulation, optimum minimum coding rate of a very-low-rate Turbo coding and spreading factor value that achieves one-cell frequency reuse in a multi-cell environment in the downlink OFDM is investigated. The required average signal-to-interference plus noise power ratio (SINR) to satisfy an average packet/block error rate (BLER), of 10^{-2} is plotted in Figure G.35 (left) as a function of the reciprocal of the coding rate, $1/R$.

In the figure, QPSK modulation is employed and Q denotes the spreading factor. As shown in the figure, the required average SINR is reduced with increasing ratio Q/R, which indicates that the suppression of severe inter-cell interference from the surrounding cells is in principle possible, however, at the expense of throughput. Moreover, under the same Q/R conditions, the required average SINR is reduced with decreasing code rate R up to approximately 1/6 to 1/8. Therefore, we see that the minimum coding rate providing a distinct channel coding gain is approximately R = 1/6 to 1/8. Figure G.35 (right) shows the required SINR for the average residual BLER of 10^{-3} as a function of the product of $1/R$ and Q. Assuming real-time traffic with a rigid delay requirement, we take into account hybrid ARQ with Chase combining.

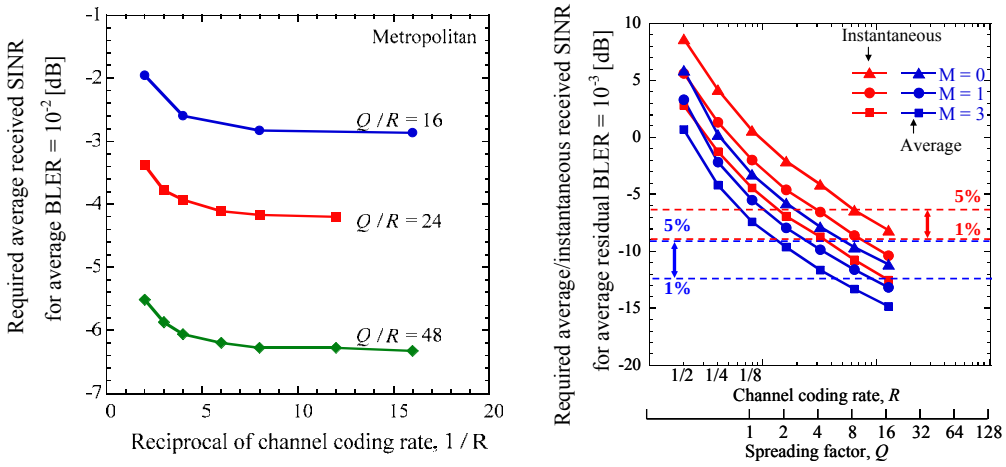

Figure G.35: Optimum minimum channel coding rate (left) and required coding rate and spreading factor for achieving one-cell frequency reuse (right).

Furthermore, we assumed two extremely different packet call times: a very long call time, where the received SINR is approximated by the average SINR (denoted as Average), and a very short call time during one packet frame duration, where the received SINR is approximated by the instantaneous SINR (denoted as Instantaneous). In the figure, the dotted lines indicate the SINR values corresponding to the 1% and 5%-point of CDF of the SINR, i.e., cell-edge conditions in a multi-cell environment. On the horizontal axis, we first decrease the coding rate from $R = 1/2$ to 1/8 maintaining $Q = 1$. Next, in order to achieve $Q/R > 8$, we further increase the Q value with a fixed $R = 1/8$. As shown in the figure, according to the increase in the Q/R value, the required SINR value is significantly improved. This is due to the effect of the improved processing gain associated with channel coding and spreading. Furthermore, assuming the same Q/R value on the horizontal axis, increasing M brings about a reduction in the required average SINR, since the time diversity gain from the hybrid ARQ improves the received SINR of a packet. From the figure, in order to satisfy the SINR value at the 1% and 5%-point of CDF, the required coding rate and the spreading factor becomes $(R, Q) =$ (1/8, 8 - 16), (1/8, 4 - 8) and (1/8, 2 - 4) for $M = 0$, 1, and 3 in the case of average SINR and (1/8, 8 - 32), (1/8, 4 - 16), and (1/8, 2 - 8) for $M = 0$, 1, and 3 in the case of instantaneous SINR. Consequently, we conclude that the spreading is inevitable to achieve one-cell frequency reuse together with the low-rate channel coding, such as $R = 1/8$.

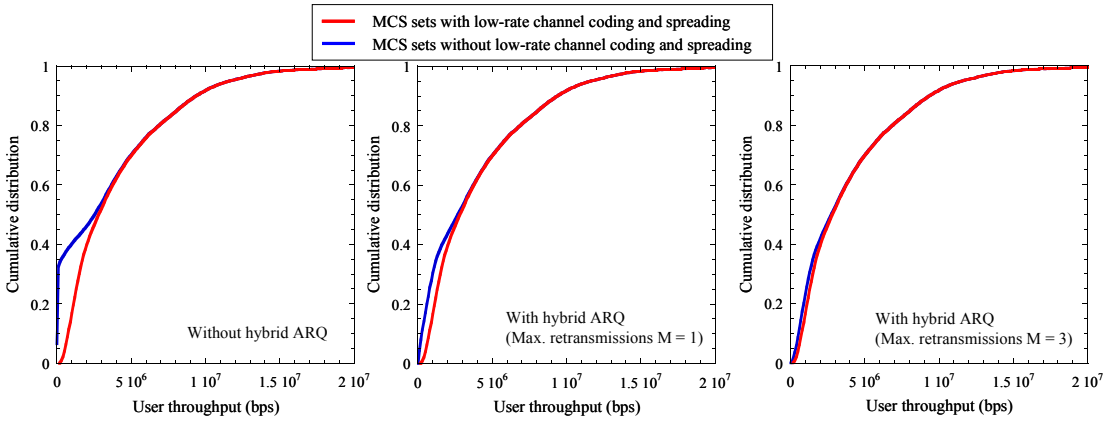

Figure G.36: Effect of low rate channel coding and required channel coding rate and spreading on user throughput in a multi-cell environment.

Next, the effect of low rate channel coding together with spreading is evaluated in a multi-cellular environment using system level simulations. In the simulations, two sets of modulation and coding schemes (MCS) are used: one with and one without spreading. The first set comprises QPSK with code rate and spreading factor $(R, Q) =$ (1/8, 16), (1/8, 8), (1/8, 4), (1/8, 2), (1/8, 1), (1/4, 1), (1/2, 1), (2/3, 1) as

well as 16-QAM with (R, Q) = (1/2, 1), (2/3, 1) and (3/4, 1). The second set includes QPSK with code rate R=1/2 and 2/3 as well as 16-QAM with rate R= ½, 2/3 and ¾.

As shown in Figure G.36, the user throughput performance is improved by employing the MCS set with low-rate channel coding and spreading compared to those without low-rate channel coding and spreading. For example, the MCS set with low-rate channel coding and spreading maintains approximately 600 kbps and 750 kbps user throughput at 5% and 10%-point of CDF, respectively. In case of hybrid ARQ with more than one retransmission, however, the benefit of low rate channel coding and spreading is negligible.

G.7.3 Comparison of FDMA and TDMA based resource partitioning among BS

Simulation Assumptions	
Simulator	Link level
Scenario	wide area cellular, frequency reuse: 7, single antenna BS and UT
Channel modelling	WSSUS Rayleigh fading with exponential power delay profile Okumara-Hata path loss model
Interference modelling	AWGN
Cell radius	Up to 2 km
OFDM parameter	512 used subcarriers, subcarrier distance: 39.0625 kHz, guard period: 6.4 μs
MCS	QPSK
FEC	no coding
Mobile speed	30 km/h, same for all mobiles - results in almost perfect link adaptation

In a wide area OFDM cellular systems, even with perfect inter-cell time synchronisation, time offsets between users in different cells due to propagation delays induce significant inter-cell interference. This appears in form of inter-carrier/adjacent band interference, if different cells are assigned adjacent portions of the available bandwidth, e.g. in a block-FDMA fashion, and in form of inter-symbol interference, if different cells are assigned the whole transmission bandwidth in successive periods of time, e.g. slot-TDMA. In order to avoid/reduce such interference, guard bands and guard periods can be introduced in FDMA and in TDMA, respectively. The aim of this analysis is that of deriving which of the two approaches is the most spectrally efficient under currently envisaged system parameters and requirements.

In a first step, the performance degradation due to time offsets in block FDMA inter-cell allocation with and without guard bands is evaluated. A worst case scenario is considered in which there are only two cells and two users which are assigned interleaved blocks of adjacent subcarriers. Moreover, equal receive power and time offsets up to ½ OFDM symbol are assumed. Results are reported in Figure G.37, left plot, in terms of uncoded BER (rawBER) for blocks of 8 and 64 subcarriers at different values of time offsets ranging from 5 μs to 16μs (cell radius of 1,5 and 4,8 km, respectively). It can be inferred that there is high performance degradation when the time offset is equal to or higher than the guard interval. For some time offsets, the rawBER curve saturates before 10^{-2}. As it is reasonably expected, significantly better performance is obtained with larger block size because the effect of inter-carrier interference is larger at the block border. Hence, for smaller blocks, almost all subcarriers might be interfered.

A better overview is offered by Figure G.37, left plot, which compares the dependency of the SNR degradation on the different values of time offsets. The SNR degradation has been computed at a rawBER of $10^{-1.77}$ corresponding to coded BER of 10^{-3}, which represents the considered QoS criterion for VoIP. The SNR degradation for the block size of 8 subcarriers is visibly much higher than for blocks of 64 subcarriers. At a time offset of 6 μs, we have a loss in power efficiency of 1.2 dB.[39] Figure G.37, right plot, shows the comparison of SNR degradation with and without guard bands. The introduction of guard sub-bands leads to a significant improvement. For time offsets larger than 5μs, in particular, the SNR degradation saturates.

To compare the spectral efficiency of the two inter-cell allocation schemes, the power efficiency loss in the block-FDMA case has to be translated into a figure of spectral efficiency loss. Given the not too high values involved, we can resort to a simple rule of thumb derived from 2G and 3G experience according to which a 4.5 dB loss in power efficiency corresponds to 50% spectral efficiency loss. In Table G.2, results

[39] Note that for block size of 8 sub-carriers the SNR degradation curve has not been plotted for time offset values larger than 6 μs, since the rawBER curve saturates before reaching the value corresponding to the required QoS.

in terms of power and spectral efficiency loss are reported for block-FDMA with blocks of 64 subcarriers, for cell radius of 2 km and reuse factor 7, with and without guard bands of 8 subcarriers.

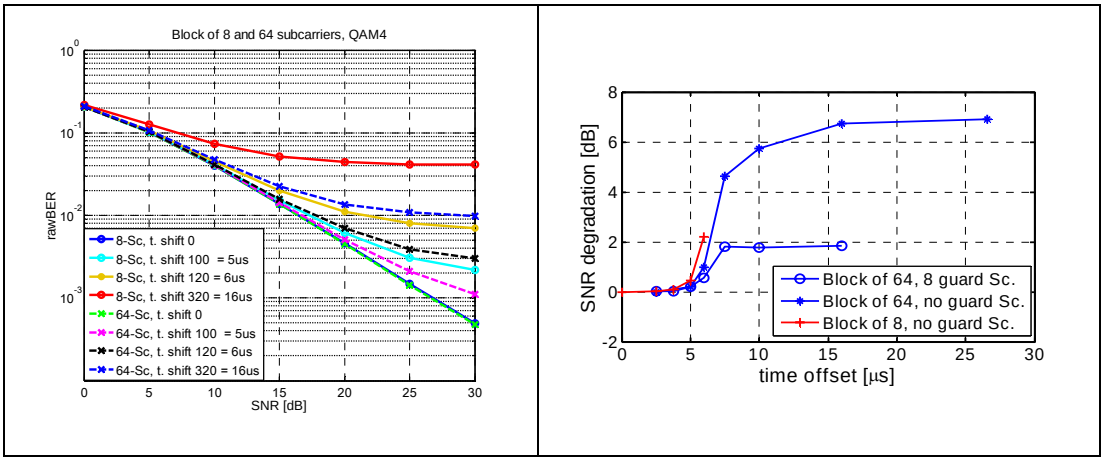

Figure G.37: left plot: raw BER for different sizes of block of subcarriers and different values of time offsets; right plot: Dependency of SNR degradation on time offset for block of 8 subcarriers and for block of 64 subcarriers with and without guard band.

In slot-TDMA, the insertion of guard periods between any pair of time-slots assigned to different cells represents an overhead which induces spectral efficiency loss and can be computed as follows. The total time consumed as guard time is given by the number of time slots multiplied by the length of the guard period that is at least equal to the maximum time offset. For TDD and HD-FDD the number of time slots assigned to different cells is 2 times the reuse factor. The maximum time offset to be taken into account depends on the considered scenario. For example, with reuse factor 16 in a macro-cellular deployment scenario with antennas above rooftop, the link of interest can be affected by interference from the second ring of interfering cells, which implies a propagation delay corresponding to four times the cell radius. The resulting overhead is then given by the ratio between the total guard time and the frame duration. Results are reported in Table G.3 for different reuse factors.

Table G.2: Power and spectral efficiency loss for block-FDMA with blocks of 64 subcarriers, with reuse factor 7, with and without guard bands of 8 subcarriers.

Reuse Factor	Additional Guard Bands Overhead [%]	Power Efficiency Loss [dB]	Spectral Efficiency Loss [%]	Total Loss [%]
7	0	6.28	69.8	69.8
7	12.5	1.80	20.1	32.6

Table G.3: Overhead due to guard periods in slot-TDMA, with reuse factor 5 and 7.

Reuse Factor	Frame Length [ms]	Number of Time Slots	Total Guard Time [µs]	Overhead [%]
5	0.7	10	133	19
7	0.7	14	186	>100

From simulation results it can be derived that it would be recommended to assign blocks of at least 64 adjacent subcarriers to different cells in order to keep the performance degradation to a reasonable level (up to 1 dB). For a reuse factor 7 and cell radius of 2 km, the spectral efficiency would be doubled through the insertion of guard bands of eight subcarriers. Moreover, it has been explained how the use of the slot-TDMA inter-cell allocation approach is restricted by the assumption of very short frame length. For the currently assumed frame length of 0.7 ms, the overhead due to the insertion of guard periods could result to be unacceptable (larger than 100% for reuse factor 7). Since the overhead depends on the number of slots which is determined by the reuse factor, a reuse factor up to 6 would be acceptable, while for reuse factors larger or equal to 7 it would be preferable to use block-FDMA.

We note that, although the results of this section have been derived under the assumption of reuse factor larger than 1, they remain valid in case of single-frequency network with interference-avoidance-based

dynamic resource management. Indeed, in the latter case, a reuse factor is implicitly implied by the size of the smallest resource units assigned to different cells.

G.7.4 Comparison of conventional and self-organised RRM in cellular networks

Simulation Assumptions	
Simulator	System level
Scenario	Short range cellular, frequency reuse 1, single antenna BS and UT
Channel modelling	Generic channel model, including path loss + shadow fading
Interference modelling	Inter-cell interference, 49-cell network (wrap-around)
Cell radius	300 m
Link adaptation	Adaptive MCS selection based on estimated SINR values
MCS	BPSK, QPSK, 16QAM, 64QAM, 256QAM, all with 1/2 coding rate
FEC	Convolutional coding $(133, 171)_{oct}$ with memory 6, codeword length 2160
Type of feedback	Only in link setup phase: measured signal power, resource candidate with corresponding interference values
Feedback delay	1 frame
Overhead	1 OFDM symbol per frame
Mobile speed	Stationary

Instead of the conventional frequency planning, a self-organised radio resource management (SO-RRM) scheme has been proposed for WINNER. There is no pre-planning on frequency bands. The whole bandwidth is accessible anywhere. Each BS, based on the UL/DL signal power and interference values measured at both the BS and the UT, does the resource allocation independently. There is no direct communication between BSs. The resources with highest possible SINR values are allocated to the new UT, and suitable PHY modes are selected in accordance with those values.

With the SO-RRM scheme, a very flexible resource allocation can be realised, which means an adaptive reuse distance is implied based on the respective interference situation of each resource in the network. This scheme also facilitates high bandwidth efficiency in the hotspot case.

Anti-dropping solutions

The long-term interference situation of a user changes when a new co-channel interferer is accepted into the network. A BS accepts a new UT when the observed UL/DL SINR is sufficient for the required transmission. Meanwhile it introduces a new interferer to the network. The updated interference at an existing UT may violate the requirements of its current PHY mode for transmission, which results in a potential dropping. In most systems, the dropping rate dominates the system capacity.

Two alternative solutions can be adopted against the dropping.

- "Reallocation": as a passive way that the scheduling algorithm reacts when channel degradation is observed during data transmission. When a reallocation is activated, new resources are allocated by implementing the similar procedure for new users.
- "Security Margin": as an alternative active method. The main idea of this method is to add a security margin into the threshold for the MCS selection, in order to increase the tolerance for the possible degradation of SINR, which is caused by new interferers. The value of such a security margin depends on many aspects. Generally a low margin does not help much in the dropping performance, while a high margin achieves a large tolerance at the cost of efficiency. Therefore a balance should be made.

Comparison between SO-RRM and conventional RRM

A 49-cell network is considered. The "wrap around" technique [80220-05] is implemented in order to allow data collection from all cells within the network. For the system level simulation, the channel is assumed time invariant. Each user has the same date rate and BLER requirements.

A simulation starts with a blank system. Users arrive at the network one by one, whose locations follow a predefined distribution. The BS starts the resource allocation scheme and allocates suitable resources to the UT. A blocking occurs when a BS cannot find sufficient resources to serve its new UT. A dropping occurs when a current transmission is destroyed be a new UT, which means either the security margin is insufficient when the active anti-dropping solution is applied, or the reallocation of resources fails in the case of the passive anti-dropping solution. The "System Capacity" is used as the criterion of system level performance. A system capacity of N is defined as that, a blocking or dropping in the system happens at the first time when the (N+1) UT joins the network.

Both uniform and non-uniform distributions of users are considered. In the non-uniform case, a hotspot is defined in the central cell. Inside each cell, the users are always uniformly distributed. A "hotspot fraction" ρ is defined to quantitatively describe the user distribution as the number of users in the hotspot cell relating to the number of users in all cells

Comparison between SO-RRM and conventional RRM

The performances of five schemes are plotted in Figure G.38. The "optimised security margin" means that the applied margin is chosen, with which the system has the highest capacity. Generally it can be concluded from the results that the SO-RRM is better than the conventional RRM at the same situation. The latter has good performance for uniform user distribution. However its inflexibility induces a remarkable loss of spectrum efficiency with non-uniform user distribution, where not all resources are accessible when many users are out of service.

With the SO-RRM, all resources are accessible in each cell. It shows its robustness to the variance of user distribution. In the cases where there are no anti-dropping solutions applied or the security is applied, the performance of SO-RRM has a performance close to the conventional RRM with a uniform-like user distribution. However with higher fraction of users located at the hotspot cell, the flexibility of SO-RRM starts showing its efficiency. When all users are located in the hotspot, a 7 times higher number of users can be served

It is also observed that reallocation improves the system capacity with any user distribution. In a system with uniform user distribution, an increase of 60% can be achieved. A passive solution gains at the cost of reallocation efforts. This benefit decreases when the hotspot fraction gets higher, which means a low necessity of reallocation.

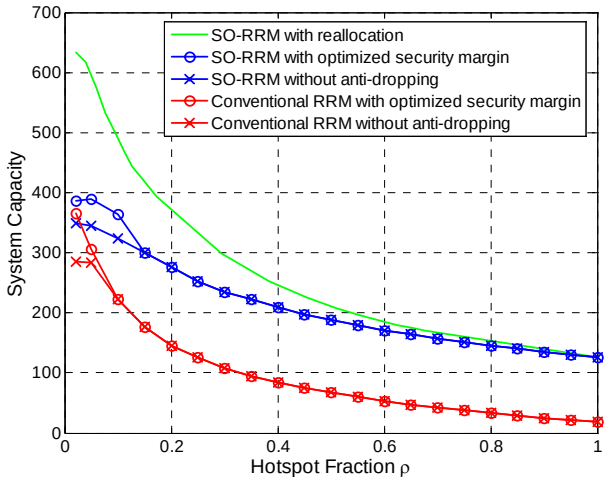

Figure G.38: Comparison of system performances with different RRM schemes.

The effect of a security margin varies for different user distribution and different resource management schemes. In a system with uniform user distribution or a system with low hotspot faction, the margin is effective in the performance improvement. However, when the fraction of users in the hotspot increases, the margin brings less improvement, and even lowers the system capacity. In a system with a high hotspot fraction, the probability of a new user located outside the central cell is very low. That is, it happens rarely that an existing transmission suffers from an outage that is caused by the new co-channel interferer. In this situation, the security margin is only an obstacle.

G.7.5 VAA technology with adaptive pre-selection aided by MC-OLSR protocol

Simulation Assumptions	
Simulator	Combined system and link level simulator
Scenario	Short range using virtual antenna arrays; $M_T = 1$; $M_R = 1$; cell radius = 320 m; mobile speed 5 km/h; VAA size = 2
Channel modelling	B1 clustered delay line
Interference modelling	no inter-cell interference
MCS	1: QPSK
FEC	no

This issue was analysed in context of radio resource control and management and more specifically the optimum pre-selection and assignment of the relay nodes at the system level for the purposes of enhancing the space-time coded cooperative transmission with the use of virtual antenna arrays (VAA) [DGA04] at the link level was investigated. To this end the MC-OLSR protocol enhanced with cooperative relaying was exploited, and this work was performed on the basis of the *Adaptive approach to antenna selection and space-time coding* analysed in [WIND24] and the *Multi-Constrained Optimised Link State Routing protocol (MC-OLSR)* proposed in [WIND31] and [WIND32] respectively. In the example depicted in Figure G.39, VAA is constituted by RN 1 and RN 2, whereas the nodes 0 (BS) and 9 (UT) are the source and destination ones respectively.

The performance comparison between the conventional and the space-time coded cooperative transmission with the use of virtual antenna arrays, when the adaptive pre-selection mechanism aided by the MC-OLSR protocol is active, is presented in Figure G.39. There is a noticeable improvement in the region of higher SNR values, however the BER curves start more or less from the same point. The reason for this situation is that if there are transmission errors between the BS and the first-hop RNs, they propagate and diminish the performance of the cooperative transmission during the second hop. This proves the necessity for further, joint cross-layer optimisation.

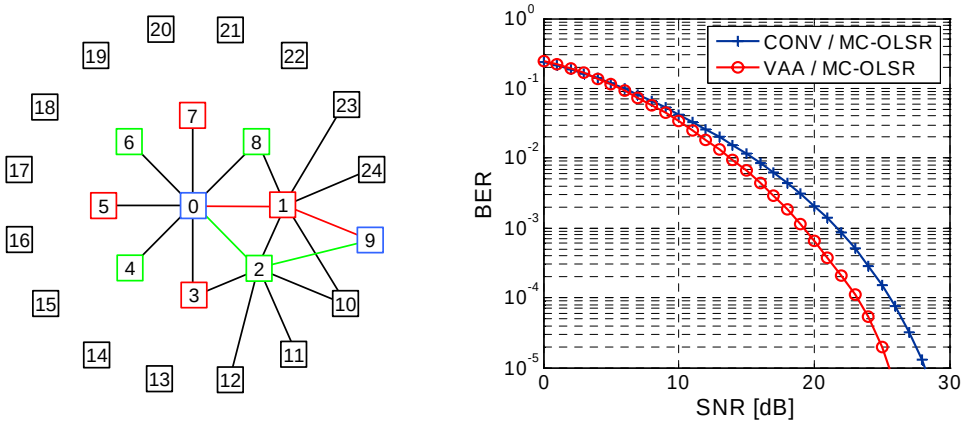

Figure G.39: Space-time coded VAA technology – scenario and performance.

References

[3GPP-TR25.212] 3GPP TSG RAN, "High speed downlink packet access: Physical layer aspects", TR 25.212.

[3GPP-WG1#42] 3GPP TSG RAN WG1#42: ZTE, CATT, RITT, Huawei, "Comparison of Structured LDPC Codes and 3GPP Turbo-Codes", R1-050840.

[3GPP-TS25.331] 3GPP TS 25.331, "RRC Protocol Specification".

[3GPP-TR25.891] 3GPP TR 25.891, "Improvement of RRM across RNS and RNS/BSS (post-Rel-5)", Release 6, v0.3.0 (draft version), 2/2003.

[80211n04] IEEE 802.11n, "Structured LDPC Codes as an Advanced Coding Scheme for 802.11n," IEEE Doc. 802.11-04/884r0, August 2004.

[80211n-05] IEEE doc 802.11-05/150r1: "WWiSE IEEE 802.11n Proposal", 2005.

[80216-04] IEEE Std 802.16-2004, "Air Interface for Fixed Broadband Wireless Access Systems".

[80216e-05] IEEE doc 802.16e-05/006r2: "LDPC coding for OFDMA PHY", available online from http://www.ieee802.org/16/tge/

[80216e05b] IEEE P802.16e/D8, 2005, "Air Interface for Fixed and Mobile Broadband Wireless Access Systems".

[80220-05] "IEEE 802.20: Evaluation Criteria", September 2005.

[Ace05] M. Aceña, S. Pfletschinger, "A computationally efficient algorithm for throughput maximization in OFDMA", *10th International OFDM-Workshop*, Hamburg, Germany, Aug.-Sept. 2005.

[AN05] IST-Project IST-2002-507134, "Ambient Networks", http://www.ambient-networks.org/

[AY05] A. Adinoyi and H. Yanikomeroglu, "Practical cooperative communication through fixed relays", accepted to Wireless World Radio Forum, December 2005.

[BBB+99] J. J. Beek, P. Börjesson, M. L. Boucheret, D. Landström, J. Arenas, P. Ödling, C. Östberg, M. Wahlqvist, and S. Wilson, "A Time and Frequency Synchronization Scheme for Multi-user OFDM" IEEE Journal of Selected Areas on Communications, vol. 17, pp. 1900-1914, Nov. 1999.

[BCK03] A. Bourdoux, B. Come, N. Khaled, "Non-reciprocal transceivers in OFDM/SDMA systems: Impact and mitigation", *RAWCON 2003*, Boston, August 2003.

[Bin90] J. A. C. Bingham, "Multicarrier modulation for data transmission: an idea whose time has come", IEEE Communications Magazine, Vol. 28, pp. 5-14, May 1990

[BM04] G. Barriac, U. Madhow, "Space Time Communication for OFDM with Implicit Channel Feedback", IEEE Trans. on Information Theory, vol. 50, pp.3111-3129, Dec. 2004

[Bon04] T. Bonald, "A score-based opportunistic scheduler for fading radio channels", European Wireless Conference, Barcelona, Feb. 2004.

[BR04] L. Bazzi, and T. J. Richardson, "Exact Thresholds and Optimal Codes for the Binary-Symmetric Channel and Gallager's Decoding Algorithm A," IEEE Trans. on Info. Theory, vol. 50, no. 9, Sept. 2004.

[BSB97] J. J. Beek, M. Sandell, and P. Börjesson, "ML estimation of time and frequency offset in OFDM systems", IEEE Transactions in Signal Processing, vol. 45, pp. 999-1008, July 1997.

[Cam98] J. Campello, "Optimal discrete bit loading for multicarrier modulation systems", Proceedings of International Symposium on Information Theory, p. 193, August 1998.

[Cam99] J. Campello, "Practical bit loading for DMT", Proceedings of ICC 99, Vancouver, Canada, pp. 801-805, June 1999.

[CCB95] P. S. Chow, J. M. Cioffi, J. A. C. Bingham, “A practical discrete multitone transceiver loading algorithm for data transmission over spectrally shaped shannels”, IEEE Trans. Commun., Vol. 43, pp. 773-775, April 1995.

[CENELEC01] EN 50360, “Product standard to demonstrate the compliance of mobile phones with basic restrictions related to human exposure to electromagnetic fields (300 MHz - 3 GHz)”, European Committee for Electrotechnical Standardization (CENELEC), July 2001.

[CENELEC02] EN 50385, “Product standard to demonstrate the compliance of radio base stations and fixed terminal stations for wireless telecommunication systems with the basic restrictions or the reference levels related to human exposure to radio frequency electromagnetic fields (110 MHz - 40 GHz) - General public”, European Committee for Electrotechnical Standardization (CENELEC), European Standard, August 2002.

[CEO02] G. Cherubini, E. Elefthriou and S. Oelcer, “Filtered Multi Tone Modulation for very High Speed Digital Subscriber Lines,” IEEE Journ. On Select. Areas on Commun., vol. 20, n.5, pp. 1016-1028, June 2002.

[CF02] J. Chen and M.P.C. Fossorier, “Near Optimum Universal Belief Propagation Based Decoding of Low-Density Parity Check Codes”, *IEEE Transactions on Communications*, Vol. 50, No. 3, March 2002

[CFO+03] E. Costa, A. Filippi, S. Ometto, M. Weckerle, E. Schulz, “Asynchronous uplink transmission in FMT-FDMA systems,” in Proc. IEEE International Symposium on Personal, Indoor and Mobile Radio Communications (PIMRC), Bejing, China 2003.

[ChC00] M. Chang, K-C. Chen, “Frequency-Domain Approach to Multiuser Detection in DS-CDMA,” IEEE Comm. Letters, vol. 4, no. 11, pp. 331-333, Nov., 2000.

[CSB05] E. Costa, P. Slanina, V. Bochnicka, E. Schulz, G. Spano' Greco, " Downlink based Intra- and Inter-cell Time and Frequency Synchronisation in OFDM Cellular Systems", Proceedings of World Wireless Congress 2005, San Francisco, May 2005.

[DAO05] M. Döttling, D. Astély, and M. Olsson, “A Multi-User Spatial Domain Link Adaptation Concept for Beyond 3G Systems,” *Proc.PIMRC 2005*, Berlin, Germany, September 2005.

[DFL+04] R. Dinis, D. Falconer, Chan Tong Lam et al., “A Multiple Access Scheme for the Uplink of Broadband Wireless Systems,” Globecom 2004.

[DGA04] M. Dohler, A. Gkelias, H. Aghvami, “A Resource Allocation Strategy for Distributed MIMO Multi-Hop Communication Systems”, IEEE Communications Letters, Volume 8, Issue 2, February 2004, pp. 99-101.

[DVB00] "Interaction channel for satellite distribution systems", ETSI EN 301 790, V1.2.2, pp. 21-24, Dec. 2000.

[Ekm02] T. Ekman, Prediction of Mobile Radio Channels. Modelling and Design. Ph.D. Th., Signals and Syst., Uppsala Univ,http://www.signal.uu.se/Publications/abstracts/a023.html

[ER01] A. Ebner and H. Rohling, "A Self-Organized Radio Network for Automotive Applications", Proceedings of the 8th World Congress on Intelligent Transport Systems, Sydney, Australia, October 2001.

[Eri04] N.C. Ericsson, Revenue Maximization in Resource Allocation: Applications in Wireless Communication Networks. Ph.D. Thesis, Signals and Systems, Uppsala Univ., Oct. 2004. http://www.signal.uu.se/Publications/abstracts/a043.html.

[FSE+04] S. Falahati, A. Svensson, T. Ekman and M. Sternad, "Adaptive modulation systems for predicted wireless channels," *IEEE Trans. on Communications*, vol. 52, Feb. 2004, pp. 307-316.

[FA02] David D. Falconer and S. Lek Ariyavisitakul, "Broadband Wireless Using Single Carrier and Frequency Domain Equalization", Proceedings WPMC 2002, pp. 27 - 36, vol.1, Honolulu, USA, Oct. 2002.

[FCS04] A. Filippi, E. Costa, E. Schulz, “Low Complexity Interleaved Sub-carrier Allocation in OFDM Multiple Access Systems,” in Proc. IEEE VTC’04, Los Angeles, California, USA, Sept. 2004.

[FDGH05a] M. Fuchs, G. Del Galdo, and M. Haardt. A novel tree-based scheduling algorithm for the downlink of multi-user MIMO systems with ZF beamforming. In *Proc. IEEE Int. Conf. Acoust., Speech, Signal Processing(ICASSP)*, volume 3, pages 1121–1124, Philadelphia, PA, March 2005.

[FDGH05b] M. Fuchs, G. Del Galdo, and M. Haardt. Low complexity space-time-frequency scheduling for MIMO systems with SDMA. Submitted to *IEEE Transactions on Vehicular Technology*, September 2005.

[FH96] R. F. H. Fischer, J. B. Huber, “A new loading algorithm for discrete multitone transmission”, Proceedings of GLOBECOM 96, London, UK, pp. 724-728, November 1996.

[FK05] D. Falconer, S. Kaiser, editors, “Broadband frequency Domain-Based Air Interfaces for Future-Generation Wireless Systems”, WWRF Working Group 4 White Paper, Version 0.16, Feb. 18, 2005.

[GA93] Mohinder S. Grewal and Angus P. Andrews (1993), “Kalman Filtering Theory and Practice”. Upper Saddle River, NJ USA, Prentice Hall.

[Gal63] R. G. Gallager, “Low-Density Parity-Check codes,” Ph.D Thesis, Cambridge

[GBD03] F. Guilloud, E. Boutillon and J-L. Danger, “λ-Min Decoding Algorithm of Regular and Irregular LDPC Codes”, 3rd International Symposium on Turbo-Codes & Related Topics.

[GRC02] D. Galda, H. Rohling, E. Costa, H. Haas, E. Schulz, “A Low Complexity Transmitter Structure for OFDM-FDMA Uplink Systems,” in Proc. VTC Spring 2002, pp. 1737-1741, 2002.

[HBD00] J.S. Hammerschmidt, C. Brunner, C. Drewes, "Eigenbeamforming - a novel concept in array signal processing", Proc. VDE/ITG European Wireless Conference, Dresden/Germany, Sept. 2000

[HP98] Guidelines for limiting exposure to time-varying electric, magnetic, and electromagnetic fields (up to 300 GHz), International Commission on Non-Ionizing Radiation Protection, Health Physics, vol. 74, no. 4, pp 494-522, April 1998.

[Hug91] D. Hughes-Hartogs, “Ensemble modem structure for imperfect transmission media”, US Patent No. 5054034, October 1991.

[IN05] C. Ibars, M. Navarro, "Reduced complexity iterative multiuser detector for beyond 3G CDMA systems", IST Mobile & Communication Summit 2005 (IST 2005). Dresden (Germany), June 19-23, 2005.

[JB03] E. A. Jorswieck and H. Boche, “Transmission Strategies for the MIMO MAC with MMSE Receiver: Average MSE Optimization and Achievable Individual MSE Region”, IEEE Trans. On Signal Processing, vol. 51, pp. 2872-2881, Nov. 2003

[JDL+04] J.P. Javaudin, C. Dubuc, D. Lacroix, M. Earnshaw, "An OFDM Evolution to the UMTS High Speed Downlink Packet Access," in Proc. of VTC Fall 2004, Los Angeles, USA, 26-29 September 2004.

[JFH+05] V. Jungnickel, A. Forck, T. Haustein, S.Schiffermüller, C. von Helmolt, F. Luhn, M. Pollock, C. Juchems M. Lampe, S. Eichinger, W. Zirwas, E. Schulz “1 Gbit/s MIMO-OFDM Transmission Experiments,” Proc. IEEE VTC Fall 2005, Dallas, Texas.

[JVS+03] C. Jones, E. Valles, M. Smith and J. Villasenor, “Approximate-Min* Constraint Node Updating for LDPC Code Decoding”, IEEE MILCOM 2003.

[KBLS06] T. T. Kim, M. Bengtsson, E. G. Larsson, and M. Skoglund, “Combining Short-Term and Long-Term Channel State Information over Correlated MIMO Channels”, Submitted to ICASSP 2006.

[KF98] F. R. Kschischang, B. J. Frey, “Iterative Decoding of Compound Codes by Probabilistic Propagation in Graphical Models,” Journal on Select. Areas Commun., pp. 219-230, 1998.

[KLF01] Y. Kou, S. Lin and M. Fossorier, “Low Density parity-check codes based on finite geometries: A rediscovery and more,” IEEE Trans. Inform. Theory, vol. 47, pp. 2711-2736, Nov. 2001.

[LC02] D. Lee and K. Cheun, “Coarse Symbol Synchronization Algorithms for OFDM Systems in Multipath Channels”, IEEE Communication Letters, pp. 446-448, Vol. 6, no. 10, Oct. 2002.

[LGA01] D. Lacroix, N. Goudard, M. Alard, "OFDM with guard interval versus OFDM/OffsetQAM for high data rate UMTS downlink transmission," in Proc. of VTC Fall 2001, October 2001, Atlantic City, USA.

[LHYT01] Y. Liu, R. Hoshyar, X. Yang, R. Tafazolli, "Joint Routing and Packet Scheduling for Enhanced Uplink UTRA-FDD with Fixed Relay Stations," in Proc. IEEE Vehicular Technology Conference, Dallas, Texas, USA, September 2005.

[LHYT02] Y. Liu, R. Hoshyar, X. Yang, R. Tafazolli, "An Integrated Radio Resource Allocation Framework for Enhanced Uplink UTRA-FDD with Fixed Relay Stations," 14th IST Mobile and Wireless communications Summit, Dresden, Germany, June 2005.

[LWB+02] D. Landström, S. K. Wilson, J.-J. van de Beek, P. Ödling and P.O. Björjesson. “Symbol time offset estimation in coherent OFDM Systems”, IEEE Transactions on Communications, vol. 50, pages 545-549, Apr. 2002.

[LWZ04] Y. Liu, T. Weber, W. Zirwas, "Uplink performance investigations of the service area basd beyond 3G system JOINT," in Proc. Kleinheubacher Berichte, Kleinheubach, Germany, October. 2004, MS No.: KH2004-A-0051.

[LZ05] T. Lestable and E. Zimmermann, “LDPC Codes Options for Next Generation Wireless Systems”, Wireless World Research Forum (WWRF), WG5, San-Diego, 2005

[MB01] Y. Mao, A. H. Banihashemi, “Decoding Low-Density Parity-Check Codes with Probabilistic Scheduling,” Comm. Letters, 5:415-416, Oct. 2001.

[MBL+05] M. Muck, P. Bernardin, P. Labbe, X. Miet, D. Pannicke, and J. Schoenthier, “Prototyping of a hybrid 5GHz/60GHz OFDM WLAN system in the framework of IST-BroadWay,” Wireless World Research Forum, 13th meeting, Mar. 2-3, 2005, Jeju Island, Korea.

[MCD05] M. Muck, M. de Courville, P. Duhamel, ”A Pseudo Random Postfix OFDM modulator - Semi-blind channel estimation and equalization,” *accepted by IEEE Transactions on Signal Processing*, 2005.

[MKK+05] N. Maeda, T. Kataoka, H. Kawai, K. Higuchi, J. Kawamoto, M. Sawahashi “Experiments on Real-Time 1-Gbps Packet Transmission Using Antenna-Independent AMC in MIMO-OFDM Broadband Packet Radio Access,” Proc. IEEE VTC Fall 2005, Dallas, Texas.

[MS02] M. M. Mansour and N. R. Shanbhag, “Low-Power VLSI Decoder Architectures for LDPC Codes”, IEEE ISLPED 2002.

[MY05] S. Myung and K. Yang, “A Combining Method of Quasi-Cyclic LDPC Codes by The Chinese Remainder Theorem”, IEEE Comm. Letters, Vol.9, N.9, Sept. 2005.

[MYK05] S. Myung, K. Yang and J. Kim, “Quasi-Cyclic LDPC Codes for Fast Encoding”, IEEE Trans. on Info. Theory, August 2005.

[OJEC99] 1999/519/EC: EU Council Recommendation of 12 July 1999 on the limitation of exposure of the general public to electromagnetic fields (0 Hz to 300 GHz), Official Journal of the European Communities, July 1999.

[OY03] J.-E. Oh, K. Yang, “Space-time codes with full antenna diversity using weighted nonbinary repeat-accumulate codes,” IEEE Trans. Commun., vol. 51, pp. 1773–1778, Nov. 2003.

[Pfl05] S. Pfletschinger, “From cell capacity to subcarrier allocation in multi-user OFDM”, *IST Mobile & Wireless Communications Summit*, Dresden (Germany), 19 – 23 June 2005.

[PI05] S. Pfletschinger and C. Ibars, “From cell capacity to subcarrier allocation in OFDMA”, *submitted to European Transactions on Telecommunications*, Sept. 2005.

[Rap91] C. Rapp, “Effects of HPA-Nonlinearity on a 4-DPSK/OFDM Signal for a Digital Sound Broadcasting System”, Proc. 2nd European Conf. on Satellite Comms., Liege, Oct., 1991, pp. 179-184.

[RM00] D. M. Rowitch, L.B. Milstein, “On the performance of hybrid FEC/ARQ systems using rate compatible punctured Turbo (RCPT) codes,” IEEE Trans. on Comm., vol. 48, no. 6, pp. 948-958, June 2000.

[SA03] M. Sternad and D. Aronsson, “Channel estimation and prediction for adaptive OFDM downlinks," IEEE VTC 2003-Fall, Orlando, October 2003.

[SD01] A. Stefanov, T. Duman, “Turbo-coded modulation for systems with transmit and receive antenna diversity over block fading channels: System model, decoding approaches, and practical considerations,” IEEE J. Select. Areas Commun., vol. 19, no. 5, pp. 958–968, May 2001.

[SEA01] M. Sternad, T. Ekman and A. Ahlén, “Power prediction on broadband channels”, IEEE Vehicular Technology Conference VTC01-Spring, Rhodes, Greece, May 6-9 2001.

[SFF+99] M. Speth, S. Fechtel, G. Fock, and H. Meyr, “Optimum Receiver Design for Wireless Broadband Systems Using OFDM-Part I” IEEE Transactions on Communications, vol. 47, pp. 1668-1677, Nov. 1999.

[SF04] M. Sternad, S. Falahati, “Maximizing throughput with adaptive M-QAM based on imperfect channel predictions,” *IEEE PIMRC 2004*, Barcelona, Sept. 2004.

[SFS05] M. Sternad, S. Falahati, T. Svensson and D. Aronsson, ”Adaptive TDMA/OFDMA for wide-area coverage and vehicular velocities”, IST Summit, Dresden, July 2005.

[SGF95] Johan Sköld, Björn Gudmundson, Jan Färjh ,“Performance and Characteristics of GSM-based PCS”, VTC 1995.

[SU05] A. Soysal and S. Ulukus, “Transmit Directions and Optimality of Beamforming in MIMO-MAC with Partial CSI at the Transmitters”, Proc. of CISS, Jan. 2005.

[SW02] A. Springer, R. Weigel, "The Physical Layer of the Universal Mobile Telecommunications System," Berlin; Heidelberg; New York: Springer, 2002.

[SWW+04] E. Schulz, M. Weckerle, T. Weber, M. Meurer, "The OFDM based beyond 3G air interface JOINT featuring interference reduction by joint detection and joint transmission", in Proc. 8th WWRF Meeting, Beijing, China, Feb. 2004, pp. 1-11

[TB04] S. Tomasin and N. Benvenuto, “A Reduced Complexity Block Iterative DFE for Dispersive Wireless Applications”, Proc. VTC 2004 fall, pp. 1693-1697.

[THB04] J. Tousch, M-H. Hamon and J. Benko, “Turbo-Codes Complexity Estimates”, IEEE 802.11n Proposal 1385-r1, Nov. 2004.

[Tse98] D.N.C. Tse and S.V. Hanly, “Multiaccess fading channels—Part I: Polymatroid structure, optimal resource allocation and throughput capacities”, *IEEE Trans. Information Theory*, vol. 44, no. 7, pp. 2796-2815, Nov. 1998.

[Vai92] P.P. Vaidjanathan, Multirate Systems and Filter Banks, Englewood Cliffs, NJ: Prentice Hall

[VF00] J. Vogt, and A. Finger: “Improving the Max-Log-MAP turbo decoder”, *IEEE Electronincs Letters*, vol. 36, no 23, pp. 1937–1939, 2000.

[VH04] V. Stankovic and M. Haardt, “Multi-user MIMO downlink precoding for users with multiple antennas”, in Proc. Of the 12-th Meeting of the Wireless World Research Forum (WWRF), Toronto, Canada, Nov. 2004

[VH05a] V. Standovic and M. Haardt, “Multi-user MIMO downlink beamforming over correlated MIMO channels”, in Proc. International ITG/IEEE Workshop on Smart Antennas (WSA05), Duisburg, Germany, April 2005

[VH05b] V. Stankovic and M. Haardt, “Improved diversity on the uplink of multi-user MIMO system”, in Proc. European Conference on Wireless Technology (ECWT 2005), Paris, France, October 2005

[VTL02] P. Viswanath, D.N.C. Tse and R. Laroia, “Opportunistic beamforming using dumb antennas”, IEEE Transactions on Information Theory, vol. 48(6), June 2002.

[WER03] L. Wischhof, A. Ebner, H. Rohling, M. Lott, and R. Halfmann, "SOTIS -A Self-Organizing Traffic Information System", Proceedings of the 57th IEEE Vehicular Technology Conference (VTC '03 Spring), Jeju, Korea, 2003.

[Win84] J.H. Winters “Optimum Combining in Digital Mobile Radio with Cochannel Interference” in IEEE Journal on Selected Areas in Communications, Vol. SAC-2, No 4, July 1984

[WIND21] IST-2003-507581 WINNER, “D2.1 Identification of Radio-Link Technologies”, June, 2004.

[WIND22] IST-2003-507581 WINNER, “D2.2 Feasibility of multi-bandwidth transmissions”, October, 2004.

[WIND23] IST-2003-507581 WINNER, “D2.3 Assessment of Radio-Link Technologies”, February, 2005.

[WIND24] IST-2003-507581 WINNER, “D2.4 Assessment of adaptive transmission technologies”, February, 2005.

[WIND25] IST-2003-507581 WINNER, “D2.5 Duplex arrangements for future broadband radio interface”, October 2004.

[WIND26] IST-2003-507581 WINNER, “D2.6 Assessment of multiple access technologies”, October 2004.

[WIND27] IST-2003-507581 WINNER, “D2.7 Assessment of Advanced Beamforming and MIMO Technologies”, February 2005.

[WIND31] IST-2003-507581 WINNER, “D3.1 Description of identified new relay based radio network deployment concepts and first assessment of comparison against benchmarks of well known deployment concepts using enhanced radio interface technologies”, Oct. 2004.

[WIND32] IST-2003-507581 WINNER, “D3.2 Description of identified new relay based radio network deployment concepts and first assessment by comparison against benchmarks of well known deployment concepts using enhanced radio interface technologies”, February 2005.

[WIND35] IST-2003-507581 WINNER “D3.5 Proposal of the best suited deployment concepts chosen for the identified scenarios”, December 2005.

[WIND41] IST-2003-507581 WINNER “D4.1 Identification and definition of cooperation schemes between RANs –first draft”, June 2004.

[WIND42] IST-2003-507581 WINNER “D4.2 Impact of cooperation schemes between RANs –first draft”, February 2005.

[WIND43] IST-2003-507581 WINNER “D4.1 Identification and definition of cooperation schemes between RANs –final deliverable”, June 2005

[WIND44] IST-2003-507581 WINNER, “D4.4 Impact of cooperation schemes between RANs – final deliverable”, November 2005.

[WIND54] IST-2003-507581 WINNER “D5.4 Final Report on Link Level and System Level Channel Models”, September 2005.

[WIND63] IST-2003-507581 WINNER, "D6.3 WINNER Spectrum Aspects: Assesment report". December 2005.

[WIND71] IST-2003-507581 WINNER, "D7.1 System requirements", July 2004.

[WIND72] IST-2003-507581 WINNER, "D7.2 System Assessment Criteria Specification", July 2004.

[WIND76] IST-2003-507581 WINNER, "D7.6 WINNER System Concept Description", October 2005.

[WOSS05] Wei Wang, Tony Ottosson, Tommy Svensson, Arne Svensson, Mikael Sternad. "Evaluations of a 4G Uplink System Based on Adaptive Single-Carrier TDMA". Proceedings IEEE Vehicular Technology Conference Fall, Dallas, Texas, USA, Sep 2005.

[YNA01] E. Yeo, B. Nikolie, and V. Anantharam, "High Throughput Low-Density Parity-Check Decoder Architectures," IEEE Globecom 2001.

[Yu02] W. Yu and J.M. Cioffi, "FDMA capacity of Gaussian multiple-access channels with ISI", *IEEE Trans. Commun.*, vol. 50, no. 1, pp. 102-111, Jan. 2002.

[Yu04] W. Yu, W. Rhee, S. Boyd, J.M. Cioffi, "Iterative water-filling for Gaussian vector multiple-access channels", *IEEE Trans. Information Theory*, Jan. 2004.

[ZB04] P. Zarrinkhat, and A. H. Banihashemi, "Threshold Values and Convergence Properties of Majority-Based Algorithms for Decoding Regular Low-Density Parity-Check codes," IEEE Trans. on Comm., vol. 52, no. 12, Dec. 2004.

[ZF04] J. Zhang, and M. Fossorier, "A Modified Weighted Bit-Flipping Decoding of Low-Density Parity-Check Codes," IEEE Comm. Letters, vol. 8, no. 3, March 2004.

[ZF05] J. Zhang, M. Fossorier, 'Shuffled iterative decoding', IEEE Trans. on Comm., Vol. 53, No. 2, February 2005

[ZZ05] H. Zhong, and T. Zhang, 'Block-LDPC: A Practical LDPC Coding System Design Approach', IEEE Trans. on Circ. And Syst.-I: Reg. Papers, Vol. 52, N. 4, April 2005.